Recipient c-kit+ Cells Contribute to Regeneration of Endothelial and Smooth Muscle Cells in Allograft Vessels

Ni, Zhichao

Awarding institution:
King's College London

Recipient c-kit^{+} Cells Contribute to Regeneration of Endothelial and Smooth Muscle Cells in Allograft Vessels

By

Zhichao Ni

A thesis submitted to King's College London
For the degree of Doctor of Philosophy

School of Cardiovascular Medicine and Sciences
Faculty of Life Science & Medicine
King's College London

September, 2018

Acknowledgements:

I wish to express my sincere gratitude to my supervisor Professor Qingbo Xu for his support during the past three-years of my PhD study. Prof Xu's expertise and advise were incredibly important and I will always thoroughly appreciate his support. I would also like to acknowledge my secondary supervisor Dr. Yanhua Hu who performed and orchestrated all the *in-vivo* surgeries and for her unconditional support both at academic and personal level throughout.

Special appreciation goes to my colleagues Dr. Claire Potter and Dr Jiacheng Deng. As a foreign student, I wowuld like to thank Dr. Potter for enthusiastically introducing me to science, as well as British culture. I am very grateful to Dr. Deng, for teaching me data intepretation and manuscript writing.

I am grateful for Mr Zhongyi Zhang's assistance in preparation of paraffin sections in my project and express my thanks to Dr Witold N. Nowak who shared his expertise in flow cytometry with me. I must additionally thank Mrs. Sherrie King, who has given her unselfish help throughout my PhD. study journey.

I would like to acknowledge the support of all the members from the groups of Professor Qingbo Xu and Dr. Lingfang Zeng, in particular, Dr. Xuechong Hong, Dr Alexandra Le Bras, Dr. Yao Xie, Dr Ioannis Kokkinopoulos, Dr. Baoqi Yu, Dr. Shirin Issa Bhaloo, Dr. Wenduo Gu, Dr. Ka Hou Lao, Dr. Ana Moraga, Dr. Junyao Yang, Dr.Angshumonik Angbohand, Mr. Mazdak Ehteramyan and Mr. Jose Morales De Los Santos. It is hard to imagine how difficult life would have been without all of these important colleagues and friends.

Lastly and most importantly, I must say thank you to my wife Mrs. Xingxing Zhong, my parents and all of my family members. It is their support and love that motivates me to move forward and take adventures and that has helped me fulfil my ambitions so far.

Declaration

I, Zhichao Ni declare that this PhD thesis and the research to which it refers is a product of my own work. Information derived from other sources and work carried out with the assistance of others, has been appropriately cited and acknowledged.

Abstract

Rationale: Transplantation-accelerated arteriosclerosis is one of the major challenges for long-term survival of patients with solid organ transplantation. Though stem/progenitor cells (SPCs) have been implicated to participate in this process, the origin of these SPCs and the underlying mechanisms behind their contribution to disease have not been fully defined.

Objective: The objective of our study was to investigate the role of c-Kit$^+$ SPCs in allograft-induced lesion formation, and to explore the underlying mechanisms.

Methods and Results: c-Kit$^+$ SPCs were detected in allograft-induced neointima lesions using immunostaining. By using an inducible lineage tracing mouse model, we showed that c-Kit$^+$ SPCs are an important source of neointimal smooth muscle cells (SMCs) and endothelial cells (ECs), contributing to neointima formation in an aortic allograft transplantation model. We performed allograft transplantation between different donor and recipient mice, as well as bone marrow transplantation experiments, demonstrating that c-Kit$^+$ SPCs-derived cells originate from non-bone marrow tissues of recipient mice, but not donor mice. ACK2, which specifically binds and blocks c-Kit function, ameliorates allograft-induced arteriosclerosis. Stem cell factor (SCF) and vascular endothelial growth factor (VEGF) levels were significantly increased in blood and neointimal lesions after allograft transplantation. C-Kit$^+$ SPCs were harvested from grafts to investigate underlying mechanisms in vitro. Mechanistically, SCF facilitated cell migration through SCF/c-Kit axis and downstream activation of small GTPases, MEK/ERK/MLC and JNK/c-Jun signalling pathways, while VEGF induced c-Kit$^+$ SPCs migration via AKT/FAK signalling.

Conclusions*:* Our findings provide evidence that recipient non-bone marrow-derived c-Kit$^+$ SPCs migrate to allograft lesions, differentiate into SMCs and ECs contributing to vascular remodelling in an allograft transplantation model. Mechanisms involving cell migration may provide insights into pathogenesis and treatment of vascular diseases.

Table of Contents

Abbreviations

4-OHT	4-hydroxy-tamoxifen
7-AAD	7-aminoactinomycin
ac-LDL	Acetylated-low density lipoprotein
ADAMs	A disintegrin and metalloproteinases
AGEs	Advanced glycation end products
AKT	Protein kinase B
AMPCs	Adventitial macrophage progenitor cells
ANOVA	Analysis of variance
AP-1	Activator protein 1
APCs	Antigen presenting cells
Arp2/3	Actin related protein 2/3
ATP	Adenosine triphosphate
BAC	Bacterial Artificial Chromosomes
BSU	Biological service unit
CABG	Coronary artery bypass surgery
CAV	Cardiac allograft vasculopathy
CDC42	Cell division control protein 42 homolog
CDKs	Cyclin-dependent kinases
CDR	Complementarity determining region
CFP	Cyan fluorescent protein
CFU	Colony forming unit
Co-IP	Co-immunoprecipitation
CRE	Cre recombinase
CRISPR/CAS	Clustered Regularly Interspaced Short Palindromic Repeat/ CRISPR associated proteins
crRNA	Short CRISPR RNA
Cyfip2	Cytoplasmic FMRP interacting protein 2
DAPI	4', 6-diamidino-2-phenylindole
DMSO	Dimethyl sulfoxide

DSBs	DNA double-strand breaks
EBP	Elastin-binding protein
ECFCs	Endothelial colony-forming cells
ECMs	Extracellular matrices
ECs	Endothelial cells
ELISA	Enzyme-linked immunosorbent assay
Ena/VASP	Enabled/vasodilator-stimulated phosphoprotein
EndMT	Endothelial to mesenchymal transition
eNOS	Endothelial Nitric oxide synthase 3
EPCs	Endothelial progenitor cells
EPs	Endothelial progenitors
ER	Estrogen receptor
ERK	Extracellular signal regulated kinases
ESPCs	Endothelial stem/progenitor cells
Fab	Fragment Antigen-binding
F-actin	Filamentous actin
FAK	Focal adhesion kinase
Fas/FasL	First apoptosis signal receptor/ Fas ligand
FAT/ FERM	Focal adhesion targeting domain
Fc/ FcR	Fragment crystallisable/ Fragment crystallisable receptor
FGF	Fibroblast growth factor
GAPs	GTPase activating proteins
GEF	Guanine nucleotide exchange factor
GFP	Green fluorescent protein
GFR	Glomerular filtration rate
GLISA	Small GTPase linked immunosorbent assay
GP130	Glycoprotein 130
GPCRs	G protein-coupled receptors
GPI	Glycosylphosphatidylinositol
gRNA	Guide RNA

GTPases	Rho family small guanosine triphosphate binding proteins
H&E	Haematoxylin and eosin
HDAC	Histone deacetylase
HDR	Homology-directed repair
HIF-1	Hypoxia-inducible factor-1
HLA	Human leukocyte antigen
HRP	Horseradish peroxidase
HSCs	Hematopoietic stem cells
Hsp90	Heat shock protein 90
HVR	Hypervariable region
ICAM	Intracellular adhesion molecular
IF	Immunofluorescence
IFN-γ	Interferon gamma
IHC	Immunohistochemistry
INR	International normalised ratio
JAK/STAT	Janus kinases/ Signal transducer and activator of transcription proteins
Klf4	Kruppel-like factor 4
LBD	Ligand-binding domain
LDL	Low density lipoprotein
LFA1	αLβ2-integrin
LIF	Leucocyte inhibitory factor
MAC/CD11b	$\alpha_M\beta_2$-integrin
MADM	Mosaic analysis with double markers
MAPKs	Mitogen-activated protein kinases
MHC	Major histocompatibility complexe or myosin heavy chain
MLC	Myosin light chain
MLCK	Myosin light chain kinase
MMPs	Matrix metalloproteinases
MRTF-A/B	Myocardin related transcription factor-A/B
MSCs	Mesenchymal stem cells

mT/mG	Membrane-targeted tdTomato/membrane-targeted Green fluorescence protein
MTMMPs	Membrane-type MMPs
MTOC	Microtubule-organizing centre
MYPT1	Myosin binding subunit
NC	Non-collagen
NFAT	Nuclear factor of activated T-cells
NHEJ	Non-homologous end joining
NK	Natural killer
NO	Nitric Oxide
NYHA	New York Heart Association
PAK1	p21-activated Kinase
PAMPs	Pathogen associated molecular patterns
PBS	Phosphate-buffered saline
PDGF	Platelet derived growth factor
PDL1	Programmed death-ligand 1
PFA	Paraformaldehyde
PI	Propidium iodide
PI3K	Phosphoinositide 3-kinase
PIP2	Phosphatidylinositol(4,5)- bisphosphate
PIP3	Phosphatidylinositol(3,4,5)- trisphosphate
PKCα	Protein Kinase C-α
PLC	Phospholipase C
PMT	Photon multiplier tube
PP1	Protein phosphatase
PRRs	Pattern recognition receptors
PS	Phosphatidylserine
PTEN	Phosphatase and tensin homolog
qPCR	Quantitative Real-Time Polymerase Chain Reaction
RAC	Ras related C3 botulinum toxin substrate
RAGs	Recombination-activating genes

RB	Retinoblastoma protein
RFP	Red fluorescent protein
RHO	Rho family of GTPases
RIAM	Rap1-GTP-interacting adaptor molecule
RNAi	RNA interference
ROCK	Rho-associated protein kinase
ROS	Reactive oxygen species
RT	Reverse transcription
SBE	Smad-binding elements
SCF	Stem cell factor
SDF-1	Stromal cell-derived factor-1
SM22	Transgelin
SM22/TagIn	Smooth muscle protein 22/Transgelin
SMCs	Smooth muscle cells
SMMHC	Smooth muscle myosin heavy chain
SMPCs	Smooth muscle cell progenitor cells
SNPs	Single Nucleotide Polymorphisms
SPCs	Stem/progenitor cells
Src	Proto-oncogene tyrosine protein kinase Src
SRE	Serum response element
SRF	Serum response factor
TADs	Transcription activation domains
TALEN	Transcription activator-like effector nuclease
TBST	Tris-buffered saline and Tween20
TCR	T cell receptor
TGFβ1	Transforming growth factor β1
TH	T helper
TIE1/2	Tyrosine kinase with immunoglobulin like and EGF like domain1/2
TIMPs	Tissue inhibitors of MMPs
TNF-α	Tumour necrosis factor-α

tracrRNA	Trans-activating crRNAs
TUNEL	Terminal UTP nick end-labelling
UEA-1	Ulex europaeus agglutinin-1
VCAM	Vascular cell-adhesion molecule
VEGF	Vascular endothelial growth factor
VH/ VL	Variable domain in heavy chain/ light chain
VLA4	α4β1-integrin
VVOs	Vesiculo vacuolar organelles
WASP	Wiskott-Aldrich syndrome protein
WAVE	WASP-family verprolin-homologous protein
WH2	WASP-homology 2
WPRE	Woodchuck hepatitis virus posttranscriptional regulatory element
WT	Wild type
X-gal	5-bromo-4-chloro-3-indolyl galactosidase
YAC	Yeast Artificial Chromosomes
YFP	Yellow fluorescent protein
ZFN	Zinc-finger nuclease
α-SMA	α-smooth muscle actin

List of Figures

List of Tables

Chapter 1: Introduction

1.1 Blood Vessels

Blood vessels transport blood from the heart to all the tissues and organs in the body (Figure 1.1). Three major types of vessel comprise the whole circulatory system: arteries, capillaries and veins. Blood is pumped from heart into the circulation sequentially from the arteries into capillaries and ultimately veins. During this process, oxygen and nutrients are delivered to tissues throughout the body and deoxygenated blood then returned to the lungs for re-oxygenation.

Figure 1.1

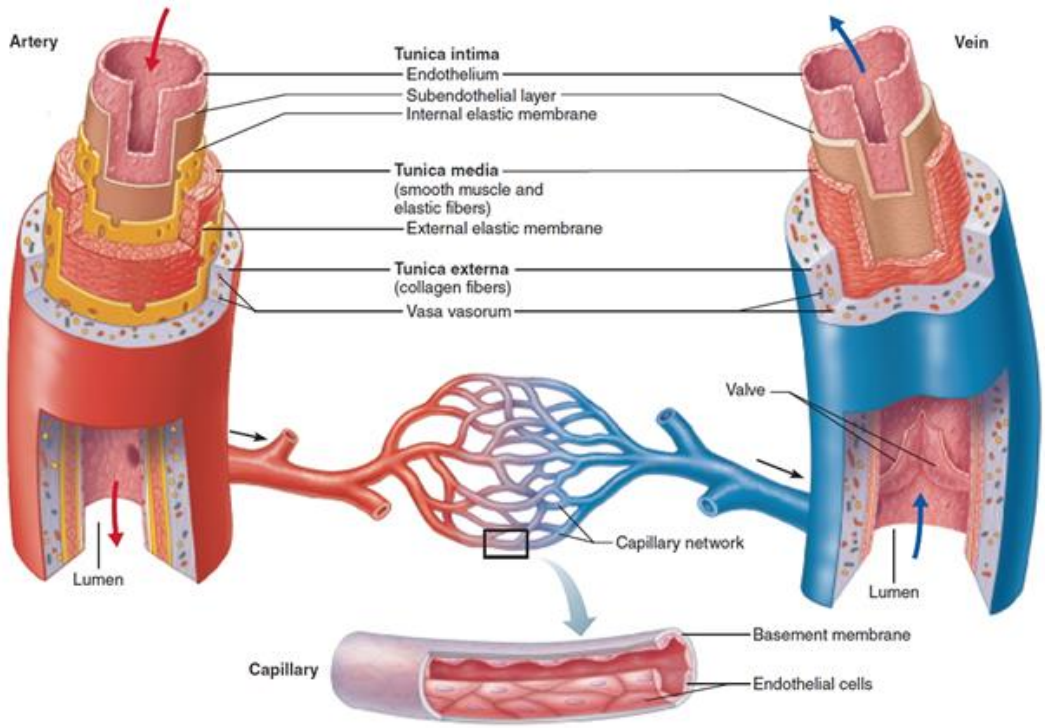

Figure 1.1 Blood vessels. Oxygenated blood is pumped from the left ventricle of the heart and circulates throughout the body. Deoxygenated blood returns to the right atrium where it is pumped to the lungs for re-oxygenation. Both artery and veins are comprised of tunica intima, tunica media and tunica adventitia layers. Tunica intima consists of endothelial cells and basement membrane. Tunica media consists of smooth muscle cells and elastic fibres. Tunica adventitia includes several cell types and connecting tissues. (Figure Source: https://healthjade.com/aortic-aneurysm.)

1.1.1 Arteries

According to their diameter, arteries can be divided into the subcategories of large arteries and arterioles. All large arteries have a classic three-layered structure including tunica adventitia, media and intima. The outermost layer is the tunica adventitia, which is comprised of connective tissue (mainly collagen), fibroblasts, nerves, resident stem/progenitor cells (SPCs), adipocytes and *vasa vasorum*. Smooth muscle cells (SMCs), elastic fibres and collagens make up the media layer. The inner layer is the tunica intima, which is covered by a single layer of endothelial cells (ECs) in direct contact with blood flow. Extracellular matrices (ECMs), form the subintimal layer and participate in the structural integrity of EC. Large arteries can be further subdivided into either elastic or muscular arteries. In elastic arteries such as the aorta and the carotid artery, there are SMCs distributed throughout the intima as well as in subintimal layers. In the media layer, multiple layers of SMCs are surrounded by elastin fibres forming SMC contractile units. This elastin structure is required to provide strong flexibility within elastic arteries that must expand due to high blood pressure. Elastic arteries are normally located close to the heart. Muscular arteries such as the femoral, ulnar and radial arteries, are smaller and generally branch from elastic arteries. Rather than mitigate systolic and diastolic pressure fluctuation, they are found in areas according to tissues or organs demand.

When the diameter of an artery is less than 0.3mm, it can be defined as an arteriole. Although arterioles also have a three-layer structure, all three layers are thinner than in large arteries and constitute of 1 to 2 layers of smooth muscle cells in the media. Arterioles branch into capillaries.

1.1.2 Veins

Similar to arteries, veins can be separated into the large veins or venules according to diameter. Large veins are also made up of three layers of tissue. However, the venous media layer contains fewer SMCs compared to same size of artery. Additionally, most veins are equipped with valves to prevent backflow. The *venae cavae* are the two largest veins returning deoxygenated blood back into the atrium. The inferior *vena cava* returns blood from the lower body, and the superior *vena cava* returns blood located above the heart. Other large veins such as subclavian vein and jugular vein, are generally called large collecting vessels. Venules are small veins with a diameter

of less than 1mm. The total number of venules in the body contain approximately 25% of the blood in the whole venous system. Distinct to arterioles, venules have a thinner structure and are equipped with pores.

1.1.3 Capillaries

Capillaries are formed from a sole EC layer and have a diameter of less than 10μm. The main function of capillaries is substance exchange from arterioles to parenchymal cells within the microcirculation[1]. According to structure, capillaries can be divided into three types including continuous, fenestrated and sinusoid capillaries. Continuous capillaries provide an uninterrupted lining layer, in which ECs are connected by intercellular junctions, allowing only small molecules to pass through. Both fenestrated and sinusoidal capillaries have pores within cells or intercellularly, which allow big molecules and even cells to pass through capillary. ECs seated upon basement membrane along with pericytes which are also known as mural cells[2]. Pericytes and ECs can be connected by integrin and gap junctions. These structures allow pericytes to exchange substances with neighbouring cells. Identifying features of pericytes vary in different tissues. For example, pericytes located near venules express the proteins desmin and αSMA proteins, whereas those within capillaries solely express desmin but not αSMA. Recently, according to surface markers, pericytes have been divided into two types which are type I ($nestin^{-}NG2^{+}$) and type II ($nestin^{+}NG2^{+}$) pericytes. It has been shown that type I pericytes are involved in adipogenesis and fibrosis, whereas type II pericytes function in myogenesis, angiogenesis and neurogenesis. It has now been widely accepted that pericytes have a role in tissue regeneration.

1.1.4 Vascular Function and Disease

The basic function of blood vessels is to transport blood and exchange nutrients into target tissues. A blood vessel has no autorhythmicity and therefore cannot independently transport the blood. Instead, blood within vessel is primarily propelled under pressure derived from the heart. Meanwhile, the vessels can also regulate blood pressure via adjusting their diameter by the autonomic nervous system control. Through vessel contraction and dilation, system blood pressure can be maintained at a stabilized level when increased flow is required into a specific vascular bed. Once pumped from the heart, blood firstly flows into the aorta followed by peripheral arteries under the pressure difference. Afterwards blood is squeezed into arterioles. Arterioles

are widely distributed in all of the organs and constitute the largest source of vascular resistance. When the arterioles lumen diameter decreases, or media wall gets thicker, blood pressure would increase. At the end, blood continues to flow from arterioles into capillaries, during which blood velocity sharply drops. Two transport types are responsible for molecule exchange between capillaries and tissues. One is transcellular transport within single endothelial cells, in which molecules larger than 3nm such as albumin and proteins would pass across via vesicles. Another one is paracellular transport, in which molecules smaller than 3nm such as water, ions and gas could cross the capillary wall through clefts between ECs. In some specific tissues such as blood brain barrier however, cells have no paracellular transport because of tight junctions and therefore the molecules can only pass by transcellular transport. Through venous vascular system, blood is collected back into the heart.

Vascular diseases are a class of diseases in which vascular function is damaged because of various pathological factors. ECs dysfunction occurs early in vascular diseases. ECs dysfunction, increases permeability in large vessel, allowing large molecules or even inflammatory cells accumulation and potentially resulting in haemorrhage (erythrocyte), atheroma (lipid accumulation) or vasculitis (inflammatory cells accumulation). During pathogenesis, large vessels can be occluded leading to downstream vessel ischemia or even cellular necrosis in patients. Depending upon the location of lesion, vascular disease can be divided into arterial and venous disease. Atherosclerosis is an inflammatory disease characterised by endothelial cell dysfunction, leukocyte infiltration, lipid oxidation and fatty streak accumulation with disturbed laminar flow due to the development of atheromatous plaques. Fibrous plaque expansion and protrusion into the lumen of vessels can lead to acute clinical syndromes, such as cerebral or myocardial infarction, or develop into thrombosis, hemorrhage, ulceration, and calcification. Similarly, arteriosclerosis is defined by arterial lesion due to non-lipid mediators. Aortic dissection is another kind of media layer disease, in which blood flows in the vessel wall and tears layers apart. Hypertension and connective tissues disorders are predisposing causes in aortic dissection. Venous insufficiency, because of venous reflux, which is caused by diseases such as vein thrombosis and phlebitis, is the most common in venous diseases. Venous insufficiency can lead to complications such as varicose veins and ulcers. Lower limb deep vein thrombosis is one severe vein disease and can increase

risk of pulmonary embolism. When the clot flows into pulmonary arteries via the circulation, it can be fatal. As the principal underlying cause of cardiovascular disease, the leading cause of death and morbidity worldwide; atherosclerosis and arteriosclerosis have enormous clinical relevance.

1.2 Organ Dysfunction and Transplantation

Organ dysfunction refers to a condition in which the tissues lose their homeostasis capability and eventually function. Organ failure can be induced due to many pathological factors such as sepsis, nonsteroidal anti-inflammatory antibiotics, and accumulation of biological by-products. Heart failure occurs when the heart is unable to pump sufficient blood to meet metabolic demands. Patients who suffer from severe heart failure may show symptoms such as dyspnoea, lower limb swelling and coughing blood. Alternatively, hepatic failure results from insufficient synthetic or metabolic function. This may arise from risk factors such as hepatitis virus, chemical exposure or cancer. New York Heart Association (NYHA) divides heart function into four classes according to severity of symptoms. NYHA IV is the terminal or end stage of heart failure in which situation patients can not undertake physical activity without discomfort. In counterpart, glomerular filtration rate (GFR) being below 15 (ml/min/1.73m^2) in kidney is defined as end-stage renal disease. In patients with chronic liver disease, a diagnosis model for end-stage liver disease has recently been implemented. This model combines several serum biomarkers including bilirubin, creatinine and international normalised ratio (INR) for prothrombin time. Beside drugs, all the patients with organ failure disease need urgent and powerful treatment. For example, implantation of left ventricular assist devices are necessary for patients who are at cardiac end stage, to prevent mortality. For patients with kidney or liver failure, dialysis is one widely used treatment. During this process, waste can be filtered out of the body to replace dysfunctional kidney/liver.

Organ transplantation, which refers to an organ being removed from one body to another as recipient, is alternative treatment for severe organ failure patients. Several organs including heart, lung, liver and kidney have been successfully transplanted and organ transplantations are currently widely performed in clinic. In general, organ transplantation can be divided into auto-transplantation, allo-transplantation, iso-transplantation and xenotransplantation. Auto-transplantation refers to a surgery to

transplant a regenerated tissue to other injury places from the same person, such as skin transplantation and vein graft transplantation for coronary artery bypass surgery (CABG). Iso-transplantation means transplanting tissues to genetically identical recipients (such as transplantation between identical twins), whereas xenograft indicates organ transplantation from one species to another. The most common type of organ transplantation in clinic is allo-transplantation, which refers to a surgery process transferring organs between genetically non-identical members from the same species. In past decades, organ transplantation has gone through rapid development and significantly improved survival rate of organ failure patients. In fact, it was shown that in the United States, the one-year survival rate after cardiac transplantation has been over 90%[3]. One year survival rate post liver[4] and kidney[5] transplantation is within 80-95%. Because of surgical technique advancement and introduction of immunosuppression drugs, short term (within six months or 1 year) graft failure has dramatically decreased below 10%. Cyclosporine and tacrolimus are examples of immunosuppression drugs which target on T cells and inhibit their activation. Data has shown that the rate limiting enzyme in T cells activation is a serine–threonine phosphatase, called calcineurin. With calcineurin stimulated, phosphorylated nuclear factor of activated T-cells (NFAT) is dephosphorylated and translocates from cytoplasm into nucleus promoting target gene activation[6]. Both cyclosporine and tacrolimus could inhibit calcineurin function and thereafter arrest T cells activation. Sirolimus and everolimus could inhibit T cells proliferation via targeting mTOR[7]. Because the lymphocyte lacks salvage pathways for synthesis of guanosine nucleotides, mycophenolate acid could inhibit lymphocyte DNA metabolism, by directly blocking de novo guanosine nucleotides synthesis.

To note, although short term survival rate in organ transplantation patients has significantly increased, long term graft failure is still high. For example, 5 years graft failure is around 20% and 10 years organ failure can reach to 40% high. Several risk factors were reportedly involved in organ failure after transplantation and these factors can be generally divided into four categories, including transplant rejection, recipient factors, transplant factors and treatment related factors. Although acute rejection mediated by T lymphocytes can be partly inhibited via immunosuppression drugs, the innate immune system could react towards the graft tissue. Patient's recovery response to graft transplantation varies due to individual differences. Patient's age and

complications with diabetes, dyslipidaemia, hypertension, cancer and viral infection could all severely effect and therefore reduce long term survival rate for organ transplantation patients. Donor transplant condition also affects organ transplantation result. For example, when the graft transplant is dysfunctional due to primary factors or during transfer process, organ dysfunction would be anticipated. Meanwhile, factors such as donor age, sex and potential infection would all contribute to graft failure. Furthermore, improper treatment or side effects after organ transplantation would as well lead to severe graft dysfunction. Although immunosuppression drugs could decrease rates of acute graft rejection, they would at the same time increase patients risk for infection and cancer. Cyclosporine as calcineurin inhibitor, has nephrotoxicity, which would result in renal graft dysfunction[8]. In addition, the timing on dialysis before transplantation has also been demonstrated an independent risk factor for kidney transplantation failure.

1.3 Allograft Vasculopathy/Arteriosclerosis

Although all risk factors above could contribute to graft failure, various studies revealed that in large proportion, graft failure does not result from primary organ dysfunction, but from ischemia due to narrowed arteries. For example, after cardiac transplantation, allograft ischemia could occur earlier in less than 2 h, and nearly all the graft could undergo ischemia within 6 h. When ischemia further progresses, vasculopathy/arteriosclerosis develops. Cardiac allograft vasculopathy (CAV) is a chronic disease in which the graft coronary artery lumen becomes narrow while the vessel wall becomes thick and hard (Figure 1.3). CAV could lead to severe graft damage, even to heart failure or sudden death. Most recent report showed that 5 and 10 years post cardiac transplantation, occurrence rate of CAV is around 30 and 50%, respectively[9]. Notably, 5 years survival rate in patients with CAV is merely 75%, lower than the patients without vascular disease. In fact, CAV is reported to be leading cause for long term transplant organ failure. Similar to other organ transplantation, CAV is caused by both immunologic and non-immunologic factors. CAV is characterized by diffuse lesions within vessel wall. CAV Lesions can be divided into vasculitis, intimal hyperplasia and atheroma plaque[10]. Initially after transplantation, inflammatory cells including lymphocytes and macrophages accumulate at intima layers leading to ECs inflammation, which is called vasculitis. Then injured ECs express cytokines or growth factors production that can activate proliferation of SMCs or fibroblasts within the

intima layer. Meanwhile, these proliferating cells also secrete ECMs such as collagen and fibronectin leading to vascular wall fibrosis. In fact, intimal hyperplasia mainly includes dysfunctional ECs, proliferating SMCs, clotting development and fibrotic ECMs. When inflammation further develops, atheroma plaque occurs which characterized by accumulation of degenerative materials such as inflammatory cells, SMCs, lipid, calcium and fibrous ECMs. As compensation, SMCs in the media layer would stretch out to form aneurysms, which keep lumen diameter in a relatively constant level. Over time, atheroma progresses in size and thickness, eventually reaching to SMCs remodelling capacity or plaque rupture occurrence. The plaque protrudes into the vascular lumen, narrowing the vessel and restricting the blood flow. When the plaque ruptures, debris and small clot would spread into small vessels resulting in lumen closure and acute major vascular event. To note, all CAV lesions would occur simultaneously but not separately. Other factors, rather than entirely vasculitis, are involved. Inflammatory cells also participate in intimal hyperplasia and atheroma plaque processes. Furthermore, data has shown that inflammatory cells do not solely limit in ECs layer, but could extend to all three layers of the vessel. Compared with native atherosclerosis, CAV also has its pathological characters. For example, CAV could occur with a concentric but not eccentric stenosis. In addition, the lesion is likely to diffuse in all the vessel but is not limited to some focal sites.

Figure 1.3

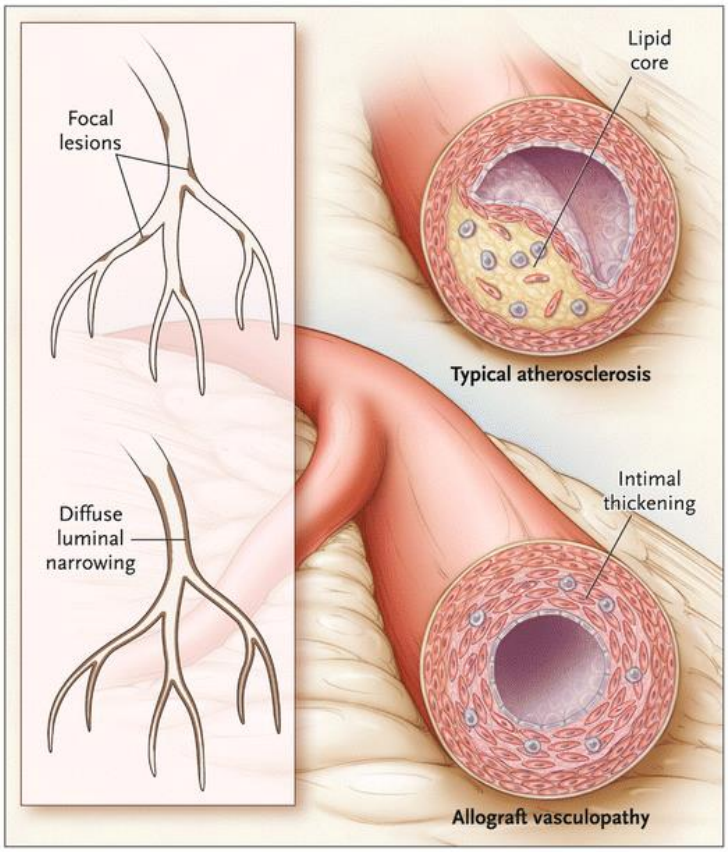

Figure 1.3 Cardiac allograft vasculopathy (CAV). Post transplantation surgery, inflammatory cells accumulate at intima layers leading to ECs activation. Dysfunctional ECs express cytokines and stimulate SMCs or fibroblast proliferation. These ECs secrete ECMs leading to vascular wall fibrosis. Vasculitis, intimal hyperplasia and atheroma plaque are typical pathological process. SMCs migrate from media layer into the intima layer as a response to lumen narrowing. Over time, atheroma progresses in size and thickness, forming the lesion. The lesion protrudes into the vascular lumen, narrowing the vessel and restricting the blood flow. When the plaque ruptures, clot occludes the lumen. Typical cardiac allograft vasculopathy (CAV) lesion is concentric but not eccentric stenosis. CAV, Cardiac allograft vasculopathy; ECs, endothelial cells; SMCs, smooth muscle cells; ECMs, extracellular matrices. (Figure Source: Colvin-Adams M, Harcourt N, Duprez D. Endothelial dysfunction and cardiac allograft vasculopathy. Journal of cardiovascular translational research[11].)

1.3.1 Immune Response

Similar to other organ transplantation, both cellular and humoral immune response are involved in CAV. Cellular immune response is a result of activated T lymphocytes which exert direct cytotoxicity or release cytokines in response to exogenous antigens. Humoral immune response refers to immunity mediated through antibodies and/or complement system. Furthermore, the innate immune system is also known to be involved in CAV pathology.

1.3.1.1 Cellular Immune Response

Immune response to non-self-antigens are recognized by recipient immune system[12]. From the transplant tissue staining, it was shown that T cells are present at higher levels and infiltrate within the neointima[13]. Three mechanisms are responsible for T cell response. Firstly, when the donor tissue is allo-transplanted to recipient, recipient T cells recognise intact donor molecules complex with peptide on donor antigen presenting cells (APCs) , leading to extremely strong and acute rejection which is called direct recognition[12]. Secondly, indirect recognition also play an important role in allo-graft rejection[12]. Distinct from direct recognition, in indirect recognition, donor antigen, is digested, internalised and presented by recipient APCs. Afterwards recipient APCs are recognized by T lymphocytes. Third, semi-direct pathway is also shown involved in T cells activation, although the mechanism is unclear[14]. In semi-direct recognition, by intracellular exchange between donor cells and recipient APCs, donor MHC is presented by host APCs inducing T cells response. Afterwards, activated T cells resulted from pathways above, would then secrete inflammatory cytokines such as IL-2 and IFN-γ[15]. Effector cells such as macrophages, T cells and B lymphocytes are activated by these cytokines. When these inflammatory cells are recruited to ECs and towards the whole vessel wall layers, vasculitis is induced.

1.3.1.2 Humoral Immune Response

Humoral immune response also contributes in CAV formation. Under inflammatory molecules regulation, B lymphocytes and monocytes are activated in response to HLA molecules. Activated B lymphocytes secrete specific antibodies which bind to donor antigens. These antibodies are recognized by phagocyte or complement system, both of which exert damage to the allograft tissues. Clinical studies have confirmed that HLA-specific antibodies expression[16] and complement activity[17] are increased within

the neointima, which correlated with poor result of transplantation. After transplantation, B cell receptor binds with the antigen activating intracellular endocytosis and presenting the antigen on the surface of a MHC II molecule. T helper (T_H) cells activate B cells to differentiate into plasma B cells or memory B cells. Plasma B cells are responsible for antibody production, whereas memory B cells are inactive and trigger rapid production of antibodies when exposed to a previously recognised epitode. Antibodies belong to the glycoproteins immunoglobulin superfamily. All antibodies are Y shaped proteins, which consist of two heavy chains and two light chains giving antigen binding domains. The domains on the chain determine function of antibodies. Fragment crystallisable (Fc) region in heavy chain is constant and defines the isotype of antibodies, which include IgA, IgD, IgE, IgG and IgM. When binding with respective specific Fc receptor (FcR) on antigen, these antibodies exert distinct effects. All isotype of antibodies have their specific complex structure. For example, IgD/E/G are monomer, whereas IgA is a dimer and IgM is one pentamer. Fragment antigen-binding (Fab) is the region consisting of part of heavy chain and the whole light chain. Variable domain in heavy chain (V_H) and light chain (V_L) are located in the Fab region, and variety in this domain is because of the hypervariable region (HVR) or complementarity determining region (CDR). Three genes are located on HVR/CDR and variety of variable domain relies on V (D) J recombination. With specific differences in domain structure, antibodies recognize targeted antigen. Subsequently, antibodies can be recognized by monocytes. Under cytokines stimulation, monocytes transform into macrophages, and phagocytose targeted cells. Alternatively, complement system is activated and recruited. Complement system is part of the immune system, involved in innate and adaptive immune process. Complement system is composed of several plasma proteins, which are produced from the liver. Once triggered, they would recruit phagocytes or form cell killing membrane attack complex. Three signalling pathways including classic complement pathway, alternative complement pathway and lectin pathway consist of the complement system.

1.3.1.3 Innate Immune Response

The Innate immune system is an evolutionarily preserved defence system, which recognises and eliminates exogenous antigen. Damage associated molecular patterns (PAMPs), refers to exogenous antigen. When PAMPs on microbes bind with pattern recognition receptors (PRRs) on host innate inflammatory cells, inflammation

is triggered. Classic PRRs include mannose receptors, scavenger receptors and Toll like receptors. For example, toll-like receptors induce mononuclear cell activation which occurs in organ transplantation[18]. Inflammatory cells such as monocyte/macrophage, mast cells, phagocyte, granulocytes, dendritic cells and natural killer (NK) cells are involved in the innate immune system. When immunoreaction persists within the graft tissue, fibrosis follows under the influence of cytokines and as a consequence thickens the neointima[19]. IFN-γ and TGF-β can activate macrophages to infiltrate into the neointima, and propagate lesion size by tissue remodelling and matrix deposition[20].

1.3.1.4 Donor Derived Immune Response

In addition to recipient immunoreaction, donor grafts also provide immune cells contributing to CAV process. After transplantation, donor immune cells migrate into recipient lymph nodes and present antigens. In fact, by transplanting transgenic heart to wild type (WT) animals, donor dendritic cells can be detected within 3h, which probably initiate recipient T cells activation[21]. Meanwhile, donor lymphocytes activity was also be detected after transplantation. It was shown that after transplantation, donor $CD4^+$ T cells were activated as a response to MHC class II on recipient B cells[22]. When $CD4^+$ T cells from donor graft were depleted, autoimmune antibodies decreased. Furthermore, ligands expressed on donor graft are also related to lesion formation. Programmed death-ligand 1(PDL1) is a ligand, which transmits an inhibitory signal reducing T cells proliferation. Data was shown that PDL1 expression on donor grafts inhibited allograft rejection by modulating T cells activation[23]. However, selectin molecules from donor cells can accelerate neointima formation via binding and recruiting leucocytes[24].

1.3.2 Allograft Transplantation Mouse Model

Rodent models in allotransplantation provide deep understanding of underlying mechanisms and potential therapeutic approaches[25]. Heterogenic heart transplantation mouse model was established since 1973[26]. This surgery involved the transplantation of heart graft to a recipient mouse. This important model provides researchers the opportunities to further study alloreactivity, although in the expense of a challenging microsurgery technique. When the graft is transplanted into immunocompetent recipients, acute rejection occurs because of MHC molecules

mismatch. MHC molecules can be divided into class I and class II groups, which are recognized by CD8 and CD4 T cells, respectively. CD4 and CD8 reactions vary in different organ grafts. Histocompatibility is decided by specific MHC in each strain. MHC haplotype in C57BL/6J and BALB/c mice are $H2^b$ and $H2^d$, respectively. This is the basis why these two strains are commonly used in allo-transplantation mouse models. For example, it was shown that when transplanting a C57BL/6J ($H2^b$) kidney to a BALB/c ($H2^d$) mouse or vice versa, allo-graft rejection occurs at a post-transplantation level[27]. Within the MHC mutant animals, allo-immune reaction would also develop. B6.H-2^{bm12} is a spontaneous mutation within the β-chain on class II MHC molecules[28]. When a heart from a B6.H-2^{bm12} mouse was transplanted to a C57BL/6J ($H2^b$) mouse, CAV developed demonstrating the involvement of CD4 T cells. Besides of cellular immunity, humoral immune rejection activities are also prevalent in allo-transplantation. It was shown that, when transplanting serum antibodies to $RAG1^{-/-}$ mice, acute rejection can be induced[29]. Recombination-activating genes (RAGs) encode enzymes which are important in the rearrangement and recombination of antibodies and T cell receptors via manipulating V (D) J recombination. T cell receptor (TCR) recognizes MHC molecules. Similar to antibodies, diversity of TCR relies on V (D) J recombination. Therefore, in $RAG1^{-/-}$ mice, both mature T cells and B cells mediated antibodies cannot be produced[30]. In previous study, data showed that although adaptive system is damaged in $RAG1^{-/-}$ mice, CAV could still occurs because of NK cells involvement[31]. Using the same $RAG1^{-/-}$ mice, and transferring donor alloantibodies, C4d was found deposited in graft artery. Because C4d is a protein which is involved in classic complement system pathway, this result indicated that complement system also contributed to allo-immuno reaction after transplantation.

To simplify the disease model and directly visualize vascular processing pathology, a vascular allograft accelerated arteriosclerosis mouse model was developed. Currently, three different types of surgery are mainly used to recapitulate this animal model. The first artery allograft transplantation was established in 1994, in which donor vessel grafts from B.10A (2R) (H-2^{h2}) were transplanted to carotid arteries of recipient C57BL/6J (H-2^b) mice via side-to-end suture[32]. Another artery allograft transplantation was performed by transplanting 1cm donor thoracic aorta to recipient infrarenal aorta by end-to-end anastomosis[33]. In 2000, our previous laboratory group work developed a simple and effective vascular graft allo-transplantation mouse model[34]. With the

assistance of a cuff similar to vein graft transplantation surgery[35], a segment of artery graft from C57BL/6J (H-2^b) mice was transplanted to BALB/c (H-2^d) by end-to-end connection[34]. With these artery allo-graft transplantation mouse models, the functions of these molecules in this disease can be further understood. For example, intracellular adhesion molecular (ICAM) is one glycoprotein, which is located on the surface of ECs and inflammatory cells. ICAM plays a important role in developing vasculitis by recruiting leucocyte infiltrating into vessel wall. When donor graft derives from $ICAM^{-/-}$ mice is allotransplanted, arteriosclerosis lesion can be analysed with the mice expressing ICAM. IFN-γ is another cytokine regulating T cells proliferation and macrophage accumulation in the neointima. When IFN-γ gene was knocked out, recipient mice would not develop severe lesion after allograft transplantation[36]. In addition, it was shown that IFN-γ could also upregulate MHC and adhesion molecules on circulating cells as well as vessel wall. This may provide us with an insight in the role of IFN-γ in this immune incompatible mouse model[37].

Mouse models do not successfully recapitulate clinically relevant transplantation pathology. Anatomical and utilisation of surgery procedures are different in both settings. Transplantation surgeries in mice do not involve immunosuppressive drugs to prevent acute graft rejection and this is one major difference compared with current clinical transplantation. Differences between animal models and the clinic must be safely addressed cautiously and in strict compliance with laws and regulations.

1.3.3 ECs Dysfunction

ECs dysfunction is a hallmark of vascular disease. ECs are the first target of the immune system after organ transplantation. EC rejection by inflammatory cells results in ECs dysfunction, which is characterised by increased permeability and inflammatory cell accumulation. After antigen molecules on ECs are recognized by immune cells, they are directly attacked either by cytotoxic or by inflammatory cell secreted cytokines, such as IL-2, IFN-γ and TNF-α. Adhesion molecules expression such as VCAM and ICAM, is increased within ECs leading to recruitment of inflammatory leucocytes. Recruited inflammatory cells further exacerbate EC dysfunction by increasing vascular permeability. These immune cells may secrete cytokines such as PDGF and TGF-β, both of which stimulate SMCs proliferation and ECMs accumulation in the intima layers. As a consequence of ECs dysfunction, clotting molecules, platelet, lipid and ECMs

accumulation within the intima layer may develop and potentially encourage intimal hyperplasia. When this process develops, apoptosis of ECs may be observed.

1.3.4 Endothelial Stem/Progenitor Cells (ESPCs)

When ECs within the donor graft become dysfunctional or are eliminated in response to immune activation, host cells may integrate into the ECs layer either for repair or further impairment. Although its function is still under debate, re-endothelialisation in CAV lesion by recipient cells has been confirmed in a number of studies. Endothelial stem/progenitor cells (ESPCs) are able to proliferate and differentiate into ECs. However, there is no clear consensus on the precise definition of these cells. To prevent any confusion in this thesis, ESPCs from bone marrow source mentioned below are referred as endothelial progenitor cells (EPCs) whereas endothelial progenitors (EPs) mean the resident ESPCs distributed at the several locations (for example, vessel wall, spleen, liver, heart and lung).

1.3.4.1 Endothelial Cells (ECs) Differentiation

ECs are identified by their specific markers such as CD31, tie-2, vWF, VE-cadherin, VEGFR, and endothelial nitric oxide synthase (e-NOS). Up-regulation of ECs gene expression relies on promoter activation. The ETS domain is one gene containing 3 α-helices and 4 β-sheets interacting with a core sequence of 5′-GGA(A/T)-3′ being identified in nearly all ECs related gene promoters[38]. ETS family proteins are important transcription factors binding with the ETS domain. Classic ETS family proteins are identified based on similar conserved domains and the most important is the pointed domain which functions by binding with the ETS domain third α-helices [38]. To date, 19 ETS family proteins have been identified within human ECs. Amongst all of them, ETS1/2 are the most important transcription factors and relatively well-established in ECs differentiation. ETS1 is composed of 440/441 amino acids within the pointed domain from the N-terminal towards to acidic transactivation domain. The ETS binding domain is flanked by two auto-inhibitory domains. ETS proteins were reported to consist of several isoforms when undergoing alternative splicing. On gene level, ETS1 and ETS2 loci are located in the same chromosome with FLI1 and ERG, respectively, in head to head orientation[39]. ETS1/2 are expressed in ECs for endothelial tube formation. Under angiogenesis stimuli such as hypoxia and inflammation exist, their expression are increased. ERG and Fli1 as another two ETS family proteins are

responsible for vascular integrity. However, the elimination of these two transcript factors does not necessarily result in ECs death indicating their roles can be compensated by other ETS family proteins. ETS family transcript factors such as ETV6, ELK3, and ETV2 are also involved in vascular integrity via ECs differentiation. Several mechanisms have been identified in the regulation of ETS family transcript factors Post-genetic modification such as phosphorylation, acetylation, ubiquitination and sumoylation are responsible for ECs gene expression. Alternatively, by binding with other transcript stimulators such as FoxC2 and klf2, ECs gene expression can be regulated. Although, a large profile of transcript factors have been associated with ETS family proteins, the precise effect is unclear. Homo-dimerization or polymerization may control the activity of ETS family proteins. Other transcript factors such as SCL, GATA, Fox and klf transcription factors have been shown to be related to ECs gene expression.

1.3.4.2 ESPCs Identification

Since the first time that the CD34 and VEGFR2 double positive cells showed potential to proliferate and differentiate into the mature EC-shaped cells expressing ECs markers such as CD31, E-selectin and eNOS, several methods have been suggested to identify putative ESPCs[40]. It was proposed that uptake of acetylated-low density lipoprotein (ac-LDL), binding with ulex europaeus agglutinin-1 (UEA-1) and differentiation potential to cells expressing ECs markers are specific characters of ESPCs[40]. However later on, large amount of studies suggest that this method alone is far from sufficient to define ESPCs, since the potential described above is shared amongst other cell types. Therefore, ESPCs were later identified by another *in vitro* method termed colony-forming assay. After one-week culture on fibronectin-coated dishes, adhering central rounded cells surrounded by thin flat cells can be observed. After selecting with specific ECs markers, targeted cells are nominated as the colony forming unit-Hill (CFU-Hill) ESPCs[41]. However it was again refuted by the fact that hematopoietic monocyte and/or immune cells could mimic CFU-Hill ESPCs[42, 43]. With the addition of failure to form new blood vessel and the slow rate of proliferation *in vivo*, these captured CFU-Hill cells were suggested to resemble hematopoietic lineage cells. Another population termed endothelial colony-forming cells (ECFCs) were recommended within an alternative EC/PCs colony forming assay[44, 45]. Under this method, the peripheral cells were cultured on collagen I coated plate with suitable

culture medium. After not more than 3 weeks, adhering cells expressing ECs markers were suggested to mimic ECFCs. In fact, ECFCs in this method were shown forming heterogeneous populations with hierarchy proliferating potential *in vitro*. More importantly, ECFCs were able to generate novel capillary like ECs in both *in vitro* and *in vivo.* This indicates that ECFCs are a sub-population of real ESPCs. To date, proposed ESPCs in most studies are identified by various stem/progenitor markers such as CD34, c-kit, and CD133 with/without some ECs markers such as CD105, CD106, CD144, VEGFR 1/2 and TIE2, although none of marker patterns have been shown exclusively in ESPCs.

1.3.4.3 Circulating Endothelial Progenitor Cells (EPCs)

Bone marrow was the first proposed to harbour ESPCs or EPCs. It has been demonstrated that in bone marrow niche, EPCs homeostasis is under regulation of several cytokines (such as VEGF, Ang-1, SDF-1 and SCF). These cytokines are known to be secreted by surrounding cells such as pericytes and ECs. Once these secreted cytokines bind to their corresponding receptors (for example, VEGFR, TIE-2, CXCR4, c-kit and Notch) respectively, EPCs begin to migrate, proliferate or differentiate following its related signalling pathway. In disease states such as hypoxia, induced hypoxia-inducible factor-1 (HIF-1) increases expression of VEGF along with Ang-1 within the bone marrow microenvironment[46]. When stromal cells sense the change of VEGF concentration, eNOS are phosphorylated via the VEGFR/Akt-dependent signalling pathway[47]. With the mechanism of S-nitrosylation, MMP9 is activated[48]. Then increased level of MMP9 rapidly alters quiescent bone marrow niche by cleaving membrane bounded SCF on stromal cells into soluble form. Soluble SCF could mobilize c-kit$^+$ EPCs from the bone marrow and into the circulation[49]. SDF belongs to the chemokines family. Under hypoxia, SDF along with its corresponding receptor CXCR4 is upregulated within stromal cells[50]. AMD3100 is a mobilizing agent which acts as an antagonist of CXCR4. Reversible blocking of SDF/CXCR4 binding in the bone marrow by AMD3100 mobilized EPCs[51]. In addition, family of integrins is also involved in EPCs mobilization. Data was shown that α4-integrin is an important molecule to mediate EPCs adhesion. Disruption between α4-integrin and fibronectin results in EPCs mobilization and thereafter increases ischemic neovascularization[52].

1.3.4.4 Resident Endothelial Progenitors (EPs)

Recent studies showed that the circulating or bone marrow derived EPCs cannot explain all the new vessel formation in the vessel wall[53]. In fact, apart from bone marrow cells, non-bone marrow cell sources (such as vessel wall, muscle, adipose tissue, dermis, intestine and liver) of EPs are recently reported to distribute in local tissues. Among all of these vascular tissues, vessel wall is one rational organ to harbour EPs. According to definition, resident EPs are cluster of local cells with potential to proliferate and differentiate into ECs. In fact, several population of EPs have been identified within vessel wall. For example, EPs were isolated from both human umbilical vein endothelial cells (HUVECs) and human aortic endothelial cells (HAECs)[53]. When cultured *in vitro*, these EPs showed potential to generate multiple ECs colonies including ECFC with both high and low proliferating potential, similar to umbilical cord blood derived ESPCs. Side population of c-kit^{+} cells within endothelial layer were also demonstrated to be able to generate functional vessel[54]. Elimination of c-kit impaired function within these EPs such as proliferating and vasculogenesis potential, which cannot be rescued by wild type bone marrow transplantation. Peripheral vascular endothelium is also reported to harbour one side population of EPs, characterized by Hoechst dye efflux ability in CD31^{+}CD45^{-} EC fraction[55]. Although these EPs showed similar surface marker to conventional ECs, the gene hierarchy within them is completely diverse. It was suggested that this population of EPs is quiescent but possesses self-expanding and colonies forming potential *in vitro*. When these cells were transplanted to ischemia mice, they showed potential to form *de novo* vessel. In addition to endothelium, a distinct niche namely the vasculogenesis zone locates between the media and adventitia layer was also reported. It was reported in this region, one population of EPs exist, with a high expression of CD34 along with VEGFR2 and TIE2 but not CD31 and CD45[56]. These EPs have the potential to generate *de novo* functional vessel verified by sprouting and capillary-formation assays. In fact, all three mural layers within coronary arteries were reported to harbour proliferating c-kit^{+}VEGFR2^{+}EPs which connect with other supporting cells[57]. Once these EPs are cultured and injected in a stenosis induced immunosuppressed dogs, they generate vasculogenesis in all large, medium and small vessels forming complete human coronary arteries. But still, caution is never non-necessary similar to However, it needs to be taken into account for EPCs identification from bone marrow, since niche mentioned are not excluded from other pro-angiogenic cells (for example, HS/PCs,

fibroblast, mesenchymal stem cells (MSCs) and pericytes), all of which also have a self-renew feature. Along with other factors including growth factors, laminal flow, hypoxia and oxidized stress, EPs are proposed to be stimulated by secreted paracrine factors from pro-angiogenic vascular cells to adjust from a quiescent state and transfer into a proliferation state along with migration to injury site, similar to bone marrow derived EPCs.

Figure 1.3.4.4

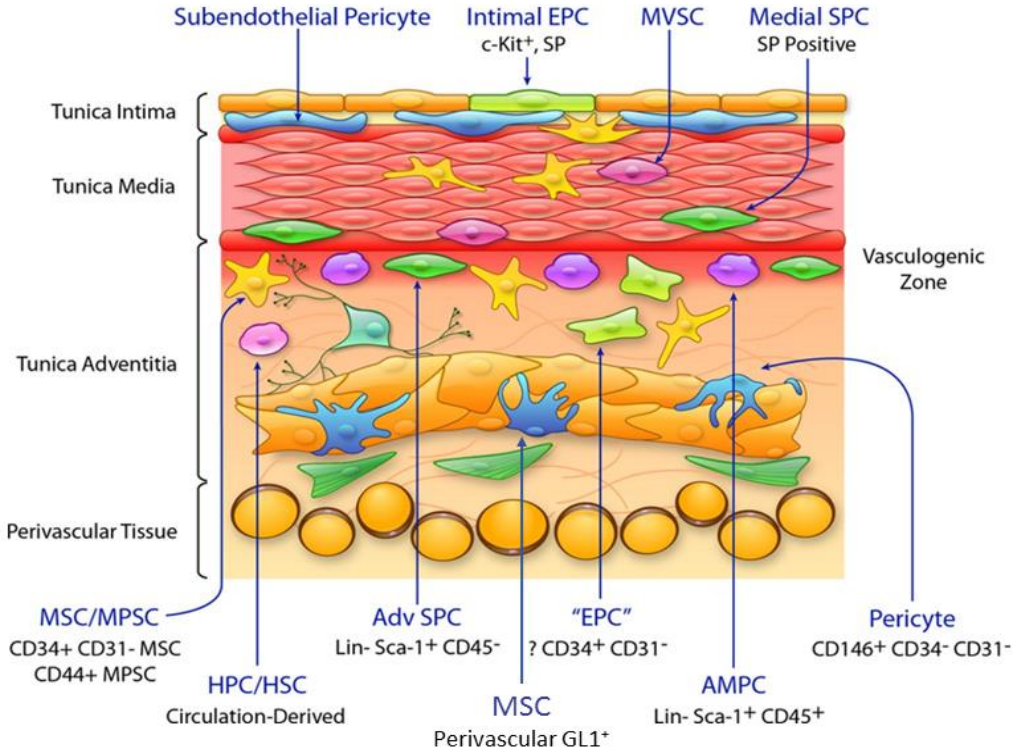

Figure 1.3.4.4 Vascular wall resident Stem/Progenitor cells (SPCs). SPCs are distributed across all of three vessel walls. EPs mainly locate in the intima and vasculogenesis zone. In media layer, MSCs are detected along with side population of progenitor cells. Adventitia harbour most abundant populations of SPCs, including adventitia SPCs, EPs, HSCs, MSCs and perivascular SPCs. All of these populations of SPCs can be recruited under vascular signals. SPCs, stem/progenitor cells; EPs, endothelial progenitor cells; MSCs, mesenchymal stem cells; HSCs, hematopoietic stem cells; AMPCs, adventitial macrophage progenitor cells. (Figure Source: Psaltis PJ, Simari RD. Vascular wall progenitor cells in health and disease. Circulation research[58].)

The lung and heart were also reported to harbour resident EPs. It was found that the lung tissue possesses a pool of c-kit$^+$ cells located in bronchioles as well as alveolar wall niche[59]. Expression of NANOG, OCT3/4, SOX2, and Kruppel-like factor 4 (Klf4) indicate multipotent potential within these adult c-kit$^+$ human lung stem cells. In fact, it was shown that these cells are self-renewing, clonogenic, and multipotent involved in lung homeostasis[59]. However, debate exists concerning the role of c-kit$^+$ cells during lung homeostasis or in the other words, the terminal fate of this population of cells. It was initially reported c-kit$^+$ cells could repopulate SMCs and/or epithelial cells[59]. This was however later disproved by one study, to show that these c-kit$^+$ pulmonary progenitor population cells were actually EPs acquiring endothelial lineage but not SMCs or epithelial cell lineage[60]. This was verified by another lineage tracing study. This study showed that in c-kit$^{kit/CreER}$; ROSA26-RFP, RFP (because of c-kit promotor induced Cre recombination activation) was only expressed in lung vascular endothelial but not epithelial cells[61]. Within the heart chamber, c-kit$^+$ SPCs with potential to differentiate into terminal non-hematopoietic cells, were thought derived from bone marrow and involved in *de novo* cardiomyocyte formation[62]. However, subsequent studies denied this phenomenon and found that bone marrow source of c-kit$^+$Lin$^-$ HSCs showed no ability to differentiate into cardiomyocyte[63] . Delivery of bone marrow derived c-kit$^+$ cells did not increase the left ventricle function[64]. Although c-kit$^+$ cells do contribute to *de novo* cardiomyocytes, the percentage is only approximately 0.03 in both growing and adult mouse heart. Considering cellular fusion, the percentage could fall to below approximately 0.008[65]. Afterwards these c-kit$^+$ cells were shown to guide mainly ESPCs towards an endothelial fate when using a lineage tracing method[65]. However, it is worthy to point out that whether these c-kit$^+$ cells acquiring ECs fate are indeed EPs or pre-existing ECs still need further investigation to determine.

1.3.4.5 Source of ESPCs in Allograft Vasculopathy

It is vital to identify the source of ESPCs in AV. It was speculated that after ECs damage, donor derived cells would be activated, and this could contribute to ECs regeneration. However, this was challenged by other studies claiming that lost ECs can be replaced by recipient source of cells. In one study from our lab it was shown that after vascular allograft transplantation, all ECs in donor graft were absent due to apoptosis or necrosis within 4 weeks[66]. Meanwhile, recipient source of circulating

ESPCs would be activated to regenerate damaged endothelium and generate microvessel neo-vasculogenesis. The intermediate situation is also reported, in which both donor and recipient source of cells contribute to mixture of ESPCs and involve in ECs regeneration[67]. An explanation of this disparate phenomenon is because of different model or treatment used. For example, although similar in some aspects, the whole immune system is not the same between the mouse and human. Therefore, after allo-transplantation, severity of immune reaction can be distinct between animal models and human tissue, which could partly explain the different results generated from various groups. In other words, severity of donor graft injury could possibly decide whether they still preserve enough potential to involve in ECs regeneration. Afterwards, it is also important to clarify the source of recipient ESPCs. It was shown that approximately 30% of regenerated ECs derive from bone marrow in mouse[66], whereas in rat only few bone marrow cells contribute to ECs regeneration[68]. These disparity results may be due to differences within species and technique used. Another important issue to address is whether ESPCs from other sources such as vessel wall, adipose tissue or spleen are involved in AV and if so, the precise mechanisms involved need to be clarified.

1.3.4.6 ESPCs Regeneration in Allograft Vasculopathy

After allo-immune reaction induced ECs dysfunction, damaged ECs and inflammatory cells release chemokines in a autocrine and paracrine fashion within the graft vessel wall. Chemokine attraction, mobilises and homes ESPCs to graft vessel. After aortic transplantation in mice, SDF-1 is upregulated within the graft recruiting $CXCR4^+$ stem cells towards the neointima[69]. Meanwhile, when interacting with adhesion molecules expressed on graft endothelium, ESPCs could adhere to the vessel. ECs dysfunction would also lead to ECMs exposure and subsequently platelet adhesion, both of which facilitate ESPCs adhesion. During ESPCs migrating and homing process, ESPCs to ECs commitment can develop occur simultaneously. Although evidence of ESPCs to ECs differentiation is lacking in CAV, studies on this process are many in other animal models. So far, literature describes ECMs, SDF, VEGF and sheer stress as main contributors of EC commitment from ESPCs. ESPCs to ECs commitment is under the governance of transcription factors, partly played by histone deacetylases (HDACs). HDACs mediated histone deacetylation is a process in which acetyl is removed from the N-terminal lysine residues on acetylated histones, altering chromosome structure

and enabling the access of transcript factors to DNA and initiating differentiation of SPCs. HDACs involvement in ESPCs differentiation to ECs can stem from the inhibition of HDACs and the downregulation of ECs markers and in turn can be rescued by Hox-A9 overexpression[70]. HDAC-3 was specifically reported to induce sca-1^+ embryonic stem cells to differentiate into ECs and accelerate re-endothelialisation of injured arteries. Other HDACs such as HDAC-1, 2,4,7,8 were also suggested for ECs differentiation. However, the precise mechanisms are unestablished as deacetylation and the result of enhanced EC markers could be the result of other HDACs including HDAC3 and possibly not from a master enzyme regulator[71]. Another important regulator among ECs differentiation are microRNAs. Various microRNAs including microRNA – 10, 16, 18a/b, 31, 99b, 107, 126, 148b, 150, 155, 214, 221, 349, 484, 513, 574-3p, let7 are highly expressed within ESPCs[72]. During ESPCs differentiation process, certain microRNAs are upregulated and subsequently targeting specific genes to enhance ECs commitment. For example, microRNA-21 was shown to be involved in ECs differentiation[73]. Besides of promoting ESPCs differentiation, microRNAs also conversely inhibit this process. It was shown that microRNA-107 inhibit EPCs differentiation by decreasing HIF-1β expression[74].

1.3.5 SMCs Phenotype Change in Allograft Vasculopathy

Smooth muscle cells (SMCs) provide the main structure in media layer of vessel wall. Several markers including α-smooth muscle actin (α-SMA), smooth muscle myosin heavy chain (SMMHC), calponin and SM-22 are currently used to identify SMCs. Traditionally SMCs are divided into two sub-types: quiescent/contractile and proliferative. Normally mature SMCs are restricted in the media layer regulating the physical vessel tone via constriction. However, in an injured environment with the presence of inflammatory mediators and allo-transplantation, SMCs undergo proliferation and ECM secretion within the intima. During persist stimuli, media quiescent SMCs undergo phenotype alteration losing their contractile property and acquiring dedifferentiating SMCs characters. These dedifferentiated SMCs usually contribute to AV plaque formation and narrow the vascular lumen. Data showed that AV can be alleviated when SMCs proliferation inhibitor such as sirolimus is used[75]. When AV further develops, apoptosis of SMCs can be observed and propagate lesion instability. Plague can disintegrate from the wall and block passage of blood flow leading to an acute cardiovascular syndrome. It was thought that SMCs only form

during embryo stage and SMCs development ceases during postnatal stage[76]. However, it was later found that smooth muscle stem/progenitor cells (SMPCs) are one important source of SMCs in adult[77].

1.3.5.1 SMCs Differentiation

During embryonic stage, SMCs are derived from the neural crest, proepicardium, mesothelium, secondary heart field, somites, mesoangioblast, pericytes and SPCs. The question of how such various origin integrate into one communal cell type is still unknown. But at least in recent decades, one transcript factor serum response factor (SRF) along with its coactivator myocardin families have been an integral part of SMCs regulation. The enhancer element proximal to oncogene c-fos promoter[78] and sarcomeric-restricted genes[79] (such as skeletal α-actin, α- myosin heavy chain, cardiac and skeletal myosin light chain 2, and cardiac troponin T), serum-response element (SRE) was identified as one CCArGG box or CArG box element responsible for target gene regulation. Structure of CArG box located within 2-3kb distant to promoters in various SMCs restricted genes[80]. Later, gene encoding SRE binding protein was cloned, identified and named as serum SRF[81]. According to its structure, SRF belongs to transcript factor within MADS box family. This consist of one N-terminal structure binding with DNA and/or protein along with one C-terminal phosphorylation sites that recruit SRF-associated factors. SMCs differentiation under SRF has been addressed by several mechanisms including increasing SRF expression, modulating affinity between SRF and SRE, SRF alternative splicing, chromatin-associated accessibility of SRF to CArG box and multiple complex assembly. Myocardin family mainly including myocardin[82] and myocardin related transcription factor-A/B (MRTF-A/B)[83] was found to be important cofactors of SRF but not directly binding to target DNA. Structural analysis of the myocardin family revealed that the N-terminal begins with RPEL motifs which is related to G-actin binding. This binding domain functions by interacting with smad1 and SRF. The SAP domain is related to chromosome function and the coiled-coil motif stabilises leucine zipper of protein on binding with SRF. C-terminal region ends with the transcription activation domains (TADs) and is known to activate MRTF-A/B. Myocardin exerts its effect on several SMCs genes including α-SMA, SMMHC, calponin, SM-22, and SM myosin light chain kinase (MLCK) by binding with SRF to regulate cell differentiation. Binding with smad3, myocardin initiates interaction between smad3/ smad-binding elements

(SBE) and this effectively increases SMCs gene expression[84]. Activation of myocardin can also be upregulated via binding between transcript factors coactivators such as SRC3 and GATA4. Conversely, several mechanisms are related to myocardin activation inhibition. For example, interaction with repressors such as Foxo4, SOX9, HRT-2 and uPAR caused inhibition of myocardin. On the other hand, ability of myocardin binding to SRF can be inhibited by competing proteins such as Runx2, TDG, HERP1and GATA factors. MRTF A/B can be retained outside the nucleus by binding with actin monomers and this prevent MRTF A/B from translocating into the nucleus exerting functions[85]. In addition, binding between SRF/myocardin complex and DNA could be inhibited by several transcript factors including Msx transcription factors (Msx1 and Msx2), Yap1, and the Klf4. In fact, transcript factors such as SRF, NKX2.5, Smad3, Mef2, Foxo and TEAD are all related to SRF/myocardin complex binding. Last, post-translocation modification such as phosphorylation, acetylation/de acetylation and/or ubiquitination is also related to myocardin expression.

1.3.6 Smooth Muscle Progenitor Cells (SMPCs)

Recently, data has shown that smooth muscle progenitor cells (SMPCs) are preserved until postnatal stage in both physiologic and pathologic processes. The source of SMPCs is highly debated. Bone marrow derived HSCs were thought as one source of SMPCs from circulation involved in SMCs differentiation[86]. Several population of SMPCs are identified in all three layers within vessel wall. One population of SMPCs with the markers such as sca-1, c-kit, CD34 along with VEGFR2, was firstly found harbouring within adventitia of vascular wall[87]. This was confirmed by later study that sca-$1^{+}$$CD34^{+}$ SMPCs expressed on adventitia are under regulation of a sonic hedgehog (Shh) signalling[88]. Recently, another population of $CD146^{+}$ SMPCs were identified within the adventitia from embryonic to postnatal stage[89]. Lineage tracing study revealed that transcript factor $Gli1^{+}$ SMPCs could proliferate and differentiate into SMCs, contributing to neointima formation after vascular injury[90]. Apart from adventitia, media layer was also demonstrated to harbour SMPCs. It was reported that one side population of SMPCs with sca-1^{+}c-kit $^{-/low}$CD34 $^{-/low}$$lin^{-}$ profile are among mature SMCs. Once cultured with TGFβ or PDGF, they differentiate into SMCs[91]. Then nearly at the same time, another study draw one bold and shocking conclusion that it was not mature SMCs but $SMMHC^{-}$ multipotent vascular stem cells give rise to SMCs during vascular disease[92]. While later this conclusion was proven not convincing

enough because of the issues such as unspecific lineage model, lacking of z-stack microscope use as well as incorrect media isolation protocol[93], this study provide one potential substitute candidate for SMCs differentiation. When existing SMCs is severely injured, SMPCs could repopulate *de novo* SMCs. Later it was shown that a population of sox10^{+} multipotent vascular stem cells possess SMCs differentiation potential[94]. Even further, more recent study showed that subpopulation of SMMHC $^{+}$ cells are capable of dedifferentiating into SMPCs with induction of stem/progenitor transcript factor klf4[95]. This enhances the potential of SMPCs to migrate and differentiate into several type of cells including ECs, SMCs and hematopoietic lineage cells. The endothelium is also able to induce SMCs transdifferentiating via mechanism of endothelial to mesenchymal transition (endMT) although the rate is only 0.01% to 0.03%[96].

1.3.6.1 SMPCs in Allograft Vasculopathy

From traditional point of view that SMCs from intima or media layer undergoing phenotype change during AV lesion formation it is easy to draw the conclusion that SMCs are all from donor source. However, various studies showed that it is not the case. Similar to ESPCs origin in AV, origin of SMCs varies in different studies. A study showed that SMCs in CAV is donor origin[97]. However, in mouse aorta allograft transplantation model the result showed that SMCs are of recipient origin[98]. Also chimeric population source of cells including both donor and recipient origin is reported[67]. Therefore, percentage of donor and recipient origin possibly also depends on lesion development stage (Figure 1.3.6.1). Furthermore, source of recipient SMPCs in AV is also debated. It was demonstrated that after cardiac transplantation, more than 80% of host SMPCs derive from bone marrow[86]. However, our group draw an opposite conclusion that bone marrow source of SMPCs were not involved in vascular allograft lesion formation. A possible reason to explain this discrepancy is whether high-resolution microscope was used in the study. Low resolution microscope could possibly not distinguish two markers being from one cell or two adjacent cells.

Figure 1.3.6.1

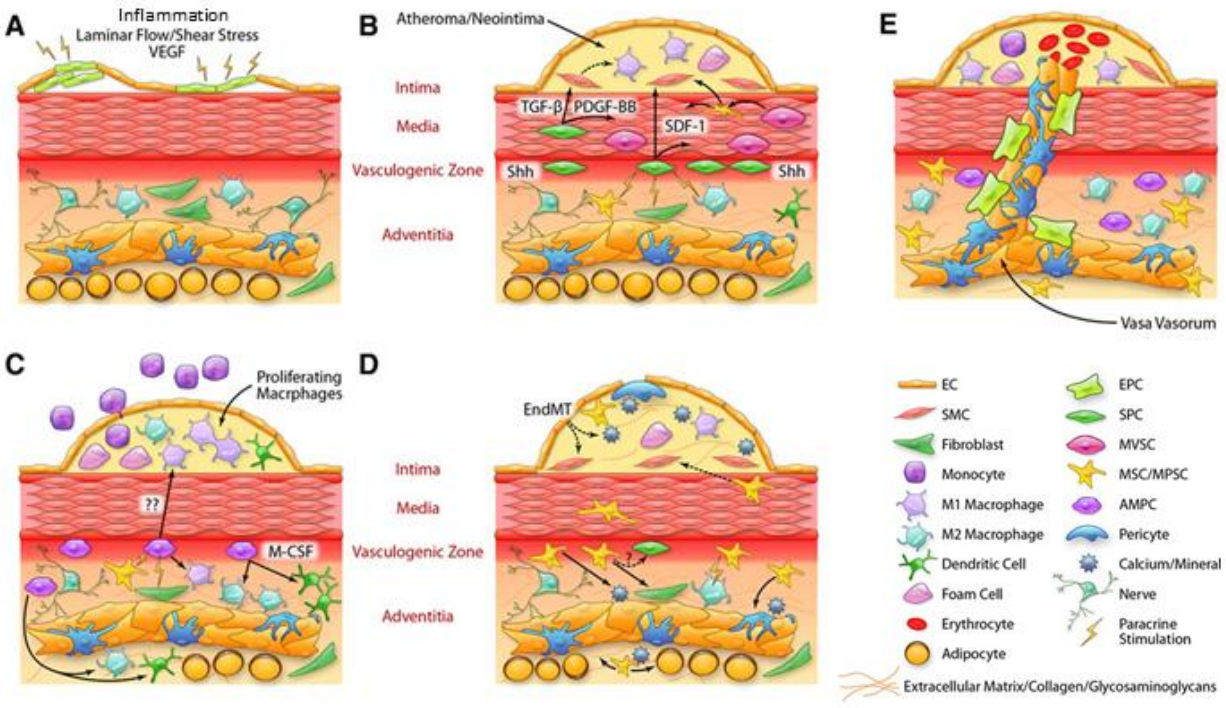

Figure 1.3.6.1 Proposed role of SPCs in allograft vasculopathy. A. ESPCs replace injured ECs after intima injury. **B.** SPCs from various sources along with/without phenotype changed SMCs are recruited under cytokines such as SDF-1 and VEGF. Under TGF-β and PDGF stimulation, SPCs differentiate into SMCs contributing to neointima formation. **C.** During lesion formation process, macrophage or HSCs are also recruited and serve as inflammatory cells formation. **D.** Pericytes and EndMT are also involved in atherosclerosis progress. **E.** Vasa vasorum and vessel remodelling are enriched in graft vessel. SPCs, stem/progenitor cells; AV, allograft vasculopothy; ESPCs, endothelial stem/progenitor cells; SDF-1, stromal derived factor-1; VEGF, vascular endothelial growth factor; TGF-β, transforming growth factor-β; PDGF, platelet derived growth factor; HSCs, hematopoietic stem cells; EndMT, endothelial to mesenchymal transformation. (Figure Source: Psaltis PJ, Simari RD. Vascular wall progenitor cells in health and disease. Circulation research[58].)

1.3.6.2 SMPCs Maintenance and Modulation in Allograft Vasculopathy

In vivo, SMPCs reside in the vascular niche, which refers to the microenvironment for stem cells to maintain their homeostasis. Once vascular injury is induced such as allo-immune attack in graft, these cells are mobilized under the stimulation of circulating cytokines. Afterwards, relying on cytokines and ECMs, SMPCs home to injured graft. In response to persistent stimulation from cytokines, ECMs and sheer stress, they acquire terminal cells fate. Within adventitial layer, phenotypic maintenance of SMPCs are under control of sonic hedgehog (SHH) signalling pathway. This is demonstrated by the fact that decreased number of adventitial SMPCs within aortic root was achieved, because of SHH knockout[88]. This study also showed that the mechanism in SHH signalling silencing SMCs differentiation is through decrease expression of SRF/myocardin, and overexpression of their related repressors including klf4, msx1 and foxo4. Similar to mature SMCs, SMPCs were shown cable of migrating when local injury occurs. It was shown that in response to vascular injury, chemokines such as CCL1/2/5 are highly expressed within SMCs culture medium. When CCL1/2 activates CXCR2 on the surface of cells, SMPCs are recruited through via Rac1/p38 signalling[99]. Alternatively, data was shown that SMPCs would migrate in response to SDF[100] and leptin[101] via mechanism of increasing cell chemotaxis and/or cell cytoskeleton regulation. During and/or after SMPCs homing to injured tissue, SMPCs to SMCs differentiation begins. Several signalling pathways regulate SMCs differentiation. Firstly, a mechanism called actin treadmilling is a classic cellular process. During this process, F-actin polymerization derived from G-actin results in unbound of MRTF-A/B with G-actin. Then unbounded MRTF-A/B transfer from the cytoplasm to the nucleus to bind with SRF to induce SMCs gene expression[102]. Epigenetic modification is another pivotal mechanism regulating SMCs differentiation. For example, it was reported that spliced HDAC-7 could enhance SRF/myocardin complex binding with targeted SMCs promoter genes[103] , whereas at the same time HAT-p300 could increase myocardin expression, both for SMCs differentiation. Extracellular matrix can also promote SMPCs differentiation. It was reported that under the collagen IV induction, sca-1^+ SMPCs underwent SMCs differentiation which can be abrogated by integrin α_1, β_1, and α_v inhibitors[104]. MicroRNAs are also shown as potential players for specific genes to induce SMPC differentiation. For example, micro RNA -10 could function by inhibiting HDAC4, which induces SMCs gene expression[105], while micro

RNA -1 targets on klf4 and promotes SMCs differentiation[106]. It was also shown that micro RNA -143/145 cluster could function at SRF and its coactivators[107, 108]. SMPCs to SMCs differentiation could be further enhanced by several growth factors such as TGF-β and PDGF. TGF-β is a multifunctional cytokine regulating cellular physiology and specifically induces SMCs differentiation by modulating all related transcript factors and/or their coactivators including smad2/3, klf4/5, SRF and myocardin. PDGF as another important cell differentiation regulator is also shown involved in SMCs gene upregulating via promoting SRF/myocardin complex. This process is via the Ras/Raf/MEK/ERK pathway[109].

1.4 Animal Model

After genome sequencing, it was found that mouse and human share extensive similarity between each other. Mouse model is therefore widely used in biomedical research for deep understanding human disease and specific gene function. There are several other advantages to use mouse as animal model. Mice have a high reproduction capacity and this in turn saves money and time. The physiological and pathological mechanisms is generally similar to humans. For example, by using C57BL/6 or BALB/c strain mice, animal models can be easily established because of their stable and detectable gene expression. Luckily, mouse gene is comparably easy to manipulate which enables the examination of the functions of specific genes feasible. Fluorescently-tagged genes in transgenic mice is one good example. In this mouse model, fluorescent reporter gene such as GFP or RFP can be added into the mouse genome loci facilitating the tracing of target genes. Alternatively, overexpression and knock of target gene such as leptin knock out (db/db) mice is also commonly used in various diabetes related studies. Human pathogenesis can even be directly observed in immunodeficiency mouse model. CB17 SCID (severe combined immunodeficiency) is one strain mouse with spontaneous SCID mutation, which results in lymphocyte deficiency. Although sharing similarity with other strains of mice in terms of appearance, they can receive human tumour cells enabling direct observation of tumour progression. In addition, mouse models also provide researcher opportunities to study on pharmacokinetic parameters of novel drugs/exogenous compounds.

1.4.1 Wild Type Mouse Strain

Inbred strains, which is defined as the mice with similar genetic background are widely used in medical research. Advantage in inbred stain mouse mainly includes known background, which facilitates medical studies. C57BL/6 mice, one type of wild type black mouse, is the first mouse strain whereby their full genome sequence is known. Besides utilised for physiological and pathological animal model, C57BL/6 mice are also used in transgenic mouse models. The sub-strains of C57BL/6J (from Jackson Lab) and C57BL/6N (from National Institute of Health) mice are not entirely identical at genetic level[110]. For example, one nonsynonymous mutation occurs on cytoplasmic FMRP interacting protein 2 (CYFIP2) within C57BL/6N, resulting in altered response to cocaine and methamphetamine, whereas C57BL/6J did not[111]. This indicates that when choosing mouse strain, it is important to avoid false interpretation because of incorrect animal model. BALB/c is an albino, inbred strain mouse. The reason to cause albinism is a common mutation in tyrosinase gene, which is responsible for melanin pigment production [112]. Similar to C57BL/6 mice, BALB/c strain is easily bred and has minimal weight variations. Because of similar immunology features, BALB/c is commonly used in cancer and immunology animal models.

1.4.2 Transgenic Mouse Model

Gene expression altering to influence protein function, is the basis of some human genetic diseases. This indicates that any sequence variation, such as deletion or recombination on specific nucleotide loci or chromosome, would result in predictable cellular response. Although it is impossible to modulate gene in human beings, animal models provides a solution to this problem. In fact, *in vitro* cultured cells have provided mechanism clues in underlying human disease. However, these models are unable to accurately mimic human physiological or pathological state. Human disease models are also difficult to replicate purely by *in vitro* work. Therefore, establishment of mouse model provides researchers opportunities to validate their hypothesis *in vivo*. With modulation on target genes, function of candidate genes as well their mechanism can be detected. Gene manipulation has advanced rapidly since the discovery of DNA. For example, studies in bacterial genome have developed genetic recombination and engineering technique. With this important knowledge, method in manipulating gene in mouse model was finally established, facilitating greater understanding in human

disease. Early mouse genetics were largely based on spontaneous mutations such as SCID mice[113]. After these mutant mice were inbred with wild type animal, number of mutant animal can be preserved and expanded. However, low frequency in spontaneous mutation is one apparent drawback in this mouse model. Techniques in chemical and/or physical mutation was later introduced[114]. However, difficulty in target gene manipulation leads to the emergence of direct target recombination technique. Main recombination techniques include mutation gene insertion and gene trap approaches. Insert mutation or random integration mutants can be realized by DNA insertion/ integration in the mouse genome[115] by using transposons[116]. Gene trap represents one recombination technique, in which inserted target genes along with report genes such as fluorescent proteins or β-galactosidase are recombined into the host genomic sequence. In this case, report genes are regarded as the molecular tag for further analysis. This means that only when report genes are detectable at transcriptional level, gene manipulation such as insertion or integration can be considered successful. The most widely used reporter mouse mice are ROSA26- RFP mice[117]. Rosa26-RFP or Rosa26-CAG-loxP-stop-loxP-tdTomato-WPRE transgenic mice were constructed by gene trap technique. In this animal model, Rosa 26 is a locus which is located at chromosome 6 and widely used transgenic mice construct. Stop codon is flanked by loxP sites. Other cell components such as CAG promoter (to enhance tdTomato gene expression) and woodchuck hepatitis virus posttranscriptional regulatory element (WPRE) (to stabilize mRNA) were also added into this animal model. For example, the animals used in our study were c-kit$^{kit/CreER}$; ROSA26-RFP mice. These mice were generated by crossing c-kit$^{kit/CreER}$ with Rosa26-RFP or Rosa26-CAG-loxP-stop-loxP-tdTomato-WPRE transgenic mice. In c-kit$^{kit/CreER}$ knock in mice, CreER is under regulation of c-kit promoter. In c-kit$^{kit/CreER}$; ROSA26-RFP mouse model, Cre recombinase was maintained by ER in cytoplasm. Once the animals were injected with tamoxifen, Cre is guided by ER components to translocate into the nucleus and recombines the loxp flanked stop codon sequence. C-kit^{+} cells are labelled with tdTomato/RFP signal, which is permanent regardless of cellular differentiation state. Currently, gene manipulating can be steadily carried out because of development in modern gene techniques. This provide researchers with g more opportunity to test their hypothesis concerning to human pathology/physiology.

Novel gene manipulation can be utilised for other purposes. Transgenic mice were not created until year 1981 and since then several groups have developed strategies to insert exogenous DNA sequences into mouse genome[118]. Specifically, defined gene sequence was transferred to pronuclei of fertilized eggs via microinjection. Then the fertilized eggs were transferred into pseudopregnant female animals. With transgenic mice, several human physiological and disease models were more effectively replicated. Transgenic mice assist scientists to observe target gene expression *in vivo.* By inserting report genes, target gene expression during disease progression can be visualized. Inducing cytoside gene expression, specific cells can be deleted, and the role of these cells can be analysed. Diphtheria toxin A gene is one well studied example in which when it is activated under a specific promoter, target cells under control of this promoter can be executed[119]. Thirdly, transgenic animal model further facilitates conditional target gene expression. Classic genetic tools are inducing tetracycline/doxycycline-inducible mice, creER/loxp system, IPTG/LAC operator-repressor animal model and CRISPR-cas9 technique. However, there are various limitations that need to be established. For example, off-target induced mistakes severely hindered success rate in transgenic animal model. Strains of mice with stable expression of specific phenotype were produced. Transgenic gene size is a factor to limit traditional vector insertion. However, use of Bacterial Artificial Chromosomes (BAC) and Yeast Artificial Chromosomes (YAC) vector systems allow for large chromosomal segment homologous recombination[120]. In other words, more complicated large genomic can be transferred into transgenic animal and the role of specific SNPs can be analysed.

1.4.2.1 Knock Out Mouse Model

Knock out strategy is one transgenic based animal model. In this model selected gene is specifically deleted from the genome. Tradition knockout begins with designing vectors carrying gene of interest homologue to target gene, along with positive selection neomycin resistance (NEO^R) gene and negative selection herpes simplex virus thymidine kinase (HSV-TK) gene. Then via homologue recombination, exogenous mutation gene replaces endogenous gene reaching gene knockout. After microinjection genomic altered germ cell into a recipient female enables the development of knockout animal and by crossing with WT mice, phenotype alterations can be expanded and preserved. From this animal model, loci function

during physiological and pathological state can be detected. For example, p53 knockout ($p53^{-/-}$) mice provide clues regarding how the loss of tumour suppressor p53 gene activates tumors progression[121]. Animal source of antibodies for therapeutic purposes were hindered because of immunogenic mismatch. However, by using heavy- and κ light-chain genes disrupted transgenic mice, large scale of human polyclonal antibodies were achieved from hybridoma cell lines [122]. In addition, knockout transgenic animal models provide invaluable unknown information. For example, it was found that some disease related genes could induce embryo lethality.

1.4.2.2 Gene Recombination Mouse Model

Global gene knockout could indeed mimic disease development at certain degree. However, global knockout could also severely complicate disease aetiology analysis. In other words, global knockout of target gene leads to the inability to detect the exact role of knockout genes in specific cells for pathogenesis. Therefore, conditional knockout animal model such as Cre/loxp and FLP-FRT systems were developed (Figure 1.4.2.2). Cre/loxp system consists of two vital components which are Cre recombinase and loxP sites. Cre recombinase is encoded by a cre gene derived from bacteriophage P1. This enzyme mediates recombination of target sequence located between loxP sites[123]. In transgenic mice models, activity of Cre recombinase is under control of specific promoters. loxP sites are a pair of the sequences which flank one inserted gene. By breeding with each other, Cre/loxP transgenic mice are produced. Depending on orientation of loxP in one DNA strand, excision and inversion would occur. Specifically, when the pair of loxP are in same direction, flanked gene would be cut by Cre recombinase. However, when loxP are in opposite direction, flanked sequence is inverted during recombination. In addition, loxP can also be located at different DNA strand promoting translocation of gene segment. FLP-FRT recombination system, similar to Cre/loxP, is also consist of FLP recombinase and FRT sites. FLP recombinase, with its meaning to invert DNA, was found in the yeast[124]. Same as Cre/loxP, FLP exerts recombination once recognizing FRT. To note, initial FLP recombinase only works at 30°C, and therefore cannot function within mammalian cells. By using these systems, gene knockout models under the regulation of specific promoters can be performed. Recombination of genes can now be controlled at a specific time point. Cre recombinase fused with human estrogen receptor (ER) is one good example (Figure 1.4.2.2). ERs belong to

the steroid hormone superfamily of nuclear receptors functioning in binding with estrogen[125]. ER is composed with five distinct domains. N-terminal begins with A/B domains which play a role in binding with co-regulator to regulate target gene expression. Subsequently, C domain encodes DNA binding domain responsible for binding between ERs and target genes. Following D domain which is a hinge region for cell signalling, E/F domains occupy C-terminal containing ligand-binding domain (LBD) binding with a specific ligand. In absence of a ligand, ERs are preserved in and activated form in the cytoplasm, by binding to heat shock protein 90 (Hsp90) ,one chaperone to prevent inactivated ERs from degrading[126]. After binding with ligand such as estrogen 17β-oestradiol, ERs separate from Hsp90 and translocate into nucleus[127]. Therefore, ER and Cre fused CreER could translocate between cytosol and nucleus following ER pattern, with which Cre could access to the loxP sites in genes to function in recombination. Tamoxifen, or its active metabolite 4-hydroxy-tamoxifen (4-OHT) is one widely used activation drug. Tamoxifen is one estrogen antagonist by binding with the ER. When ER binds with tamoxifen, it will not exert normal function such as promoting cell growth, although it will still translocate from the cytosol into the nucleus[128]. The presence of endogenous estrogen 17β-oestradiol activation is one huge block in CreER mice application. Therefore, several mutants with modified ER was performed to overcome this obstacle among $CreER^{TAM}$ (mouse mutant ER) and $CreER^{T}$ (human mutant ER). However, both of these procedures was seen to be ineffective due to low efficiency and high doses of tamoxifen resulted in cell death. This was not solved until the development of models including *CreER*^{T2} mice[129] and MerCreMer mice[130]. In both animal models, fusion proteins were responsive to tamoxifen at a higher rate.

Figure 1.4.2.2

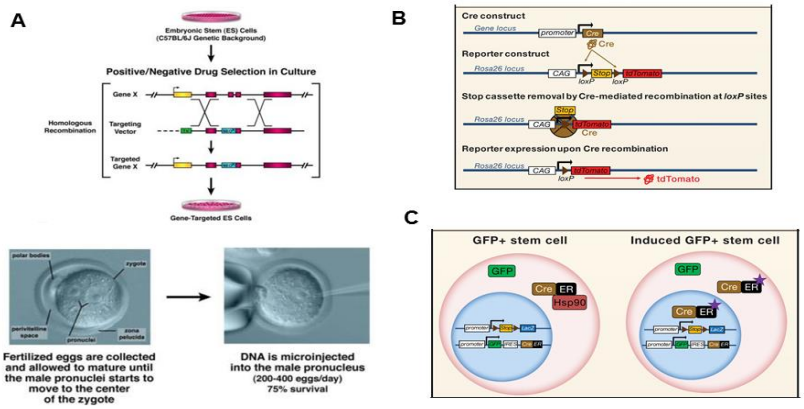

Figure 1.4.2.2 Strategy of gene recombination mouse model. A. Vectors, which contain genomic sequence are transferred to pronuclei of fertilized eggs via microinjection. Then the fertilized eggs are transferred into pseudopregnant female animals. **B.** Schematic representation of Cre-loxP system. Cre recombinase is expressed under s[131]pecific promoter. Cre could recombine loxP to remove the stop cassette. Once stop codon is cut, the reporter gene is expressed in specific cells. **C.** $CreER^{T2}$, is kept inactive in the cytoplasm by heat shock proteins Hsp90. Once binding of tamoxifen, $CreER^{T2}$ is released from the chaperone and translocates into to nucleus. Cre would then recombine at loxP sites. (Figure Source: **A**, Doyle A, McGarry MP, Lee NA, Lee JJ. The construction of transgenic and gene knockout/knockin mouse models of human disease. Transgenic research. 2012;21:327-349[118]; **B** and **C**, Kretzschmar K, Watt FM. Lineage tracing. Cell. 2012;148:33-45[132].)

1.4.2.3 Combined Recombination Mouse Model

In a gene knock in technique, a piece of mutant sequence replaces target host sequence in target sites. Although traditional transgenic mouse models provide various treasurable results, its drawbacks have been also noted during application. For instance, transgenic promoter sequence could result in the change in target gene leading to pathological alteration. In opposite, with knock in technology, mutant gene could be inserted with known sequence without incurring problems such as location variety and isoform recombination, which frequently occurred in traditional random integrated transgenic mouse model. Meanwhile, by combing knock in strategy with conditional knock out silence genes sequence, conditional gain of gene function can be achieved. In fact, this combined transgenic mice model has been wildly used in research. For example, since knock in mouse model could enable expression of specific gene under compartment promoter, target gene excision in specific cells can be achieved. Similarly, CreER recombinase could make sequential control in target gene expression feasible. Further, by crossing with Cre/CreER knock in mice with Rosa26-reporter mice, cell fate can be traced.

New site-specific recombinases such as Dre-rox recombination system[133] was more recently established. Dre was also found from P1-like phage, performing similar function to Cre recombinase. Distinct to Cre enzyme which recognize loxP recombination sites, Dre would perform recombination when in present of rox. Dre-rox recombination system has been provento perform recombination in both E.coli and animal models[133]. Furthermore, conditional control, similar to CreER, was developed by binding Dre with progesterone fusion protein. Combined system was utilised by combing two or more recombination systems. This model is designed to test occurrence sequence in specific physiological event. This is particularly important in my SPCs study area. For example, result from stem cells study with single recombination system is always interfered by existing terminal cells. It was under debate whether cardiomyocytes labelled in kit-CreER animal are from existing cardiomyocytes or stem cells[65]. By combing Cre-loxP and Dre-loxP systerms, it was shown that only few non-cardiomyocytes generate *de novo* cardiomyocytes[134]. Although the conclusion in this study is still controversial because of the toxicity issue of two system in one cells, this combined system provides one potential method in solving problems within stem/progenitor cells. Also, the split protein system showed potential in intersectional application. It was shown that Cre can be split into two parts which are the Cre-N and the Cre-C. They could spontaneously form back into full length functional Cre once reconstitution via α- complementation[135]. One potential application is to put two fragments under regulation of two different promoters, once these two promoters are activated at the same time, Cre could perform its function.

1.4.2.4 Recent Development in Transgenic Mouse Models

Furthermore, there are other techniques being currently used in gene engineering technique. RNA interference (RNAi) is one method, to silence target gene expression by inducing double stranded RNA formation. Through designing RNAi sequence under regulation of a promoter, RNAi could silence target genes in selected cells. Moreover, when combing recombination system in the embryo, spatiotemporal gene knock out or knock down can be established. However, to note, knockdown by RNAi is incomplete and with the problem uncertainty of off target effects. Therefore, cluster of techniques based on engineered nucleases system composed of DNA/RNA recognition component and cleavage protein were developed. These systems could

specifically cut DNA double strands to produce DNA double-strand breaks (DSBs), which would then stimulate DNA repair mechanisms, including non-homologous end joining (NHEJ) and homology-directed repair (HDR). Zinc-finger nucleases (ZFNs) consist of zinc-finger protein which is used to recognize target DNA, and nuclease which functions in cutting DNA strand[136]. Similarly, another example is transcription activator-like effector nuclease (TALEN), which is composed of a transcription activator-like effector protein and nuclease[137]. 30 amino acids with conserved ββα configuration compose the zinc-finger protein[136], whereas transcription activator-like effector protein is composed of a series of 33–35 amino acid repeat domains[137]. Then following specific sequence, target sequence can be recognized and modified including knockout, insertion or mutation. Recently, CRISPR/CAS which denotes clustered regulatory interspaced short palindromic repeats system, was introduced to manipulate genomes within both non-mammal[138] and mammal[139] cells. In fact, CRISPR/CAS In fact, CRISPR/CAS was discovered from the immune response in bacteria to provide protection against invading foreign DNA in viruses by utilising RNA guided cleavage[138]. Short CRISPR RNA (crRNA) derived from spacer and CRISPR DNA would anneal for trans-activating crRNAs (tracrRNAs) to form guide RNA (gRNA). Then following gRNA, CAS protein can cut spacer or invading DNA gene from host genome. With all of these transgenic tools, more animal models mimicking human disease can be built. Potentially in the future, human genetic diseases can hypothetically be cured by the development of advanced genetic editing tools.

1.4.3 Lineage Tracing

Lineage tracing studies are a way of dynamically observing change in one population of targeting cells, and/or their progenies. This technique provides vital information in understanding location, function and differentiation state in selected cells. Currently it has become one common *in vivo* technique in observing how cells behave within the tissue and correlate with neighbour cells. Similar to other early techniques, lineage tracing has also gone through several stages (Figure1.4.3).

1.4.3.1 Direct Observation

Direct observation of certain cells, enables researchers to visualise that they derived from pre-existing cells. Moreover, one embryo cell could give rise to various functional distinct cells and form in different tissues. When the cells are exposed to various

factors such as X-ray and drugs, direct observation facilitate physiological alteration observation on mitosis, migration and apoptosis within cells. Although direct observation is non-invasive and provides researchers opportunities to observe in real time on both cellular migration and proliferation. However, when cells are located in intact tissues or organs, direct observation is not achievable. Besides, when cellular features are similar to other cell types in terms of morphology, it is difficult to recognise the intended cell type. Therefore, cells being labelled with dyes were developed which is not toxic. Dyes used to label target cells include carbocyanine, fluorescein-conjugated dextran and horseradish peroxidase (HRP)[132]. Dye labelling was then replaced by report genes. This is because reporter genes do not spread to neighbour cells.

Figure 1.4.3

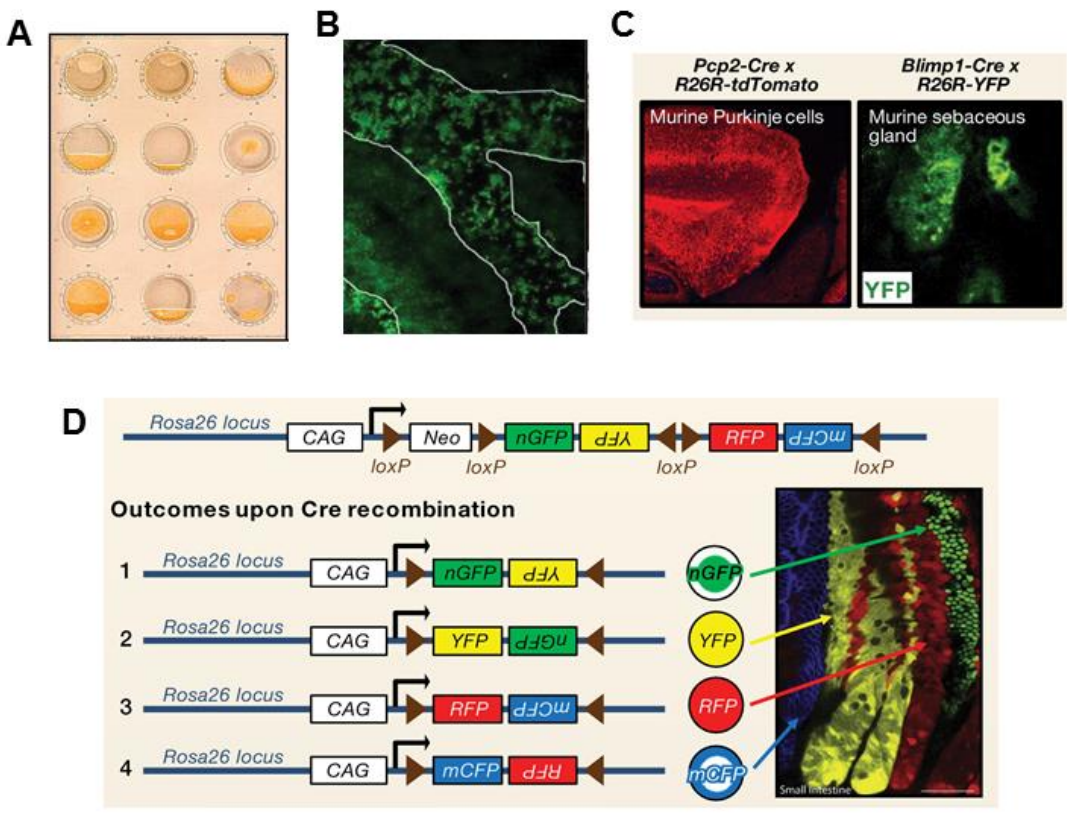

Figure 1.4.3 Lineage tracing. **A.** Direct Observation. **B.** Chimeric lung tissues with GFP^+ and GFP^- cells. **C.** Cre recombination labelled tdTomato and YFP tissues. **D**. Congetti transgenic mouse with designed multiple colour reporter strategy. GFP, green fluorescence protein; YFP, yellow fluorescence protein. (Figure Source: Kretzschmar K, Watt FM. Lineage tracing. Cell. 2012;148:33-45[132].)

1.4.3.2 Reporter Genes

Reporter gene can be strictly divided into two categories: bioluminescent and fluorescent reporter genes. Although both reporter genes are detectable and facilitate tracing the fate on target cells, they have distinct mechanism to generate light. Bioluminescence can be generated from reporters by chemical reaction. This technique is enlightened from the firefly, which can generate light itself and can be seen in darkness. In a luciferin reaction, in the absence of oxygen and enzyme, substrate luciferin expressed no luminescence. However, once catalysed in presence of luciferase and oxygen, luciferin would be transferred into oxyluciferin and release the light[140]. Another widely used example is β-galactosidase which could hydrolyse colourless substrate 5-bromo-4-chloro-3-indolyl galactoside (X-Gal), and release indolyl molecule which would be subsequently oxidized into an indoxyl, an indigo blue substrate[141]. In a fluorescent setting, a different UV wavelength is emitted compared to the absorbed UV wavelength. This is due to loss of energy once exposed to the given substance. Therefore, specific substances can be detected at a specific UV spectrum. Also, multiple fluorescent labelled substances can be detected in the same setting. In fact, currently several fluorescence proteins including green (GFP), red (RED), yellow (YFP) and cyan (CFP) are widely used in various studies. Confocal microscopes are extensively used to detect fluorescence signal. Simply, a laser beam with specific wavelength being filtered from beam splitter, focuses on specimen and excites fluorescence. Mirror galvanometer is an electromechanical instrument which senses an electric current by deflecting a light beam with a mirror. To gain the three dimension data, focus could change successively achieved at a focal depth. Emitted fluorescence goes through a pinhole lens to reach detector or photomultiplier tube (PMT), where fluorescence intensity is collected. After the photon light signal is transferred into photoelectrons and further amplified, PMT signal is decoded into a digital signal and analysed by the computer.

Advantage in bioluminescence reporter is its relatively low background because it can be detected with no light and therefore no external factors would interfere. Bioluminescence subtracts do not exist within the mammal cells and so the detected bioluminescence signal would not result from endogenous background. However, fluorescent reporters always have high background, since some cells or tissues could express fluorescence, referred as autofluorescence. For example, heme shows high

red autofluorescence. Another advantage in bioluminescence reporter is that bioluminescence signal can be used for quantification. Bioluminescence reporter expression could be detected at a high range of signal. Meanwhile, bioluminescence reporter could metabolise resembling the pattern of targeted protein. Therefore, bioluminescence reporter could spatiotemporally reflect the change in target proteins. However, fluorescence proteins are always very stable. They would accumulate but not detect the change in labelled proteins. Therefore, fluorescence proteins are not appropriate tools for quantification in target gene expression. Furthermore, when detecting fluorescence proteins, laser light used, is always with high energy. This could result in photo bleaching and even directly cellular toxicity leading to false negative results. On the other hand, fluorescence proteins also show their virtue in some other aspects. First, fluorescence proteins are bright once activated and can be further amplified by its counterpart antibodies, whereas in opposite, bioluminescence reporter is always very dim in terms of light leading to relatively low sensitivity. Then by using confocal microscope, accurate site can be detected. Further, the image with 2D or 3D could facilitate judging cell distribution in spatiality. Moreover, because of various fluorescence proteins mentioned above, more than one antigen can be detected in one cells by using co-localization study.

Table 1.4.3.2 Character of fluorescence proteins

Class	Protein	Excitation[c] (nm)	Emission[d] (nm)	Brightness[e]	Photostability[f]
Far-red	mPlum[g]	590	649	4.1	53
Red	mCherry[g]	587	610	16	96
	tdTomato[g]	554	581	95	98
	mStrawberry[g]	574	596	26	15
	J-Red[h]	584	610	8.8*	13
	DsRed-monomer[h]	556	586	3.5	16
Orange	mOrange[g]	548	562	49	9.0
	mKO	548	559	31*	122
Yellow-green	mCitrine[i]	516	529	59	49
	Venus	515	528	53*	15
	YPet[g]	517	530	80*	49
	EYFP	514	527	51	60
Green	Emerald[g]	487	509	39	0.69[k]
	EGFP	488	507	34	174
Cyan	CyPet	435	477	18*	59
	mCFPm[m]	433	475	13	64
	Cerulean[g]	433	475	27*	36
UV-excitable green	T-Sapphire[g]	399	511	26*	25

(Table Source: Shaner NC, Steinbach PA, Tsien RY. A guide to choosing fluorescent proteins. Nature methods. 2005;2:905-909[142].)

1.4.3.3 Chimeric Mouse Models

Chimeric mouse model helps to detect the role of specific cells. When transplanting cells which are tagged with reporter genes, to wild type recipient, the function of transplanted cells can be tested. When bone marrow is transplanted to sub-lethally irradiated mice, distribution and function of labelled cells determine the role of bone marrow cells in mice physiology or pathology. Although this approach is invasive and needs surgery, transplantation could distinguish different role of specific cells between host and recipient animals. When transplanting human SPCs into immune compromised mice, disease pathology can be observed[143]. Moreover, it was shown that combing unlabelled and labelled embryos together produces mosaic chimeric animals, which can be used to trace cells fate and their relationship with neighbouring cells. For example, by using mosaics animal models, notch signalling is proven vital in adhering ECs stalk cells with each other[144]. Second application of mosaics chimeric animal is detecting cells component and its related dynamic change in the target tissue. For instance, by using multicolour mosaics mouse models, leukemic cells have been shown to consist of clonal architectures and dynamic change with disease processes. In addition, by comparing differences between mutant and wild type cells at a specific site, gene function related to disease can be detected.

1.4.3.4 Transgenic lineage tracing

Appearance of genetic approaches has pushed lineage tracing study one step further. For example, in Rosa26 β-geo[145] mice, all of the cells would express reporter gene which can be detected exogenously and this is quite useful in chimeric studies. With this animal model, labelled cells can be tracked using the techniques such as flow-cytometry and microscopy. Further, when combing recombination techniques (described above) with transgenic reporter gene modified mouse models, quite various disease mouse models were built. The Rosa26-CAG-loxP-stop-loxP-tdTomato-WPRE transgenic mouse is a widely used animal model. In fact, this mouse model has many synonym abbreviations including Rosa26-CAG-LSL-tdTomato, Rosa-LSL-tdTomato, Rosa26-Tomato and Rosa26-RFP. In this thesis, Rosa-RFP mice were crossed with Cre/CreER transgenic/knock-in mice. Stop codon which is flanked by loxP sites would be cut (with or without tamoxifen induction in terms of purpose in studies) within target cells which showed recombinase. Subsequently, the fate of selected cells can be

traced. Recently, a multicolour report gene construct strategy was also induced. For example, mosaic analysis with double markers (MADM) mouse model[145] splits GFP or RFP gene in two DNA strands and separated by loxP and Cre recombination would result in gene reconstitution of fully functional reporter genes. Membrane-targeted tdTomato/membrane-targeted EGFP (mT/mG) double-fluorescent reporter mouse[146] was artfully designed with the Rosa26-CAG-loxP- tdTomato -loxP- GFP structure that the cells without recombination would express tdTomato signal, whereas after recombination, cells are tagged by GFP. Multicolour reporter mice are able to generate multiple reporter colours, can provide us with evidence that most tissues consist of multiple clones and are potentially not derived from a single cell. For example, brainbow mouse was developed by combing more than two florescence reporters. With this mouse model, at most 10 combo colours can be generated[147]. Similarly, the confetti mouse uses four different reporter genes to show clonal hierarchy[148]. However, to note, the principle of multicolour reporter mice is based on Cre recombinase random recombination. Therefore, conclusions from every study using this animal need to be cautiously judged, since the rule of this random recombination related to cellular physiology is still unclear.

1.5 Cell Migration

Migration is one basic cell physiology, related to SPCs recruitment in AV. The development of fluorescence microscopes enables us to visualise, how motile structure forms and locates underlying motor protein assembly. This motile structure is crucial in regulating cellular posture and position, in response to every extracellular biophysical force. These adjustments are mainly controlled through cytoskeleton transformation (Figure 1.5).

Figure 1.5

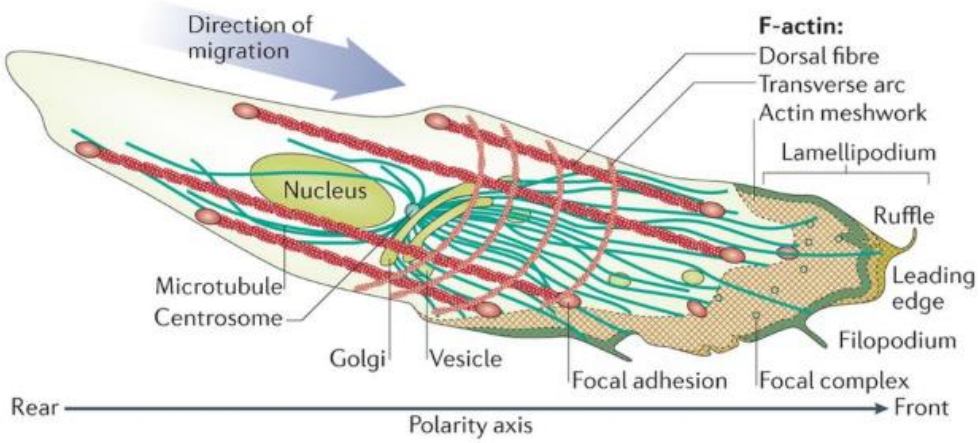

Figure 1.5 Motile cytoskeleton components. In response to surrounding signals, F-actin forms protrusion including filopodia and lamellipodia in front of cells. MTOC and Golgi apparatus in the meantime orient to the leading edge for cell migration. Adhesion complex forms at the cell membrane to regulate F-actin movement. Myosin activity provides traction tension for cell migration. F-actin, filament actin; MTOC, microtubule-organizing centre. (Figure Source: Mayor R, Etienne-Manneville S. Nature reviews. Molecular cell biology. 2016;17:97-109 [149].)

1.5.1 Filament Assembly

The cytoskeleton network mainly consist of three biopolymer component types including actin, microtubule and intermediate filaments, based on rigidity[150]. Actin filament is one form of polymer built by dimer pairs of globular actin monomers. One actin filament consists of two distinct ends, which are point (fast growing) and barbed (slow growing) end. Two ends are made of distinct concentrations of actin monomers. The barbed end is six times higher than the point end. Homeostasis is regulated by the concentration of free actin monomers that the actin filament is exposed to. In other words, assembly (polymerization) or disassembly (depolymerisation), depends on a

setting critical concentration. When the concentration of free actin monomers is higher than the critical concentration, actin filaments polymerize. By contrast, actin filament goes through depolymerisation when concentration is lower. Within the cell, when the concentration of free actin monomers is between critical concentrations at two end, asymmetric changes occur. In this situation, point end would grow whereas barbed end would shrink. This means that when actin filaments translocate from the places with low free actin monomers concentration to higher concentration places, the length stays roughly the same. This phenomenon is called treadmilling[151]. Microtubules are rod-like, hollowed polymers with high rigidity. Microtubules are made of protofilaments which are assembled from tubulin protein. Similar to actin filaments, motility of microtubule is also regulated by treadmilling. Intermediate filaments such as vimetin, sesmin, keratin and lamin are flexible proteins. Instead of generating polarized force, they are stable and do not treadmill. All of these components comprise the cell cytoskeleton. When the cells sense surrounding signals such as chemokines, actin would polymerize and translocate, functioning as an engine to produce cell protrusion. Actin filaments assembly are the basis for cells to move forward which are carried out by several accessory proteins.

Actin filaments assembly begins with actin nucleation. A nucleus would firstly form and rapidly promote F-actin development. Nucleation is one rate limiting step in polymerization, because intermediate actin dimer is not stable. Currently, three mechanisms are responsible for nucleation. The first mechanism is to form a branch from an existing actin filament. When recognizing nucleation promoting factors such as WASP/WAVE family proteins, Arp2/3 complex forms to generate a branched structure from an existing filament. The structure of Arp2/3 complex is similar to actin. In the inactive state, it is not bounded with ATP. Once binding with ATP molecules, the Arp2/3 complex is activated for conformation change[152]. Then WASP/WAVE proteins recruit Arp2/3 complex and actin monomers to initiate branch formation from existing actin filaments. A second mechanism is via formins, which could bind actin FH2 domains to form stable dimers and initiate actin nucleation. The last nucleator-spire has four actin monomer-binding WASP-homology 2 (WH2) domains. Therefore, a spire could stably bind with four actin monomers to form a short single nascent filament and finally incorporate into a mature filament. After nucleation, F-actin continues to grow, which refers to actin elongation. After forming dimer actions by FH2

domains, formins keep attaching at the filament end. Then adjacent domain FH1 further recruits profilin actin monomers for rapid elongation. Enabled/vasodilator-stimulated phosphoprotein (Ena/VASP) is another protein to promote filament elongation. Similar to formins, Ena/VASP could bind profilin actin to form tetramers[153]. However, filament growing is not unlimited because of capping proteins. Capping proteins could interact with filament end to terminate filament elongation. To note, both formins and VASP could inhibit activity of capping proteins. Therefore, the filament elongation rate can be regulated. Cofllin is another regulator for actin dynamics[154]. It was shown that cofllin could uncap barbed ends of old filaments and then release free actin monomers[155]. Released free actin monomers bound with ATP are recycled to replenish actin concentration at the leading edge. After these free actins bind to the new end of filament, direction of F-actin can be determined. When these proteins cooperate and are properly regulated, control of rate in actin elongation can be acquired.

1.5.2 Protrusion Formation

F-actin would then connect distal point of adhesion to sense the signal. On the other hand, F-actin could also generate force to facilitate cell migration. F- actin in cell protrusion can be divided into filopodia and lamellipodia[156]. Filopodia locates at cell tip and would protrude out of cell body by treadmilling when sensing chemical or mechanical stimuli. Because there is VASP attaching at the tip, filpodia could keep elongating without being capped or branched. Another kind of F-actin is lamellipodia, which binds to branches of existing filaments. Distinct from filpodia, it was found that protrusion of lamellipodia relies on elastic Brownian ratchet mechanism[157]. When the slow barbed end of a filament binds to cell membrane, thermal energy would bend the filament to store elastic energy. Bending the filament also permits more actin monomers to connect. When elastic energy is released during filament unbending, the cell membrane would be pushed forward by driving force prompting cellular protrusion. With this character, lamellipodia would grow in setting direction when receiving the environment signal.

Formation of protrusions in both filopodia and lamellipodia, are under regulation of Rho family small guanosine triphosphate binding proteins (GTPases) mainly including Rac, Cdc42 and Rho. GTPases are molecular switches and regulated by

conformational states[158]. When they are bound to GTP catalysed by guanine nucleotide exchange factors (GEFs), they are activated to promoting downstream signalling. Conversely, when they are bound to GDP by GTPase activating proteins (GAPs), they are inactivated. Once activated, Cdc42 could bind to WASP protein and Rac relieves WAVE from its inhibition of proteins. Then a conserved region called VCA domain in both WASP and WAVE is exposed and binds to Arp2/3 complex. In this way, filaments can be elongated and protrude. Meanwhile, WAVE/WASP could also regulate Rac/Cdc42 in a feedback loop to precisely control the filament length. Besides forming protrusions, Cdc42 could also orient the microtubule-organizing centre (MTOC) and Golgi apparatus to the leading edge[158]. Then MTOC polarity occurs in which microtubules form protrusions and deliver vesicles from Golgi to the leading edge providing necessary proteins. In addition, Cdc42 could activate downstream kinase PAK1, which could further upregulate Cdc42 activity through a positive feedback loop. Although GTPases themselves could induce cell protrusion and polarity, signal amplifying is still needed when chemoattractant derived from gradient difference is low between front and rear of the cell. PIP_3 is one crucial molecule which functions in transmitting and magnifying the signal. Generation of PIP_3 is stimulated by PI3K and inhibited by phosphatase PTEN. It was shown that, in migrating cells, PI3K accumulates at the leading edge whereas PTEN is restricted at the rear of the cells[159]. Further, PI3K could positively activate and control localization of Cdc42 and Rac.

1.5.3 Adhesion Complex

Although filaments could form and protrude, actin polymerization would also occur in body and rear of the cells[160]. Meanwhile, within the cells, newly formed actin bundles could at the same time flow back leading to generation of retrograde flow, which produce the force, in opposite to direction of cell migration. Besides actin bundles, myosin could also contribute to retrograde flow formation[161]. Therefore, cellular translocation rate is one combined result, determined by both forward traction force and retrograde flow force. Then how this balance was regulated was later explained by a clutch theory[160]. This theory claimed that, when actin interacts with clutch or adhesion complex assembled by integrin and adhesion proteins such as vinculin and talin, traction force can be effectively transmitted to cytoskeleton actin facilitating cell migration. Conversely, failure in binding between actin and adhesion molecules results in weaker forward traction force and thereafter backward movement in cells. Also,

focal adhesions could also stabilize stress fibres in the leading edge and prevent filaments from deadhesion.

1.5.3.1 Integrins

Integrins are one important family of receptor to support cell migration. Each integrin, as a transmembrane receptor, consists of two heterodimeric molecules which are α and β chains. The long N-terminal of integrin binds with extracellular matrix. C-terminal tail within cytoplasmic domains functions in binding with intracellular components. Activation of the extracellular part could lead to conformation change in both α and β chains. Then altered interactions between these two chains provides the intracellular binding site for signalling molecules such as small GTPases and phosphorylated tyrosine kinases and this facilitates signal relay from extracellular space to cytoplasm. Meanwhile, intracellular signals can also be transmitted out of cells through integrins, by which affinity and activity can be regulated[162]. When the cells migrate, exogenous signals would be firstly sensed by filopodia, and then growing number of integrin interacts with the extracellular matrix. As the integrin grows into a cluster, nascent adhesion forms when myosin II is absent[163]. At this moment, although nascent adhesion is still unstable and cannot sustain cytoskeleton force from F-actin, high force derived from myosin II and F-action could promote integrin accumulation.

1.5.3.2 Adhesion Molecules

When integrin cluster continues to develop, several group of proteins such as talin, vinculin, paxillin, and α-actinin, are recruited to form mature focal adhesion[164]. In addition to forming cell adhesion, these proteins could also transmit signal and facilitate cell migration. Talin is the first identified protein, which directly binds with integrin. Talin is composed of an N-terminal head and a C-terminal rod domain. In native physiology, talin keeps an autoinhibition state by head to rod binding. However, once activated by kinases such as PKCα, RIAM, PIP_2, talin adopts an extended conformation, which facilitates its binding with integrin. Then whole rod domain would stretch and expose more sties, for binding with vinculin or actin. At these moment, talin could function in forming focal adhesion and as one mechanosensor, which transmit the signal into the cytoplasm for cells to regulate traction force, especially when in response to actin retrograde flow. Meanwhile, actomyosin contraction could further promote talin conformation change to expose more binding sites. Another vital binding

protein is vinculin, which is consist of N-terminal globular head and C-terminal rod tail. Similar to talin, vinculin would also maintain autoinhibited form when in native. Once activated, they would be recruited by talin and also stretch to expose binding sites for other proteins. Head domain of vinculin is responsible for binding with talin, whereas the rod domain could bind with Arp2/3, paxillin, VASP and catenins[165]. Because of its role in transmitting the cell force, loss of vinculin would result in adhesion dysfunction. It was shown that binding of talin and vinculin promote more actin fibre bundling to generate force and in a positive loop, increased contractility force could recruit more binding proteins[166].

1.5.4 Myosin II Contractility

The myosin light chain (MLC) phosphorylation could increase myosin II contractility and therefore promote tension transmission. By producing tension when ATP is present, Myosin molecules could promote actin filament sliding. Meanwhile, myosin could also involve in adhesion tension transmitting via binding with actin filament. Myosin molecules contain two heavy chain and two light chain. From appearance, a myosin heavy chain can be divided into head, neck and rod tail regions. The head globular domains contain binding regions and could bind with both actin filament and ATP. Following is the neck domain which serves as a lever arm, to transfer and amplify the chemical energy derived from ATP hydrolysis into kinetic energy. The rod tail regions form in dimerization structure and could bind with another myosin molecular resulting in an anti-parallel bipolar structure when activated. The MLC divided into essential light chain and regulatory light chain, binds at the neck region of the heavy chain to regulate myosin function. It was shown that inactivated myosin maintains an assembly-incompetent form though head and tail auto-interaction. However, when regulatory light chain is phosphorylated, head and tail interaction is unfold and then assembly-competent state forms[167]. Thereafter myosin could bind with filament or another myosin molecular. Several kinases have been reported involved in MLC phosphorylation such as MLC kinase (MLCK) and Rho-associated (ROCK). For example, after stimulation from Ca^{2+}–calmodulin, MLCK is activated to unfold myosin auto-interaction. RohA could bind with ROCK and expose its kinase domain to phosphorylate MLC. In opposite, MLC phosphatase are responsible for MLC dephosphorisation. MLC phosphatase is made of three subunits which are catalytic region protein phosphatase (PP1), myosin binding subunit (MYPT1) and a third

subunit. When MYPT1 bound to working MLC, PP1 is activated to remove the phosphate group from MLC and revert myosin into inactivate state. Activated ROCK could phosphorylate MYPT1 at two inhibitory sites and dysfunctions MLC phosphatase[168]. In addition, by phosphorylating different site in both MLC and MHC, PKC is also reported to induce myosin activity. Myosin is not directly involved in protrusion network, but functions in protrusion regulation. When myosin II is knockout, although lamellipodia could remain intact, protrusion production rate cannot be regulated[169]. Myosin regulates protrusion rate by transmitting contractile force to actin, and act along with adhesion molecules as clutch to push membrane forward at the leading edge. In addition, level of active myosin is dispensable for assembly of nascent adhesion. By promoting integrin cluster exposing cryptic sites of binding proteins and posture conformation, myosin regulates F-actin binding with adhesion complex. Meanwhile, through disperse adhesion molecules, leading edge could stretch from central to peripheral edge under myosin tension force.

1.5.5 Focal Adhesion Disassembly

When focal adhesion forms at the leading edge, it is still not stable. F-actin disassembly occurs at the same time to reorganize protrusion structure. This F-actin reorganization was reported result of intracellular signal, transmitted from adhesion complex[170]. Then with assistance of retraction force exerted by myosin motor, cell detachment occurs. Deadhesion would also occur in rear part of cells and facilitate cells translocation. However, it is worth to point out that, distinct to adhesion complex in the leading edge, rear part of the cells have larger and more mature adhesion structure. Therefore, proteins or cellular kinases are needed to translocate within cells via microtubules to promote adhesion disassembly[171]. Focal adhesion kinase (FAK) is a cytoplasmic tyrosine kinase playing an important role in signalling cascade. FAK is composed of three pivotal parts which are N-terminus FERM, central kinase domain and C-terminus focal adhesion targeting (FAT) domain. When FAK is inactive, FERM auto-binds with kinase domain to inhibit its catalytic capability. Upon activated, FERM domain is phosphorylated, and promote recruitment of SH2 contained adaptor proteins such as Src[172]. Then more sites in FAK structures are further phosphorylated to induce binding and activation of other kinases. It was shown that in FAK deficiency cells, cells could still adhere but fail to migrate, which indicates that FAK is mainly responsible for adhesion turn over[173]. After cell turn over, FAK downstream signalling

would further activate Rac and ERK favouring filament elongation. In fact, it was shown that adhesion in cell rear is always strong like an anchor. Therefore, high tension provided by myosin II is needed for cell detachment. In addition, several FAK downstream singling pathways have been reported to contribute to cell migration. For example, FAK/Src complex is responsible for p130cas recruitment and phosphorylation. Then recruited Cas/Crk complex promote Rac activation through protein DOCK180[174]. Another signalling to promote cell migration is stimulated when FAK binds with PI3K and Grb7. When PI3K and Grb7 are both activated by FAK, they cooperate in promoting cells migration[175]. N-WASP can also be activated directly by FAK, to facilitate Arp2/3 complex formation for actin polymerization. Meanwhile, FAK could also induce Rac/Cdc42 activation by binding with paxillin[176]. Paxillin is another important component of focal adhesion and relay the signal from extracellular into the cells. Paxillin contains five repetitive leucine-rich LD motifs at the N-terminus and four cystein-histidine-enriched LIM domains at the C-terminus. LD domains provide docking sites for focal adhesion related proteins such as FAK, Src, talin and vinculin. When N-terminus site is phosphorylated, paxillin is activated and recruited to focal adhesion site. When interacting with FAK/Src complex, paxillin can be activated to induce ERK/MLCK signalling, which promote adhesion turn over and cell migration[177]. Afterwards, myosin and stress fibre promote rear part to translocate. This process would help to pull the cell forward. To note, all migrating process is rapid and also in dynamic change, which means when the first round of migration finishes, the next round would begin or has already begun. During the same time, organelles are also dragged by F-actin and myosin to move along the cell membrane and assist cellular integrity.

1.5.6 Extracellular Matrix

ECMs provide a structural platform for the vascular wall and interact with vascular cells to regulate diverse cellular biological process (Figure1.5.6). Meanwhile, cells could produce *de novo* ECMs for vessel wall development and remodelling. Pathological cytokines could do harm to ECMs homeostasis leading to vascular wall stiffness. ECMs can be divided into two forms which are interstitial and pericellular ECMs. Pericellular ECMs contact cells to prevent cells from ripping apart, whereas interstitial ECMs bind with each other to create a complex network. In a vessel wall, ECMs provide support for the basement membrane. Internal elastic laminae locate at the

outmost of intima layer comprise of elastin. Internal elastic laminae and basement membrane can be connected by connective tissues. ECMs are also rich in collagen and elastin fibres within media layer, to enable separation and lubrication to SMCs. The outmost layer is the adventitia tunica, in which layer of the ECMs is comprised of external elastic laminae and interstitial ECMs. Main forms of ECMs in the vascular wall include collagens, elastin, fibronectin (FN), laminins, proteoglycans (PGs), and glycosaminoglycans (GAGs) which are highly acidic and hydrated molecules. Surrounding cells are responsible for ECMs production within different layers. For example, collagen and elastin are derived from SMCs and in adventitial layer ECMs are produced by fibroblast[178]. The vascular cells interact with ECMs through integrin and support cells to proliferate, survive and/or differentiate. Several types of ECMs could exert distinct effect on target cells. For example, basal laminae proteins such as collagen-IV and laminin could enhance SMCs contractile gene expression, whereas interstitial matrix proteins could improve SMCs proliferating rate. ECMs damage would contributes to cellular biology changes and promote vascular wall remodelling or disease. Meanwhile, small molecules can be released from ECMs as matrikines which also provide signals for surrounding cells.

Figure 1.5.6

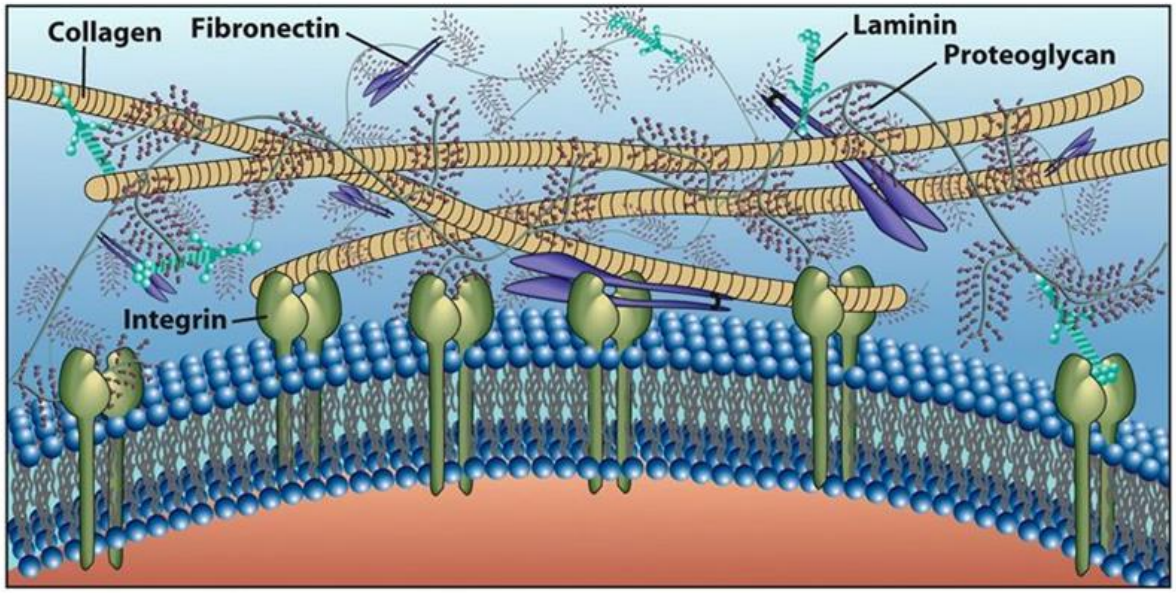

Figure 1.5.6 Extracellular Matrices (ECMs). ECMs within the vascular wall contain several types including collagens, elastin, fibronectin, laminins, proteoglycans, as well

as glycosaminoglycans. According to distribution, they are divided interstitial and pericellular ECMs. SMCs and fibroblast are mainly responsible for ECMs production within the vessel wall. Besides maintaining vessel structure, ECMs contact with neighbouring cells and regulate vessel wall homeostasis. ECMs, extracellular matrices; SMCs, smooth muscle cells. (Figure Source: http://slideplayer.com/slide/9806334/.)

1.5.6.1 Collagen

Collagen is known as a tropocollagen triple helices, as referred as microfibril[179]. Each chain of collagen consists of repeating glycine-prolin-lysine (Gly-X-Y) motifs serving for triplet formation. Collagen formation begins from a Non-collagen (NC1) domains and the triplex structure can align in a C- to N-terminal direction. During this process, under assistance of vitamin C, a hydroxyl base is added to prolin and lysine by prolyl hydroxylase and lysyl hydroxylase, respectively. Then glycosylation occurs by adding either glucose or galatose to hydroxylysine, and thereafter collagen chains twist into triplets. When peptide at each terminal end is cut, tropocollagen forms. Through aldol condensation reaction, hydroxylysine and hydroprolysyl are oxidized forming cross link between two tropocollagen molecules to form microfibrils. Afterwards they pack into fibrillary collagen. For example, collagen I and III belong to the fibrillary collagen form and this provides vessel wall tensile strength. They can be stabilized by other macromolecules such as decorin and biglycan[180]. However, some collagens have interruptions by non-collagen structures within their triple helical structures favouring them to interact with other molecules. For example, by tail to tail interaction, NC1 domain in collagen IV could initiate dimer triple and helical structures formation. Similarly, tetramer and multiple complex comprise of the collagen network. At last, collagen molecules could also bind with other kind of ECMs forming multiplexin.

Collagen could directly interact with cells by integrin. With integrin signalling, cells fate is regulated. For example, interaction between collagen and α1β1 integrin stimulates SMCs proliferation through MAPK pathway[181], whereas α2β1 mediate SMCs migration[182]. Meanwhile, distinct form of collagen could also show different impact on cells. When SMCs are cultured in collagen IV, SMCs would express more contractile phenotype because of SRF binding, whereas in collagen I environment, SMCs could transform into an inflammatory form[183]. When collagen IV NC1 domain molecules such

as arresten was put into ECs culture medium, angiogenesis was inhibited[184]. Similarly, neostatin derived from collagen-XVIII could also inhibit neovascularization[185]. Afterwards, in response to distinct collagen, SMCs or fibroblast would secrete different ECMs. When collagen is excessively produced, vessel fibrosis and stiffness would occur with more collagen binding by hydroxylysine or hydroprolysyl oxidization.

1.5.6.2 Elastin

Elastin is an elastic protein allowing the tissue to recover its origin shape after stretching or contracting. By linking to a small soluble precursor tropoelastin, the complex elastin would form. Tropoelastin is firstly synthesised and transported from the cytoplasm to the extracellular space. This process is facilitated by the elastin-binding protein (EBP), which prevents tropoelastin from degradation. Once tropoelastin is delivered outside of the cells, EBP would recycle back into the cytoplasm[186]. Each tropoelastin consist of hydrophobic and hydrophilic domains. The hydrophilic domains contain Lys-Ala (KA) and Lys-Pro (KP) motifs that are involved in crosslinking during the formation of mature elastin. Assembly process is mediated on microfibrils, which serve as a scaffold. Elastin is produced in both media and adventitia layers and is mainly located at the space between the internal and external elastin laminae. Elastin fibre consists of fibrillin microfibrils and elastin core, allowing the elastic recoil. Elastic recoil is important for the vasculature to maintain its structure when they bear dynamic blood flow. Fibrillin microfibrils could provide Elastin with scaffold facilitating elastin deposition and assembly. Elastin fibres cover SMCs in a concentric fenestrated elastic laminae, which serves as a basic unit of the artery wall[187].

Elastin binds with SMCs via the elastin receptor, which consist of EBP, neuraminidase and a protective protein[188]. When binding with this receptor, elastin suppresses migration and proliferating in SMCs. Meanwhile, contractile character in SMCs can be maintained. Elastin can assist and preserve myofilament stability through activating Rho GTPase. Data showed that when culturing SMCs on elastin, SMCs would preserve quiescent state with contractile filament[189]. However, elastin form could also affect SMCs state. For example, when elastin is cleaved and release its fragment EDP, this released segment binds with SMCs receptor inducing SMCs migration. Elastin also exerts its effect on inflammatory cells. In opposite to other ECMs such as lamina or collagen, Elastin reduce leukocyte adhesion in the neointima. Elastin gene mutant

results in uncontrolled SMCs proliferation and intima hyperplasia[190]. Data was shown that mice with elastin gene knockout would die because of vascular occlusion[191].

1.5.6.3 Fibronectin

Fibronectin is a glycoprotein dimer. C-terminal of each chain is bonded by disulfide bond. There are mainly of two types in fibronectin, which are soluble plasma fibronectin and insoluble fibronectin composing ECMs. Each fibronectin consists of I, II, III three motifs. Different to motif I and II which function in intra-chain bond and matrix assembly, motif III mainly functions by binding with cells by interacting with integrin. This interaction is because of RGD sequence (Arg–Gly–Asp) within III motif. Fibronectin is crucial in cell physiology. For example, when vascular injury is induced and bleeding occurs, plasma soluble fibronectin can be activated to form the clot protecting the tissue. Then ECs or ESPCs are recruited to injury sites for angiogenesis or vasculogenesis. Meanwhile SMCs, fibroblast and leucocyte also accumulate at wound site to secret proteases digesting soluble fibronectin. Afterwards, insoluble fibronectin along with other ECMs such as collagen is secreted to resemble origin structure of the tissue. During this process, SMCs are promoted into phenotypic change from contractile type and into a proliferate state. These characters also mediate fibronectin involving neointima formation. It was shown that by alternative splicing fibronectin motif, leucocyte and SMCs accumulation are decreased. Vitronectin also has a similar function in vessel wall remodelling[192].

1.5.6.4 Laminins

Laminins are large proteins to serve a component of basement membrane. Laminins are composed of heterotrimeric proteins including α, β, γ chains. With cross like structure, three short arms are used for binding with other laminins, and the long arm is for binding with cells. To form a matrices network, laminins interact with other ECMs by fibronectin, vitronectin and perlecan. Laminins locate at the basement membrane in the vessel wall. Laminins surround and bind cells with distinct isoform. It was shown that within the endothelium, α4 and α5 are highly expressed. Whereas in SMCs basement membrane, α1 and β2 expression are increased[193]. They exert several functions in vessel wall. For example, Laminins can inhibit leucocyte invasion. Laminins isoform expression were thought to be derived from the pericytes to regulate leucocyte transmission. Meanwhile, because laminin could directly anchor with ECs

by integrin, it was thought that laminins could also convey mechanical signalling from the lumen. In addition, SMCs phenotype can also be maintained by laminins in the basement membrane. Other ECMs such as PGs and GAGs could function in LDL binding, which is associated with atherosclerosis formation. All of these ECMs could all cooperate together to regulate homeostasis within the vessel wall.

1.5.6.5 Metalloproteinase

ECMs homeostasis is regulated by proteases or metalloproteinases. Metalloproteinases include matrix metalloproteinases (MMPs), a disintegrin and metalloproteinases (ADAMs), and ADAMs with a thrombospondin motif (ADAMTS)[194]. Their proteases activity relies on their catalytic site, which consist of a conserved motif HEXXHXXGXXH and a zinc ion. Metalloproteinase can be divided into soluble and membrane anchored form. Among all of these enzymes, MMPs are the main enzymes to degrade all ECMs[195]. By modulating connective tissues or adhesion molecules, migration and/or proliferation can be regulated. Tissue inhibitors of MMPs (TIMPs) could inhibit MMPs activity, to prevent excessive ECMs degradation. MMPs and TIMPs commonly maintain ECMs balance, which is crucial for vessel wall remodelling. N-terminal of MMPs is a signal peptide domain, which is crucial for MMP activity. When the signal peptide domain is bound to the catalytic domain, MMPs are inactive. However, once signal peptide domain is cleaved from the catalytic domain, MMPs are activated. Most MMPs also have a haemopexin-like domain to respond to a known ligand. Some Membrane-type MMPs (MTMMPs) anchor on the cell surface by a cytoplasmic tail or by direct binding by glycosylphosphatidylinositol (GPI). Currently, 23 MMPs have been identified in human beings[196]. According to recognized molecules structure and subtracts, MMPs can be divided into collagenases, gelatinases, stromelysins, matrilysins, MTMMPs and other MMPs. Once produced, MMPs would be secreted into the plasma when binding with heparin sulfate glycosaminoglycan known as a pro-MMPs form. Alternatively, MTMMPs would reside on the cell surface. Several factors could activate pro-MMPs including alteration in heat, PH and chemical agents. Protease could also activate pro-MMPs. For example, in non-active form, pro-MMP2 bind with TIMP2 and MT1-MMP as a complex. N terminal inhibitory domain of TIMP could inhibit function MT1-MMP. However, when TIMP is removed from this complex, MMP2 can be activated by signal peptide domain cleavage. Alternatively, signal

peptide domain can be cleaved by another MT1-MMP[197]. In some cases, distinct MMPs would cooperate for ECMs degradation. For example, collagenase MMP1 and MMP8 could recognize and unfold their triple helix in collagen fibril. This signal chain is subsequently degraded by gelatinases[198].

1.5.7 Cell Migration within Vessel Wall

Vessel wall is composed by several cells types including leucocyte, ECs and SMCs as shown above. Cell migration is pivotal for vascular homeostasis and vessel remodelling. To move to targeted sites, cells would either float from the circulation to the tissue such as leucocyte or crawl locally on ECMs surface such as ECs and SMCs, in response to signals (Figure 1.5.7).

Figure 1.5.7

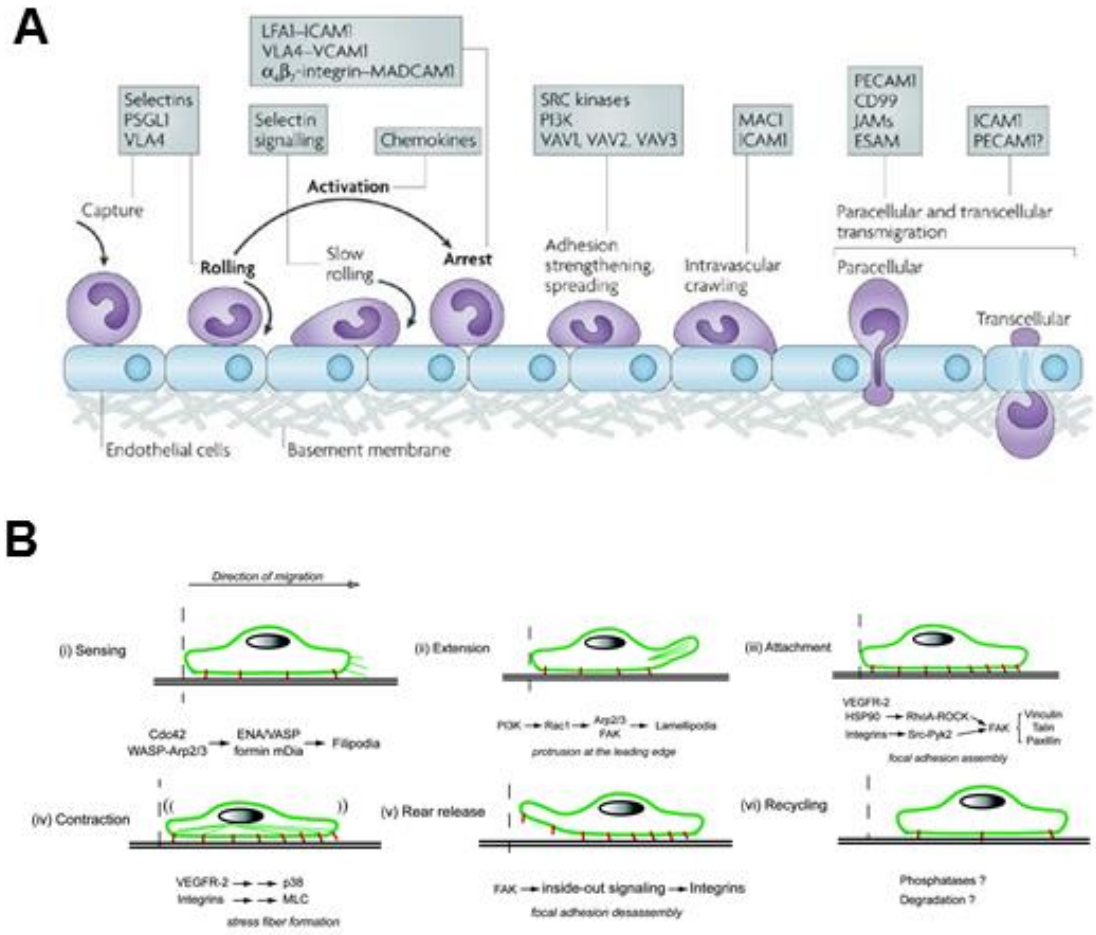

Figure 1.5.7 Cell migration in vascular wall: A. Leucocyte migration contains continues stages including rolling, capture, adhesion strength and transmigration. During these stages, molecules such as selectin, integrin, adhesion molecules and chemokines facilitate leucocyte capture on ECs surface. Via paracellular or transcellular route, leucocyte transmigrate into basement membrane. **B.** ECs and SMCs begin to crawl in response to signal within the vessel wall. All the stages include sensing, extension, attachment, contraction, rear release and recycling. Vascular cells crawling is one continues process. ECs, endothelial cells; SMCs, smooth muscle cells. (Figure Source: **A**, Ley K, Laudanna C, Cybulsky MI, Nourshargh S. Getting to the site of inflammation: The leukocyte adhesion cascade updated. Nature reviews. Immunology. 2007;7:678-689[199]; **B**, Lamalice L, Le Boeuf F, Huot J. Endothelial cell migration during angiogenesis. Circulation research. 2007;100:782-794 [200].)

1.5.7.1 Leucocyte Migration

Leucocyte migration is one continues process which involves several stages including rolling, capture, adhesion and transmigrating for vessel wall remodelling. Circulating cell recruitment begin to roll by selectins molecules such as L-selectin, P-selectin and E-selectin[201]. When binding and interacting with selectins expressed on inflammatory ECs, leucocytes adhere to ECs layers. By leucocyte interaction, more inflammatory cells are recruited to the endothelium. With the blood flow, leucocytes roll on the ECs surface and form a stronger interaction by binding to selectins. Selectin engagement triggers activation of downstream pathways such as PI3K and MAPK signalling. Meanwhile cell rolling can also be mediated by integrin. It was shown that several integrin types such as $\alpha_4\beta_1$-integrin (VLA4), $\alpha_L\beta_2$-integrin (LFA1) and $\alpha_M\beta_2$-integrin (Mac, CD11b) could maintain cell rolling, when interacting with immobilized vascular cell-adhesion molecule 1 (VCAM1) expressed on ECs[199]. In response to ECs inflammation, ECs would be rapidly mobilized to express both ICAM-1 and VCAM-1. Meanwhile, chemokines are also produced by ECs and presented on ECs luminal surface. Alternatively, leucocytes could also generate chemokines, which is endocytosed by ECs or binds with glycosaminoglycans on ECs layer. The most classic G protein-couples receptors (GPCRs) on leucocyte could bind these chemokines inducing signalling cascades change and provide signals, referred as inside-out signalling[202]. Several factors are responsible for integrin activation. For example, in monocyte, GPCRs downstream molecular, phospholipase C (PLC) is activated for VLA4 activation once stimulated by chemokines. Meanwhile, via small GTPase activation such as RAP1 and RhoA, activity of LFA1 can be regulated. In fact, signal transmitting can be achieved through adhesion molecules such as talin and vinculin. With inside-out singling, integrin is driven from bent low-affinity conformation to extended high-affinity state and binds with inflammatory molecules. Afterwards leucocyte stops rolling and is captured on ECs surface. Also, activated integrin could transmit signalling by out-inside singling to tight this interaction. For example, tyrosine kinase Src could be rapidly recruited to integrin. The resulted cytoskeleton arrangement occurs and collaborate with activated integrin to form cell adhesion. The effect in leucocyte capture varies depending on integrin types.

Once captured by inflammatory ECs, leucocytes continue to crawl transmitting ECs connection. While transmigration, monocyte firstly crawl into intercellular space between ECs to sense the weak site by MAC/ICAM complex[203]. Binding of ICAM and MAC induces MAPK signalling activation, to increase ECs contraction via regulating myosin motor. Therefore, intercellular space can be open for leucocyte transmigration. Guided by both chemokines and sheer flow, monocyte transmigrate through interaction with ECs. During this process, cell migration is also facilitated by intercellular interaction between leucocyte and ECs. In fact, it has been demonstrated that this interaction is favoured by a docking structure, in which binding molecules accumulate and serve as a binding site. Similar to migration pattern on extracellular matrix, monocyte could move through paracellular route. For example, junction molecules such as PECAM1 and ICAM could bind as a ligand for leucocyte receptors and mobilize the cells. These molecules would cluster and form a concentration gradient to guide cells to migrate[204]. In opposite, VE-cadherin which cannot mobilize leucocyte would keep away from the docking structure[205]. With reduced ECs intracellular adhesion, more space is opened for monocyte migration and meanwhile by adjusting adhesion molecules in a favoured site, monocyte could move inwards. In addition to paracellular route, monocyte could also migrate through transcellular pathway[206]. This process minorly occurs but could be rapid. Monocyte transcellular migration is achieved by vesiculo vacuolar organelles (VVOs). VVOs is a specific ECs organelle that is formed by cabelolea and cytoskeleton, contributing to endothelial permeability. With this structure, VVOs could transport fluid and macromolecules from the lumen to the cytoplasm. In this case, once integrin expressed on leucocyte surface is recognized by ECs adhesion molecules, cabelolea translocate from cytoplasm to cell membrane and thereafter construct intracellular channels facilitating leucocyte migration. Transcellular transmigration is prone to occurring in weak ECs layer in response to ECs dysfunction.

After transmigration through ECs monolayers, leucocyte continue to migrate into the basement membrane. As discussed above, ECs basement consist of ECMs including collagen and elastin, connected by proteoglycan perlecan. During process of penetrating basement membrane, leucocyte would firstly seek the weak point because of asymmetric distribution of ECMs. The weak sites in basement

membrane locate at the sites, where ECMs are less deposited or the gap between pericytes and ECMs. Meanwhile, these sites are also permissive for cytokines. To note, ECMs such as glycosaminoglycans (GAGs) could also bind to cytokines for leucocyte proliferation or chemotaxis. Furthermore, ECMs could also activate integrin signal on leucocytes when migrating.

1.5.7.2 ECs Migration

ECs migration is involved in angiogenesis, a process in which blood vessel arise from pre-existing vessel. During AV, vascular occlusion results in hypoxic environment. Quiescent ECs are then activated by proangiogenic factors to shape the new lumen, with new connections to supply surrounding cells demands for oxygen and nutrients. Proangiogenic stimuli are mainly chemokines, ECMs and sheer stress. After ECs injury, cytokines such as vascular endothelial growth factor (VEGF) and angiopoietin are released. VEGF is a signal molecule, which binds to its corresponding receptor vascular endothelial growth factor receptor (VEGFR). VEGFR belongs to tyrosine kinase receptor and is widely expressed on ECs. VEGFR is consist of an extracellular domain, a transmembrane region and intracellular domain. Until currently, in total four VEGF subtype (A/B/C/D) and three VEGFR (1/2/3) are found in VEGF/VEGFR signalling. When extracellular domain of VEGFR is activated by VEGF, VEGFR undergoes dimerization and relays signals into the cytoplasm. Intracellular tyrosine kinase is then activated for transphosphorylation on specific tyrosine kinase, which could recruit SH2 containing adaptors to convey downstream signalling. Then activated Rac and Cdc42 produced ECs protrusion, which is amplified by PI3K signalling. Several studies also showed that intercellular interaction inhibit ECs migration. Data was shown that VEGF is efficient in dissociating adhesion between ECs to facilitate ECs migration[207]. Angiopoietin is another cytokine released during ECs dysfunction. Four forms angiopoietin are now identified which are angiopoietin (1/2/3/4). Receptors of angiopoietin are Tie-1 and Tie-2. Similar to VEGF/VEGFR signalling, Tie1/2 activation also mediates phosphorylation on specific tyrosine kinase. This stimulates downstream migration signalling. In addition to migration, angiopoietin also stabilizes nascent vessel. It was shown that angiopoietin could stimulate ECs to release cytokines such as TGF-β and PDGF. SMCs or pericytes are recruited under these cytokines to contribute to ECs stability via secreting ECMs.

ECMs are another stimulus inducing ECs migration. ECMs type determines pattern of ECs migration. During normal state, ECs attach to ECMs and preserve endothelium integrity. However, once ECMs are eradicated, ECs migration is initiated because of altered ECMs. For example, collagen I and fibronectin could support ECs migration[208]. Meanwhile, ECMs could function as cytokines scaffold to reserve cytokines. These cytokines could positively or negatively regulate ECs migration. Therefore, when ECMs are degraded during vascular remodelling, reserved cytokines can be released in the vascular microenvironment to control angiogenesis. Furthermore, interaction between ECs and ECMs also plays an important role in ECs migration. Through integrin as well as intracellular adhesion molecules, cytoskeleton connects ECs to ECMs. Adhesion and de-adhesion processed can be therefore regulated because of different type and gradient of ECMs. Integrin expression on ECs can also be regulated by cytokines. For example, $\alpha_v\beta_3$, $\alpha_v\beta_5$ and $\alpha_5\beta_1$ on ECs are upregulated by VEGF for angiogenesis[209]. Shortly after integrin engagement, FAK undergoes conformational change and controls deadhesion signal. Sheer stress could also induce ECs migration. In physiological state, the endothelium is protected by glycocalyx expressed on ECs. However, after allo-graft transplantation, ECs are directly exposed to sheer stress. Once stimulated by sheer stress, ECs would polarize by cytoskeleton remodelling. Signals from sheer stress is sensed by integrin to activate Rho family GTPases to generate protrusion. Meanwhile, RhoA is also activated to provide contraction required for rear detachment and migration.

1.5.7.3 SMCs Migration

Similar to ECs, SMCs migration after vascular injury is also regulated by several factors including cytokines, ECMs and sheer stress. In AV, SMCs are induced to migrate towards the lesion site. Platelet-derived growth factor (PDGF) is one cytokine to induce SMCs migration. PDGF is a dimeric glycoprotein composed of two subunit such as PDGF-AA, PDGF-BB, PDGF-AB, PDGF-CC and PDGF-DD. Its corresponding receptor is PDGFR, which is a tyrosine kinase receptor and includes two isoforms PDGFR-α/β. PDGFR is composed of extracellular immunoglobulin like domain and intracellular tyrosine kinase domain. Once binding with PDGF ligand, PDGFR dimerises to activate downstream signalling. However, the effect on SMCs migration depends on PDFG isoform. For example, PDGF-BB induces SMCs mobilization, whereas PDFG-AA inhibits SMCs migration. Meanwhile, besides of

direct simulation, PDGF-BB could also induce SMCs to secret cytokines such as FGF-2 in an autocrine fashion for migration[210]. Fibroblast growth factor (FGF) is another cluster of signalling proteins and data showed that FGF-2 facilitates SMCs motility[211]. Receptor of FGF is FGFR, which is also a tyrosine kinase receptor to pass signal into cytoplasm.

In uninjured vessel, SMCs are trapped in elastin in the media layer. Elastin favours SMCs contractile state with little capability to proliferate and migrate. During these state, ECMs and SMCs are relatively stable to adhere with each other. However, during allograft induced arteriosclerosis, component of ECMs are altered to induce SMCs to migrate. ECs dysfunction provides inflammatory cells opportunities in continuing to break through the basement layer. In this process, inflammatory cells secrete metalloproteinase to degrade ECMs, mainly elastin in graft media layer. Meanwhile, to restore the injured tissue, soluble fibronectin accumulates in lesion. Then fibronectin, stimulates intimal myocyte, fibroblast or inflammatory cells to secret fibrotic ECMs such as collagen I and collagen IV. On the other hand, soluble fibronectin is replaced by insoluble fibronectin. Subsequently, along with other fibrotic ECMs, fibronectin stimulates phenotypic change of SMCs from a contractile state to a proliferating type. Mobility of SMCs is meanwhile upregulated. Several fibrotic ECMs induce SMCs migration including fibronectin, collagen I, collagen IV, and lamina[212]. Once integrin adheres with ECMs, signal would be transmitted into SMCs cytoplasm triggering cells to migrate via cytoskeleton arrangement.

Haemodynamic factors would also affect SMCs phenotype change and migration. During normal state, SMCs layer is covered by ECs layer. SMCs sense sheer stress via ECs signalling. By ECs secreted cytokines, SMCs homeostasis is regulated under normal shear stress. However, after ECs dysfunction or death, SMCs are directly exposed to shear stress. The balance between percentage of contractile and proliferation SMCs form is interrupted. Meanwhile, because of intima hyperplasia, normal shear stress is transformed into oscillatory shear stress. It was shown that oscillatory shear stress promotes SMCs phenotype transformation into synthetic form. Under this state, mobility of SMCs is increased. Then guided by chemokines attraction, SMCs migrate to intima layer involved neointima formation. With the neointima further proceeding, ESPCs are recruited to the endothelium layer for ECs regeneration. Along with residual ECs, newly formed ECs would cover SMCs on lesion surface again.

Because of the intruded lesion, AV plaque is naturally divided into two parts according to blood flow direction. In upstream regions, blood flow is high shear stress and directly strike the vessel wall. In this case, high shear stress induces ECs to secrete nitric oxide (NO) which decreases SMCs migration but increases SMCs apoptosis[213]. Therefore, in lesions upstream, SMCs are prone to form a necrotic core and rupture. In downstream of the lesion, low shear stress or oscillatory shear stress induce PDGF and TGF secretion from ECs. Then under the influence of these cytokines, proliferation and migration capability of SMCs are upregulated to support intima thickening[214].

1.6 Hypothesis and Aims

1.6.1 Rationale

After vascular allo-transplantation, both recipient and donor derived inflammatory cells accumulate in the vascular graft, leading to allograft vasculopathy / arteriosclerosis neointima formation. However, the source of other accumulating vascular cells, including ECs and SMCs, is still uncertain. Recently, several SPC populations have been identified from various tissues, however the role of these cells in allograft vasculopathy / arteriosclerosis are still not clear.

1.6.2 Hypothesis

We hypothesized that SPCs from both donor and recipient source tissues are involved in vascular allograft accelerated arteriosclerosis lesion formation and that the recipient source of these SPCs could be various tissues including vascular wall and bone marrow.

1.6.3 Aims

1.6.3.1 Aim 1: To investigate SPCs population in the vessel wall and bone marrow;

Immunostaining of C57/6J animal tissue was used to identify SPCs in both the vessel wall and bone marrow.

1.6.3.2 Aim 2: To establish a lineage tracing mouse model;

C-kit $^{kit/CreER}$; Rosa26-RFP knock in mice were established to trace the fate of SPCs under physiological conditions.

1.6.3.3 Aim 3: To detect the fate of SPCs in allo-graft induced arteriosclerosis;

Vascular allo-transplantation surgery was performed between Balb/c mouse and c-kit $^{kit/CreER}$; Rosa26-RFP transgenic animal, to study SPCs fate from donor and recipient mice, respectively. Furthermore, by creating chimeric mice, the role of bone marrow or non-bone marrow derived SPCs in allograft accelerated arteriosclerosis could be identified.

1.6.3.4 Aim 4: To study the underlying mechanism of SPCs migration.

SPCs migration is known to depend on cytokines. Therefore, mobility pattern of SPCs within vascular allograft under the influence of specific cytokines were tested.

Chapter 2: Methods

2.1 Mice and Artery Allograft Procedure

All animal breeding and surgeries were performed according to required standards in the biological service unit (BSU) at the James Black Centre of King's College London and all procedures were approved by UK Home Office License (PPL70/8944). Chow diet with 12-hour light and 12-hour dark environment at 25 °C was applied to all mice. C-kit $^{kit/CreER}$ knock-in mice (generated from a C57BL/6 background) were a kind gift from the Zhou laboratory, Shanghai Academy of Science, China[61]. Rosa26-RFP reporter mice were purchased from the Jackson Laboratory, USA. C57BL/6J and Balb/c mice were purchased from Harlan, Blackthorn, Bicester, UK. C-kit $^{kit/CreER}$; Rosa26-RFP mice were generated by crossing c-kit $^{kit/CreER}$ and Rosa26-RFP reporter mice, and tracing the fate of c-kit^{+} cells as reported previously[61]. Briefly, the number of c-kit $^{kit/CreER}$ animals was firstly expanded by crossing C-kit $^{kit/CreER}$ with C57BL/6 wild type (WT) mice. Then c-kit $^{kit/CreER}$ mice were crossed with Rosa26-RFP reporter mice. Therefore in theory, the chance to obtain the mice with c-kit $^{kit/CreER}$; Rosa26-RFP genotype from this strategy was 25%. Genotyping was performed via conventional PCR to ensure expression of the target alleles: c-kit-creER (mutant allele: forward: 5'-GCCTTCTATCGCCTTCTTGACG-3'; reverse: 5'-CAGTCGGCACAAAAGCATCAC-3'). ROSA-RFP (mutant allele: forward: 5'- AAGGGAGCTGCAGTGGAGTA-3'; reverse: 5'- CCGAAAATCTGTGGGAAGTC-3'. WT allele: forward: 5'-GGCATTAAAGCAGCGTATCC-3'; reverse: 5'-CTGTTCCTGTACGGCATGG-3').C-kit $^{kit/CreER}$; Rosa26-RFP mice expressing RFP (red fluorescent protein/Tdtomato) signal under the control of the c-kit promoter occurred once tamoxifen induction. 5 pulse intraperitoneal injections of Tamoxifen (Sigma, T5648) dissolved in corn oil (20 mg/ml) on 5 consecutive days ensured Cre recombinase efficiency (0.1–0.15 mg tamoxifen per gram of mouse body weight).

Aorta transplantation was performed between Balb/c mice and C-kit $^{kit/CreER}$; Rosa26-RFP, chimeric mice and wildtype C57BL/6J mice aged 8-12 weeks. Randomised selection of male and female mice was applied in experiments. The allograft transplantation procedure was performed as described previously[66, 98] (Figure 2.1). Briefly, branching artery of donor aorta segments were carefully enclosed by

electrocoagulation to prevent bleeding. Segments were immersed into heparin to prevent coagulation. After the recipient mice were anaesthetised with phenobarbital, a single 20mm incision in the middle of the neck to expose the right common carotid artery. Both distal and proximal ends of the right common carotid artery then were then immobilised by two clips. A cut at the middle of the artery between the two clips was applied and each end was placed within a 1mm cuff. Donor graft was joined to recipient artery by covering over of the cuff. After tight ligation of aortic segment with cuff at each end without bleeding, clipper at each end was released carefully followed by suture of the muscle and skin. Proper observation was exerted on post-surgery mice. For antibody delivery, after aortic segments were implanted to carotid artery, 100 μg ACK2 or control IgG in 30% pluronic F-127 gel (Sigma, P2443) was delivered to the adventitial side of the transplanted aortic grafts.

Figure 2.1

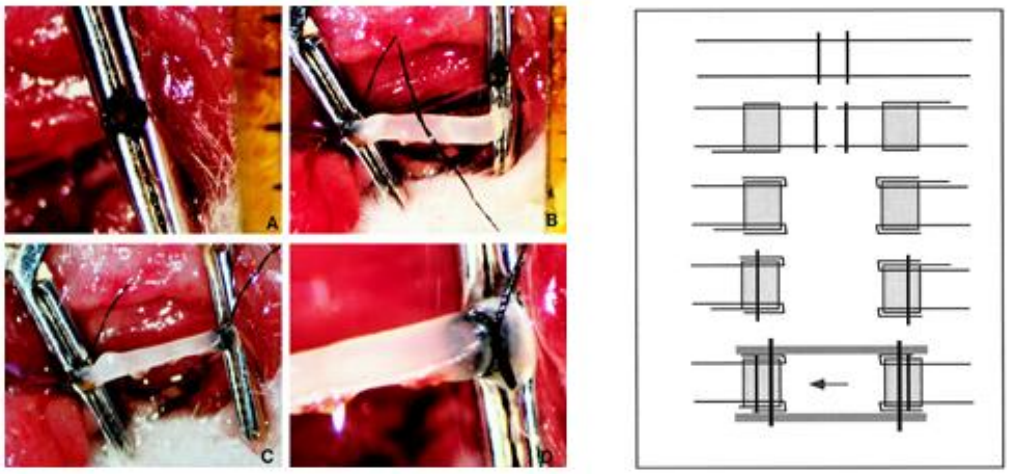

Figure 2.1 Artery allograft procedure. The right common carotid artery was ligated and dissected between the middle ties. The vessel segment passed through a cuff at each end. The vessel end and cuff were then fixed with microhemostat clamps. Vessel segment was turned inside out to cover the cuff. The aortic segment (1 cm) was harvested and grafted between the 2 ends of the carotid artery by sleeving the ends of the vessel over the artery cuff and suturing them together. The vascular clamps were removed; pulsations were seen in the grafted vessel. (Figure Source: Dietrich H,

Hu Y, Zou Y, Dirnhofer S, Kleindienst R, Wick G, Xu Q. Mouse model of transplant arteriosclerosis: Role of intercellular adhesion molecule-1. Arteriosclerosis, thrombosis, and vascular biology. 2000;20:343-352[34].)

2.2 Immunofluorescence and Immunohistochemical staining.

For immunofluorescent staining of mouse tissues, tissues were first collected, washed with PBS and fixed in 4% paraformaldehyde (PFA, Santa Cruz, sc-281692) at 4 °C for 2-3 h. Tissues were then dehydrated in 30% sucrose solution (BDH, 102747E) overnight at 4 °C, embedded in OCT and frozen at -80°C. Tissues were cut to a 10-µm thickness using a CryoStar Cryostat (Thermo Scientific). Frozen sections were firstly fixed in 4% PFA for 10 min, followed by permeabilisation and blocking in 5% donkey serum supplemented with 0.1% Triton X-100 for 1 h at room temperature. Tissues, cells or sections were then stained with primary antibodies in 5% donkey serum overnight at 4 °C, incubated with Alexa Fluor-conjugated secondary antibodies (Invitrogen, 1:500) for 1 h at room temperature, followed by DAPI (Molecular Probe, D1306) staining for 8 min. The control group were solely incubated in PBS with 5% donkey serum over night at 4 °C and then sequentially put secondary antibodies and DAPI. All slides were mounted with anti-fade mounting medium (Dako, s3023). Images were acquired using a Leica (TCS SP5) confocal microscopy by myself but not blinded. Primary antibodies used in this study are shown in Table 2.2.

For immunohistochemical staining of mouse tissues, tissues were firstly fixed in 4% PFA, dehydrated, and embedded in a paraffin block. Serial sections were cut to a 5-µm thickness and stained with haematoxylin and eosin following a standard protocol.

Table 2.2 Primary antibodies used for Immunofluorescence

Antibody	Dilution used	Provider	Code
c-Kit	1:50	R&D	AF1356
c-Kit	1:50	Santa Cruz	sc-5535
CD34	1:100	BD Pharmingen	553731
CD34	1:100	Santa Cruz	sc-7045

Sca-1	1:200	Abcam	ab51317
RFP	1:500	Rockland	600-401-379
α-SMA	1:100	Sigma	A5228
SM22	1:100	Abcam	ab14106
Calponin	1:100	Abcam	ab46794
SCF	1:100	Santa Cruz	sc13126
CD31	1:100	BD Pharmingen	553370
VE-Cadherin	1:100	Santa Cruz	sc-6458
vWF	1:200	Santa Cruz	sc-8068
e-NOS	1:200	BD Pharmingen	610297
VEGF	1:200	Santa Cruz	sc-53462

2.3 Aorta Preparation for Endothelial *En-face* Imaging

Three-month old wild type (C57BL/6J) or C-kit $^{kit/CreER}$; Rosa26-RFP mice were sacrificed by cervical dislocation. PBS was injected into the left ventricle of the heart to wash blood from the aortas, followed by a PFA injection to fix the endothelial cells. The hearts along with the aortas from the aortic root to bifurcation of the abdominal aorta into the common iliac arteries were then isolated intact. Aortas were carefully dissected from the hearts and all heart muscle along with extravascular connective tissue around the aortas was gently removed. Aortas were then put into a solution of PBS with 5% donkey serum (Dako, Agilent Technologies, Denmark) and 0.2% Triton X-100 (Sigma-Aldrich, USA) at room temperature for permeabilisation of the cell membrane and blocking. After 4 h, the tissues were washed with PBS 3×5 min. The

tissues were then cut into pieces and divided into the control and the treatment groups. The control group were solely stained with VE-cadherin, whereas treatment tissues were stained with VE-cadherin and targeting antigens.

The treatment group vessels were incubated with antibody against VE-cadherin, CD34, c-kit and RFP (Table 2.2) at a concentration of 1:100 in PBS with 2% donkey serum over night at 4 °C. Meanwhile the control group vessels were incubated with antibody against VE-cadherin at a concentration of 1:100 in PBS with 2% donkey serum. The following day, the tissues were washed with PBS 3x5 min and treated with the appropriate secondary antibodies, diluted in PBS at a concentration of 1:500. After 1 h incubation at room temperature, tissues were washed 3×5min with PBS and the nucleus was then stained with 4', 6-diamidino-2-phenylindole (DAPI) solution (Sigma-Aldrich, United Kingdom) for 5 min at room temperature. The aortas were washed 3x5 min with PBS and were then ready for mounting. The aortas were first cut into cross-sectional rings of similar size before they were opened directly onto slides (Thermo Scientific, Germany). The rings were opened with the endothelium facing upwards. A drop of fluorescent anti-fade mounting medium (Vector laboratories, United Kingdom) was added before lowering the glass cover slip (Hirschmann-Laborgeräte, Germany) and the slides were stored at 4°C overnight. Tissues were imaged using the Leica SP5 confocal microscopy by myself but not blinded. Images were analysed using ImageJ.

Table 2.3 Primary antibodies used for intima *en-face* tissue preparations

Antibody	Dilution used	Provider	Code
VE-Cadherin	1:100	Santa-Cruz Biotechnology	sc-6458
CD34	1:100	Santa-Cruz Biotechnology	sc-7045
c-kit	1:100	Santa-Cruz Biotechnology	sc-5535
RFP	1:500	Rockland	600-401-379

2.4 Aortic Adventitia Preparation for *En-face* Imaging

Wild type (WT) mice were sacrificed by cervical dislocation. Hearts, along with the aortas from the aortic root to the bifurcation of the abdominal aorta into the common iliac arteries, were isolated intact. The aortas were carefully dissected from the hearts and all heart muscle along with extravascular connective tissue around the aortas was gently removed. Once whole aortas had been digested in 0.4 mg/ml collagenase at 37 °C for 6 min, the adventitia was gently separated from the media of each aorta by peeling the layer up and over the vessel. Adventitia was then put into a solution made of PBS with 0.2% Triton X-100 at room temperature for permeabilisation of the cell membrane for 15min after which the tissue was blocked in 5% donkey serum. The treatment group adventitial tissues were incubated with a rat monoclonal antibody raised against sca-1, CD34 and c-kit with the concentration of 1:100 in PBS with 2% donkey serum, whereas the control group adventitia was solely incubated in PBS with 2% donkey serum over night at 4°C. After the tissues in both treatment and control groups had been washed with PBS 3x5 min, they were treated with the secondary antibodies diluted in PBS at a concentration of 1:500. The processes of DAPI staining process, slide preparation and image process are as the ones in the endothelial *En-face* method 2.3.

Table 2.4 Primary antibodies used for intima *en-face* tissue preparations

Antibody	Dilution used	Provider	Code
Sca-1	1:200	Abcam	ab51317
CD34	1:100	Santa-Cruz Biotechnology	sc-7045
c-kit	1:100	Santa-Cruz Biotechnology	sc-5535
RFP	1:500	Rockland	600-401-379

2.5 Cell Isolation

Graft cell harvest was performed by cutting the whole vessel into 1 mm small pieces followed by collagenase digestion at 38 °C for 30 min. During this process, frequent stirring of pieces of artery ensured full digestion of the tissue. Bone marrow cells were acquired via flushing of PBS through mouse femur and tibia. Spleen tissue was

pulverised. All isolated cells were passed through a 40 μm cell strainer (Falcon, 352340) to remove excess tissue and/or large clots. Bone marrow and spleen cells were incubated with a red blood cell lysis buffer (eBioscience, 00-4333) for 20 min to remove peripheral red blood cells. All prepared samples were kept on ice for flow cytometry analysis.

2.6 Flow Cytometry Analysis

Harvested cell pellets were labelled with antibodies at 1:50 dilution for 30 min on ice. After centrifugation and discarding of excess supernatant, the cell pellets were re-suspended in PBS and then were ready for analysis. Stained cells were collected on BD LSR Fortessa II flow cytometry (Becton Dickinson) and data was analysed in Flowjo Software. The antibodies applied in this project are shown in table 2.6.

Table 2.6 Antibodies used for flow cytometry analysis

Antibody	Dilution used	Provider	Code
anti-CD34-Alexa Fluor647	1:100	BD bioscience	560233
anti-CD117(c-kit)-PE	1:100	Biolegend	105807
anti-Ly-6A/E(Sca-1)-PE/Cy7	1:100	Biolegend	108114
anti-CD29(Intergrinβ-1)-PE	1:100	BD bioscience	562801
anti-CD31(Pecam-1)-PE/Cy7	1:100	Biolegend	102523
anti-CD45- Alexa Fluor647	1:100	Biolegend	103124
anti-CD146-FITC	1:100	eBioscience	11-1469-41
anti-CD201(EPCR)-PE	1:100	eBioscience	12-2012-80
anti-CD140a(PDGFRa)-APC	1:100	eBioscience	17-1401-81

anti-CD105(Endoglin)-PE	1:100	eBioscience	120407
anti-CD44-PE/Cy7	1:100	eBioscience	103029
anti-Ki-67-FITC	1:100	eBioscience	11-5698-82

2.7 Bone Marrow Reconstitution

The procedures used in the creation of chimeric mice were performed as previously described[98]. Briefly, harvest of donor bone marrow cells by flushing mouse femurs and tibias with PBS was followed by removal of excess tissue and/or large clots via passing cells through a 40 μm cell strainer in a similar procedure described above. Harvested cells were stored in serum free medium. A lethal dose of whole-body irradiation (900 rads X-Ray) was applied to recipient mice. 6 h later, chimeric mice were established via bone marrow transplantation in which 5×10^6 unfractionated donor bone marrow cells were injected into the tail veins of irradiated recipient mice. An animal model for further use was acquired following tamoxifen induction of the similar strategy described above, on chimeric mice two weeks after bone marrow transplantation. The efficiency of bone marrow transplantation was determined by RFP detection using flow cytometry described above. Allograft transplantation of aortic segments from Balb/c mice to chimeric mice was not performed until the full reconstitution of bone marrow in chimeric mice and establishment of animal model.

2.8 Mouse Vascular Stem/Progenitor Cell Isolating and Culture

The procedure used for mouse vascular stem/progenitor cell (SPCs) isolation and culture was performed as previously described. Briefly, isograft of vena cava to carotid artery of recipient was performed (both donor and recipient were C57/BL6J mice). Grafts were harvested two weeks after surgery and then cut open and spread onto one 0.2% gelatin (Sigma, G1393) coated T25 flask (culture conditions were set at 37°C with 5% CO2). To ensure cell growth, complete stem cell culture medium consisting of DMEM (ATCC, 30-2002), 10% EmbryoMax ES Cell Qualified FBS (Millipore, ES-009-B), 10 ng/ml leukaemia inhibitory factor (Merck Millipore, LIF1050), 0.1 mM 2-mercaptoethanol (GIBCO, 31350-010), 100 U/ml penicillin-streptomycin (GIBCO,

15140122) and 2 mM L-glutamine (GIBCO, 25030081) was used. SPCs labelling was achieved in sequence by using sca-1(Miltenyi Biotec, 130-092-529) and c-kit (Miltenyi Biotec, 130-091-224) microbeads kit according to manufacturer's instruction. The culture medium was prepared following the recipe described above. Once at 80% confluence, SPCs were digested by trypsin (Glico, 25300-054) and passaged at a ratio of 1:3. The culture medium was changed every other day.

2.9 Cell Sorting

A sca-1$^+$ population of cells was obtained using an anti-Sca-1 MicroBead kit (FITC) (Miltenyi Biotec, Germany) and following the manufacturer's instructions. The cells were first harvested using trypsin-EDTA after they had been washed with PBS. After incubation at 37 °C for 2 min, complete medium was added. The resulting cell suspension was centrifuged at 300 g for 10 min after which the supernatant was aspirated and the cell pellet was resuspended in 90µl MACS buffer (PBS, 0.5% serum and 2 mM EDTA) plus 10 µl of Anti-Sca-1-FITC per 10^7 cells. The suspension was mixed well and incubated in a 4 °C refrigerator for 10 min. 2 ml MACS buffer was then mixed with the cell suspension before it was centrifuged once more at 300 g for 10 min. After aspirating the supernatant, the cell pellet was resuspended in 80 µl of MACS buffer and 20 µl Anti-FITC microbeads per 10^7 cells. The suspension was mixed well and incubated at 4°C for 15 min. After mixing with 2 ml of MACS buffer the suspension was then centrifuged a final time at 300×g for 10 min. Once the supernatant had been aspirated and the cell pellet had been resuspended in 500 µL MACS buffer, the cell suspension was transferred to a pre-washed column in the magnetic field of a MACS Separator. After all the cells had passed through the column, the column was washed three times, each time with 500µl MACS buffer. New buffer was added only when the column reservoir was empty. The column was removed from the magnetic field of the separator and placed in a suitable collection tube. Afterwards, 1 ml buffer was loaded into the column and then was pushed by the plunger to flush out the magnetically labelled cells. The cell suspension was centrifuged at 1000 rpm for 5 min. After the supernatant was fully aspirated the cell pellet was resuspended in complete medium and the Sca-1$^+$ cells were transferred to 0.04% gelatin coated flasks. The c-kit$^+$ cells were sorted using the CD117 microbead kit (Miltenyi Biotec, Germany). Briefly, the cells were harvested by using trypsin-EDTA as previously described. After the cell suspension had been centrifuged at 300 g for 10 min, the supernatant was aspirated.

The cell pellet was then resuspended in 80 µl MACS buffer and 20 µl of c-kit microbeads per 10^7 total cells. The suspension was mixed well and incubated at 4 °C in the refrigerator for 15 min. The suspension was then centrifuged at 300 g for 10 min after 2 ml MACS buffer had been added to the suspension. Once the supernatant had been aspirated and the cell pellet had been resuspended in 500 µl MACS buffer, the cell suspension was transferred to a column in the magnetic field of a MACS Separator. Then the magnetic sorting was carried as described for sca-1(Figure 2.9).

Figure 2.9

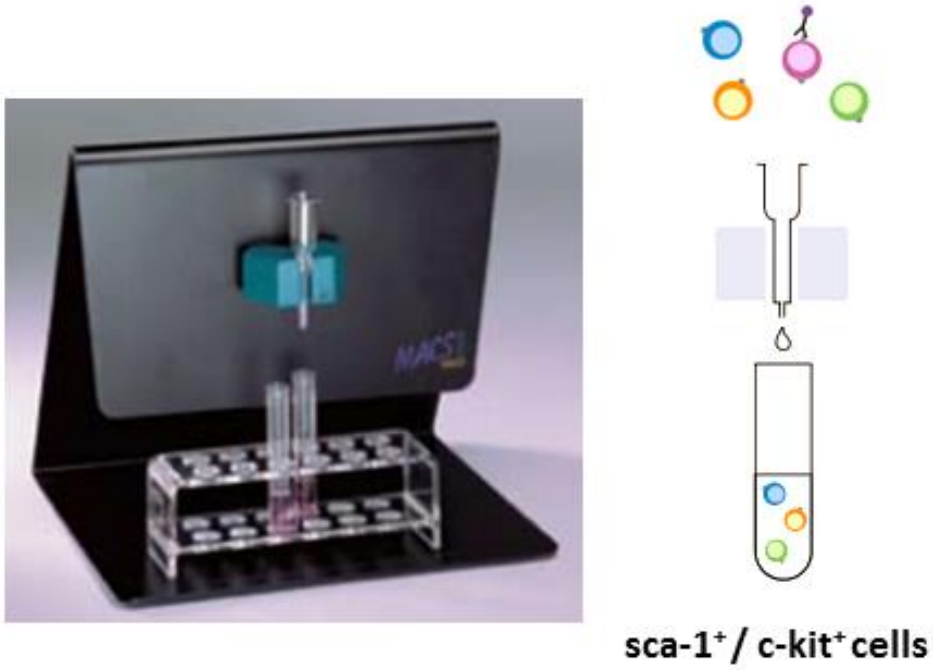

Figure 2.9 Cell Sorting. Cell pellets were incubated with microbeads containing antibody coated magnetic microbeads in MACS buffer. After labelling, cells were passed through a column in a magnetic field to exclude non-labelled cells. Magnetically labelled cells were then pushed out from the column and these positive sca-1$^+$ and/or c-kit$^+$ cells were further cultured.

2.10 Transwell Migration Assay

Transwell migration assays were performed using transwell kits (Corning Costar, 3464) with 8.0 µm pore membrane filters (Figure 2.10). Seeding 1×10^6 SPCs with 100 µl

serum free medium in the upper chamber at 37 °C for 10 min was followed by loading gradients SCF (Pepro Technology, 250-03) (0, 1,10,100 ng/ml) or VEGF (Pepro Technology, 450-32)(25, 50,100ng/ml) in a total of 600 µl serum free medium into the lower chamber. In experiments concerning c-kit blocking antibody ACK2 (eBioscience, 14-1172-85) or IgG antibody as control, antibody was loaded in both upper and lower chambers. AKT inhibitor X (Millipore, 124020) was loaded similarly. After 18h incubation, medium from both upper and lower chambers was discarded. The migrating cells on the reverse surface of the transwell filter were sequentially fixed in 4% PFA for 10 min and then stained with 1% crystal violet solution (Sigma Aldrich, HT90132) for 15 min (both processes were at room temperature). Non-migrating cells remaining on the top of transwell filter were removed by cotton swabs ensuring the images recorded captured only migrated stained cells on the reverse surface. Cells were counted at 5 random fields of the view under the microscope (at 20×).

Figure 2.10

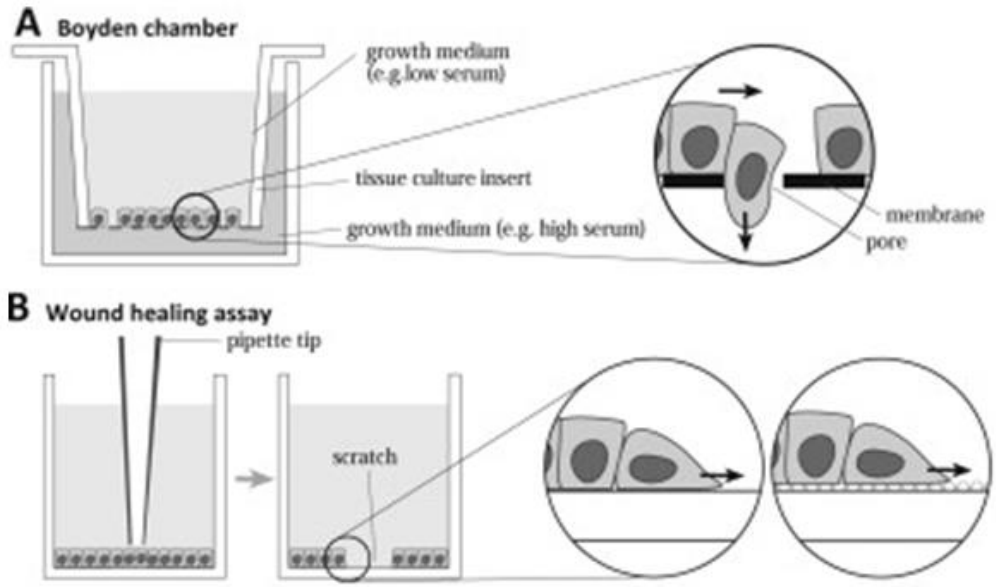

Figure 2.10 *in vitro* Migration Assay. A, Transwell migration assay. Cells migrate through a pore in the membrane. **B**, Wound healing assay. Cells were scratched from a dense monolayer a pipette tip to produce a cell free area. Closure of the wound area represents rate of cell migration. (Figure Source: Kramer N, Walzl A, Unger C, Rosner

M, Krupitza G, Hengstschlager M, Dolznig H. *In vitro* cell migration and invasion assays. *Mutation research*. 2013;752:10-24[215].)

2.11 Scratch-wound Healing Assay

SPCs were seeded in culture medium in a 12-well plate (Figure 2.10). The density was 1×10^5 cells per well. Once at 80% confluence, a scratch in the surface coverage of cells was made using a 1000 µl pipette tip and culture medium was removed. Images of the initial width of the gap were obtained under the microscope (at 20x) in 5 fields. A concentration gradient (0, 1, 10,100 ng/ml) of murine stem cell factor (SCF) (Peprotech, AF-250-03) in the serum free medium was added to the cells. After 16 h culture, images in 5 fields were recorded. Mean area change between the two sides of the scratch compared with that in the initial scratch was shown as data indicated.

2.12 BrdU Proliferation ELISA Assay

Cell proliferation was tested using the cell proliferation ELISA, BrdU (colorimetric) kit (Roche, USA). Briefly, 5000 VPCs and APCs were added to a 96 well plate (Sigma-Aldrich, Corning-Costar, USA) which had been coated with 0.04% gelatin and incubated with complete medium overnight. After the complete medium was removed, 100 µl serum free medium with various concentrations of SCF (0, 1, 10,100 ng/ml) was added into the wells to culture the cells for 18 h. Afterwards 10 µl BrdU labelling solution was added per well and the cells were incubated for an additional 2 h after which the medium was removed. 200 µl FixDenat was added per well for 30 min and then removed. Subsequently 100 µl anti-BrdU-POD working solution was added per well for extra 90min and then removed. Once every well had been washed with 300 µl washing solution 3 times, 100 µl substrate solution was added and then the absorbance of the samples measured at 450 nm (reference wavelength is 690 nm) in a platereader (Life science, Tecan, Infinite M200 Pro, United Kingdom).

2.13 Protein Extraction and Quantification

Cells were lysed on ice for 40 min by a lysis buffer consisting of RIPA buffer (Thermo Fisher, 89901), phosphatase inhibitor tablets (Roche, 04906837001,) and protease inhibitor tablets (Roche, 05892970001). The resulting cell lysate was transferred to a 1.5ml crystal clear microcentrifuge tube (Starlab, E1415-1500) and sonicated using a Branson Sonifier 150 at level 1 for twice, each time for 8 seconds. After 15 min

centrifugation at 15000 g speed at 4 ºC, supernatant was collected and transferred to a new 1.5ml microcentrifuge tube. Quantification of protein concentration was performed by DC Biorad protein assay according to manufacturer's instruction. Briefly, reagent A and reagent B were sequentially mixed with sample, absorption was read at 750 nm and protein concentration was measured according to a resulting standard curve.

2.14 Western Blot

The loading buffer was prepared using 4 X LDS sample buffer (life-technologies, Thermo-Fisher, United Kingdom) supplemented with 10% 2-mercaptoethanol. The 30µl sample volume was made of protein samples, loading buffer and distilled water. Specifically, the composition of the loading sample is that 30µg protein samples diluted with distilled water made up 3/4 and LDS buffer 1/4. Once loading samples had been prepared, they were centrifuged for a short time and incubated at 95°C for 10 min.

NuPAGE 4-12% bis-tris Gels (life-technologies, Thermo-Fisher, United Kingdom) were loaded into a running gel tank, and the comb was carefully removed. First running buffer was added to the wells to remove excess acrylamide. After the running buffer (50 ml 20X running buffer + 950 ml PBS) had been added, the samples plus the ladder (Bio-rad, United Kingdom) were loaded into the wells. Any remaining wells were loaded with the 1X LDS to keep the pH balance within the gel. The electrophoresis apparatus was then attached to an electric power supply running at 140 V for 90 min, after which the gel was gently removed from the plastic plates. Transfer buffer consisting of 100 ml 100% methanol (life-technologies, Thermo-Fisher, United Kingdom), 25 ml 20X NuPAGE transfer buffer (life-technologies, Thermo-Fisher, United Kingdom), and 375 ml distilled water was prepared, and used to soak Amersham nitrocellulose Blotting membrane (GE healthcare life science, United Kingdom) and filter paper, which was laid across the gel to make the gel sandwich. Then the transfer process is at the power supply 35 V for 90 min.

After washing with TBST (prepared from tris buffered saline (TBS) tablet (AMERCO, United Kingdom), 0.1% Tween-20 (Sigma-Aldrich, USA) and 100 ml distilled water), the membrane was blocked with 5% non-fat dried milk in TBST for 1 h at 4 °C with shaking. Afterwards the membrane was washed in TBST 3x5 min. The membrane was incubated with primary antibody in TBST overnight at 4 °C with shaking after

which the membrane was washed in TBST, 3x5 min. The membrane was then incubated with secondary antibody for 1h, before it was washed in TBST 3x5 min. To develop the membrane Amersham ECL Western Blotting Detection reagent (GE healthcare life science, RPN2106, United Kingdom) was applied for 2 min at room temperature, the membrane was then put inside plastic film in a hypercassette and developed using Amersham hyperfilm (GE healthcare life science, United Kingdom) in the developing machine (Ecomax, Protech, United Kingdom)**.** Primary antibodies applied in this project are listed in table 2.14.

Table 2.14 Primary antibodies used for western blot

Antibody	Dilution used	Provider	Code
anti-p-ckit	1:200	Cell Signaling	3391S
Anti-c-Kit	1:50	Santa Cruz	sc-5535
anti-MEK1/2	1:200	Cell Signaling	4694S
anti-p-ERK 1/2	1:500	Santa Cruz	sc-16982-R
anti-p-MEK1/2	1:200	Cell Signaling	9154S
anti-ERK 1/2	1:1000	Cell Signaling	4695P
anti-p-JNK	1:200	Santa Cruz	sc-6254
anti-JNK	1:200	Santa Cruz	sc-474
anti-p-c-jun	1:100	Santa Cruz	sc-16312
anti-c-jun	1:100	Santa Cruz	sc74543
anti-p-MLC	1:200	Cell Signaling	3675S
anti-MLC	1:500	Cell Signaling	3672S

anti-p-AKT1/2/3	1:200	Santa Cruz	sc-7985-R
Anti-AKT1/2/3	1:500	Santa Cruz	sc-8312
anti-p-FAK	1:200	Abcam	ab81298
anti-GAPDH	1:1000	Santa Cruz	sc25778

2.15 G-LISA RhoA/Rac1/Cdc42 Activation Assay

GTPase family activation was measured using a G-LISA activation assay kit (Cytoskeleton) including RhoA (BK124-S) / Rac1 (BK128-S) / Cdc42 (BK127-S) according to the manufacturer's instructions. G-LISA was developed to detect small GTPases activity. Similar to ELISA assay, small GTPases effect proteins were coated in the plate. Only GTP but not GDP bounded G protein could bind on the plate. After luminescence reaction, amount of specific GTP bounded G protein could be detected from absorbance number. Briefly, cell lysate was collected from SCF treated SPCs and protein extraction was performed as in 2.13. Measurement of the protein concentration was using detection solution followed manufacturer's instructions. For GTPase family activation measurement study, loading of equalized lysate to one 96 well plate was performed (assay blank was acquired by loading lysis buffer only in some wells). For the purpose of mixing the samples in each well, the plate was placed on an orbital shaker at a speed of 400 rpm for 45 min at 4 ºC. After samples were mixed with antigen presenting buffer for 2 min and cultured with diluted anti-RhoA/Rac1/Cdc42 primary antibody at 400 rpm speed on shaker for 45min. Secondary antibody and HRP detection reagent was then sequentially added to samples. Reactions were terminated by HRP Stop Buffer. Absorbance was read at 490 nm.

2.16 Cellular Cytoskeleton Immunostaining

SCF was loaded on SPCs in 8-well slide. Samples were collected at specific time points and fixed with 4% PFA for 10 min. 0.1% Triton X-100 blocking buffer was applied to samples 1h for blocking and permeabilisation. Staining was achieved by

sequential incubation of samples with focal adhesion primary antibodies including vinculin (Abcam,ab18058,1:50) and p-FAK (Abcam,ab81298,1:100) overnight at 4 °C, secondary antibodies plus phaloidin-488 (Invitrogen, A12379) a high-affinity filamentous actin (F-actin) probe 1h at room temperature and DAPI on slides 8 min for nuclei staining. All slides were mounted with anti-fade mounting medium.

2.17 Mouse ELISA Assay

Concentration measurement of SCF and TGFβ from serum of C57/6J mice or MMP2 and MMP9 from SPCs culture supernatant was achieved via quantification ELISA kit according to the standard protocol provided by manufacturer, respectively. The ELISA kits applied were including Mouse/Rat SCF Quantikine ELISA Kit (R&D, MCK00), Mouse TGF beta1 ELISA Kit (Abcam, ab119557), Total MMP-2 Quantikine ELISA Kit (R&D, MMP200), and Mouse Total MMP-9 Quantikine ELISA kit (R&D, MMPT90). Briefly, in purpose of collecting serum samples, sacrifice of mice was performed by over dose of phenobarbital. Blood from vena cava of mice was collected and blood serum was transferred to a new 1.5 ml vial tube. In terms of cultured cells, supernatant was collected from post-treatment medium. Dilution of collected serum or supernatant was according to each assay. Following each kit protocol, absorbance was read at 450 nm and that at 540 nm or 570 nm was used as wavelength correction.

2.18 RNA Extraction

Total RNA was isolated from SPCs, which had been treated with 100 ng/ml SCF in serum free medium for different time periods (2, 5, 15, 30, 60 min), using the RNeasy Mini kit (QIAGEN, United Kingdom). Briefly, after the cells had been washed with PBS to thoroughly remove the culture medium, 350 µl RLT buffer was added to disrupt the cells. Lysate was then pipetted into a QIAshredder spin column placed in a 2 ml collection tube and centrifuged for 2 min at full speed. Subsequently 350µl ethanol was added to the homogenized lysate and mixed well by pipetting. The sample was then transferred to an RNeasy spin column placed in a 2 ml collection tube and centrifuged at 8000g for 15s. After the flow-through had been discarded, 700µl RW1 buffer was added to the RNeasy spin column and afterwards the sample was centrifuged at 8000g for 15 s to wash the spin column membrane. Once the flow-through had been discarded, 500 µl RPE buffer was added to RNeasy spin column and the sample was centrifuged at 8000g for 2min. This process was repeated twice.

After the flow-through had been discarded, the RNeasy spin column was placed in a new 1.5 ml collection tube and 30µl RNase-free water was added to the RNeasy spin column. After the sample was centrifuged at 8000g for 1min, the RNA was diluted into the solution collected in the collection tube. The RNA concentration was detected using the NanoDrop 1000 Spectrophotometer (Thermo scientific, United Kingdom). Quality of RNA was controlled according to A260/280 ratio. Absorbance at 260 nm measures the RNA concentration and 280 nm measures the protein concentration in the sample. Proper RNA A260/280 ratio ranges between 1.8 and 2.2. The RNA sample was then ready to be used for reverse transcription and polymerase chain reaction (RT-PCR).

2.19 Reverse Transcription (RT) and Quantitative Real-Time Polymerase Chain Reaction (qPCR)

Reverse transcription was performed using the Qiagen kit following the manufacturer's instructions. 14 µl solution including 1 µg RNA sample, with 2 µl gDNA wipeout buffer (QIAGEN, United Kingdom) and distilled water was incubated at 42 °C for 2min in a thermal cycler (Techne, United Kingdom) to eliminate contaminating gDNA in the RNA sample. This 14µl sample was combined with 4 µl reverse transcription buffer (QIAGEN, United Kingdom), 1µl RT primer mix (QIAGEN, United Kingdom) and 1µl quantitative reverse transcriptase (QIAGEN, United Kingdom). The total 20µl reaction solution was incubated in the thermal cycler at 42 °C for 15min and then at 93°C for 3min. After the reverse transcription reaction process, 80 µl RNAse-free water was added to dilute the sample. Afterwards, 2 µl of cDNA samples were added to 10µl sybergreen mix (ThermoFisher, United Kingdom), 1.5 µl primer plus 6.5 µl RNAse-free water. The total cocktail was loaded into a 96 well plate after which the plate was centrifuged at 800 rpm for 1min to mix the sample well. The plate was loaded into the polymerase chain reaction (PCR) machine (Eppendorf, Mastercycler, United Kingdom) to react.

2.20 Conventional Polymerase Chain Reaction (PCR)

Genotyping for the target genes in Kit-CreER; Rosa26-RFP mice, employed polymerase chain reaction (PCR). Amplification of target DNA was achieved by mixture of cDNA with target primers and taq DNA polymerase. After transferring and

running resulting products on 2% agarose gel (Invitrogen, 16500-500), observations of target bands were acquired using a Biospectrum AC Imaging system.

2.21 Agarose Gel Preparation and Observation

2 g of agarose powder (#16500500, Invitrogen) was added to 100 mL 1x TAE buffer (#EC872, National Diagnostic). The mixture was heated to boiling point in a microwave for two minutes. Once the agarose had cooled down to around 60°C, 10 µl of SafeView nucleic acid stain (#NBSSV, NBS Biologicals) was added into the solution. The gel mixture was carefully poured into a Horizon horizontal gel cast electrophoresis apparatus with the well comb inside. Once the gel had reached room temperature and solidified, the gel was gently placed into 1x TAE buffer and the comb was carefully removed. 25 µl of amplified DNA samples together with 5 µl of 6x loading buffer were loaded into each well. Electrophoresis was performed at 160 V for 20 minutes. DNA fragments were visualized under UV light using a Biospectrum Imaging System 500.

2.22 Statistics

All data are presented as mean±standard error of the mean (SEM). Statistical analysis was performed using Graphpad Prism 6 software. Two-group comparisons were conducted via t-test, while more than two-groups were assessed via analysis of variance (ANOVA) followed by Dunnett's multiple comparison tests. $p<0.05$ was considered statistically significant.

Chapter 3: Results

3.1 Stem/Progenitor Cells (SPCs) Distribution in Aorta

For detecting SPCs in mouse aorta, immunostaining of SPC markers including sca-1, CD34 and c-kit on aortic cryosection was performed (Figure 3.1A). SPCs were shown to be mainly distributed in adventitial and endothelial layers. Bone marrow cells were reported to harbour SPCs. Immunostaining in our study showed that bone marrow source of cells also expressed these three markers (Figure 3.1B). *En-face* immunostaining determined the distribution of SPCs in intima layer (Figure 3.1C). Further confirmation of the presence of SPCs in the adventitia layer was via adventitia *en-face* staining (Figure 3.1D).

Figure 3.1

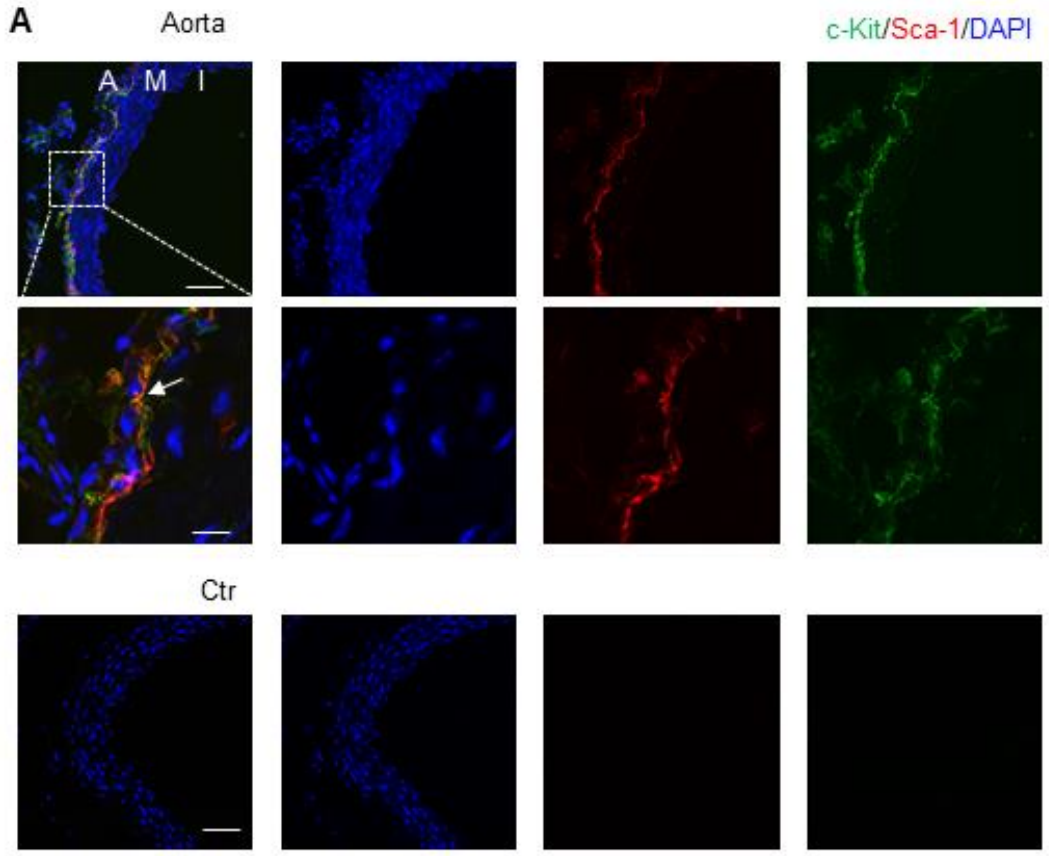

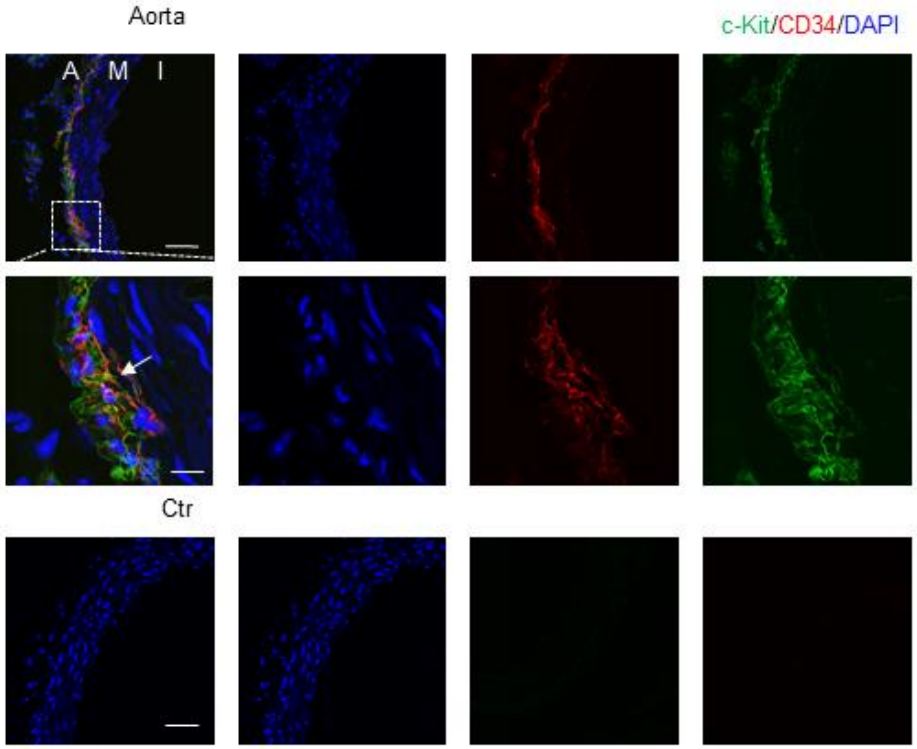
Aorta
c-Kit/CD34/DAPI
A M I
Ctr

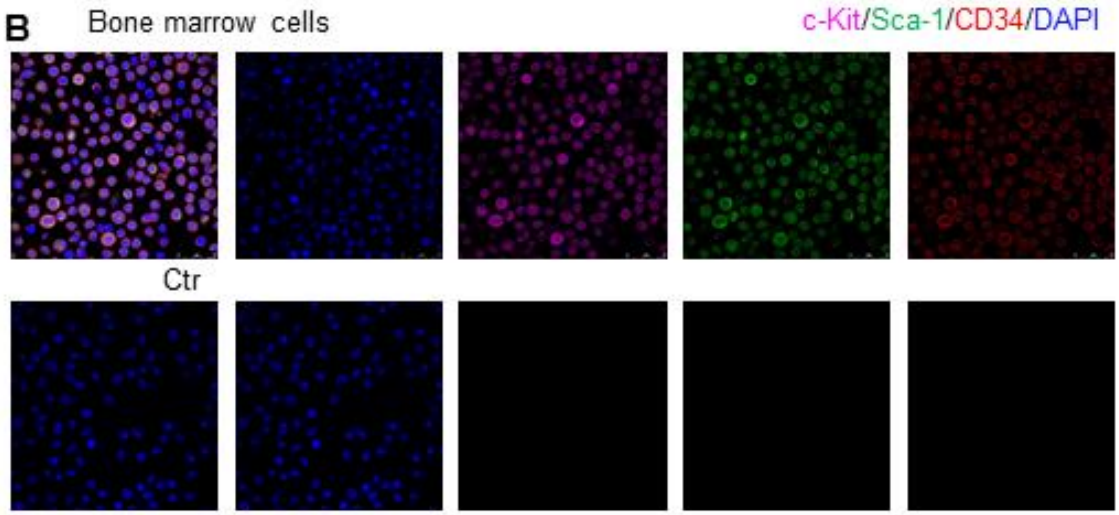
B
Bone marrow cells
c-Kit/Sca-1/CD34/DAPI
Ctr

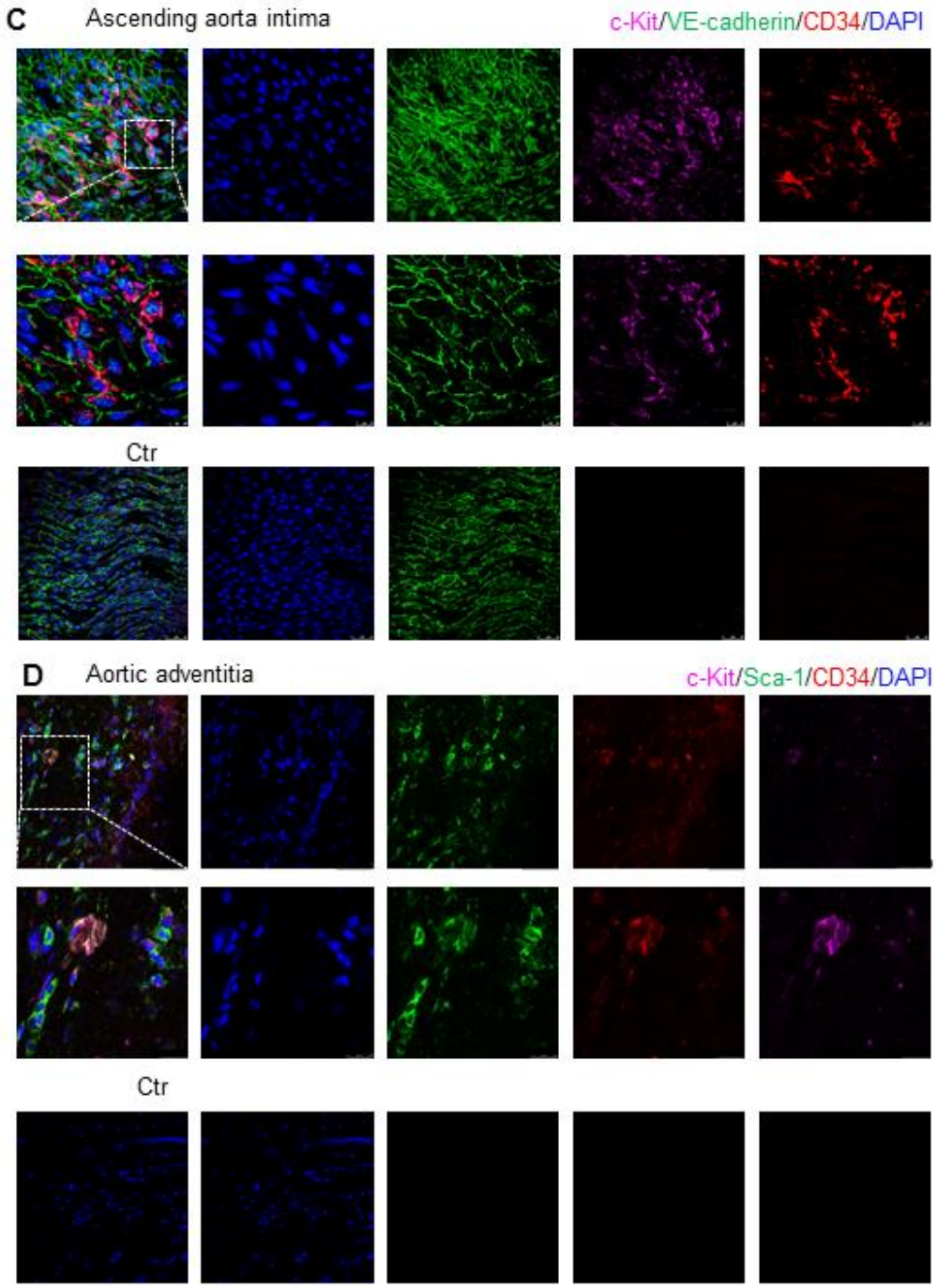

Figure 3.1 SPCs distribution in aorta and bone marrow. Representative images of normal aorta (**A**) and bone marrow (**B**) from wildtype mice stained for c-Kit, Sca-1 and CD34 (n=3 experiments). Arrows indicate vascular SPCs. *En-face* staining of aortic intima (**C**) and adventitial (**D**) layers showing SPCs stained with c-Kit, Sca-1 and CD34 from wildtype mice (n=3). VE-cadherin, an endothelial marker is used to establish the presence of the intima. Scale bars, 100 μm, and 20 μm in the enlarged images. A, adventitia; M, media; I, intima; Ctr, control.

3.2 SPCs in c-kit$^{kit/CreER}$; ROSA26-RFP Mouse

To further address the role of SPCs *in vivo*, a c-kit$^{kit/CreER}$; ROSA26-RFP mouse was employed[61]. Gene construct of this knock-in mouse was achieved through insertion of one piece of cDNA sequenced for Cre recombinase (Cre) combines with a mutant estrogen receptor (ER), into one allele of wild type C57/6J DNA strand, in the frame of promoter sequence of c-kit gene (in this way generation of CreER were acquired under control of c-kit promoter sequence). Rosa26-RFP or Rosa26-CAG-loxP-stop-loxP-tdTomato-WPRE transgenic mice were constructed by gene trap technique. In this animal model, stop codon is flanked by loxP sites. Cross breeding was then performed between c-kit$^{kit/CreER}$ mice and ROSA26-RFP fluorescent reporter mice (Figure 3.2A). Upon tamoxifen injection (five pulses of tamoxifen intraperitoneal injection in five consecutive days), ER component is activated to drive CreER from the cytoplasm into the nucleus and this process only occurs when the cells expressed the c-kit promoter gene. The stop codon framed by a loxP sequence being cut by Cre therefore resulted in red fluorescent protein (RFP) labelling. Since RFP specifically labelled c-Kit$^+$ cells in these mice, we were able to use this mouse model to trace the fate of c-Kit$^+$ SPCs *in vivo*. It should be noted that RFP labelling is permanent in these cells once labelled, regardless of further changes in c-Kit expression, as most SPCs will lose their SPC markers once they differentiate. Kit-CreER; Rosa26-RFP mice were pulsed with tamoxifen and analysed for RFP expression one week later (Figure 3.2A). Flow cytometric analysis showed successful labelling of RFP in cells from bone marrow as well as aorta (Figure 3.2B). We also observed a population of cells expressing both RFP and c-Kit in the aortic adventitia, with a large portion of these RFP$^+$ cells co-staining with Sca-1 and/or CD34, whereas some RFP$^+$ cells were also found to reside in the medial and endothelial layers (Figure 3.2C). Interestingly, few resident c-Kit$^+$ SPCs-derived RFP$^+$ cells were found to co-express smooth muscle marker α-smooth muscle actin (α-SMA) in the media (Figure 3.2D). RFP labelling of c-Kit$^+$ cells was also observed in lung, spleen and liver (Figure 3.2E). Collectively, these data showed that tamoxifen administration in Kit-CreER; Rosa26-RFP mice successfully labelled c-Kit$^+$ cells.

Figure 3.2

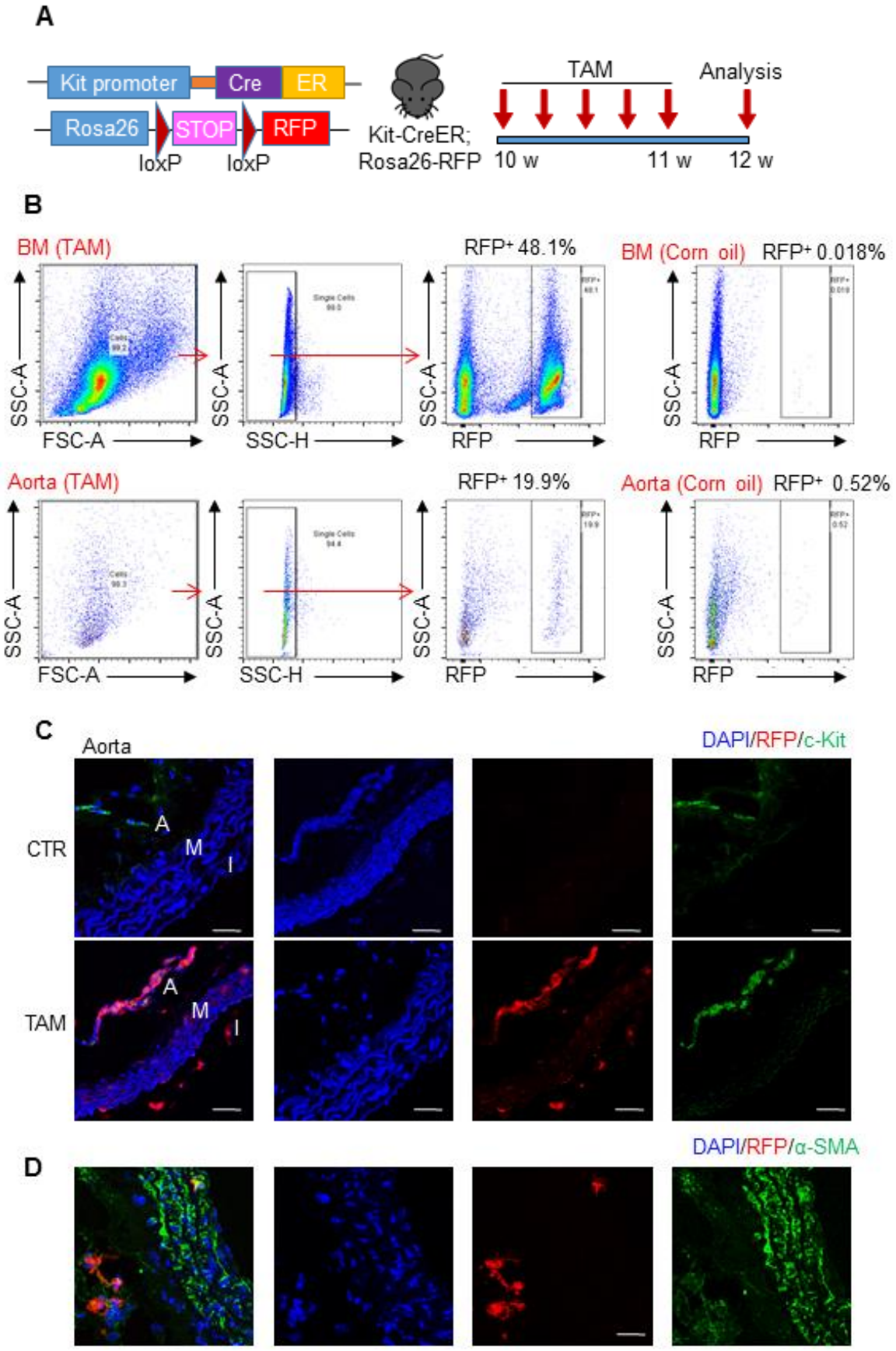
A
Kit promoter
Cre
ER
Rosa26
STOP
RFP
loxP
loxP
Kit-CreER;
Rosa26-RFP
TAM
Analysis
10 w
11 w
12 w
B
BM (TAM)
RFP+ 48.1%
BM (Corn oil)
RFP+ 0.018%
SSC-A
FSC-A
SSC-H
RFP
Aorta (TAM)
RFP+ 19.9%
Aorta (Corn oil)
RFP+ 0.52%
C
Aorta
DAPI/RFP/c-Kit
CTR
TAM
A
M
I
D
DAPI/RFP/α-SMA

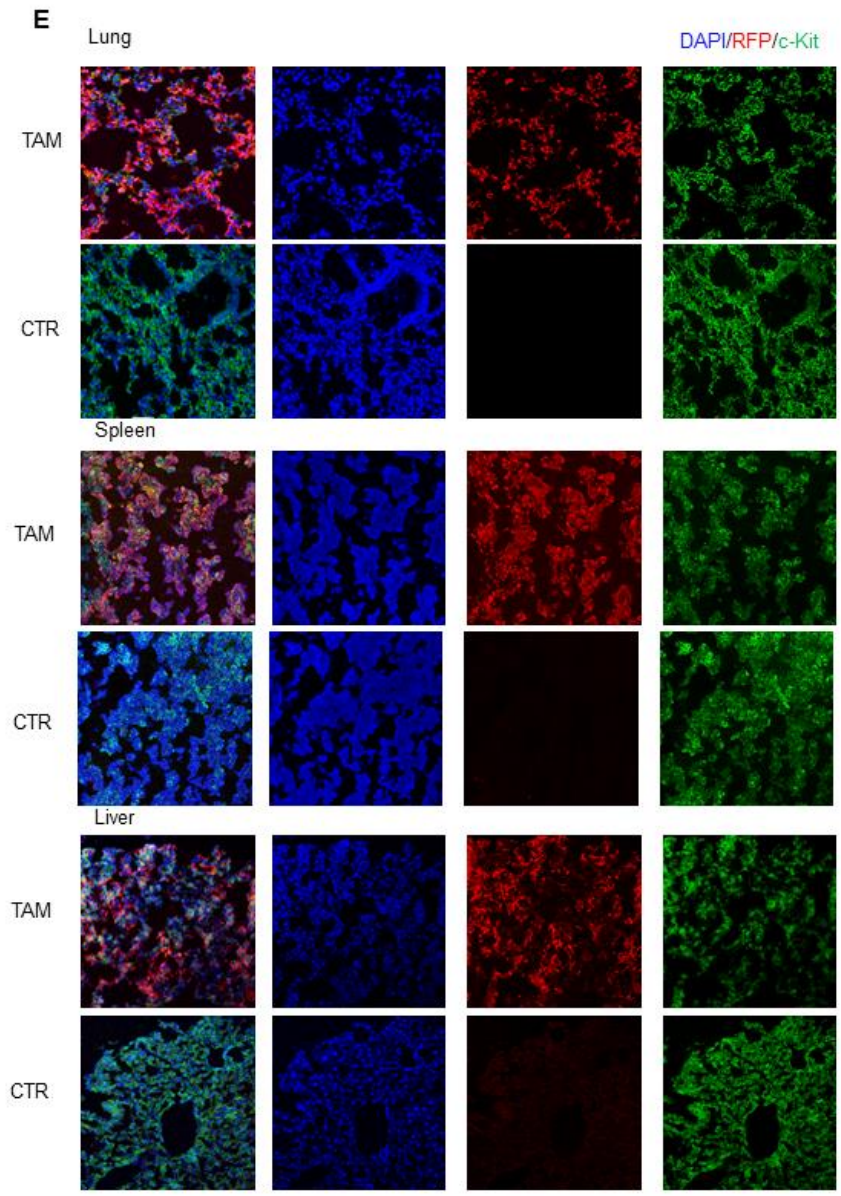

Figure 3.2 Establishment of Kit-CreER; Rosa26-RFP mouse model. A, Strategy for Kit-CreER; Rosa26-RFP mice generation and experimental schedule of tamoxifen-induced RFP labelling of c-Kit$^+$ cells and analysis. **B**, Representative flow cytometric analysis of RFP$^+$ cells in bone marrow and aorta (n=3 experiments). **C**, Representative images showing RFP labelling in vascular SPCs staining for RFP, c-Kit. Scale bars, 100 μm. n=3 experiments. **D**, Representative immunostaining images showing normal aorta from Kit-CreER; Rosa26-RFP mice (n=3) stained with RFP and α-SMA. Scale bars, 50 μm. **E**, Representative images showing RFP$^+$ labelling of c-Kit$^+$ cells in lung, spleen and liver (n=6 mice per group). Scale bars, 100 μm. A, adventitia; M, media; I, neointima; CTR, corn oil control; TAM, tamoxifen.

3.3 C-kit^{+} SPCs in Aortic Intima Layer were not Derived from Bone Marrow

To determine if c-kit^{+} SPCs distribution in endothelial layer, we employed *en-face* immunostaining of c-kit$^{kit/CreER}$; ROSA26-RFP mouse for the full length of aorta, which began from the aortic root and extended to the bifurcation of the abdominal aorta into the common iliac arteries, focusing on the tissue intima (Figure 3.3A). According to aorta anatomy, the artery was divided into five parts. Data showed that positive RFP staining within the intima mainly located at the sites above descending aorta, whereas at the location below the thoracic aorta, no c-kit^{+} SPCs were distributed within the EC layer (Figure 3.3A). Then chimeric mice were developed to detect whether these c-kit^{+} SPCs were derived from bone marrow. Chimeric mice were generated in which bone marrow cells from Kit-CreER; Rosa26-RFP mice were transferred to irradiated wildtype C57BL/6J mice. These chimeric mice were then pulsed with tamoxifen, subjected to allograft transplantation and further graft analysis (Figure 3.3B). Reconstitution of bone marrow was shown after transplantation and was determined via flow cytometry and immunostaining in bone marrow and blood cells (Figure 3.3C). *En-face* staining was then performed on these chimeric animals. Data showed that few aortic ECs contained RFP (Figure 3.3D). This result indicated that c-kit^{+} SPCs in the intima were not derived from bone marrow. Counting of c-kit^{+} SPCs derived ECs in both c-kit$^{kit/CreER}$; ROSA26-RFP mouse and chimeric animal were summarized (Figure 3.3E).

Figure 3.3

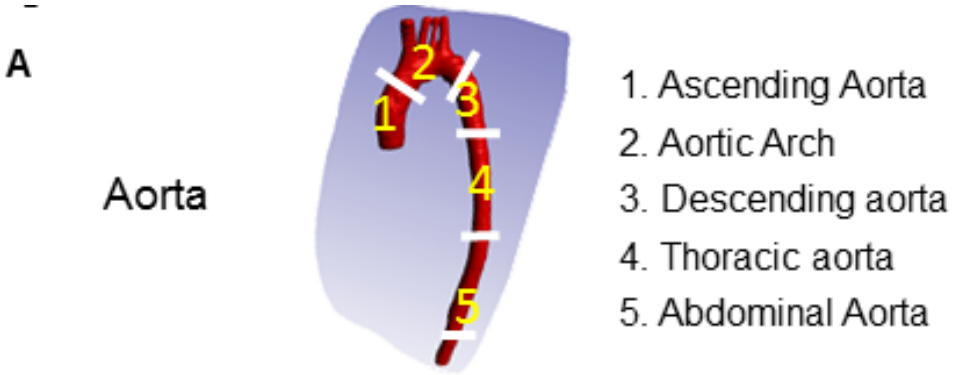

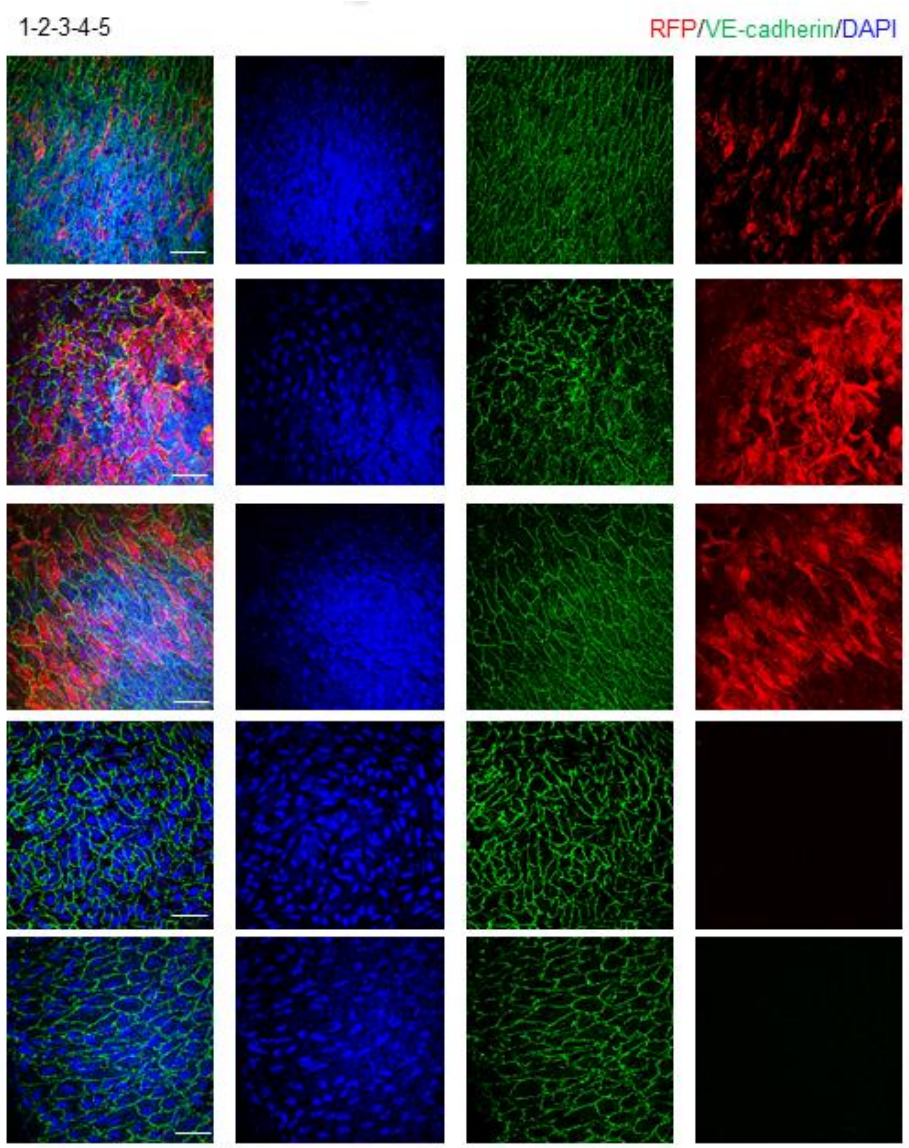
1-2-3-4-5
RFP/VE-cadherin/DAPI

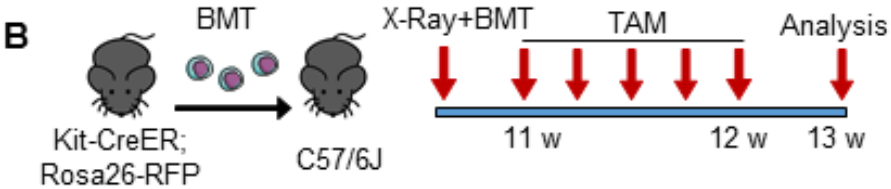
B
BMT
X-Ray+BMT
TAM
Analysis
Kit-CreER;
Rosa26-RFP
C57/6J
11 w
12 w
13 w

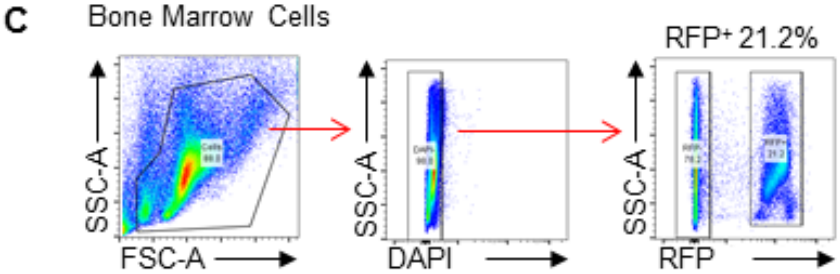
C
Bone Marrow Cells
RFP+ 21.2%
SSC-A
FSC-A
SSC-A
DAPI
SSC-A
RFP

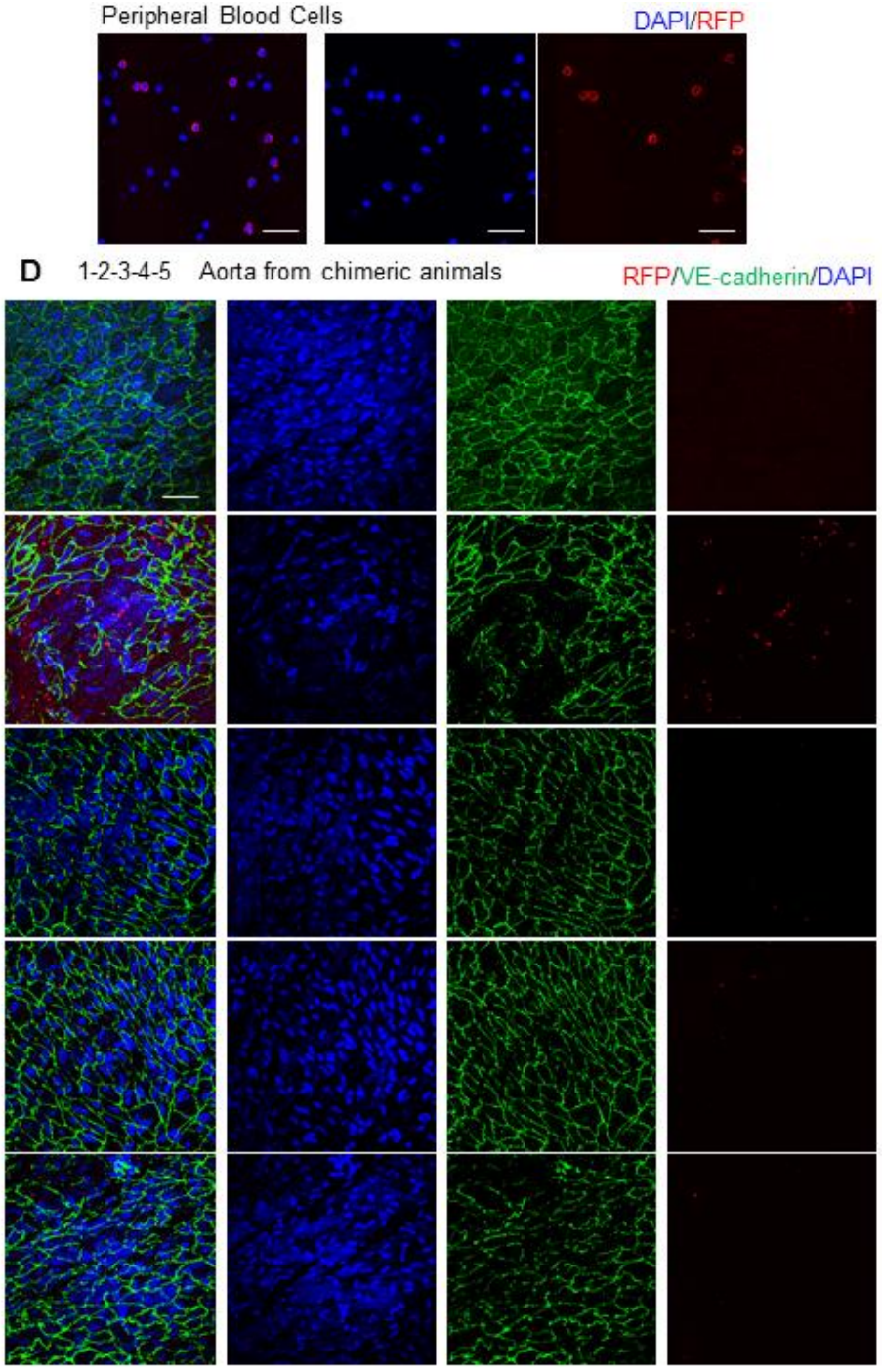
Peripheral Blood Cells
DAPI/RFP
D
1-2-3-4-5 Aorta from chimeric animals
RFP/VE-cadherin/DAPI

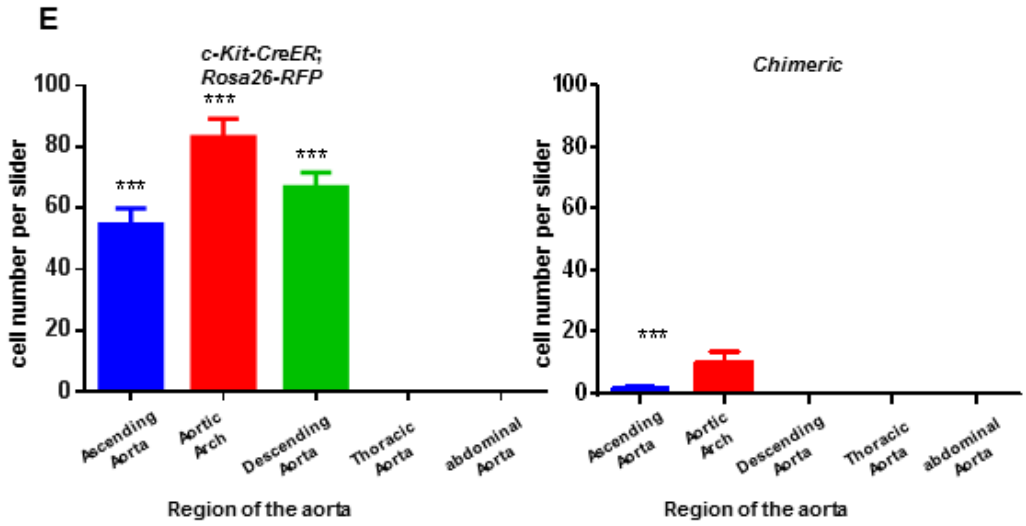

Figure 3.3 C-kit^{+} SPCs in intima layer were not derived from bone marrow. A, *En -face* staining of aortic intima showing SPCs stained with c-Kit^{+} SPC derived cells distribution according to aorta anatomy in Kit-CreER; Rosa26-RFP mice. VE-cadherin was shown as intima marker. Scale bars, 100 μm**.** Representative flow cytometric analysis of bone marrow cells from chimeric mice (n=6 mice per group). **B**, Strategy for chimeric mouse model in which bone marrow from Kit-CreER; Rosa26-RFP mice were transplanted to irradiated C57BL/6J mice, followed by tamoxifen treatment. **C,** Representative immunostaining images of peripheral blood cells stained with RFP from chimeric mice (n=6 mice per group). Scale bars, 25 μm. **D**, *En-face* staining of aortic intima showing SPCs stained with c-Kit^{+} SPCs derived cells distribution in chimeric mice (n=3 experiments). **E**, c-kit^{+} SPCs derived ECs counting in both c-kit$^{kit/CreER}$; ROSA26-RFP and chimeric animal.

3.4 c-kit$^+$ SPCs Identification in Allograft Induced Lesion

We further explored whether SPCs contribute to neointima formation in a mouse allograft model as described previously[34], in which aortic segments from BALB/c mice were transplanted to C56BL/6J mice (Figure 3.4A). Immunostaining of aortic allografts showed neointima formation after allograft transplantation (Figure 3.4B). Importantly a small number of cells expressing c-Kit, Sca-1 and/or CD34 were found in neointimal layers (Figure 3.4B), suggesting a possible role for SPCs in allograft-induced neointima formation. We next asked whether c-Kit$^+$ SPCs contribute to allograft-induced neointima formation. Kit-CreER; Rosa26-RFP mice pulsed with tamoxifen were subject to an allograft transplantation surgery, in which aorta segments from BALB/c mice were transplanted to Kit-CreER; Rosa26-RFP mice. Grafts were collected four weeks after transplantation (Figure 3.4C). Immunostaining of aortic allografts revealed a large number of RFP$^+$ cells accumulated in the neointimal lesions (Figure 3.4D), indicating that c-Kit$^+$ SPCs participate in allograft-induced neointima formation.

Figure 3.4

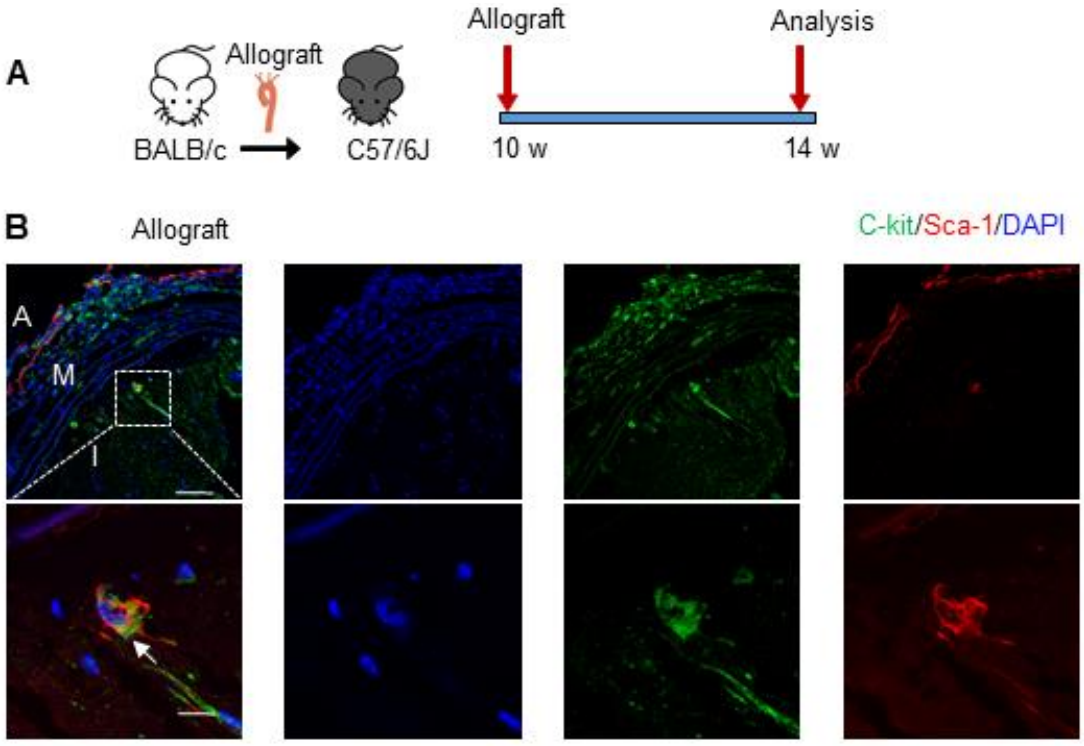

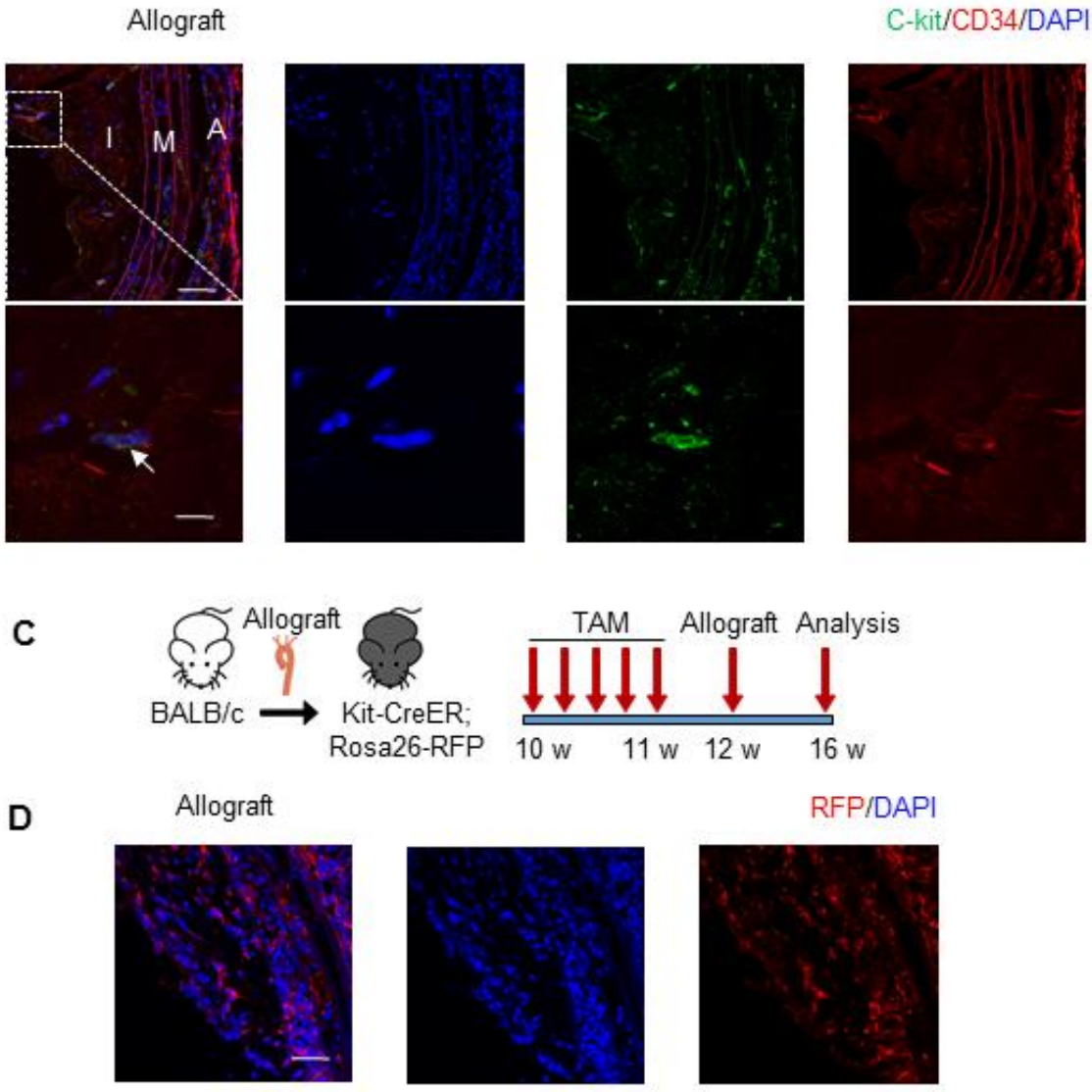

Figure 3.4 C-kit$^+$ SPCs involved in allograft induced lesion formation. A, Schematic showing allograft transplantation experiments. Aortas from BALB/c mice were transplanted to C57/6J mice and grafts were collected 4 weeks after surgery. **B**, Representative images of aortic allograft from allograft mice stained for c-Kit, Sca-1 and CD34 (n=3 experiments). Arrows indicate vascular SPCs. Scale bars, 100 μm, and 20 μm in the enlarged images. **C,** Schematic showing allograft transplantation experiments. After Kit-CreER; Rosa26-RFP mice received tamoxifen injection, aortas from BALB/c mice were transplanted to these mice and grafts were collected 4 weeks after surgery. **D**, Representative images showing aortic grafts from Kit-CreER; Rosa26-RFP mice stained with RFP antibody (n=6 mice per group). A, adventitia; M, media; I, intima or neointima; TAM, tamoxifen.

3.5 Recipient c-Kit$^+$ SPCs Differentiated into SMCs in Neointima and were of Non-Bone Marrow Source

As smooth muscle cells are the major component of neointima, we further explored whether c-Kit$^+$ SPCs may give rise to neointimal SMCs. Immunofluorescence analysis showed that SM22$^+$ and α-SMA$^+$ SMCs were abundant in neointimal lesions. Subsequently, we counted the whole numbers of RFP$^+$ cells, SMCs and the cells which co-expressed both RFP and SMCs markers in the slides. After calculation, we found that 53.54 ± 1.92% of SM22$^+$ and 37.31 ± 1.55% of α-SMA$^+$ SMCs in neointimal lesions were labelled with RFP, whereas 63.57 ± 2.39% and 30.18 ± 1.04% of RFP$^+$ cells showed expression of SM22 and α-SMA, respectively (Figure 3.5A). These data suggest that a large number of neointimal SMCs originate from c-Kit$^+$ SPCs. As RFP only labelled recipient cells in this model, our results also indicate that c-Kit$^+$ SPCs from recipient mice can differentiate into neointimal SMCs *in vivo* and contribute to neointima formation in allograft mouse model. We next sought to address whether these recipient c-Kit$^+$ SPCs originate from bone marrow or non-bone marrow tissues. Aortic graft was allotransplanted from BALB/c mice to chimeric mice (Figure 3.5 B). RFP$^+$ cells were detected in neointimal lesions (Figure 3.5C). However, few RFP$^+$ cells co-expressed SMC markers SM22 and α-SMA (Figure 3.5C), indicating that the origin of c-Kit$^+$ SPCs-derived SMCs was not bone marrow.

Figure 3.5

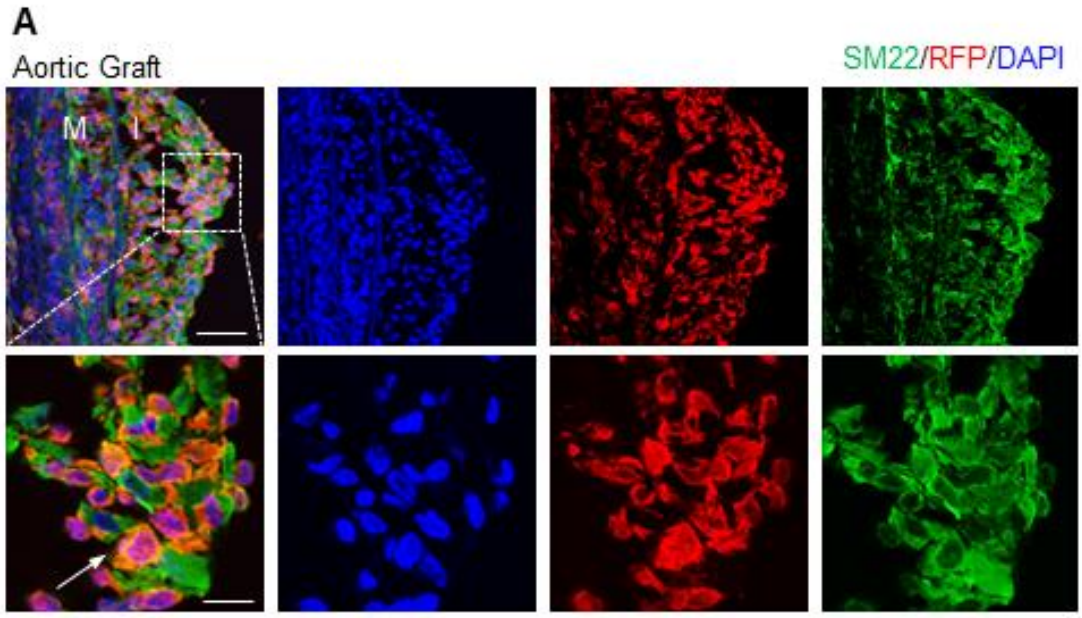

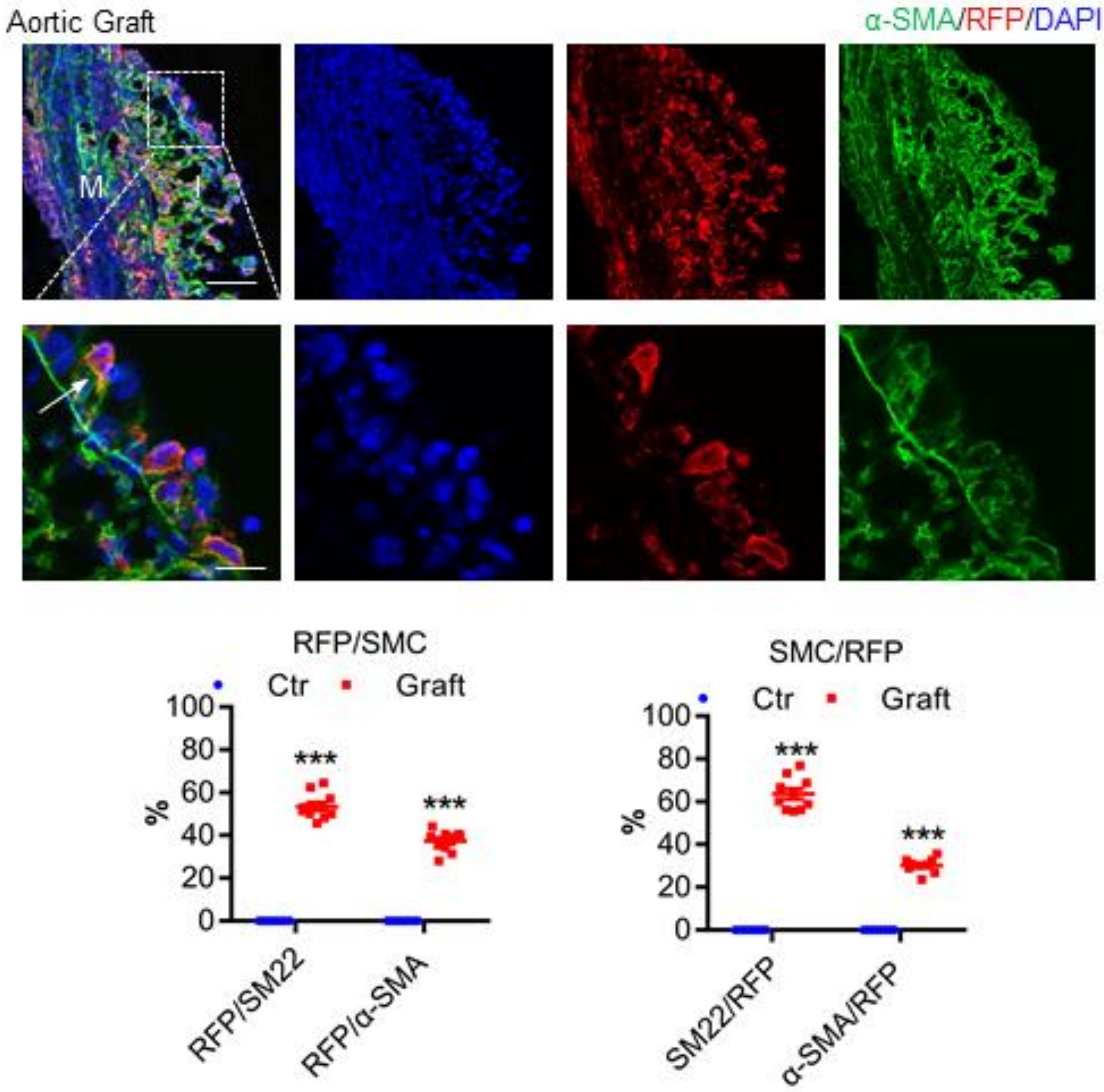
Aortic Graft
α-SMA/RFP/DAPI
M
I
RFP/SMC
Ctr
Graft
100
80
60
40
20
0
%
***
***
RFP/SM22
RFP/α-SMA
SMC/RFP
Ctr
Graft
100
80
60
40
20
0
%
***
***
SM22/RFP
α-SMA/RFP

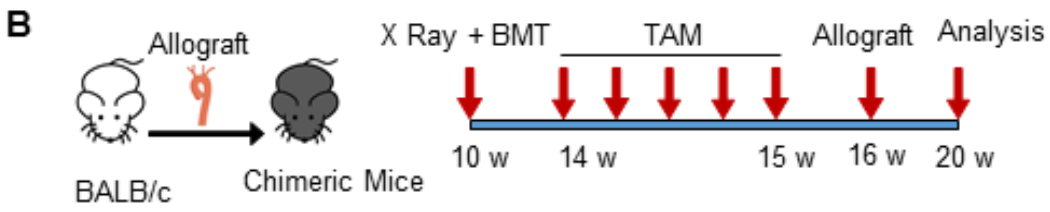
B
Allograft
BALB/c
Chimeric Mice
X Ray + BMT
TAM
Allograft
Analysis
10 w
14 w
15 w
16 w
20 w

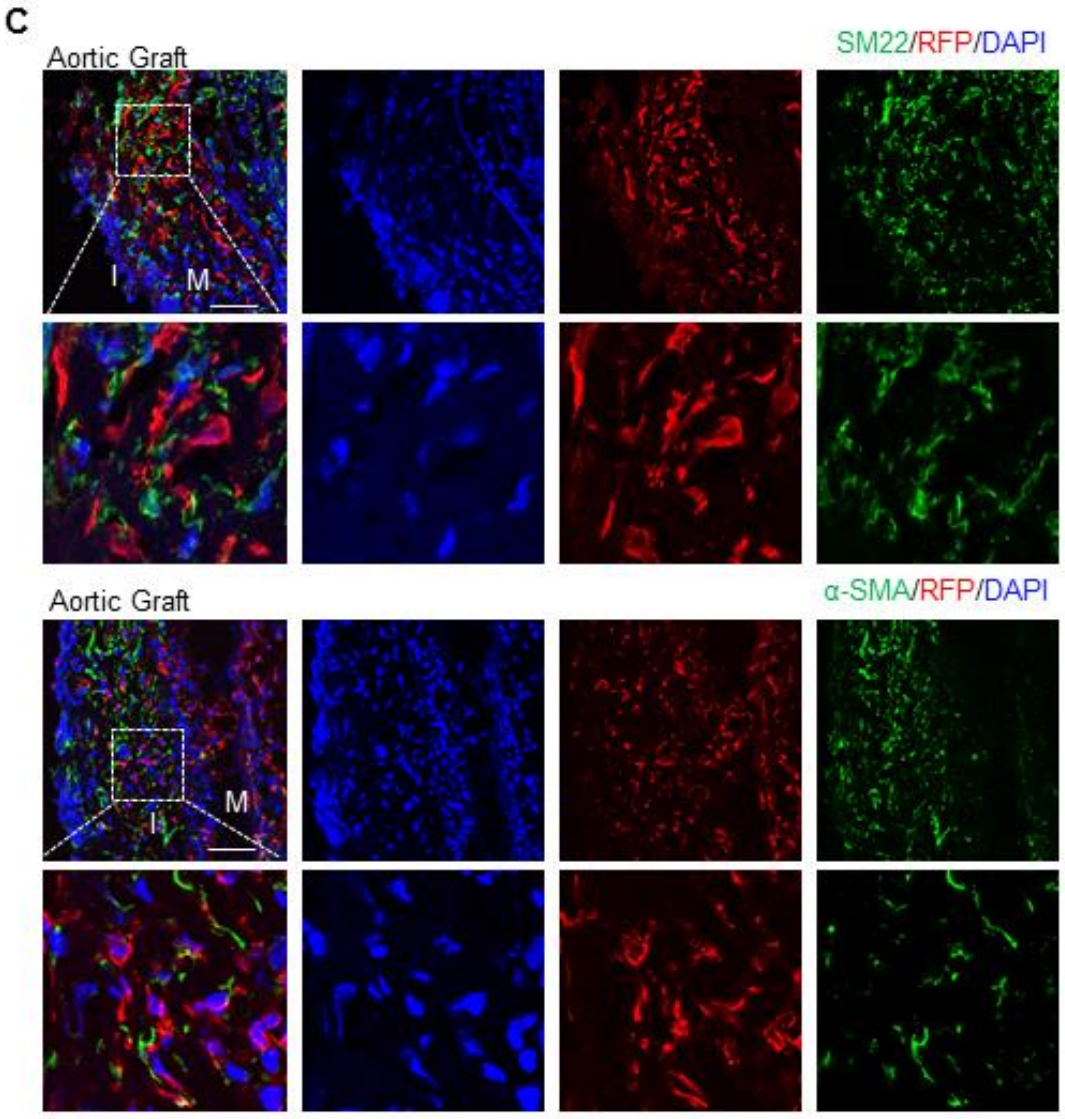

Figure 3.5 Recipient non-bone marrow source of c-kit$^+$ SPCs differentiated into SMCs in neointima. A, Representative images showing aortic allograft from Kit-CreER; Rosa26-RFP mice stained with RFP, SM22 and α-SMA. Scale bars, 50 μm, and 20 μm in enlarged images. Arrows indicate RFP$^+$SM22$^+$ or RFP$^+$α-SMA$^+$ cells. The graphs indicate percentage of RFP expression in SMCs or SMC marker expression in RFP$^+$ cells. Data are mean ± SEM, ***P<0.001, unpaired two-tailed t test, n=10 per group. **B**, Strategy for chimeric mouse model in which bone marrow from Kit-CreER; Rosa26-RFP mice were transplanted to irradiated C57BL/6J mice, followed by tamoxifen treatment and allograft transplantation. **C**, Representative immunostaining images showing aortic graft of chimeric mice with RFP, SM22 and α-SMA staining. n=6 mice per group. Scale bars, 50 μm, and 20 μm in enlarged images. M indicates media; I, neointima; Ctr, control; BMT, bone marrow transplantation; TAM, tamoxifen.

3.6 Recipient c-Kit$^+$ SPCs Differentiated into ECs for Both Luminal ECs Regeneration in Neointima and Microveseels Remodelling in Adventitia

We further explored whether c-Kit$^+$ SPCs might give rise to ECs. Immunofluorescence analysis on the animals same as Figure 3.4C showed that ECs were abundant in neointimal and adventitia lesions in the graft (Figure 3.6A and Figure 3.6B). These ECs were positive for markers including CD31 and VE-cadherin. Since ECs in the graft are responsible for both intima layer regeneration and adventitial layer neovasculogenesis, we therefore tried to detect the role of c-Kit$^+$ SPCs in both luminal ECs regeneration and adventitial microvessel remodelling. Firstly, we analysed ECs in neointima. Similar to the methods before, we count all the numbers of CD31$^+$ cells, RFP$^+$ cells, and the cells which co-expressed with CD31 and RFP. Data showed that 49.37 ± 4.06% of CD31$^+$ cells were labelled with RFP, whereas 27.34 ± 2.58% of RFP$^+$ cells showed expression of CD31 (Figure 3.6A). Then, we analysed ECs in graft adventitial layer. Data showed that 38.47 ± 4.87 % of CD31$^+$ cells were labelled with RFP, whereas 27.21 ± 2.61% of RFP$^+$ cells showed expression of CD31 (Figure 3.6B). These data suggest that c-Kit$^+$ SPCs contributed to both luminal ECs regeneration in neointima and adventitial microvessel ECs remodelling. We next addressed whether bone marrow derived c-Kit$^+$ SPCs contribute to ECs commitment. The aortic graft tissues were collected from the same animals as Figure 3.5B. RFP$^+$ cells and ECs were also detected in both neointimal lesions and adventitial layers in the grafts. In neointima layer, few luminal ECs were labelled with RFP (Figure 3.6C), indicating that the origin of c-Kit$^+$ SPCs-derived luminal ECs was not bone marrow. In adventitial microvessels, some of RFP$^+$ cells co-expressed with ECs marker CD31 (Figure 3.6D). However, none of these RFP$^+$ cells in adventitial microvessels co-expressed with VE-cadherin. Instead large number of these RFP$^+$ cells co-expressed with inflammatory ECs marker VCAM (Figure 3.6D). This result indicated that c-Kit$^+$ SPCs derived from bone marrow were involved in adventitial microvessels remodelling by differentiating into inflammatory ECs.

Figure 3.6

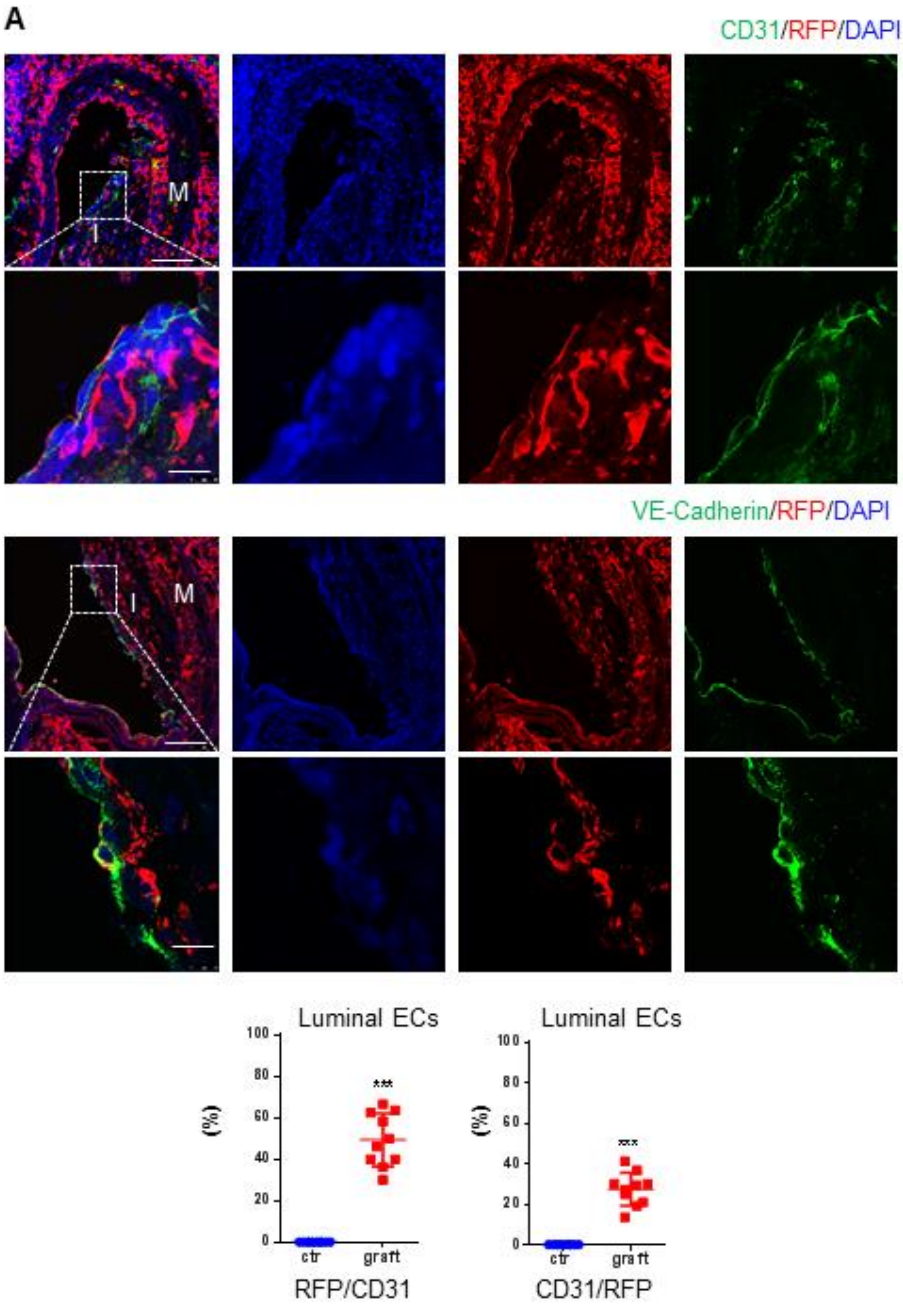
A
CD31/RFP/DAPI
M
I
VE-Cadherin/RFP/DAPI
I
M
Luminal ECs
(%)
100
80
60
40
20
0
***
ctr
graft
RFP/CD31
Luminal ECs
(%)
100
80
60
40
20
0
***
ctr
graft
CD31/RFP

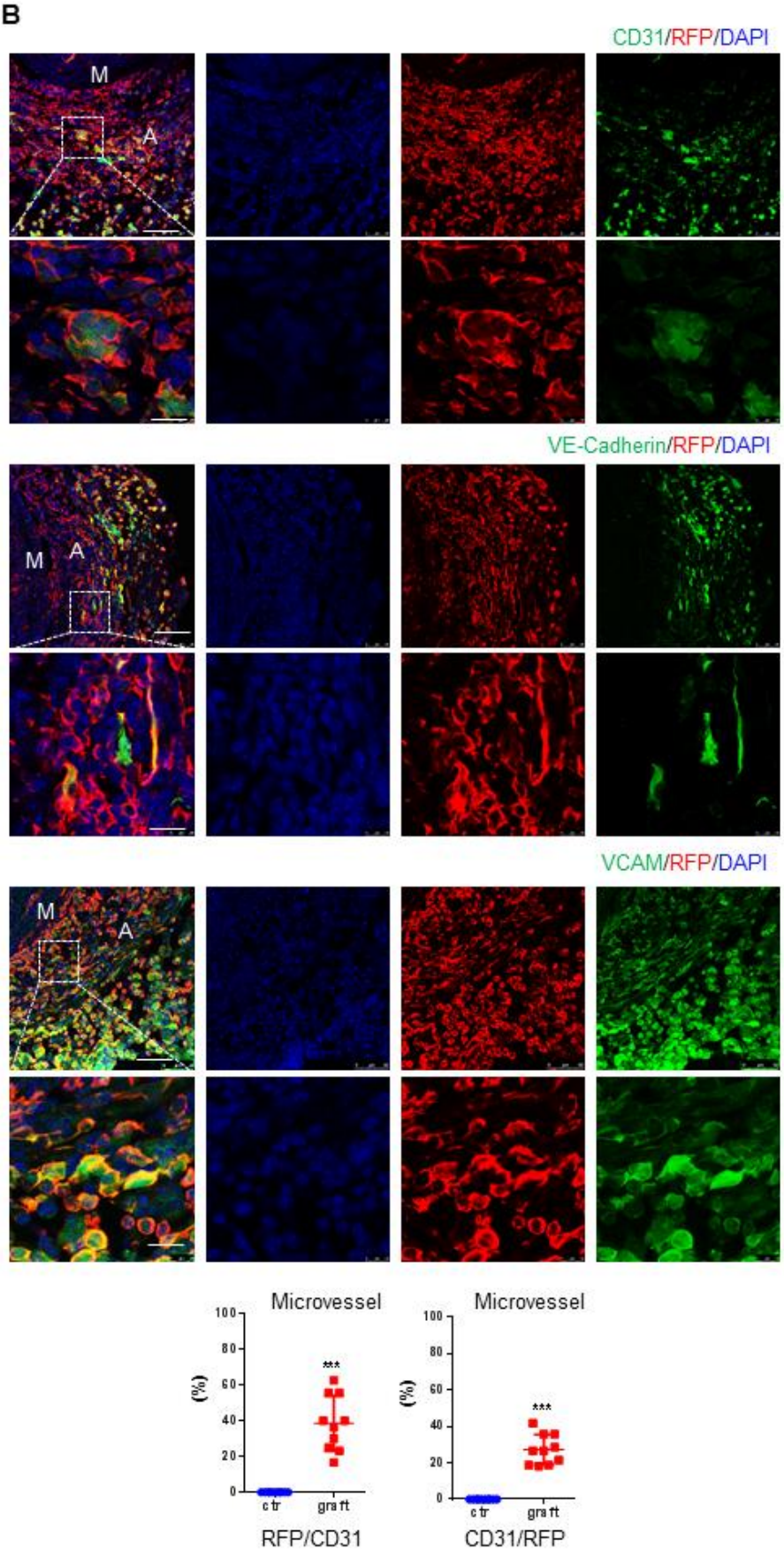
B
CD31/RFP/DAPI
M
A
VE-Cadherin/RFP/DAPI
M
A
VCAM/RFP/DAPI
M
A
Microvessel
(%)
100
80
60
40
20
0
***
ctr
graft
RFP/CD31
Microvessel
(%)
100
80
60
40
20
0
***
ctr
graft
CD31/RFP

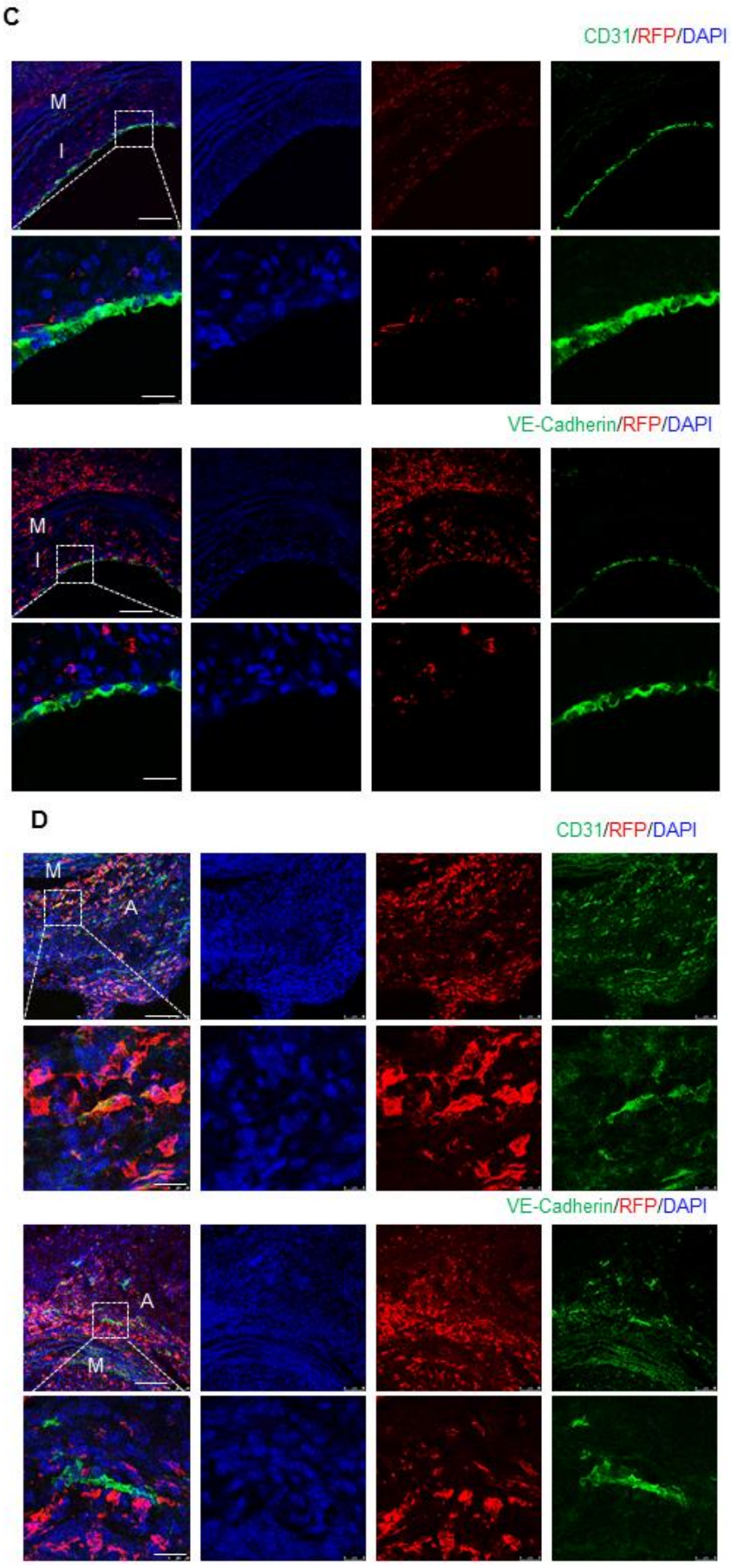
C
CD31/RFP/DAPI
M
I
VE-Cadherin/RFP/DAPI
M
I
D
CD31/RFP/DAPI
M
A
VE-Cadherin/RFP/DAPI
A
M

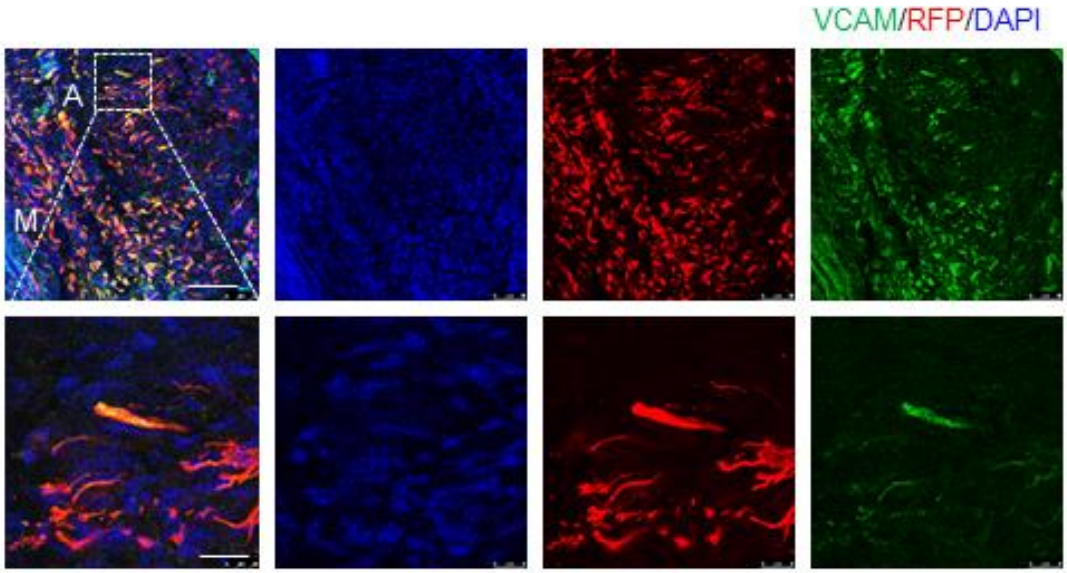

Figure 3.6 Recipient c-Kit$^+$ SPCs differentiated into ECs for both luminal ECs regeneration in neointima and microveseels remodelling in adventitia. **A**, Representative images showing luminal ECs regeneration in the neointima of aortic allograft from Kit-CreER; Rosa26-RFP mice stained with RFP, CD31 and VE-cadherin. Scale bars, 50 μm and 20 μm in enlarged images. The graphs indicate percentage of RFP expression in CD31$^+$ cells or CD31 expression in RFP$^+$ cells. Data are mean ± SEM, ****P*<0.001, unpaired two-tailed t test, n=10 per group. **B**, Representative immunostaining images showing adventitial microvessel remodelling of allograft from Kit-CreER; Rosa26-RFP mice stained with RFP, CD31, VE-cadherin and VCAM. Scale bars, 50 μm and 20 μm in enlarged images. The graphs indicate percentage of RFP expression in CD31$^+$ cells or CD31 expression in RFP$^+$ cells. Data are mean ± SEM, ****P*<0.001, unpaired two-tailed t test, n=10 per group.**C**, Representative images showing ECs regeneration in the neointima of aortic allograft from chimeric mice stained with RFP, CD31 and VE-cadherin. Scale bars, 50 μm and 20 μm in enlarged images. **D**, Representative immunostaining images showing adventitial microvessel remodelling of allograft from chimeric mice stained with RFP, CD31, VE-cadherin and VCAM. n=6 mice per group. Scale bars, 50 μm, and 20 μm in enlarged images. M indicates media layer; I, neointima; A; adventitial layer.

3.7 Donor c-Kit$^+$ SPCs Did Not Involve in Neointima Formation

To further investigate whether neointimal SMCs may arise from c-Kit$^+$ SPCs within donor graft, aortic segments from Kit-CreER; Rosa26-RFP mice were transplanted into BALB/c mice (Figure 3.7A). One week after transplantation, BALB/c mice were pulsed with tamoxifen and grafts were collected for analysis two weeks later (Figure 3.7A). Interestingly, although we observed neointimal SMCs accumulation in aortic grafts, no RFP$^+$ cells were detected (Figure 3.7B), in contrast to grafts harvested from recipient Kit-CreER; Rosa26-RFP mice. Meanwhile, ECs regeneration was detected but these ECs were not labelled with RFP fluorescence (Figure 3.7C). Collectively, these results demonstrate that c-Kit$^+$ SPCs from recipient, but not donor mice, are important contributors to neointimal SMCs in allograft model.

Figure 3.7

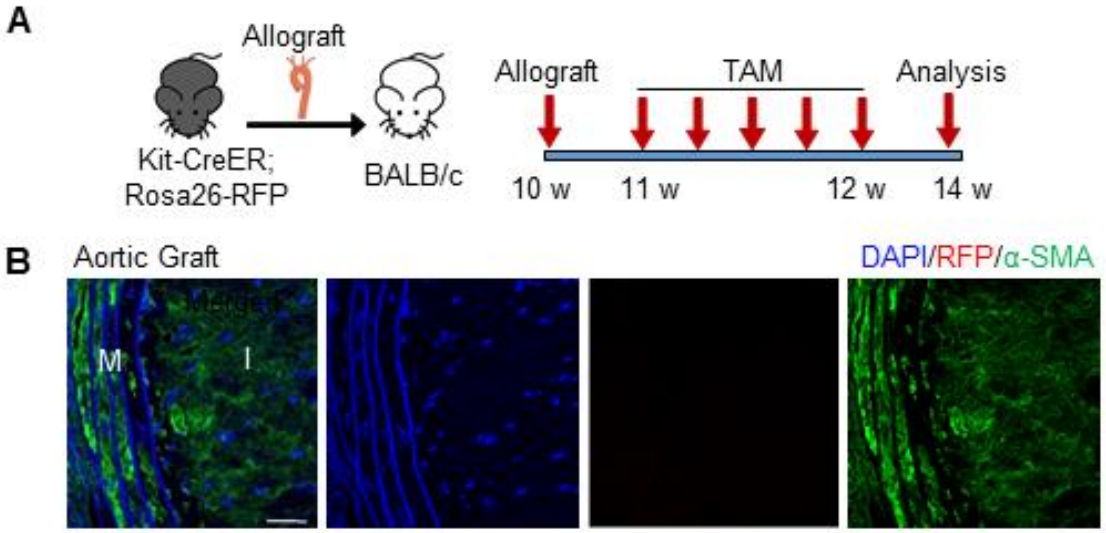

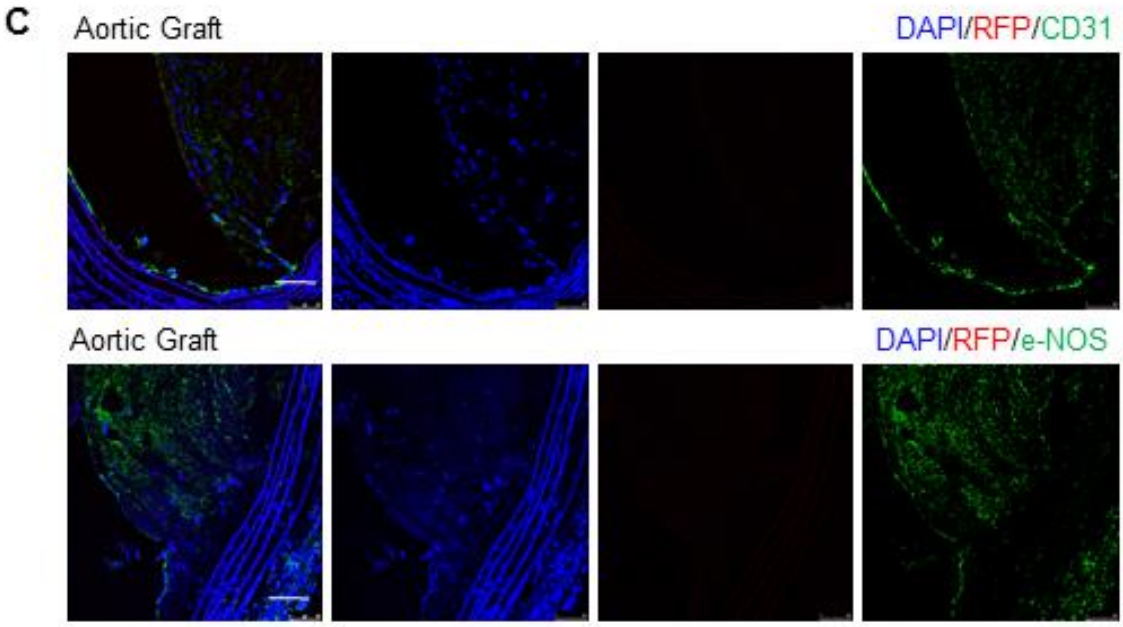

Figure 3.7 c-Kit$^+$ SPCs from donor aorta did not contribute to neointima formation. A, Schematic showing allograft transplantation experiment in which aortic segment from Kit-CreER; Rosa26-RFP mice was transplanted to BALB/c mice, followed by tamoxifen treatment. Graft tissues were collected two weeks after the last pulse of tamoxifen. **B,** Representative images showing aortic grafts stained with RFP and α-SMA from mice described in **A** (n=6 mice per group)**. B,** Representative images showing aortic grafts stained with RFP and CD31 or eNOS from mice described in **A** (n=6 mice per group)**.** Scale bars, 50 μm. M indicates media; I, neointima; TAM, tamoxifen.

3.8 SCF Induced c-Kit$^+$ SPCs Migration

We next sought to examine possible mechanisms underlying c-Kit$^+$ SPCs migration to the lesions and differentiation into neointimal SMCs. Previous reports have shown that SCF, a specific ligand for c-Kit, can mediate cell survival, proliferation as well as cell migration[216]. Significant increase of SCF concentrations in peripheral blood was observed after allograft transplantation (277.9 ± 15.45 vs 114.8 ± 12.80 pg/ml, Graft vs Control, Figure3.8A). More importantly, compared to control aorta, SCF was significantly increased in neointimal lesions of allografts where co-staining of SCF with RFP$^+$ cells was also observed (Figure 3.8A). These data suggest a possibility that accumulation of SCF in blood and neointima may induce migration of c-Kit$^+$ SPCs to the lesion sites.

To further prove our hypothesis, we isolated resident c-Kit$^+$ SPCs from vessel grafts. We first performed phenotyping of these c-Kit$^+$ SPCs and flow cytometric analysis showed that these cells expressed multiple SPCs markers including c-Kit, Sca-1, CD34, CD140, CD105, CD29, CD44 and CD201 (Figure 3.8B), confirming that these isolated c-Kit$^+$ cells displayed SPCs properties. We next determined whether SCF could induce migration of these c-Kit$^+$ SPCs *in vitro*. Both transwell migration assay (Figure 3.8C) and scratch wound healing assay (Figure 3.8D) showed that SCF significantly increased migration of SPCs in a dose-dependent manner, with a dosage of 100 ng/ml SCF resulting in the peak of cell migration. This dosage was therefore used in our subsequent experiments.

ACK2 is an antibody which has been reported to specifically target c-Kit$^+$ cells and block c-Kit function[217]. We next determined if AKC2 could also reduce SCF-induced c-Kit$^+$ SPCs migration *in vitro*. As expected, ACK2-treated cells showed a significantly lower migration rate than a control IgG group in response to SCF stimulation (Figure 3.8E). However, we noticed that blocking effects were partial. We speculated that other feedback signalling pathways could be activated after c-kit receptor kinase was blocked. However, this still needs further study to demonstrate. SCF or ACK2 treatment did not affect cell proliferation in c-Kit$^+$ SPCs (Figure 3.8F), indicating that the effect of SCF or ACK2 on cell migration did not result from cell proliferation. Taken together, our data provide evidence that SCF is a chemotactic factor that induces c-Kit$^+$ SPC migration.

Our data so far suggested that recipient c-Kit$^+$ SPCs mainly from non-bone marrow tissues contributed to neointima formation. We next asked whether blocking of c-Kit could abrogate neointima formation in our model. Therefore, ACK2 was further used in our *in vivo* experiments. Immediately after aortic graft transplantation from BALB/c mice to C57BL/6J mice, ACK2 or control IgG dissolved in pluronic F-127 gel was applied to the adventitial side of the aortic grafts (Figure 3.8G). The application of pluronic F-127 gel allows a slow release of ACK2 to the local graft microenvironment[218]. Our results showed mice that received IgG treatment developed severe neointimal formation (Figure 3.8H). In contrast, neointimal lesions were significantly reduced in ACK2-treated aortic grafts, with significant lower neointima areas and higher lumen areas (Figure 3.8H). Furthermore, the number of neointimal SMCs was much lower in ACK2-treated mice than in control mice (Figure 3.8I), suggesting that blocking of c-Kit$^+$ cells effectively impaired neointimal SMC formation. The percentage of SMCs in neointimal lesions was comparable between both groups (Figure 3.8I). Taken together, these results further demonstrate the importance of c-Kit$^+$ SPCs in neointima formation in allograft transplantation.

Figure 3.8

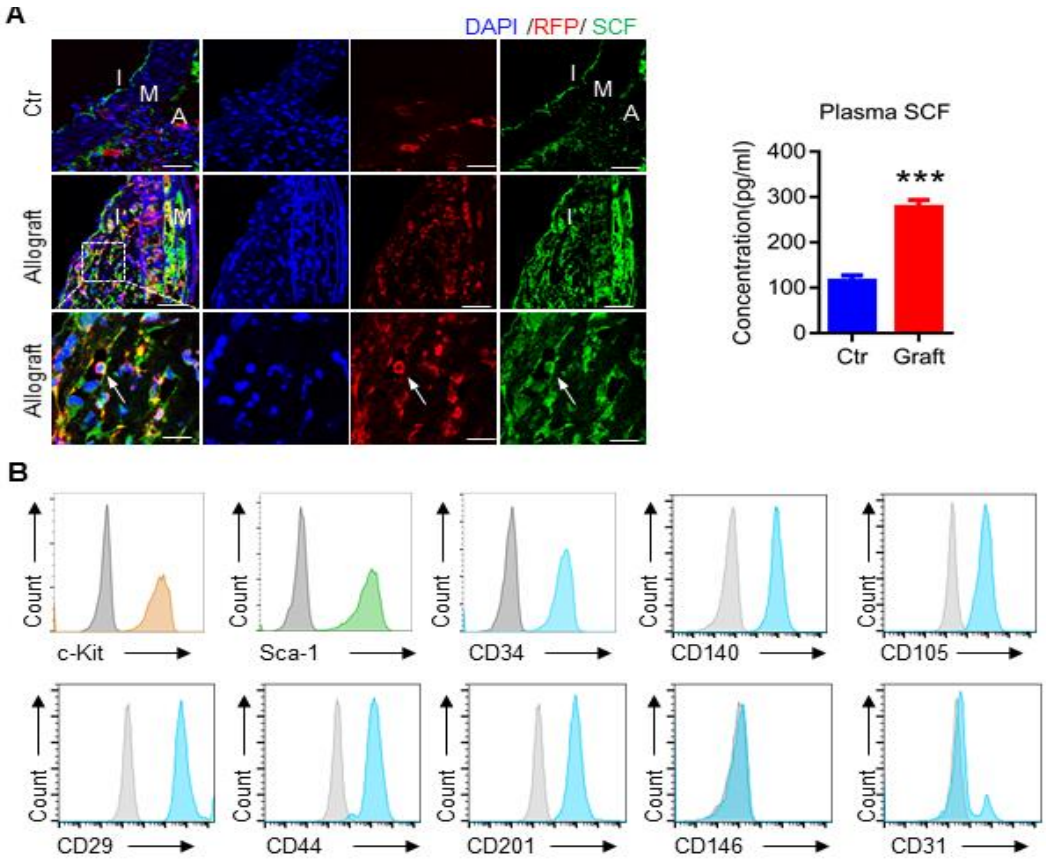

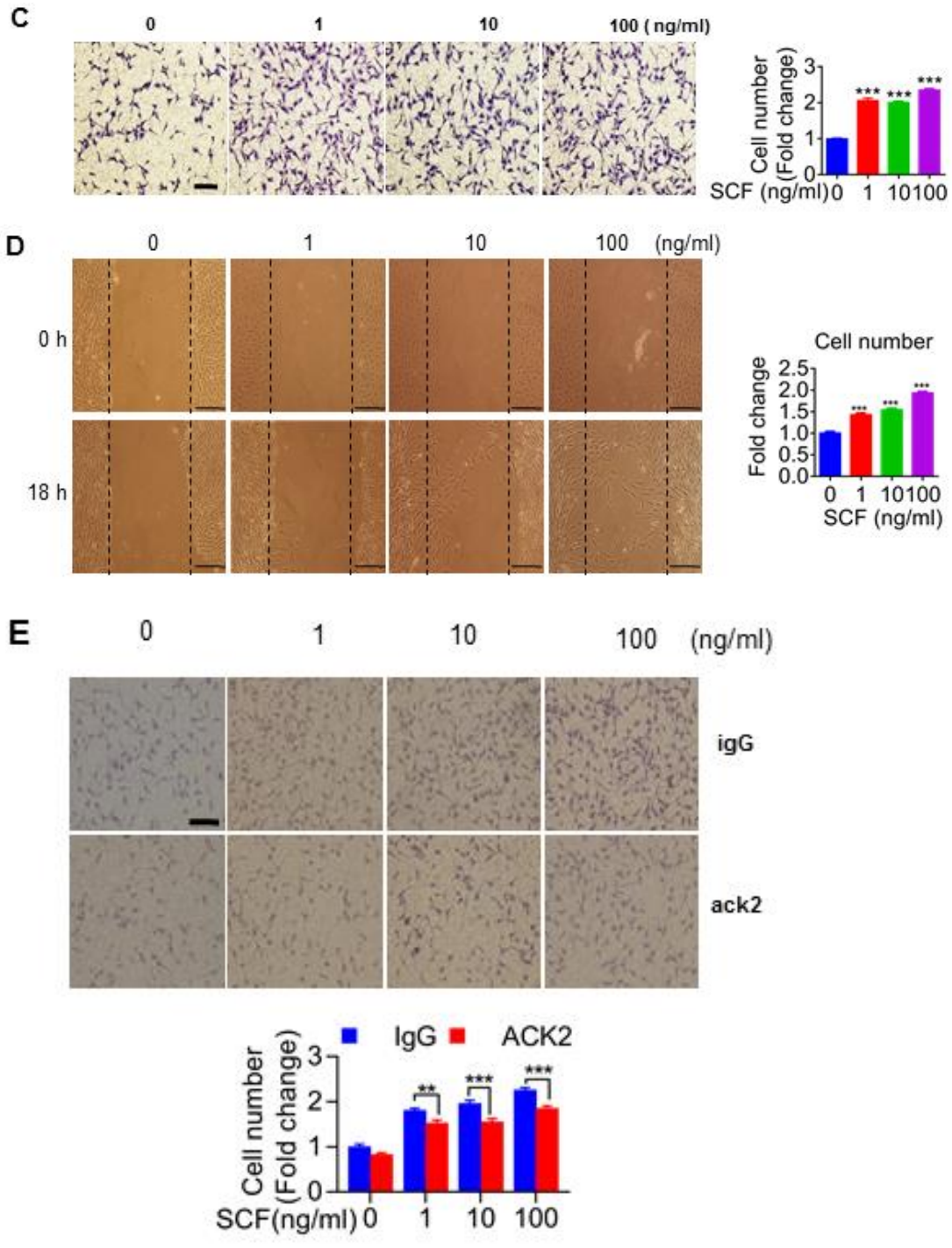
C
0
1
10
100 (ng/ml)
Cell number (Fold change)
SCF (ng/ml) 0 1 10100
D
0
1
10
100 (ng/ml)
0 h
18 h
Cell number
Fold change
SCF (ng/ml)
E
0
1
10
100 (ng/ml)
igG
ack2
IgG
ACK2
Cell number (Fold change)
SCF(ng/ml) 0 1 10 100
F
BrdU
Fold change
SCF (ng/ml)
Ki-67
Ctr
SCF
Ki-67
IgG
ACK2

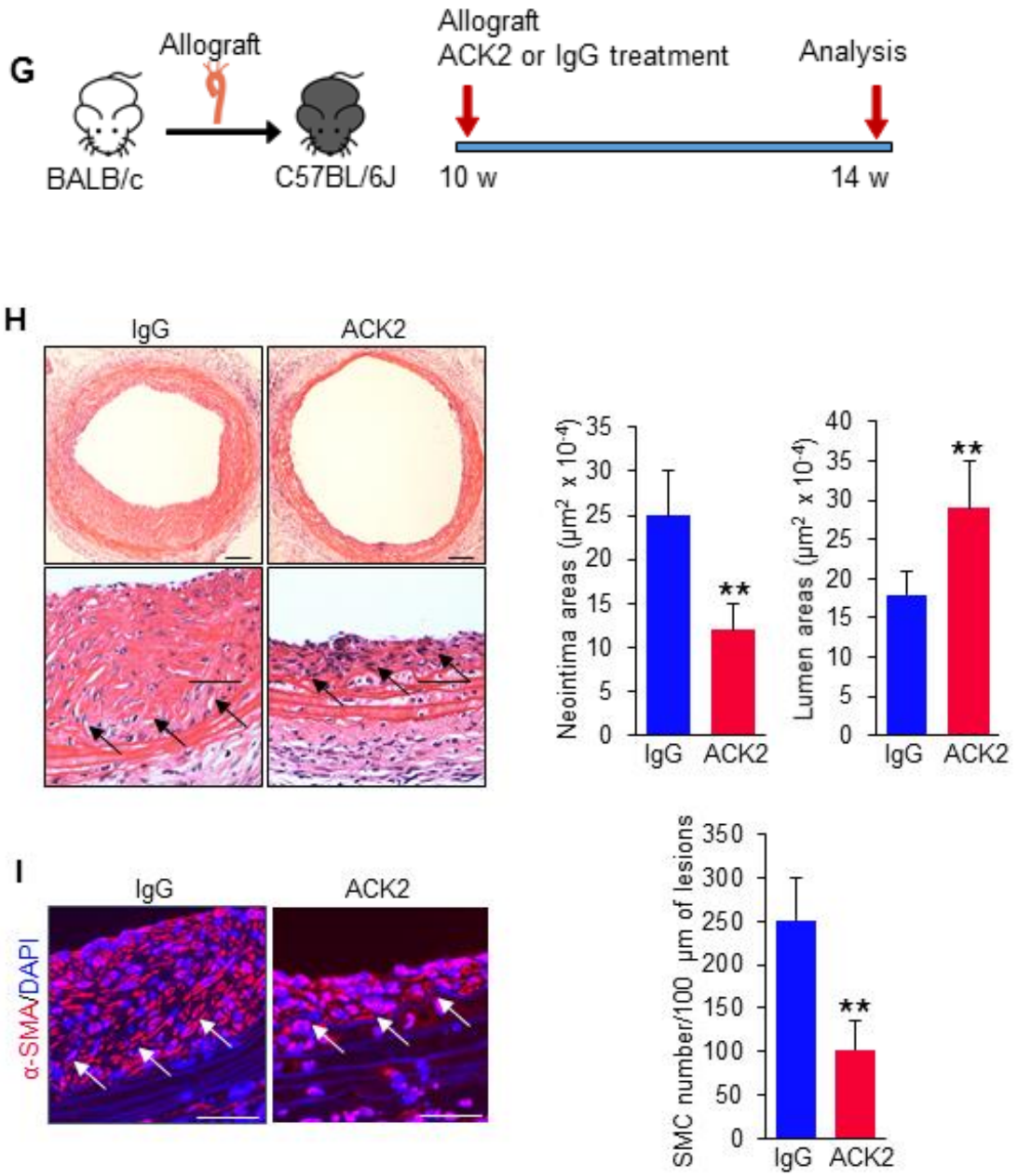

Figure 3.8 SCF induces migration of c-Kit⁺ SPCs *in vitro*. A, Representative images showing RFP and SCF staining in control and allografts (n=6 mice per group). Arrows indicate co-staining of RFP and SCF. Scale bars, 50 μm, and 20 μm in enlarged images. The graphs indicated concentration of SCF in blood plasma of control and allograft mice. Data shown are mean ± SEM, **P<0.01, ***P<0.001, unpaired two-tailed t test, n=6-7 mice per group. Ctr indicates control group. **B**. Cells were analysed by flow cytometry for their expression of surface markers including c-Kit, Sca-1, CD34, CD140, CD105, CD29, CD44, CD201, CD146 and CD31. Corresponding IgG was used as isotype controls, as indicated by tinted grey areas

(n=3 experiments). **C**, Representative images showing SCF-induced c-Kit$^+$ SPC migration, by Transwell migration assay. Scale bars, 100 μm. Graphs shown are relative cell number normalised to control. **P<0.01, ***P<0.001, one-way ANOVA with Dunnett's test, n=3 experiments, 10 fields per sample. **D**, Representative images showing migration of c-Kit$^+$ SPCs in response SCF using a scratch-wound assay. Scale bars, 100 μm. Graph are shown as fold change normalised to 0 h time point. ****P*<0.005, one-way ANOVA with Dunnett's test, n=5 per group. **E**, Representative images showing SCF-induced c-Kit$^+$ SPC migration with ACK2 or control IgG by transwell migration assay. Scale bars, 100 μm. Graphs shown are relative cell number normalized to control. **P<0.01, ***P<0.001, two-way ANOVA with Bonferroni's test, n=3 experiments, 5 fields per sample. **F**, Cell proliferation was measured by BrdU assay and Ki-67 staining in SCF-treated c-Kit$^+$ SPCs in the presence of ACK2 or IgG (n=3 experiments). **G**, Schematic showing ACK2 or IgG treatment in mouse allograft model (n=6 mice per group). **H**, Representative HE staining of aortic grafts was shown. Arrows indicate neointima lesions. Scale bars, 100 μm, and 50 μm in enlarged images. Graphs showing quantification of neointima areas and lumen areas. ***P*<0.01, unpaired two-tailed t test, n=6 per group. **I**, Representative images showing allograft stained with α-SMA. Arrows indicate neointimal lesions. Scale bars, 50 μm. Graphs showing quantification of SMC numbers per 100 μm of neointimal lesions. ***P*<0.01, unpaired two-tailed t test, n=6 per group. **F**, Percentage of SMCs in total cells was shown. All data shown are mean ± SEM. n=6 per group.

3.9 The SCF/c-Kit Signalling Pathway Regulated c-Kit$^+$ SPC Migration

Considering that reorganisation of the actin cytoskeleton is critical in triggering cell migration[219], to investigate the possible mechanisms behind this migration we first performed immunostaining to observe actin cytoskeleton and focal adhesion in c-Kit$^+$ SPCs, as phalloidin specifically binds actin, whereas phosphorylated focal adhesion kinase (p-FAK) and vinculin stain focal adhesion assembly. SCF immediately induced formation of parallel elongated stress fibres and cell spreading in cultured graft derived c-Kit$^+$ SPCs, compared to untreated cells (Figure 3.9A). Filopodia and lamellipodia were formed at the leading edge of c-Kit$^+$ SPCs within 2 min after SCF treatment. Moreover, co-staining of p-FAK, vinculin and filamentous actin (F-actin) was also observed at the leading edge (Figure 3.9A), which is indicative of cell migration. These data suggest that SCF may trigger cell migration at a very early time point. As SCF has been reported to specifically bind and activate c-Kit, we next sought to investigate whether c-Kit signalling pathways regulate this early process. Phosphorylation of c-Kit was increased by SCF within minutes (Figure 3.9B), indicating that early activation of c-Kit signalling may regulate this process. Small GTPases, which can be activated by tyrosine kinase, have been shown to be pivotal in regulating cytoskeleton reorganisation and cell migration[219]. As c-Kit is a receptor tyrosine kinase, we further performed G-LISA activation assay to test the activation of GTPases. We showed that SCF treatment led to early activation of small GTPases including cell division cell division cycle 42 (Cdc42), Ras homolog family member A (RhoA) and Rac family small GTPase 1 (Rac1) within 2 min (Figure 3.9C). Possible downstream pathways of c-Kit signalling and/or GTPases including phosphorylation of mitogen-activated protein kinase kinase 1/2 (MEK1/2), extracellular signal-regulated kinase 1/2 (ERK1/2) and myosin light chain (MLC) were also elevated shortly after SCF stimulation (Figure 3.9B). Activation of MLC may further promote cell contractility and cell motility[220]. Phosphorylation of c-Jun N-terminal kinase (JNK) and c-Jun was also observed to increase and peak at a later time point of 30 min (Figure 3.9B). Notably, ACK2 could completely or at least partially blocked the activation of c-Kit signalling, as well as migration-related pathways including MEK/ERK/MLC, JNK/c-Jun pathways (Figure 3.9D), consistent with the inhibitory effect of ACK2 on SPC migration (Figure 3.8), indicating that SCF/c-Kit signaling, upstream of MEK/ERK and JNK pathways, is critical for cell migration in c-Kit$^+$ SPCs. Because both MEK/ERK and JNK/c-Jun have

been reported to regulate expression of matrix metalloproteinase (MMP) to degrade extracellular matrix and ease cell migration[221], we further measured secretion of MMPs in cell culture supernatants. A significant increase in MMP-2, but not MMP-9, was detected after SCF treatment for 24 h and 48 h (Figure 3.9E), suggesting a possible role of MMP-2 in regulating cell migration at a later time.

Figure 3.9

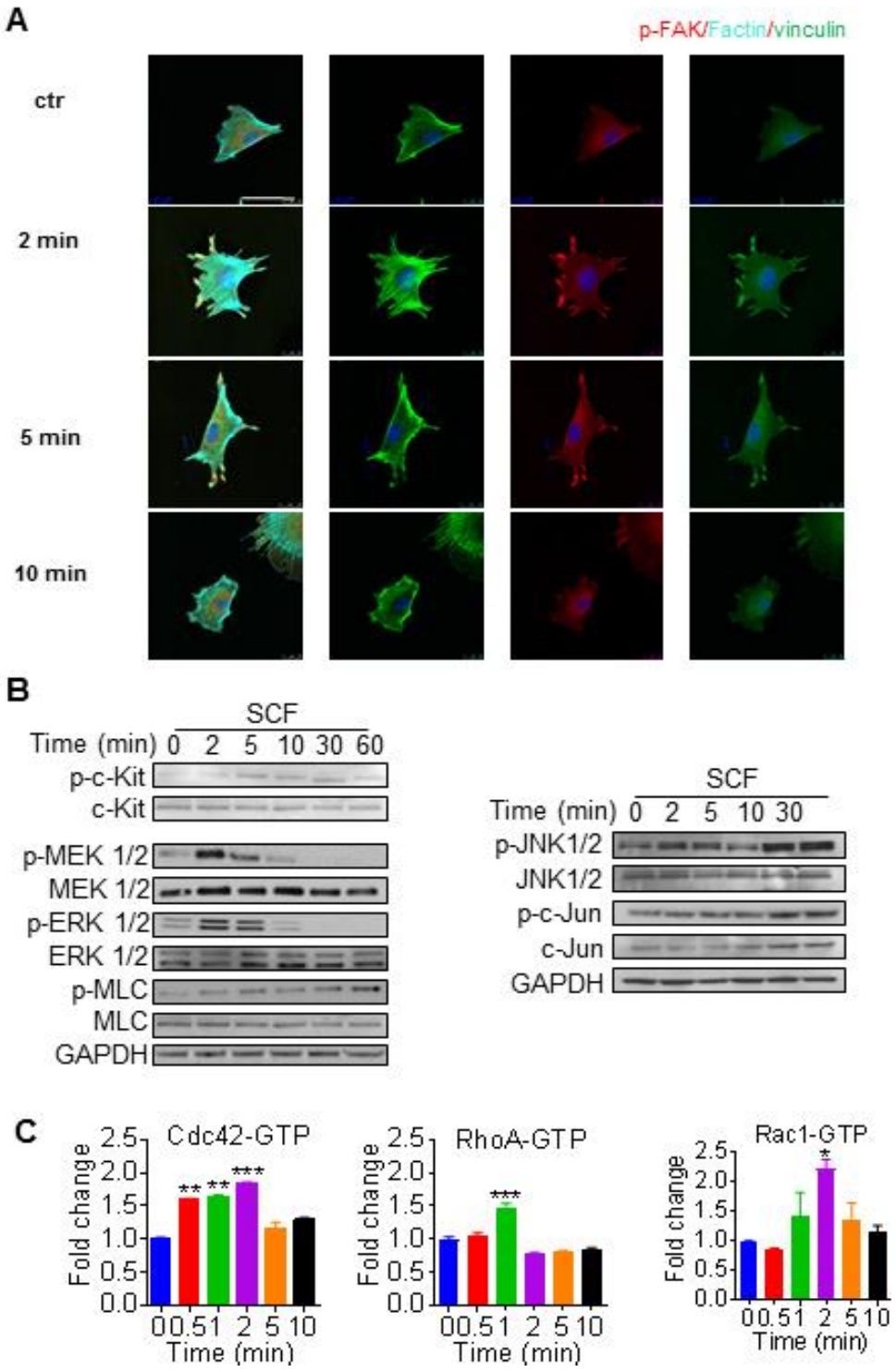

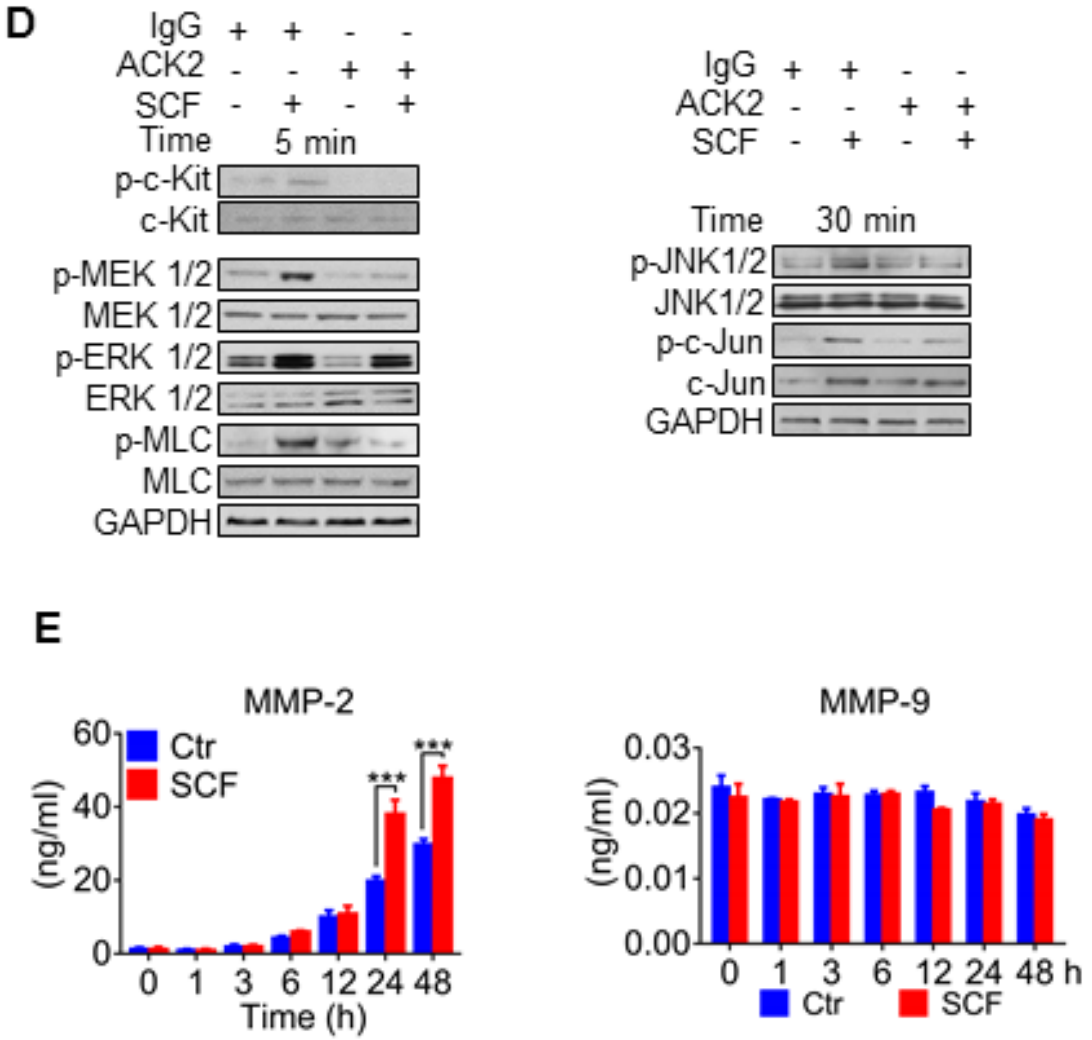

Figure 3.9 SCF/c-Kit signalling pathway in c-Kit$^+$ SPCs migration. A, Representative images showing SCF-treated c-Kit$^+$ SPCs stained with p-FAK, F-actin and vinculin (n=3 experiments). Scale bars, 10 μm. **B**, Representative western blot showing activation of c-Kit, MEK-ERK-MLC and JNK/C-Jun pathways in response to SCF (n=3 experiments). **C**, Graphs showing activation of small GTPase including Cdc42, Rac1 and RhoA in SCF-treated SPCs. *P<0.05, **P<0.01, ***P<0.001, one-way ANOVA with Dunnett's test, n=3 experiments. **D**, Representative western blot indicating signalling pathways in response to SCF for indicated times, in the presence of ACK2 or IgG (n=3 experiments). **E**, Quantification of MMP-2 and MMP-9 in cell culture supernatant from SCF-treated cells. ***P<0.005, two-way ANOVA with Bonferroni's test, n=3 experiments. A, adventitia; M, media; I, intima or neointima; Ctr, control.

3.10 VEGF Induced c-Kit$^+$ SPCs Migration

VEGF is another crucial molecule in vascular biology. Immunostaining results showed that VEGF co-stained with RFP$^+$ cells in neointimal lesions of allografts (Figure 3.10A). These data suggest the possibility that VEGF is involved in of c-Kit$^+$ SPCs regulation. We next determined whether VEGF could induce migration of these c-Kit$^+$ SPCs *in vitro*. Transwell migration assay showed that SCF significantly increased migration of SPCs, with a dosage of 50 ng/ml SCF resulting in the peak of cell migration (Figure 3.10B). This dosage was therefore used in our subsequent experiments. Cytoskeleton immunostaining was then performed to detect cell migration at a single cell level. Data showed that VEGF immediately induced formation of parallel elongated stress fibres and cell spreading in c-Kit$^+$ SPCs, compared to untreated cells (Figure 3.10C). Filopodia and lamellipodia were formed at the leading edge of c-Kit$^+$ SPCs within 2 min after VEGF treatment. Moreover, co-staining of p-FAK, vinculin and filamentous actin (F-actin) was also observed at the leading edge (Figure 3.10C), which is indicative of cell migration. These data suggest that VEGF triggered cell migration at a very early time point. The mechanism underlying VEGF-mediated cell migration was further investigated. Protein kinase B (AKT) activity is reported downstream of VEGF signalling and its expression was shown elevated shortly after VEGF stimulation (Figure 3.10D). Downstream, FAK was also found activated (Figure 3.10D) and FAK is correlated with focal adhesion digestion. An AKT inhibitor was used, and it was found that the AKT/FAK pathway can be blocked (Figure 3.10D). We next determined whether AKT inhibition could also reduce SCF-induced c-Kit$^+$ SPCs migration *in vitro*. As expected, AKT inhibitor-treated cells showed a significantly lower migration rate than a vehicle DMSO group in response to SCF stimulation (Figure 3.10E).

Figure 3.10

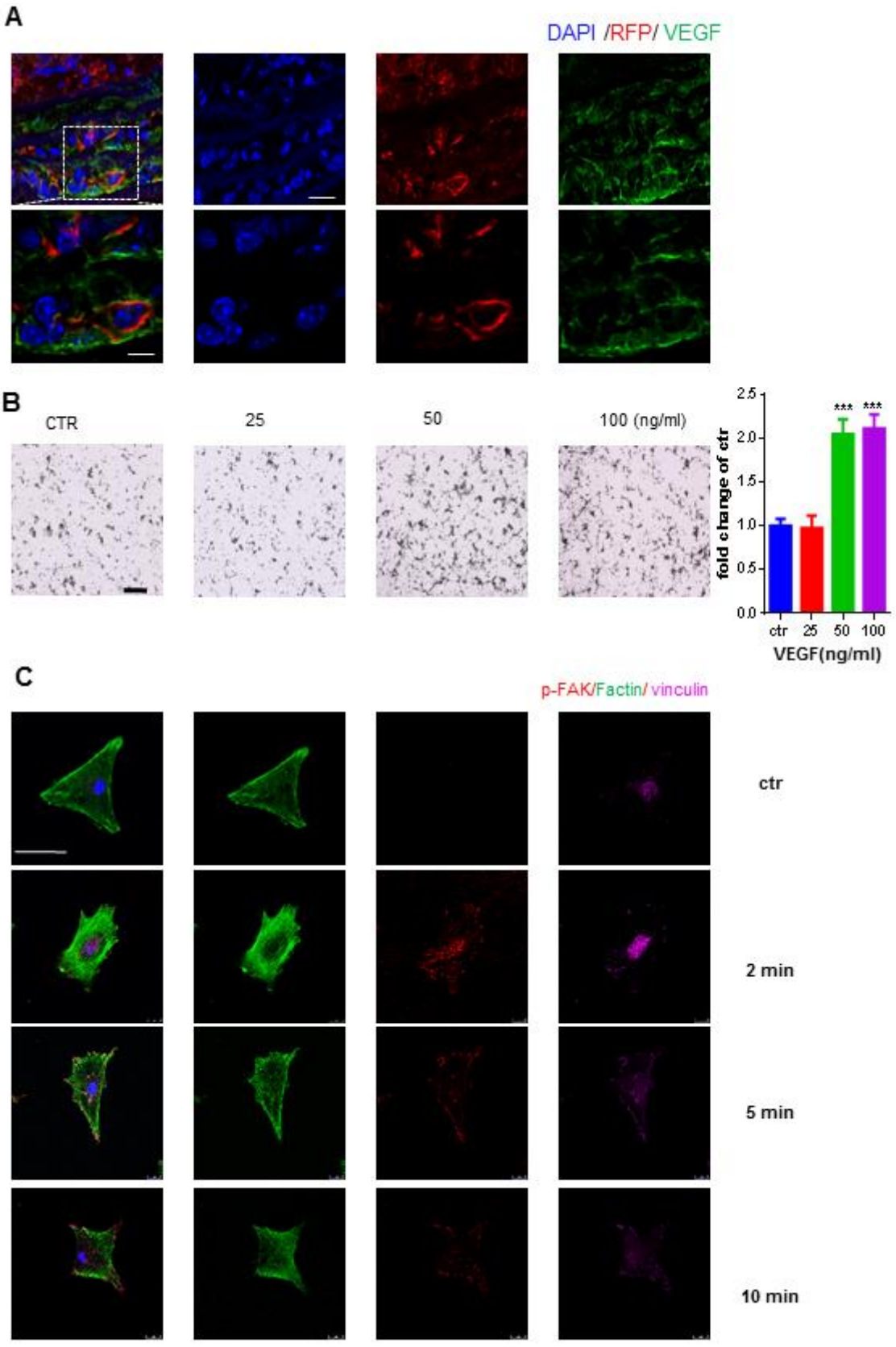
A
DAPI /RFP/ VEGF
B
CTR
25
50
100 (ng/ml)
fold change of ctr
2.5
2.0
1.5
1.0
0.5
0.0
***
***
ctr
25
50
100
VEGF(ng/ml)
C
p-FAK/Factin/ vinculin
ctr
2 min
5 min
10 min

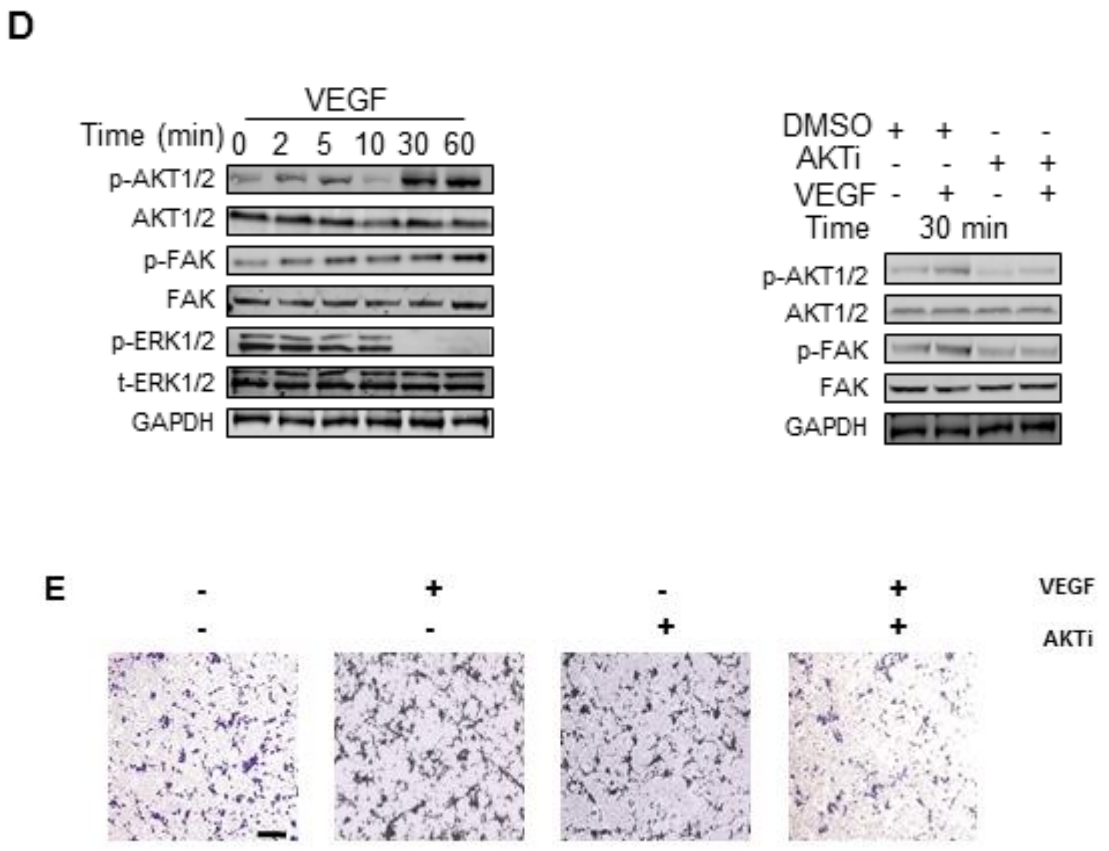

Figure 3.10. VEGF induced migration of c-Kit$^+$ SPCs *in vitro*. A, Representative images showing RFP and SCF staining in allografts (n=6 mice per group). Arrows indicate co-staining of RFP and SCF. Scale bars, 50 μm, and 20 μm in enlarged images. **B**, Representative images showing VEGF-induced c-Kit$^+$ SPC migration, by transwell migration assay. Scale bars, 100 μm. Graphs shown are relative cell number normalized to control. **P<0.01, ***P<0.001, one-way ANOVA with Dunnett's test, n=3 experiments, 10 fields per sample. **C**, Representative images showing VEGF-treated c-Kit$^+$ SPCs stained with p-FAK, F-actin and vinculin (n=3 experiments). Scale bars, 10 μm. **D**, Representative western blot showing activation of AKT/FAK pathways in response to VEGF (n=3 experiments) or in the presence of AKT inhibitor or DMSP (n=3 experiments). AKTi, AKT inhibitor; DMSO Dimethy sulfoxide. **E**, Representative images showing VEGFF-induced c-Kit$^+$ SPC migration with AKT inhibitor or control DMSO by transwell migration assay. Scale bars, 100 μm.

Chaper 4: Discussion

4.1 Summary

This study answers several important questions about vascular allograft induced arteriosclerosis. Firstly, immunostaining of wild type mice identified the location of SPCs to be both aorta and bone marrow. Additional findings from the c-kit$^{kit/CreER}$; ROSA26-RFP transgenic lineage tracing mouse model further supported this conclusion. Secondly, in an allo-transplantation study, the sources of vascular cells mainly including ECs and SMCs were determined. The results showed that 4 weeks post-transplantation, all donor derived c-kit^{+} vascular cells were absent from the graft. Meanwhile, the graft lesion was formed of c-kit^{+} vascular cells derived from the recipient mouse. When analysing cell fate using double marker staining, data showed that c-kit^{+} SPCs differentiated into both ECs and SMCs. Further analysis of the source of recipient vascular cells was performed using a bone marrow chimeric animal. It was shown that only non-bone marrow derived c-kit^{+} SPCs differentiated into SMCs. For ECs, non-bone marrow source of c-Kit^{+} SPCs differentiated into ECs for luminal ECs regeneration in the neointima, whereas bone marrow source of c-Kit^{+} SPCs mainly differentiated into inflammatory ECs for microveseels remodelling in graft adventitia. Thirdly, the pattern and underlying mechanism of cytokine inducing c-kit^{+} SPCs migration was also evaluated *in vitro*. Vascular graft related cytokines were analysed by immunostaining. Data showed that expression of SCF and VEGF were upregulated. However, the control mice we used were only those without surgery. This is not a standard control. In the future study, standard control groups such as sham surgery or autografting mice need to be established to compare with the allograft animal groups to acquire more convincing result. Using transwell and scratch wound healing assays, it was demonstrated that under the influence of these two cytokines, c-kit^{+} SPCs migration is increased. Finally, a combination of G-LISA assays, immunostaining and western blots showed that migration of c-kit^{+} SPCs can be triggered by SCF via downstream activation of small GTPases, MEK/ERK/MLC and JNK/c-Jun signalling pathways, whereas VEGF can facilitate c-kit^{+} SPCs migration via AKT/FAK pathway. These *in vitro* studies provided us the clues about on how the recruitment of c-kit^{+} SPCs within the graft tissues were regulated. However, these mechanisms still need further *in vivo* work to demonstrate in the future.

4.2 Stem/Progenitor Cells (SPCs) Distribution

SPCs are a cluster of cells with the potential for proliferation and differentiation. SPCs possess two important characteristics, which are self-renewal and differentiation potency. Self-renewal refers to the ability of cells to go through cell division while maintaining their undifferentiated state, while differentiation potency indicates that SPCs can differentiate into mature terminal cell types. Specifically, stem cells can differentiate into multiple terminally differentiated cell types, whereas progenitor cells can only transform into one (Table 4.2-1). From the point of view of replication capacity, stem cells have a nearly unlimited potential for self-renewal, whereas progenitor cells can only divide for a finite number of times. In the adult body, adult SPCs act to repair injured tissue. Several methods have been used to identify SPCs, such as cell transplantation assay, clonogenic assays and functional assays. In the above methods, several makers such as CD34, Sca-1 and c-kit are used to label the vascular SPC population. For example, c-kit or CD117 is a tyrosine kinase receptor expressed on the surface of various types of SPC. Data has shown that c-kit is an important marker for hematopoietic stem cells (HSCs). Several tissues including the skin, the reproductive organs, the gastrointestinal tract, the nervous system and the cardiac and respiratory systems have been shown to contain c-kit$^+$ cells. However, there are only few studies investigating c-kit expression and function in the vascular system. One important issue, which hinders SPC research, is that though various markers have been used to identify SPCs, a uniquely specific marker is still lacking. For example, though c-kit is widely used to represent a cluster of SPCs, other cell types such as pericytes, ECs, hematopoietic cells, mast cells and interstitial cells also express c-kit. This can severely complicate result interpretation. The study in our lab previously identified vascular SPCs with the markers including Sca-1, CD34 and c-kit[95]. Therefore, we continued to use these three makers to identify SPCs.

Table 4.2-1 Comparison between stem cells and progenitor cells

	Stem cells	**Progenitor cells**
Self-renewal	Unlimited	Limited
Terminally differentiated cell type	Multi-potency	Uni-potency

To identify localised target gene or protein expression, several techniques are normally used (Table 4.2-2). To study expression of DNA or RNA sequences, labelled complementary DNA or RNA is used as a probe to bind to and identify target gene expression, this process is referred to as *in situ* hybridization. To identify specific proteins immunofluorescence (IF) or immunohistochemistry (IHC) techniques are employed to detect target antigen. In this way, antigen distribution can be visualised in the sample. Both IF and IHC are based on antigen-antibody interactions. The difference between IF and IHC are the reporter molecules; IF uses fluorochromes, whereas IHC uses chromogenic molecules as the reporter. Alexa Fluors and Dylight Fluors are popular commercial fluorescent reporters. In IHC, a colourless substrate is converted into a coloured product after use of enzymes such as alkaline phosphatase (AP) or horseradish peroxidase (HRP). For example, when DAB is catalysed by HRP, it generates a brown pigment, which can be visualised under the microscope. IF and IHC methods can be classified as direct or indirect methods. When the primary antibody is directly linked to a fluorophore and is bound to target molecules, the antigen can be recognised. This is called a direct method. In contrast, indirect method uses the primary antibody without the fluorophore to be firstly applied to bind to the target antigen followed by a secondary antibody incubation, which carries fluorophore and binds to the primary antibody. As multiple secondary antibody molecules may bind to a single primary antibody molecule, the fluorescence signal can be amplified using this method, which facilitates sensitivity improvement. In our study, we employed indirect IF to detect target antigen expression because of its high sensitivity and specificity. However, in our study we only used PBS with secondary antibodies as the negative control. This is not appropriated. In the future, IgG primary antibodies along with secondary antibodies should be used as the standard controls in our further studies.

Table 4.2-2 Target gene/antigen localisation

	In situ Hybridization	Immunofluorescence (IF)	Immunohistochemistry (IHC)
Probe	DNA/RNA	Antibody	Antibody
Principle	DNA/RNA complementation	Antigen/antibody binding	Antigen/antibody binding
Reporter	Fluorochrome/ Chromogenic	Fluorochrome	Chromogenic
Enzyme	Yes/No	No	Yes

The stem cell niche refers to the cellular microenvironment in the specific location where stem cells are found. It maintains adult stem cells in a quiescent state. However, after stimulations such as injury, SPCs exit from this quiescent state into a self-renewal or differentiation state. Various factors contribute to the stem cell niche, including stromal cells, ECM proteins, cytokines, adhesion molecules and specific metabolic environment. The SPC niche plays an important role in the cell physiological balance. If the SPCs niche is damaged, this cell physiological balance could be broken leading to tissue/organ failure. The bone marrow was the first niche described to harbour vascular cells including SPCs[222]. According to position and function, the bone marrow niche can be subdivided into the osteoblastic niche and the vascular niche. The osteoblastic niche is located at inner part of the bone, with a hypoxic environment for SPCs quiescence. The vascular niche is located near the artery, providing a higher concentration of nutrients and oxygen for SPC mobilisation. In the bone marrow niche, SPCs do not exist in isolation. In fact, they are under the regulation of surrounding cells such as ECs and stromal pericytes. Via a paracrine effect, surrounding cells secrete growth factors facilitating SPCs homeostasis. Meanwhile, ECs and stromal cells can also directly interact with SPCs. For example, Jagged and Delta like ligand expressed on the EC surface can regulate HSCs function through the Notch/Wnt pathway. Furthermore, mobilisation of SPCs from the bone marrow niche is also regulated by signalling such as SDF/CXCR4 and SCF/c-kit axis. By repeated flushing of the whole murine femur and tibia bones with PBS, we harvested SPCs attached to

bone marrow. Co-localisation of markers including CD34, Sca-1 and c-kit markers, indicated that a large proportion of harvested bone marrow cells were SPCs.

The vascular wall is largely composed of vascular cells and ECM proteins. It was initially thought that the vessel wall environment solely played a structural role in supporting SMCs and ECs, until the identification of SPCs. Multiple studies have indicated an important role for these SPCs in vascular wall function and disease. Evidence from various groups suggests that SPCs are involved in atherosclerosis lesion formation as well as tissue regeneration. To acquire aorta specimens, cryo or frozen sectioning was performed (Table 4.2-3). Cryosectioning is a widely used technique for rapid microscope pathological diagnosis during surgery. Cryosections are also prepared in the lab for cytological analysis. Compared with paraffin sections, cryosectioning is comparatively timesaving because the tissues do not need pre-paraffin embedding. Cryosectioning is additionally beneficial for preserving antigen function. In our study PFA, instead of formalin was used. This further improves antigen preservation. However, some information can be lost if cryosectioning alone is used to detect target cell distribution in the vessel. Although aortic cryosections provides us the opportunity to study the distribution of SPCs transversely across aortic wall, the less than 20μm thickness of the specimen could easily mean we miss the target cells and restrict the view of whole vessel. Though it may be possible to reconstitute the whole aorta using many sections and a computer-based technique, this work is time-consuming and difficult to carry out. Therefore, whole mount *en-face* staining was performed, which assisted us in determining the distribution of SPCs in the whole aorta while focusing on specific layers. In our study, endothelial and adventitial layer *en-face* staining was performed. In endothelial layer *en-face* staining, the whole aortic tissue was carefully harvested. Because ECs are prone to apoptosis after animal death, perfusion fixation during harvest is necessary for cell and antigen preservation. Though some studies report that the EC layer can be distinguished from the SMC layer based on nucleus morphology, our study employed ECs specific cell surface marker VE-cadherin to distinguish ECs by their specific cobblestone structure under the microscope (as shown above). Distinct to ECs, cells within the adventitial layer are embedded in the ECM and comparatively resistant to apoptosis. Therefore, collagenase was used to digest the whole vessel and the adventitia was then carefully dissected from media layer. We found that maintaining the whole adventitial layer

intact was practically speaking rather difficult despite the tensile characteristics of this layer.

Table 4.2-3 Aortic tissue preparation

	Paraffin section	**Frozen tissue**	***En-face***
Fixation	Before embedding	After sectioning	Before Harvest
Fixing Reagent	Ice cold acetone	Ice cold acetone/PFA	PFA
Section	Microtome	Cryostat	N/A
Storage	Long term, RT	Mild, -80°C	Short, 4°C
Time Consuming	Long	Short	Intermediate
Direction	Cross	Cross	Vertical
Antibody Penetration	Three layers	Three layers	Single layer

The aorta is the largest vessel, originating from the cardiac left ventricle and extending down to the abdomen. Based on anatomy, the aorta can be divided into ascending aorta, aortic arch, descending aorta, thoracic aorta and abdominal aorta. In the current study, IF staining of SPC markers on aortic cryosections were performed. It was found that $CD34^+$ and $Sca\text{-}1^+$ cells were distributed throughout the whole aorta, whereas c-kit staining was limited to the ascending aorta and aortic arch (Figure 3.1A). This is verified by *en-face* staining as c-kit marker were solely expressed in ascending aorta (Figure3.1C and Figure 3.1D). These results firstly embodied asymmetry of SPCs markers in spatiality, which indicates that although surface antigens such as CD34, Sca-1 and c-kit are traditionally regarded as SPC surface markers, they represent distinct cell lineages which may exert functionally distinct effects on vascular wall homeostasis. Secondly, when analysing these three markers together, data showed that a certain proportion of aortic cells express triple positive staining. When studying location (Figure 4.2A), we observed a distinct distribution pattern, in which most SPCs

are distributed in the ascending aorta and aortic arch, whereas in the descending aorta, thoracic aorta and abdominal aorta we see only sporadic SPCs. This asymmetric distribution might result from distinct aortic segment origin since the embryonic stage (Figure 4.2B). In the human prenatal aorta, the ascending aorta derives from the aortic sac or truncus arteriosus, which serves as a ventricular outflow tract after birth. Meanwhile, part of the truncus arteriosus would make up the aortic arch. In total seven aortic arches form during embryonic development. The first and second aortic arch disappear with further aortic development. The third aortic arch forms the carotid artery, and the fifth aortic arch regresses very early during development or does not form at all. The sixth forms in pulmonary arch and develops into the pulmonary artery during maturation, but the connection to the dorsal aorta either disappears on the right side or becomes ductus arteriosus on the left side. Only the left fourth aortic arch persists postnatally and serves as the aortic arch. The descending aorta, thoracic aorta and abdominal aorta derive from the dorsal aorta. Separate origins of aorta segments lead to distinct microenvironments, which could partly explain the asymmetric distribution of SPCs. In addition, structure distinction in aortic segments could also be a factor, which affects SPCs distribution. From direct observation, it is easily to see that the aortic arch has more curve and branches, whereas the descending aorta is relatively straight and branchless. This morphological change influences blood flow patterns and the resulting fluid shear stress felt by the vessel wall. Curvatures and branch points experience low levels of shear stress which is thought to cause inflammation in vessel tissue. This inflammation may trigger SPC recruitment and homing to this area and thus aid vessel wall regeneration. More investigation will be required to test this hypothesis.

Figure 4.2

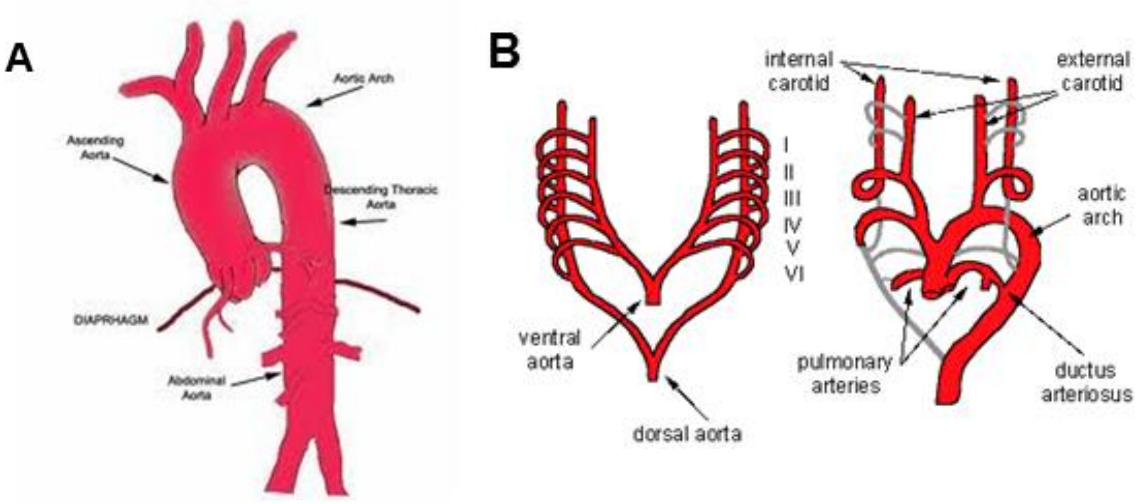

Figure 4.2 Aorta. A, aortic anatomy. The aorta can be divided into ascending aorta, aortic arch, descending aorta, thoracic aorta and abdominal aorta. **B**, aortic embryology. The ascending aorta derives from the aortic sac or truncus arteriosus. The truncus arteriosus consist of aortic arch. In total seven aortic arches form during embryo stage. The first and second aortic arch disappear in adult. The third aortic arch forms the carotid artery, and the fifth aortic arch never forms or regresses. The sixth aortic arch forms in pulmonary arch. Only the left fourth aortic arch persists until postnatal and serves as aortic arch. Descending aorta, thoracic and abdominal aorta derive from dorsal aorta. (Figure Source: **A**, https://www.pinterest.co.uk/pin/370350769327120894/?autologin=true; **B**, https://radiopaedia.org/articles/thoracic-aorta.)

4.3 SPCs in c-kit$^{kit/CreER}$; ROSA26-RFP Mouse

To answer questions in terms of the fate of SPCs, c-kit$^{kit/CreER}$; ROSA26-RFP knock-in and transgenic animal models were employed (Figure 3.2A). The C-kit$^{kit/CreER}$ mouse is one type of knock-in animal, in which a CreER sequence flanks a c-kit promoter. This means that once the cellular c-kit promoter is activated, the CreER sequence is transcribed to produce mRNA, which can then exert function at a protein level. The reporter mouse used in our study is a Rosa26-RFP or Rosa 26-CAG-loxP-stop-loxP-

tdTomato-WPRE transgenic mouse, in which the stop codon is flanked by loxP sites. By crossing these two transgenic or knock in mice, c-kit$^{kit/CreER}$; ROSA26-RFP mice were generated. Within quiescent c-kit^{+} cells, mature Cre is contained by the ER in cytoplasm. Once the animals are injected with tamoxifen, Cre is guided by ER components to translocate into the nucleus and recombines the loxp flanked stop codon sequence. C-kit^{+} cells are labelled with tdTomato/RFP signal, which is permanent regardless of cellular differentiation state. Thus, the progeny of c-kit^{+} cells maintain RFP signal even though expression of c-kit has been lost, permitting us to trace the fate of c-kit^{+} cells. We made a number of observations in this conditional inducible animal model, which have been previously reported in other studies. For example, c-kit^{+} cells were found to differentiate into ECs with lung and heart by using this animal models. However, in this animal model the role of c-kit^{+} cells in the vascular tissues is still unknown. Both c-kit$^{kit/CreER}$ and ROSA26-RFP transgenic mice were designed based on C57/6J background. Several studies have indicated that these transgenic animals including hybrid c-kit$^{kit/CreER}$; ROSA26-RFP mice share similarity with C57/6J wild type animals, in every basic aspect such as shape, fur colour, body weight and daily diet and we also found this to be the case. As c-kit$^{kit/CreER}$; ROSA26-RFP mice are used as lineage tracing mouse model therefore specification in the recombination system is crucial to the final result. In our study, two strategies were applied to ensure system reliability. C-kit$^{kit/CreER}$ is known as a one knock-in mouse model, in which the CreER sequence replaces the c-kit exosome in a one to one pattern. This means that CreER expression accurately depends on c-kit activation level. This knock in mouse model is an improved technique, compared with random integration based traditional transgenic mouse models. In traditional random integration transgenic mouse models, the designed gene would be placed in a random place within the host genome. Meanwhile, transgenic gene expression can be affected by its own exogenous promoter, which could lead to unfaithful expression of the inserted gene. Therefore, our c-kit$^{kit/CreER}$ model insures that CreER replicates c-kit gene expression to a large extent. Another issue affecting the CreER recombination model is endogenous leak. As described previously, in traditional CreER recombination mouse models, in addition to tamoxifen, endogenous oestrogen may also stimulate the ER component, inducing CreER translocation, and leading to endogenous leak. In our study, the *CreER*^{T2} sequence which is designed based on a

mutant ER component, was used in c-kit$^{kit/CreER}$ animal. In this strategy, a mutant ER component which solely recognises tamoxifen, but not endogenous oestrogen was used. This has been shown sufficient to solve this endogenous leak issue in other studies. Another issue that must be monitored in this animal model is recombination efficiency. As described before, tamoxifen injection would ensure Cre recombination, which assists cell labelling. However, tamoxifen used as breast cancer medication has been reported to induce severe side effects including osteoporosis, thromboembolism and reduced cognition. In fact, murine mortality post tamoxifen injection was observed. In our study, 5 doses of 150 µg/g (mouse weight) on five consecutive days was used in consideration of both Cre recombination efficiency and mice survival rate (Figure 3.2A). Our data showed that RFP signal could efficiently and specifically label the c-kit^{+} cells in target tissues including aorta, lung, liver and bone marrow (Figure 3.2 C and Figure 3.2E).

Table 4.2-3 Transgenic mouse

	Traditional Transgenic	**Knock In**
Gene manipulation	Random integration	Point to point replacement
Off-target	High	Low
Specification	Low	High
Efficiency	High	Mild
Exosome interruption	Yes/No	Yes
Identification before use	Yes	Yes

4.4 C-kit^{+} SPCs in Aortic Intima Layer were not Derived from Bone Marrow

In Figure3.1C, we showed that c-kit^{+} cells were distributed in the endothelial layer of WT C57/6J mouse. Therefore, endothelial *en-face* staining was also performed in c-

$kit^{kit/CreER}$; ROSA26-RFP animals to identify c-kit^+ SPCs. Further, to better represent the vascular structure, we divided the whole aorta into five parts following anatomy. From these results, it was shown that RFP signal can be observed in certain parts of the ascending aorta, aortic arch and descending aorta, but not in thoracic and abdominal aorta (Figure 3.3A). This result indicated that c-kit^+ cells were distributed in the vascular intima layer and could potentially be involved in vascular ECs regeneration. Two theories could explain c-kit^+ cells involvement in vascular ECs regeneration. The first theory is through angiogenesis, in which new blood vessels are formed from pre-existing ECs. Angiogenesis is a vital process in both physiology and pathology. Once stimulated, cell surface receptors can be activated for ECs to sprout. Several factors are reported to initiate angiogenesis. For example, data has shown that shear stress can act on ECs leading to ECs mobilisation. In addition, growth factors such as VEGF and FGF can increase ECs permeability and proliferation to facilitate angiogenesis. Under these stimuli, ECs could first release proteases to degrade the ECMs for cell mobilisation. Then with the adhesion molecules, ECs fuse into neighbouring vessels. In our study, c-kit antigen was shown to be expressed within the ECs layer and thus suggesting that these c-kit^+ cells represent a novel population of ECs that are activated under stimulation. In fact, the shear stress pattern within aorta segments is quite distinct. For example, because several branches are within aortic arch area, disturbed and low shear stress are observed in this region. In contrast, unidirectional and high laminar blood flow are detected in the descending aorta. Various studies have shown that distinct blood flow patterns have opposite effects on ECs biology, in which disturbed flow could increase angiogenesis and high shear stress decrease ECs sprouting. This could partly explain the distinct pattern of c-kit^+ cells observed in within different aortic regions within the endothelial layer. The second theory for c-kit^+ cell involvement in ECs regeneration is vasculogenesis. Vasculogenesis is a process, in which *de novo* ECs are formed from ESPCs. This process along with angiogenesis dominates blood vessel formation during embryonic stages. In postnatal stages, vasculogenesis was also shown to form small vessels such as capillaries and tumour vessels. However, the role of vasculogenesis in large vessels is still unknown. In our study, the expression of c-kit^+ cells and their progenies in endothelial layers indicate their potential as SPCs in ECs regeneration. Possibly c-kit^+ SPCs are activated and then fuse into monolayers of ECs similar to angiogenesis.

Several populations of EPs are reported harboured in the vessel wall. However, the role of these EPs in ECs homeostasis requires further study. In summary, the results of *en-face* staining indicate that c-kit^{+} cells were distributed in the vascular intima layer. However, whether these cells participate into angiogenesis or vasculogenesis cannot be confirmed by our *in vivo* work. Thus, *in vitro* work such as endothelial colony-forming cells (ECFCs) culture assay is still needed to demonstrate the stemness of these c-kit^{+} cells.

Another issue was whether these c-kit^{+} SPCs cells were derived from the bone marrow, a site which is known to harbour the SPCs. Therefore, chimeric mice which contain two populations of genetically distinct cells were created by transplanting the bone marrow cells from c-kit$^{kit/CreER}$; ROSA26-RFP to WT C57/6J irradiated mice (Figure 3.3B). This allowed us to examine the role of bone marrow derived c-kit^{+} cells. Two steps are required to produce chimeric mice. The first step is irradiation of WT C57/6J animals. Although the c-kit$^{kit/CreER}$; ROSA26-RFP mice in our study have a C57/6J background. Immune response can still be activated because the bone marrow transplantation was performed between different individuals. If bone marrow cells are directly transplanted into a non-irradiated mouse, transplantation failure would occur. Irradiation is required to clear recipient inflammatory cells to prevent transplant immune response. Irradiation exerts injury on dividing cells such as HSCs within bone marrow. The most commonly used techniques are Gamma and X-ray irradiation. X-ray irradiation was used in our study and the dose used was 900rad, which ensured total myeloablation[223]. After irradiation, immunosuppressed mice were produced, which are suitable for cell transplantation. The second process in generating chimeric mice is transplantation of bone marrow cells. After transplantation, immunosuppressed mice were rescued due to cell replenishment with the transplant cells. In the clinic, bone marrow cell transplantation is a vital treatment for malignant blood diseases such as leukaemia and multiple myeloma. In animal experiments, bone marrow transplantation can be used to obtain crucial information about bone marrow derived cells. In our study, bone marrow cells were flushed out of the femur and tibia of donor c-kit$^{kit/CreER}$; ROSA26-RFP mice, and stored in sterile cell culture medium. Donor bone marrow cells were transplanted to recipient irradiated C57/6J mice through the tail vein. Guided by molecules such as SDF-1, donor cells could home to bone marrow from the circulation. The transplanted bone marrow SPCs can be divided

into the categories of short and long term lived HSCs. Immediately after transplantation, short lived SPCs reconstitute lymphoid and myeloid lineage, whereas long lived SPCs are responsible for long term haematopoietic cells reconstitution. Approximately 21 days after bone marrow transplantation, peripheral haematopoietic lineage is fully reconstituted[224]. Because the recipient mice were myeloablated by irradiation before bone marrow transplant, they were at high risk of infection or death if the donor bone marrow cells failed to reconstitute the immune system. Therefore, survival of the mice is one positive index indicating bone marrow transplantation success. Similar to c-kit$^{kit/CreER}$; ROSA26-RFP mice, chimeric animals were given 5 doses of tamoxifen, for Cre recombination (Figure 3.3B). Afterwards, bone marrow reconstitution was also verified by flow cytometry and immunofluorescence staining. Harvested cells from chimeric mice showed RFP signal (Figure 3.3C). This indicated that both bone marrow transplantation and tamoxifen induced CreER recombination were partially successful.

After chimeric mice were created, aortic *en-face* staining was performed on collected tissue. However, no RFP signal was detected within ECs layers in all aorta tissues from aortic root to abdominal aorta. Several possible reasons could be behind this result. Failure of bone marrow transplantation is one possibility. However, our previous results (Figure 3.3C) which identified RFP in chimeric mice indicated that transplantation was partly successful. However, we also noticed that percentage of RFP^{+} cells in bone marrow were lower in chimeric mice(Figure 3.3C) than that in c-kit$^{kit/CreER}$; ROSA26-RFP mice(Figure 3.2B). In the future study, we still need to prolong the recovery time for chimeric mice after bone marrow transplantation. In addition, survival of the animals without infection or haematopoietic disease suggested that donor bone marrow has re-established the immune system within the recipient animal. Both these findings suggest no RFP signal within the ECs layer is not due to failed transplantation. Another potential reason for negative results is the failure of CreER recombination. However, positive staining in both IF and flow cytometry results demonstrated that our strategy could efficiently induce recombination and label the c-kit^{+} cells in the chimeric animals. Low efficiency labelling of specific ECs because of the knock in lineage tracing animal model may be the culprit. However, previous *en-face* staining data (Figure 3.3A) has shown positive staining of c-kit^{+} cells in c-kit$^{kit/CreER}$; ROSA26-RFP animals. Both of these results indicated that the absence of RFP

staining in chimeric mouse *en-face* staining is not because of failure in labelling target cells. Therefore, our results (Figure 3.3E) indicated that bone marrow c-kit$^+$ SPCs did not differentiate into luminal ECs in physiological state. This raised several areas of interest. The first is the true derivation of these c-kit$^+$ SPCs during vascular regeneration. Resident vascular SPCs are one potential candidate. In fact, due to their location, resident vascular SPCs might rapidly sense the signals from surrounding vascular cells and contribute to ECs vascular homeostasis, but this still needs further study. Another point of interest is that although bone marrow derived c-kit$^+$ SPCs do not contribute to vascular homeostasis, whether they are involved in disease was not clear. For this reason, a vascular allograft accelerated arteriosclerosis mouse model was designed.

4.5 c-kit$^+$ SPCs in Vascular Allograft lesion

To study the role of SPCs in vascular allograft accelerated arteriosclerosis a mouse model was established (Figure 3.4A). The model used in this study has been developed in our lab since 2000 when carotid artery or aorta was allotransplanted[34]. Obviously, mice are much smaller than humans, and naturally murine vascular diameter is very small, increasing the difficulty level of the surgery. The carotid artery and the aorta are the largest blood vessels in mice and therefore the most accessible for use in vascular allograft accelerated arteriosclerosis surgery. In this surgery 1mm cuffs are applied to stabilise and ligate the vessel end. It is well known that long term donor graft ischaemia can easily result in graft fibrosis, which is an inducement for graft failure. Cuff usage greatly reduces the duration of surgery, increasing success rates of the transplantation. Further transplantation between C57BL/6J ($H2^b$) and Balb/c ($H2^d$) mice ensues alloimmuno reaction occurrence because of mismatched MHC molecules (Figure 4.5 A). In this model, cell infiltration in both media and neointima can be observed within 2 weeks of transplantation. After 4 weeks, neointima enlargement leads to vascular stenosis. By 6 weeks, the whole lumen is occluded. In terms of specific cells, data from our lab has shown that the number of ECs derived from the donor decrease over time and entirely lost after 4 weeks[66]. In contrast, the number of host derived ECs increases and these ECs are shown to be involved in both ECs regeneration and microvessels formation (Figure 4.5 B). Similarly a recipient source of cells dominate *de novo* SMC formation in the neointima after 4 weeks[98]. For this reason, we collected the tissues 4 weeks after transplantation. In our study both

cell infiltration, lesion formation and lumen stenosis can be observed. When the tissues were further stained, SPCs were shown to be distributed in the lesion of the allograft (Figure 3.4B). However, more questions arose from this result. Firstly, although SPCs can be detected in the lesion, their fate was still left unknown. During this process, SPCs would home in and colonise the lesion, however, at the same time these cells undergo differentiation mediated by cytokines. When these SPCs terminally differentiate, they lose SPC marker expression. Because cellular marker expression is not stable during their differentiation process, lineage tracing in wild type animal cannot be realized. Furthermore, although SPCs markers including Sca-1, C-kit and CD34 are observed in the lesion, the source of these SPCs in wild type mouse model cannot be detected. Understanding whether these SPCs derive from the donor or recipient cells is vital, because the result directly affect the strategy choice during and after allo-transplantation surgeries. If the SPCs are derive from the donor animal, anti-immune drugs that protect these cells would be vital for improving graft survival rate. In contrast, if the SPCs are from recipient sources, increasing SPCs mobilisation may be one important issue for graft long term maintenance. Additionally, the mechanisms behind migration and differentiation of these cells is hard to detect using only *in vivo* animal models. For this reason, these SPCs were harvested and the underlying mechanisms investigated *in vitro*.

Figure 4.5

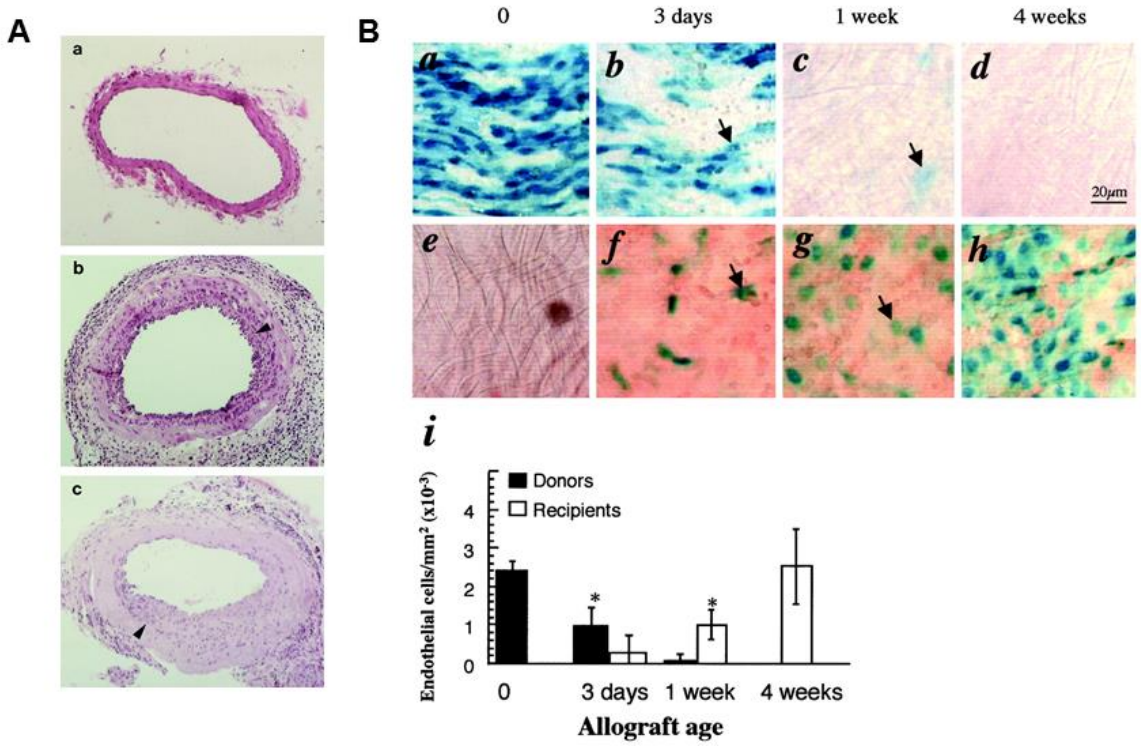

Figure 4.5 Allograft accelerated arteriosclerosis. **A**, HE-stained sections of mouse control artery and artery allografts. Common carotid arteries (a) of C57BL/6J mice, allografted 2 (b) and 4 (c) weeks after surgery. **B**, *En-face* staining of endothelial cells on aortic allografts. a through d, Freshly harvested aorta segments from TIE2-LacZ mice (a) were allografted into carotid arteries of Balb/c mice (b through d). e through h, Freshly harvested aortic segment from a Balb/c mouse (e) was allografted into carotid arteries of TIE2-LacZ mice (f through h). Blue indicates β-gal+ cells. (Figure Source: **A**, Dietrich H, Hu Y, Zou Y, Dirnhofer S, Kleindienst R, Wick G, Xu Q. Mouse model of transplant arteriosclerosis: Role of intercellular adhesion molecule-1. *Arteriosclerosis, thrombosis, and vascular biology*. 2000;20:343-352[34]; **B**, Hu Y, Davison F, Zhang Z, Xu Q. Endothelial replacement and angiogenesis in arteriosclerotic lesions of allografts are contributed by circulating progenitor cells. *Circulation*. 2003;108:3122-3127[66].)

4.6 Death Pathways were Induced in Donor Graft c-kit^{+} SPCs Derived Cells

ECs can be damaged after vascular allograft because of immune cell attack. T cells may directly trigger ECs apoptosis or B cell dominated humoral immune activity may recruit antibodies and complement components, leading to attack on ECs. Immune system involvement results in EC barrier dysfunction and adhesion molecular exposure, both of which lead to ECMs, platelets, erythrocytes and other inflammatory cells infiltrating the graft intima layer. Previous results from our lab have shown that in animal models, donor derived ECs did not survive[66] (Figure 4.5 B). In addition to immune responses, risk factors such as lipid accumulation and local infection can accelerate ECs apoptosis. In fact, acute graft failure is frequently observed after ECs dysfunction. Therefore, EC integrity and regeneration are key to graft survival rate. ESPCs are an important source of regenerated ECs. Once ECs are lost, ESPCs can be activated for vasculogenesis and form a *de novo* lumen within the lesion. However, the source of these ESPCs are still unclear (Table 4.6-1). Our results show that donor derived c-kit^{+} SPCs are not involved in ECs regeneration within allograft tissue (Figure 3.7A and Figure 3.7C). Similar to our other *in vivo* work, procedures were performed to prevent mouse model failure. For example, after the graft c-kit$^{kit/CreER}$; ROSA26-RFP was transplanted to Bab/c mice, tamoxifen was given to recipient animal. This ensured successful Cre recombination within the graft even after allo-transplantation. Therefore, there was no contribution of donor c-kit^{+} SPCs in allograft induced lesions. This agrees with our previous study that suggest regenerated ECs in allograft are not from donor origin[66]. However, studies in human tissue showed a different result. When Y-chromosome *in situ* hybridization was used to investigate female graft tissue that was transplanted into a male recipient, it was found that within transplanted coronary artery graft tissues, more than 95% ECs did not show a Y-chromosome. This indicates that in human graft tissue, most ECs are of donor origin[225]. Later, when similar protocols were performed on cardiac transplantation patients, the results showed the graft was of chimeric ECs, suggesting that only half of ECs were derived from donor resident ESPCs[67]. Contradictory conclusions observed in human and animal studies can be explained by several factors. Firstly, to increase patient survival rate post cardiac allo-transplantation, immunosuppressive drugs are regularly used. Therefore, donor ECs in human tissues may remain in the graft after markedly reduced intima injury. In contrast, to induce lesion formation, immunosuppressive drugs were not used

in a vascular allo-transplantation animal model. As shown previously, ECs were totally desquamated after allo-transplantation. Another potential source of donor derived ECs are resident ESPCs. Similar to ECs, after transplantation, SPCs could also be attacked. Immunosuppressive drugs assist to preserve function of local SPCs to differentiate to ECs. The animal model used in our study was c-kit$^{kit/CreER}$; ROSA26-RFP mouse, which allows tracing of the fate of c-kit^{+} SPCs. Our results indicate that donor derived c-kit^{+} SPCs are not involved in EC regeneration. However, to determine whether other population of SPCs such as donor sca-1^{+} and CD34^{+} cells are involved in allograft arteriosclerosis would require other animal models.

Table 4.6-1 Source of ESPCs in allograft

Species and Allograft	Organ	Method	Recipient	Donor	Bone Marrow	Reference
Mouse						
BM chimera	Aorta	TIE2/LacZ	>95%	<5%	≈30%	Hu et al[23]
BM chimera	Aorta	GFP	Majority	NA	≈20%	Feng et al[26]
Rat						
Sex-mismatch	Heart	Y-PCR	≈100%	0	<5%	Hillebrands et al[19]
BM chimera	Aorta	MHC/HIS52	>95%	NA	≈3%	Hillebrands et al[27]

Human						
Sex-mismatch	Heart	Y-probe	NA	95%	NA	Hruban et al[17]
Sex-mismatch	Heart	Y-probe	42%	58%	NA	Quaini et al[95]
Sex-mismatch	Heart	Y-probe	24.3%	NA	NA	Minami et al[28]
Sex-mismatch	Heart	Y-probe	1–24%	NA	NA	Simper et al[29]
Sex-mismatch	Kidney	MHC/Y-probe	33–66%	<30%	NA	Lagaaij et al[21]

BM indicates bone marrow; GFP, green fluorescent protein; MHC, major histocompatibility complex; NA, not available; Y-PCR, Y chromosome–specific PCR; Y-probe, Y chromosome–specific probe.

(Table Source: Xu Q. Stem cells and transplant arteriosclerosis. *Circulation research*. 2008;102:1011-1024[226].)

After EC dysfunction, SMCs accumulate in the allograft lesion. However, the source of these SMCs is still under debate (Figure 4.6-2). It was firmly believed that SMCs in the lesion were derived from media vascular SMCs. When these SMCs go thorough phenotypic switching, cell potential of migration and proliferation are upregulated[227, 228]. Increased ECM is secreted by SMCs, leading to neointima formation. However, results from our lab indicates another possible conclusion. Data show that after transplantation, no graft derived SMCs were preserved in the neointima[98] and this suggests that after surgery, SMCs undergo cell death. Several studies support this result and in fact, SMCs death is one common hallmark of arteriosclerosis[226]. In the past 20 years, local vascular wall layers harbouring SPCs, were also reported to be

involved in SMCs formation after vascular injury[87, 92]. In our study however, we did not observe any local SPCs after allo-transplantation (Figure 3.7B). This result indicated that donor c-kit$^+$ SPCs were also induced to death. Indeed, a relationship between vascular SMCs and SPCs within the vascular lesion has emerged after years of debate[89]. It was demonstrated that after mild atherosclerosis, vascular SMCs first undergo a phenotype change, to adopt vessel wall remodelling. When vascular injury becomes more severe, apoptosis of the original SMCs occurs and at the same time, SPCs are recruited to injury sites differentiating into SMCs. However, in our study, both donor SMCs and donor c-kit$^+$ SPCs were induced to death because of the severe immuno response and were therefore not involved in SMCs regeneration.

Table 4.6-2 Source of SMCs in allograft

Species and Allograft	Organ	Method	Recipient	Donor	Bone Marrow	Reference
Mouse						
BM chimera	Aorta	Y-probe	Majority	None	None	Li et al[91]
BM chimera	Aorta	LacZ	>95%	NA	10.8%	Shimizu et al[88]
BM chimera	Heart	LacZ/GFP	≈88%	NA	≈82%	Sata et al[92]
BM chimera	Aorta	SM22/LacZ	95%	None	None	Hu et al[20]

Rat						
Sex-mismatch	Heart/aorta	Y-PCR/SMA	>95%	None	None	Hillebrands et al[19]
Human						
Sex-mismatch	Heart	Y-probe	<5%	NA	NA	Hruban et al[17]
Sex-mismatch	Heart	Y-probe	16%	NA	NA	Glaser et al[94]
Sex-mismatch	Heart	Y-probe	60%	NA	NA	Quaini et al[95]
Sex-mismatch	Heart	Y-probe	<5%	NA	NA	Minami et al[28]
Sex-mismatch	Kidney	Y-probe	60–80%	NA	NA	Grimm et al[96]
Sex-mismatch	Heart	Y-probe	None	Majority	NA	Atkinson et al[97]

BM indicates bone marrow; GFP, green fluorescent protein; Y-PCR, Y chromosome–specific PCR; Y-probe, Y chromosome–specific probe; NA, not available.

(Table Source: Xu Q. Stem cells and transplant arteriosclerosis. *Circulation research*. 2008;102:1011-1024[226].)

Cell death can be divided into the pathways of apoptosis, necrosis, autophagy and pyroptosis (Figure 4.6-3). Apoptosis is a programmed cell death realised by a series processes including blebbing, cell shrinkage, and nucleus fragmentation. After the cell fragments are produced, phagocytic cells are recruited to engulf the post-apoptotic contents. Cellular apoptosis is mainly initiated by intrinsic and extrinsic pathways. Intracellular pathways are activated by stress sensed by the cells, whereas extrinsic

pathways are triggered when extracellular ligand binds with cell surface death receptor. After allograft transplantation, TNF-α and Fas ligand (FasL) concentrations are both upregulated due to inflammatory cell activation. When they bind with their receptors on SMCs, death inducing signalling complex (DISC) is formed, which triggers caspase activity. Caspases such as caspase-8 are a group of cysteine-aspartic proteases, which attack target proteins facilitating programmed cell death.

Extracellular pathways increase intracellular stress and stimulate intracellular apoptotic pathway. During this process, mitochondria are induced to swell under proapoptotic protein attack and are prone to rupture further promoting pro-apoptotic effectors to leak out. Then through mitochondrial apoptosis-induced channels, cytochrome C is released into the cytoplasm and forms the apoptosome when binding with caspase-9. With these components, organelles are digested into fragments and cleared by phagocyte without affecting nearby cells.

Necrosis is a pathological process in which cells are induced to injury and death, under extracellular factors. Distinct from apoptosis, necrosis is always detrimental and fatal. Necrosis does not follow apoptotic signalling pathways and has a distinct underlying pattern. Cellular necrosis also starts from surface receptor activation when stimulated by external factors. For example, in the vascular graft, if the lesion area grows restricting the blood flow ischaemia would then initiate SMCs necrosis in a caspase independent manner. In addition, the immune response can also trigger necrosis. During this process, reactive oxygen species (ROS) are produce and the oxygen and glucose supply are depleted which further enhances necrotic lesion development. All these factors result in the breakup of SMCs membrane and thus uncontrolled necrotic cellular products are released into extracellular space. This further upregulates the inflammatory response and recruits more phagocytes to engulf dead cells. However, phagocytosis in necrotic lesions is inefficient. In addition, inflammatory cells could also secrete cytokines. Both the remaining SMCs debris and inflammatory molecules would then function on surrounding cells to promote necrotic lesion enlargement. Meanwhile, platelets, fibroblasts and osteoblasts can be attracted by cytokines. Remnant necrotic SMCs along with ECMs, serve as a nucleating structure or necrotic core, initiating formation of complex lesions, including thrombosis, fibrosis and calcification.

Autophagy is a destructive mechanism which disassembles dysfunctional cellular components. This is executed by the autophagosome, a double membraned vesicle. When the autophagosome fuses with lysosomes, target proteins can be degraded. In SMCs, autophagy is an adaptive response, when under external stress such as starvation and ischaemia. Autophagy ensures SMCs reserve their priority functions such as survival when stress is minor. When stress become more severe, autophagy could also lead to death of unhealthy SMCs to save the energy for comparatively functionally complete SMCs. The current consensus is that in physiological states regulated autophagy promotes SMCs survival, whereas in pathological condition such as atherosclerosis, defective autophagy induces SMCs death contributing to vulnerable lesion formation. Studies have shown that autophagy related genes are regulated by a balance between two protein kinases mTOR and AMPK.

Table 4.6-3 c-kit$^+$ SPCs death

	Autophagy	**Apoptosis**	**Necrosis**
Cell lysis	No	No	Yes
Cell swelling	No	Yes/No	Yes
DNA fragment	Yes/No	Yes	Yes
Trigger	Metabolism change	Apoptosis ligand	Cell stress
Marker	LC3B, p62	DISC, Caspase, Cytochrome-c, PS	N/A
Programmed cell death	No	Yes	No
Occurrence	Biology	Biology/Pathology	Pathology
Function in vessel	Anti-atherosclerosis	Anti/pro-atherosclerosis	pro-atherosclerosis

Several questions remain unanswered in this mouse model. For example, although death of donor source of c-kit$^+$ SPCs was observed in vascular allograft lesion, cells loss rate is unclear. The technique such as terminal UTP nick end-labelling (TUNEL) was used to detect DNA fragmentation in all dead cells. However, this technique

showed no distinct staining in specific cell types such as SMCs and SPCs. When cell death is induced, their specific cell markers are prone to be lost. When different types of cells show a similar profile within the neointma, results of SPCs death rate could be incorrectly estimated. Therefore, in further study, multiple time points and techniques are needed to observe SPCs death rate, which could provide more accurate information in in a comprehensive dynamic way.

The role of SPCs death in arteriosclerosis is still unknown. As described above, autophagy is a protective process once cells are under external stress. Several methods could be used to serve as autophagy markers. Besides direct observation of the autophagosome and morphology under microscope, LC3 and p62 compartment staining could also be used to track autophagy occurrence[229]. In fact, autophagy has been shown to be involved in SPCs biology including homeostasis and differentiation within various tissues such as skeleton and cardiac muscle[131]. However, the role of autophagy in vascular SPCs are still unknown. Furthermore, cell autophagy in atherosclerotic lesions is commonly impaired. Therefore, the role of autophagy and its impaired form in SPCs regulation still needs further study.

When graft injury further develops, SPCs apoptosis and necrosis could be induced. Propidium iodide (PI) and 7-aminoactinomycin D (7-AAD) are fluorescent chemical compounds with high affinity for double stranded DNA. Because they cannot cross live cell membranes, these agents could be used to distinguish live and dead cells. Phosphatidylserine (PS) staining can be used to distinguish between apoptosis and necrosis. PS is an apoptotic marker, which translocates from the cytosol to the surface under regulation of scramblase once the cells undergo programmed death. In addition, processes such as time-lapse morphology change, DNA fragmentation, caspase activation and cytochrome c release are all used to identify SPCs apoptosis. Currently, the link between SPCs death type and injury severity is also unknown. Therefore, in future it would be worth carefully identifying percentage of apoptotic and necrotic cells in different allograft stages. Our results showed that, similarly to SMCs and ECs, SPC derived cells were also induced to death under alloimmuno reaction. However, the role of SPCs death in allograft accelerated arteriosclerosis is still unknown. Though it is clear that ECs and SMCs apoptosis leads to vascular dysfunction and unstable lesion, apoptosis of bone marrow derived macrophages is beneficial for alleviating neointima formation. Meanwhile, when undergoing external stress such as inflammatory attack

after allograft, whether SPCs are directed towards cell death or differentiation still need further study to investigate.

4.7 C-kit^{+} SPCs were from Recipient Source in Vascular Allograft

Role of the recipient SPCs within the vascular graft lesion were determined in this study, in which aorta segment of Balb/c mice were allotransplanted to c-kit$^{kit/CreER}$; ROSA26-RFP mouse (Figure 3.4C). Because the segment showed no transgenic signal, RFP fluorescence can all be regarded to derive from recipient animal. Expression of RFP signal indicated that recipient source of SPCs involved in neointima formation. In terms of specific cells type, we found that recipient source c-kit^{+} SPCs involved in endothelium regeneration (Figure 3.6A). In the literature, it was thought that after ECs dysfunction, the damaged ECs are replaced by donor preserved ECs or ESPCs. However, in our animal model, results showed that after transplantation, no donor derived c-kit^{+} SPCs were detected within neointima. Instead, recipient source of c-kit^{+} SPCs regenerated the endothelium. This result draws a structure of ECs regeneration in vascular allograft. After donor ECs and/or ESPCs were induced to cell death by alloimmune attack, recipient source of c-kit^{+} SPCs were recruited to the graft in a cytokine gradient dependent manner. Once induced to differentiate into ECs, these ESPCs replace original dysfunctional ECs. This result is crucial in understanding pathology of vascular allotransplantation arteriosclerosis. It provided the clues in refining therapeutic strategy. Combined with studies from lab before, it is currently clear that local ECs and ESPCs were rapidly lost after the surgery. Subendothlial layer was therefore exposed to the blood, risking for vascular injury. If more ESPCs attachment and ECs regeneration on ECs layer can be promoted at early stage, the graft failure rate can be possibly reduced. We hypothesized that the number of ESPCs in circulation is critical for endothelium regeneration. This is because our previous study reported that CD34^{+} progenitor cells are lower in apoE$^{-/-}$ mice[230]. This resulted in diminished ECs regeneration and partly explained the increased lesion area in apoE$^{-/-}$ mice. In fact, it has been shown that risk factors such as inflammation and oxidative stress are related to decreased number of ESPCs. ESPCs number has been regarded as one biomarker to predict cardiovascular risk because of its correlation to Framingham cardiovascular score[231]. Therefore, for further clinical application, increasing ESPCs number could be a potential target to prevent chronic vascular allograft failure. For example, data showed that although immunosuppressant drugs

such as cyclosporine and tacrolimus could inhibit inflammatory response which is beneficial to prevent acute graft failure, these drugs could also inhibit cell proliferation. When the inhibition is severe, the number of circulating ESPCs would be decreased, which could be a potential cause for chronic graft. This provided another factor for clinicians, in setting a balance between immunosuppressive drug dosage and duration. In addition, some studies also indicated that after stimulation with vascular risk factors, the number of ESPCs are increased instantly, which seems ambiguous to previous conclusion. For example, it was shown that after some acute myocardial infarctions, ESPCs were increased. The explanation of this paradox is that at the beginning of disease, ESPCs are stimulated and mobilized from their niche to injured site for compensation. However, with continuous stimuli, ESPCs dysfunction occurs resulting in a decrease of proliferation and mobilization along with increased apoptosis. All of these factors contribute to decreased ESPCs number in the long term. Therefore, as a future work, it would be beneficial to investigate the importance of dynamic change in ESPCs cell number to allograft severity. In terms of clinical settings, increasing circulating ESPCs number may raise tumour risk. Therefore, any similar strategy used into post-allotransplantation patient to promote ESPCs regeneration need be appraised on malignant risk before putting into clinic.

Our study also showed that c-kit$^+$ SPCs were involved in microvessel remodelling in the adventitial layer (Figure 3.6B). Vasa vasorum is the small blood vessel network, which supplies the blood and nutrient for the vessel wall. Within the aorta, vasa vasorum normally locate at adventitia and outer part of media. Few vasa vasorum penetrate into intima layer. Study indicated that occlusion in vasa vasorum of abdominal aorta could lead to extensive medial necrosis[232]. In allograft arteriosclerosis pathology, vasa vasorum remodelling also play an important role. It was shown that shortly after ECs injury, *de novo* formed and proliferated vasa vasorum would penetrate from adventitia into intima layer in response to ECs loss. In fact, results from our group showed that microvessel remodelling is one of earliest events occurring after vascular allograft transplantation[66]. The function of these microvessels in arteriosclerosis formation varies in different studies. Some studies demonstrate that vasa vasorum penetration helps to maintain nutrients and growth factors supply which restrict cells death within the lesion. On the other hand, other opinion insists that these neo-vascularized microvessels always have permeable ECs, which are conductive to

inflammatory cells invasion and contribute to lesion enlargement. However, when the disease further proceeds and vasa vasorum occlusion occurs, cell necrosis would be induced because of nutrient shortage. This leads to atherosclerosis complications such as lesion rupture, aneurysm and angioma. In our study when the allotransplantation was performed in chimeric mice (Figure 3.5B), results showed that bone marrow derived c-kit$^+$ SPCs were involved in adventitial microvessls formation (Figure 3.6D). This is not surprising because a study from our group has indicated before that bone marrow derived cells are responsible for neo-vacuolization[66]. After ECs were induced to death by alloimmune response, various molecules were released into circulation. Bone marrow harboured c-kit$^+$ SPCs would be therefore mobilized by cytokines. Then under attracting of chemoattractant, bone marrow derived c-kit$^+$ SPCs were recruited to the graft and when interacting with adhesion molecules expressed on graft cells, c-kit$^+$ SPCs adhered into graft tissue. These bone marrow derived c-kit$^+$ SPCs subsequently are involved in microvessels formation. Although in an early stage, newly formed microvessels could provide graft tissue the blood flow to some extent, final stage of inflammatory vasa vasorum would accelerate arteriosclerosis lesion formation. In our study, data showed that adventitial microvessels derived from bone marrow c-kit$^+$ SPCs were mainly inflammatory ECs (Figure 3.6D).

Although c-kit$^+$ SPCs are a population of cells identified by their communal surface marker c-kit, they are indicated a heterogenic population of ESPCs. For instance, in our study they are divided into bone marrow and non-bone marrow source of c-kit$^+$ SPCs. Data was shown that non-bone marrow source of c-kit$^+$ SPCs mainly functioned in intima layer regeneration (Figure 3.6A and 3.6C), whereas bone marrow derived c-kit$^+$ SPCs involve in microvessels formation (Figure 3.6B and 3.6D). Therefore, further studies are still needed to detect variation in function of different source of c-kit$^+$ SPCs. If different source of c-kit$^+$ ESPCs could be harvested properly in the future, test could be proceeded to compare function such as permeability and neo-vascularized potential in their formed cluster of cells. In addition, gene profile is worth to be established in subsequent studies in different populations of c-kit+ ESPCs. When compared with regenerated c-kit$^+$ ESPCs in the lesion, the true source regenerated ECs can be expected to be identified. This study also provides the clue for future clinical treatment. Data from previous work indicate that ECs layer regeneration is beneficial to restore vessel function, whereas microvessels development could

enhance lesion area. This means if future clinical trials could develop the treatment to upregulate non-bone marrow c-kit$^+$ ESPCs mobilization, and at the same time decrease bone marrow origin of c-kit$^+$ ESPCs attachment to the vessel wall, longer time survive of vascular graft could be expected. After allograft transplantation, inflammatory molecules such as TNF-α and IL-2 are released leading to recipient cell death. Data showed that these molecules could also impact the ESPCs function. Therefore, more future work is required to detect role of these cytokines in c-kit$^+$ SPCs function especially in ECs layer regeneration.

Using the same mouse model (Figure 3.4A), co-expression of RFP and SMCs markers including α-SMA and SM-22 indicates that recipient c-kit$^+$ SPCs differentiated into SMCs in vascular allograft (Figure 3.5A). This accorded with previous study from our lab that, in same mouse model, SMCs within plaque lesion derive from recipient but not donor sources[98]. One possible explanation of this result is that, after donor graft SMCs death since alloimmuno response from recipient inflammatory cells, cytokines as the signal were secreted into circulation. Role of these cytokines in SPCs regulation would be further discussed below. Resulted cytokines or chemokines gradient recruited recipient SPCs into lesion site to replenish SMCs within graft neointima. Subsequently, graft structure can be maintained by newly formed SMCs. Since the bone marrow is important for harbouring c-kit$^+$ SPCs, it is crucial to determine whether bone marrow was involved in SPCs replenishment and SMCs differentiation. Result from allo-transplantation surgery based on Balb/c mice to these chimeric mice (Figure 3.5B) indicated that, bone marrow source of c-kit$^+$ SPCs was not involved in SMCs differentiation (Figure 3.5C). The conclusion that SPCs derived SMCs were of non-bone marrow source agreed to previous study from our lab[98]. This is also in line with results from other groups using injury[233] and ApoE$^{-/-}$ [234] spontaneous atherosclerosis mouse models. However, one study demonstrated that bone marrow derived LacZ$^+$ cells could co-express with α-SMA markers in allo-transplant induced neointima[235]. Later this conclusion was found to be misinterpreted. Instead of real SMCs differentiation *in vivo*, this co-staining was in fact caused from overlapping between SMCs and LacZ$^+$ leukocytes. One possible reason for this false positive result, is lacking high resolution confocal microscope, a technique limitation at that moment.

Other tissues need to be tested, on whether they are source smooth muscle SPCs. A possible source was presumed to be recipient local carotid artery which is close to

anastomoses. However, in our method, instead of directly stitching graft with recipient vessel, a cuff was used to anastomose donor and recipient ends, leaving no direct contact between graft and recipient vessel. Combining with the similar study from our lab[98], local recipient SPCs seem impossible to pass anastomoses into grafts. Another possibility is the non-bone marrow tissues, such as vessel wall, spleen, liver and adipose tissues, all of which were suggested to harbour SPCs. It is rational to speculate that, once stimulated, SPCs from these tissues could be mobilized into circulation and then home to graft under chemokines. Among all of these tissues, vessel wall is the best studied. In fact, all of three vessel wall layers have been reported to harbour SPCs. For example, adventitia as one important perivascular structure, contains several population of SPCs[87, 90], which are capable of differentiating into SMCs-like cells and therefore involved in neointima formation. Meanwhile, another study before, points out that MHC^- stem cells could give rise to SMCs in neointima[92]. In addition, ECs were also shown able to transdifferentiate into SMCs-like cells in atherosclerosis lesions, via endothelial to mesenchymal transition (EndMT) mechanism[236]. Various sources of these stem cells could also partly explain heterogeneity of SMCs in vascular allograft lesions. From various studies, data indicated that SMCs, which account for the highest percentage of cell number in allograft lesions, showed high level of heterogeneity. Traditionally it was thought that this heterogeneity derived from mature donor media SMCs transdifferentiation and it reflects different stage of SMCs dedifferentiation. However, our work has proven that donor SMCs would be induced to death, and then recipient source of SPCs dominate SMCs repopulation. Different source of these SPCs could be the main reason, why the SMCs within the lesion showed distinct phenotypes and characters.

Because the donor SMCs were induced to death after transplantation, recruited SPCs within the graft, could differentiate into SMCs and repopulate vessel wall. During this process SPCs and their derived SMCs would firstly proliferate and reorganize ECMs, which contribute to vessel wall repair and lesion stability in the early stage. When inflammatory injury persists, SPCs accumulation and proliferation would be uncontrolled, which would result in luminal narrowing. In the advanced stage these recipient source of SMCs also undergo programmed cell death under cytokines such as TNF-α and IL-2. Therefore, some targets are worth focusing in future treatment. Firstly, in early stage of transplantation, SPCs mobilization and SMCs commitment is

one potential target for vascular allograft regeneration. Secondly, in long term, accumulation and proliferation of SPCs derived SMCs need to be cautiously regulated to keep the lumen area. Apoptosis and/or necrosis prevention of these newly formed SMCs is another target to inhibit advanced lesion formation. Thirdly, when choosing the drugs, the balance between inflammatory cells inhibition and SPCs function reserve need to be noticed. Both uncontrolled inflammation and SPCs dysfunction could result in graft failure. Summary of source and role of c-kit$^+$ SPCs is shown in

Figure 4.7

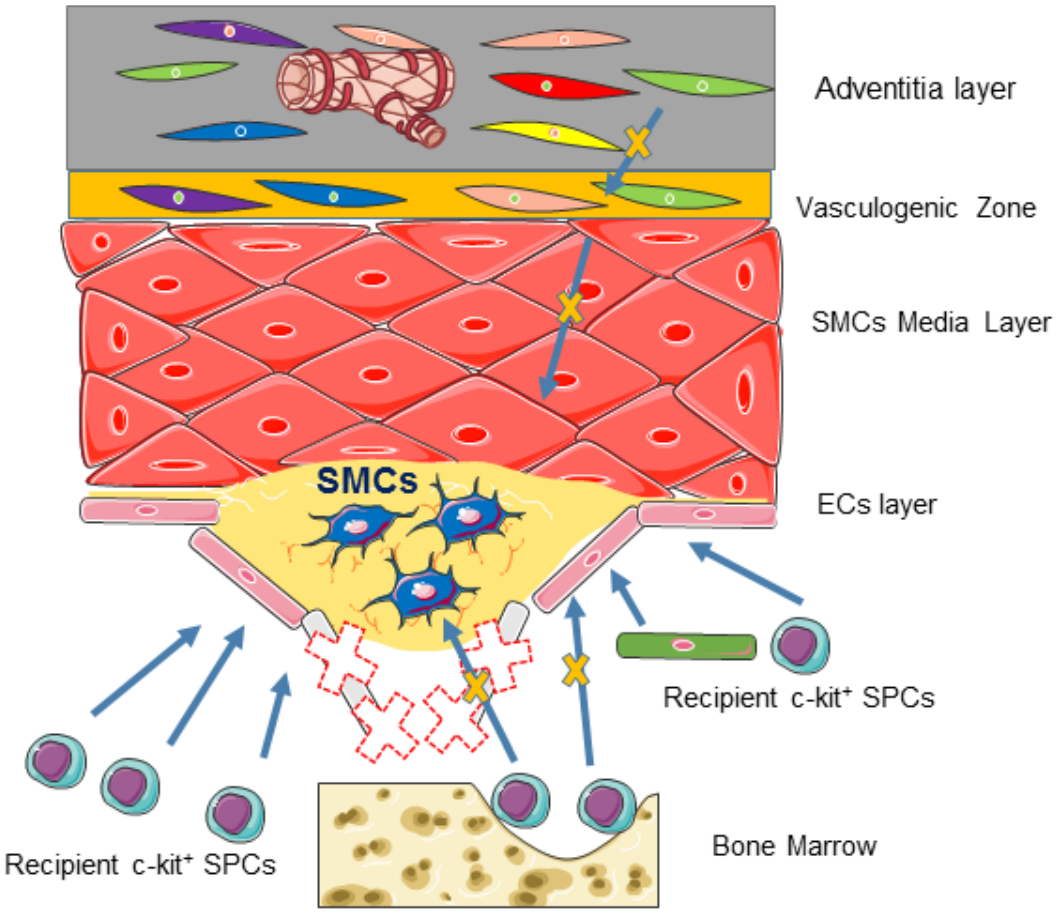

Figure 4.7 Proposed source and role of c-kit$^+$ SPCs in allograft accelerated arteriosclerosis. After vascular allo-transplantation. Donor cells were firstly induced to death. Recipient of c-kit$^+$ SPCs were recruited to the vessel wall. Non-bone marrow source of c-kit$^+$ SPCs were committed to both ECs and SMCs fate in the neointima. SPCs, stem/progenitor cells; ECs, endothelial cells; SMCs, smooth muscle cells.

4.8 C-kit$^+$ SPCs Isolation

Our study required the harvesting of SPCs from vascular grafts. Because the graft was a transplant harvested from surgery, isolated cells in our study were from various sources and for this reason mimic the cell population derived from *in vivo* work. When graft vessels are cut open and applied to the surface of a cell culture flask cells migrate from the graft vessel and after several days form colonies in the flask. After extended culture, vascular stem cells persist and expand in the flasks because of their self-renewal properties. Stem cell culture has been widely used in labs throughout the world, but various points need to be taken into consideration to ensure successful conservation of stem cells pluripotency potential. *In vivo*, stem cells are under quiescent maintenance within a microenvironment or niche, which are full of ECMs favouring stem cells adhesion. Therefore, in our study, the flasks to hold the cells were coated with 0.2% gelatin. When the flask is coated with gelatin, there is a supportive physical environment for cells to attach and grow. Cell to cell interaction is one character of stem cells in the niche. Intercellular interaction allows the cells to relay the signal, and could respond to experiment change when in stress. Our study put the 30,000 cells in 75 cm^2 area, which provide the cells a proper intensity to grow. The culture media used in our study was complete stem cells medium which consists of Dulbecco's Modified Eagle's Medium, 10% foetal bovine serum, 10 ng/mL leukemia inhibitory factor and 0.1 mM 2-mercaptoethanol. Dulbecco's Modified Eagle's Medium is one standard formula stem cell culture medium consist of necessary nutrient including amino acid, glucose, vitamin and ions. Foetal bovine serum could provide cells with growth factors supporting cells to survive and grow. Leukaemia inhibitory factor (LIF) is an IL-6 class cytokine, which inhibit cell differentiation. When binding with cell surface receptor GP130, LIF activates JAK/STAT signalling. This promotes stem cells renew while inhibit cells differentiation. 2-mercaptoethanol is a chemical reducing compound which provides a mercapto group which could scavenge oxygen or hydroxyl radicals for antioxidant. Therefore, adding 2-mercaptoethanol into the medium prevented cell from toxic radical attack. Because *in vitro*, the cells lack the protection of immune system, cells are prone to contamination. Fungi, bacterial, virus and mycoplasma are the common source of contamination which could lead to cell dysfunction or death, antibiotic was therefore loaded to ensure the SPCs were growing in a sterile environment. Meanwhile, because our cells were cultured alone, the risk of

false result from other contaminated cell lines can be avoided. When the cells grew full in the flask, cells were digested with trypsin. Trypsin belongs to serine protease family member and its optimum activity is at 37°C. Therefore, cells detachment was performed in the pre-warmed incubator. During trypsin digestion, long time touch to the cells were avoided to protect the cells from damage. After fully detachment, complete culture medium was added to inactivate trypsin. This inactivation is that the serum in the medium contains antitrypsin and macroglobulin which could stop trypsin activity. To freeze the remaining cells, dimethyl sulfoxide (DMSO) contained medium was used since DMSO can prevent water crystal to lyse the cells during cryopreservation. The reason to use the medium is considering to avoid cells staving during thawing.

Graft SPCs outgrew from our culture condition. However, the cell proportion are still unknown. To separate the target cell population, cells were sorted out of origin cells. Cell sorting could be based on cell size, shape and surface markers. Currently, several methods are used in cell sorting. Single cells sorting such as microrafts and DEPArry lab-based chip technology provided methods to sort the cells based on intracellular and extracellular properties. Florescent activated cell sorting (FACS) is based on flow cytometry to select the cells which contain target surface markers. Magnetic cell sorting makes use of column to separate labelled cells. In recent studies, one technique called buoyancy activated cell sorting was developed, in which microbubbles were bound with cells surface antigens and then through flotation, these cells could be isolated from the samples. From cost-utility ratio point of view, magnetic cell sorting was used in our study. Meanwhile, although c-kit is regarded as a stem cells surface marker, it is also expressed on other cell types such as ECs, hematopoietic cells, mast cells and interstitial cells. Therefore, another cell surface marker sca-1 was also used in our study in cell sorting. Overlapping of these two population could ensure SPCs property to the largest extent, in our study. Flow cytometry study (Figure 3.8B) identified our isolated c-kit$^+$ SPCs. From the result, positive staining of c-kit and sca-1 indicates that cell sorting was successful. Meanwhile, other cells markers were also tested in our cell population. Interestingly, several cell markers were found positively stained including CD34, CD140, CD105, CD29, CD44, and CD201. This indicates that c-kit$^+$ SPCs isolated from graft are heterogeneous cell populations, consisting of various cell types including ECPCs,

fibroblast, MSCs and pericytes. All these cell types were reported to have SPCs potential and could be involved in vascular remodelling. Mesenchymal stem cells (MSCs) are multipotent stromal cells which showed potential to differentiate into several cell types including osteogenic cells, cartilage cells, myocytes and adipose cells. In recent years, MSCs have also been demonstrated to differentiate into both ECs and SMCs to assist in vessel regeneration. This indicated the c-kit$^+$ SPCs in our study might be a population of MSCs. Several tissues were indicated to harbour MSCs including bone marrow, adipose tissue and resident vessel wall. Fibroblasts are typical biological cells which could synthesize ECMs and play critical role in vascular wound healing and fibrosis. In the vessel wall, fibroblasts normally locate at the adventitial layer. Pericytes are a population of cells that located around ECs consisting small vessel in vascular system. In tradition, both fibroblasts and pericytes exert paracrine function for surrounding cells. In recent studies however, it was shown that these cells could transform into SPCs and contribute to both vascular biology and pathology processes. This result fits our expectation, because other similar studies have indicated a heterogeneous population in SPCs. However, more work still needs to be performed in the future to demonstrate unanswered questions. For example, it is important to address whether our isolated cells were distinct populations, or they are derived from an ancestor. Although these cells express various markers, some similar study points out they may come from the same source and the various markers could be explained by the different stage of the same cells. Alternatively, if these cells do derive from multiple sources, the distinction and their respective fates need to be compared.

4.9 SCF Induced c-kit$^+$ SPCs Migration

Stem cell factor (SCF) is specific ligand for c-kit receptor. SCF exists two forms, a soluble and a membrane bound isoform. Soluble SCF is derived from membrane bound isoforms, which have been cleaved by a protease. Both soluble and membrane bound SCF can bind with c-kit to promote intracellular tyrosine kinase activation. As one typical cytokine, SCF expresses in ECs and fibroblasts. From our results (Figure 3.8A), in physiological aorta SCF was mainly expressed in the intima layer and adventitial layers, coinciding with previous studies. After transplantation, results showed that SCF spread all over the graft (Figure 3.8A). The explanation is that, when graft cells were induced to death after transplantation, SCF was released from these

cells, which could then bind with c-kit receptor and attract the c-kit$^+$ SPCs. However, from our previous studies, c-kit$^+$ SPCs were circulating in the blood. It is rational to speculate that SCF would also be released into the circulation to mobilize these cells. Therefore, ELISA assay was used in our study to investigate the change of SCF in circulation. Enzyme-linked immunosorbent assay (ELISA) is one widely used technique in clinic to detect the antigen in the sample for diagnosis. The principle of ELISA is based on antigen-antibody reaction. Target antigen could interact with specific antibody. The antibody is pre-connected with the designed enzyme. After substrate for enzyme is added, substrate reaction would produce signal, which can be detected by spectrophotometry. Intensity under standard setting is correlated with antigen concentration. Therefore, ELISA assay could accurately quantify SCF content in plasma. According to detection mode, ELISA can be divided into direct, sandwich and competitive ELISA. In direct ELISA, antigen contained buffer is directly added to the surface. Subsequently the enzyme contained antibodies are added to detect the antigen. Within this method, the enzyme can be used as amplifier, which could transfer reaction signal in a recognized and quantitative level. However, a major disadvantage in this method is that antigen capture is non-specific, especially in serum or plasma samples, which contain large number of antigens competing with surface area and decrease the chance of target antigens to stick on the plate. Sandwich ELISA is one improved technique. In this method, specific capture antibody would be pre-bounded at surface. When the sample is added into the plate, target antigen can be specifically captured by the antibody. After detecting antibodies are applied, signal could be detected. In this way, unspecific binding antigen induced problems can be avoided. Competitive ELISA is one comparatively less common used method, to detect antigen in non-purified samples. In consideration of sensitivity and specificity, our study used sandwich ELISA and found that SCF concentration was upregulated after transplantation (Figure 3.8A). In summary, both ELISA and IF staining result indicated that SCF is upregulated both locally and in circulation after vascular injury caused allo-transplantation. Also this result demonstrated that SCF could potentially mobilize c-kit$^+$ SPCs from the niche into circulation, and then attract these cells to lesion area. But this still needs *in vitro* work to demonstrate.

Cell motility allows the cells to change their position. Cell accumulation is one character of neointima. In general, motility assays can be separated into migration and

invasion assay. In the biological field, migration is defined as direct cell position change on substrate such as ECMs and plastic plate on a 2D surface, whereas invasion is regarded as ability, with which cells could break through the complex 3D matrix during movement. During invasive processes, cells need to go through series steps including attachment to ECMs, shape modification and/or ECMs digestion. For example, when leucocytes are mobilized from the bone marrow under cytokines, they migrate first in the blood without attaching to ECMs. Once recruited by local vascular chemokines, they attach on lumen surface and then invade into the vascular wall. Migration is a pre-condition of invasion. In other words, cells could not invade without migration capability. Mode of cell motility can be divided into single cell and multiple cells migration. Single cells could migrate simply by cytoskeleton rearrangement with or without attaching to ECMs, whereas multiple or collective cells migration involves cell to cell interaction. Both motility models could occur simultaneously. Animal studies demonstrated that SCF would be upregulated after transplantation. The role of SCF in c-kit$^+$ SPCs function is still unknown within *in vivo* work. Therefore, our study tested how SCF activated c-kit$^+$ SPCs in different assays in regarding to study cells migration, proliferation and differentiation.

In our study, two cell motility assays, transwell assay and wound healing assay were used to detect the effect of SCF on c-kit$^+$ SPCs migration *in vitro* (Table 4.9). Transwell assay or Boyden chamber assay is one classic method to observe cell chemotaxis. In a transwell kit, two chambers are separated by a pore membrane. When the cells could translocate from inner/upper chamber into the outer/lower surface, they are regarded going through migration. Two chambers were loaded with medium with different concentration of cytokines. Normally, cytokines concentration in outer chamber is higher than that in the inner chamber. Then the cells loaded in upper chamber could migrate under the attraction of cytokines. The membrane pore size is lower than cell diameter and this ensure that cells would not drop because of its own gravity. Only when guided under cytokines, these cells could change their morphology and pass the membrane. In our study, because SPCs size is on average around 30μm, pore size at 8μm of transwell assay kit was employed. During the assay, several other points need to be noticed. Firstly, height of medium level need to be equal. Because the liquid pressure could also drive cell to migrate, different medium level could result in false end. In our study, 100 μl and 600 μl medium were put into the inner and outer

chamber, respectively. This ensured the medium height to keep in an even level. Second, incubation time needs to be carefully controlled. If incubation time is too short, the cells could have not initiate to migrate. Conversely, when incubation time is too long, cells would migrate too extensively beyond membrane surface area limitation, which makes comparison impossible. Therefore, from previous test results, our study decided to load 1,000,000 cells and incubate for 18h, from which the result is suitable to observe. After incubation, migrated cells were fixed and stained using crystal violet. The remaining cells on the upper chamber were removed by cotton swab and then migrated cells can be counted under microscope. The advantage in using transwell assay is that this experiment could easily detect the SPCs motility capability when in response to gradient of SCF. The disadvantage is that dynamic cell migratory pattern cannot be acquired because this assay could only observe and count the cell number once at the endpoint. Another migration study used in our study is scratch wound healing assay. This assay also provided us the chance to observe cell migration but in a dynamic pattern. In this experiment, confluent SPCs on a plate were wounded by a scrape exerted by pipette tips. The rate at which cells fill in the gap can be regarded as cell migrating speed. Under the microscope, speed of cell movement can be measured dynamically. With this method, cell migration in several time points can be observed. Because uneven thick scratch could affect the result, our study used the same pipette tips in different groups trying to reduce variation between groups. Meanwhile, because heavy scratch is an external stress which could induce the cells to death. Therefore, when performing scratch wound on the cells, gentle action was preferred which minimizes the injury to cells. By using these two migration assays, our study demonstrated that SCF induced c-kit^{+} SPCs in a dose dependent manner (Figure 3.8C and Figure 3.8D). ACK2 is a blocking antibody, which could inhibit c-kit kinase activity. When ACK2 was applied into the working medium, data showed that SCF induced increase in cell migration can be partially reversed (Figure 3.8E). This indicated that effect of SCF on SPCs is through c-kit activity.

Cytoskeleton as cellular basic component is crucial in regulating cell migration (Table 4.9). By using cytoskeleton assay, SPCs migration can be detected in a single cell level (Figure 3.9A). Phalloidin is a toxin found in death cap mushroom. When it is injected into the blood, it rapidly binds with F-actin. When binding with F-actin subunit, they showed higher affinity to actin monomers leading to decreased dissociated rate

of actin subunit and then harm to filament depolymerization. Meanwhile, phalloidin could inhibit ATP hydrolysis and trap ADP. Since its high affinity to F-actin, phalloidin carrying fluorescence substrate was used as to label F-actin. Because phalloidin cannot penetrate cell membrane, this tagged antibody is commonly used in dead fixed and permeabilised cells such as which in our study, instead of live cells. Our result showed that in untreated cells, F-actin locate across the whole cell body but in a rambling pattern. However, instantly after SCF treatment, F-actin accumulate at the leading edge of membrane forming in filopodia and lamellipodia structure to sense the signal and initiate cell migration. As stated before, vinculin is a cytoskeleton protein located at the cell membrane and involve in focal adhesion formation. Along with other focal adhesion proteins such as paxillin and α-catenin, vinculin serves to bind F-actin with cell membrane. From our study, vinculin was recruited early to the cell protrusion. Unlike floating cells such as leucocyte in blood flow, SPCs migrate on ECMs in a scramble manner. Therefore, focal adhesion could serve as feet during the cell spread process. Meanwhile, FAK was also appeared at focal adhesion site. Previous data have indicated that FAK is pivotal for cell motility. FAK activation in a phosphorylation form could activate downstream proteins, which in one hand dissociate adhesion complex, and in other hand, promote further cell protrusion F-actin formation. Our result indicated that, migration of SPCs under SCF is rapidly initiated, because of cytoskeleton rearrangement (Figure 3.9A). This migration is not constant. Instead, they went through several stages, including protrusion formation, F-actin stabilization and adhesion dissociation which are series of classic migratory manners of scramble cells.

Table 4.9 Migration assays

	Transwell Assay	**Scratch Wound Healing Assay**	**Cytoskeleton Assay**
Chemokine gradient	Yes	No	No
Cell injury	No	Yes	No
Measurement	Cell count	Migration Area/ Cell count	Cytoskeleton rearrangement
Movement direction	Vertical/ Horizontal	Horizontal	Horizontal

Migration Pattern	Single cell/ Collective	Collective	Single cell
Measure timepoint	Endpoint	Dynamic	Endpoint/Dynamic
Cell state	Live	Live	Dead

In our study, incubation time of transwell assay and scratch wound healing assay were both 18h, which is long enough for cells expansion. Migratory assays result could be affected by uneven cell division. Therefore, proliferation assays were also performed in our study. Cell proliferation or division is one stem cell character. In quiescent state, cells stay in G0 phase without replication. However, once stimulated, quiescent stem cells are induced to divide. Cell division can be divided into four stages including G1, S, G2 and M phases (Figure 4.9). G1 phase is the first stage of cell division process. During G1 phase, cells enlarge in size and synthesize necessary substrate to prepare for DNA duplication. S phases is the stage when DNA duplication occurs. G2 phase continues to increase genetic materials. At the end, cells enter in M phase to divide one cells into two daughter cells.

Figure 4.9

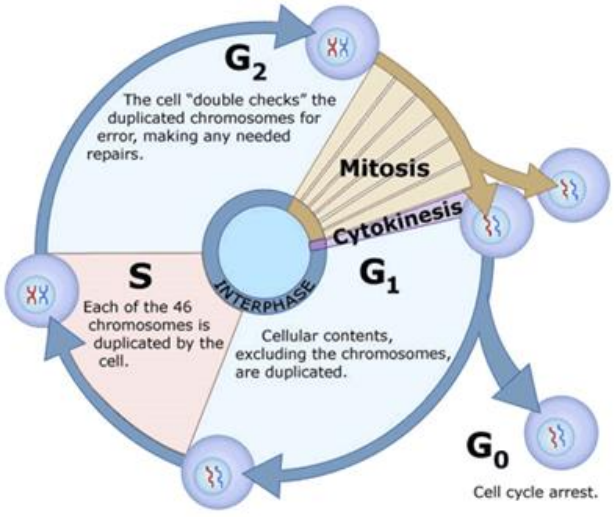

Figure 4.9 Cell cycle. Quiescent stay in G0 phase without replication. G1 phase synthesize necessary substrate for DNA duplication. S phases is responsible for DNA

duplication occurs. G2 phase continues to increase genetic materials. Cell divide in M phase. (Figure Source: www2.le.ac.uk/projects/vgec/highereducation/topics/cellcycle-mitosis-meiosis.)

During the whole cell cycle, four points control the cell proliferation. The first point is called restriction point(R-point), which locates between G1 and s phases. R-point decides whether the cells would continue further cell cycle or turn back to G0 phase. Once the cells pass the R-point, they do not need persistent extracellular stimulation to maintain the cell cycle. Then three checkpoints are responsible for cell cycle. G1/S checkpoint is located at end of G1 phase. Some studies hold the opinion that G1/S checkpoint and R-point located at the same place, but the conclusion still needs further study to demonstrate. One major target of the G1/S checkpoint is to check cellular DNA integrity. If DNA damage is detected at this point, cell cycle would be delayed or arrested at G1 phase. After the cells pass G1/S checkpoint and S phase replication, S/G2 checkpoint functions to assess if proper chromosome duplication is ready and duplicated newly formed genetic material is defective. At the end whether the kinetochore has attached to spindle fibre would be evaluated at G2/M checkpoint. Once the cells pass this point, cellular division occurs. The whole cell cycle is under regulation of cyclin. Cyclin has no enzymatic activity but could provide binding sites for downstream substrates such as CDKs. Cyclin-dependent kinases (CDKs) are a group of kinase, which could activate cell cycle through phosphorylating other proteins. Only when cyclin-CDKs complex is formed, cell cycle could be initiated. Cyclin-CDKs complex activity can be inhibited by negative regulatory molecules such as retinoblastoma protein (RB), p53 and p21. When the cell DNA is damaged under stress, these molecules would be accumulated for repaired. If the damage is too heavy and cannot be repaired, they would induce cell to death. Therefore, these negative regulatory molecules function in cell mutant and if dysfunction occurs on these molecules, cell aberration occurs. Currently, several proliferation related indexes including DNA synthesis, metabolic activity, proliferation markers and ATP consumption were used to detect proliferation rate. In our study, Brdu assay and ki67^{+} cell counting was used to detect the effect of SCF on c-kit^{+} SPCs proliferation. Brdu is a synthetic nucleoside which could function similar to thymidine. When the Brdu is loaded into the sample, it incorporates into newly synthesized DNA during S phase. After adding Brdu specific antibody, incorporated Brdu number can be detected which

represent cell proliferation rate. Ki67 is one nucleus protein associated with ribosomal RNA transcription. It locates at cell nucleus and is present in all cell cycle stages but not quiescent cells. It is a classic proliferative marker which could be used to detect percentage of proliferating cells. In our study, after 18h SCF incubation, both Brdu number in immunoassay and ki67^{+} cells percentage in flow cytometry showed no significant difference in c-kit^{+} SPCs (Figure 3.8F). This indicated that within 18h, SCF would not alter the rate of c-kit^{+} SPCs division rate. Also this meant that SCF effect on c-kit^{+} SPCs migration was not due to increase proliferation rate.

4.10 ACK2 Reduced Arteriosclerosis Lesion

SCF upregulated c-kit^{+} SPCs migration *in vitro* (Figure 3.8C and Figure 3.8D) and this can be partially inhibited by c-kit blocking antibody ACK2 (Figure 3.8E). Therefore, we wondered if ACK2 could also decrease lesion after vascular allo-transplantation. Artery stenotic lesion is one complex result during vascular adaptive remodelling. After ECs are injured from various factors, they are leaky to several cytokines or leucocyte. Meanwhile, SMCs within intima layer are induced to proliferate and secrete ECMs leading to intimal hyperplasia. During lesion development, SMCs derived from any sources would accumulate into the lesion sites forming neointima and occupying the vascular lumen. When the lesion proceeds with thrombosis accumulation in the end stage, they could obstruct the whole lumen with or without lesion rupture. Several histologic indexes are important to atherosclerosis diagnosis. Lumen area is a parameter, which is correlated to vascular ischemia. When the lumen area is large, blood is flowing fluently, whereas when it is small, blood flow is restricted due to vessel wall narrowing. Neointima area is another biomarker to diagnose atherosclerosis. Increased neointima area indicates higher risk of vascular events. Because our study mainly used collected vascular tissue, lumen area and neointima area were used as parameters to appraise vascular lesion. Vascular allograft was transplanted again from balb/c to C57/6J mice (Figure 3.8G). Meanwhile, the graft was encompassed by pluronic F127 gel with ACK2 or with igG (Figure 3.8G). Pluronic F127 gel is one triblock copolymers that maintains in gel structure at room temperature, but become liquid state at 4-5°C. Previous study indicates pluronic F127 gel is suitable for drug release. Because of these characters, pluronic F127 gel was used in our study for local antibody delivery and release. To analyse the collected tissues, H&E staining was used. Haematoxylin and eosin (H&E) stain is one principle histological method for

clinical diagnosis. In this method, haematoxylin bind with basophilic structure such as DNA and stain them in blue. Eosin tends to stain eosinophilic proteins within plasma or ECMs into red. From H&E staining, our result showed that ACK2 significantly decreased lesion area whereas increased lumen area (Figure 3.8H). In addition, there is also a significant decrease in cell number (Figure 3.8H). This can be explained by our migration result that ACK2 could inhibit SCF induced c-kit^{+} SPCs accumulation after the vascular allo-transplantation. Our previous result indicated that c-kit^{+} SPCs could differentiate into SMCs. Since SMCs accumulation is one well known culprit in arteriosclerosis formation, we therefore also performed IF staining to count the SMCs cell number. Our results showed that SMCs accumulation is also significantly decreased (Figure 3.8I). Combining with these result, we concluded that c-kit+ SPCs migration and SMCs differentiation were the cause of lesion formation *in vivo*. Therefore, ACK2 could be a potential treatment to allograft related arteriosclerosis in future clinical work.

4.11 SCF/C-kit Axis Signalling

Murine c-kit gene was cloned and sequenced in 1993[237]. When c-kit is translated into protein level, it serves as a tyrosine kinase receptor protein. C-kit, as the cell surface marker, belongs to type III receptor tyrosine kinase. On structure, c-kit is a transmembrane protein mainly consist of extracellular domain, which bind with its ligand and intracellular tyrosine domain, which is responsible for phosphate group transfer. Core size of c-kit protein is around 110kDa and when it is glycosylated, mature c-kit protein forms with the size at around 150kDa. C-kit is rapidly activated by dimerization. When two separate c-kit monomers bind with the ligand, they are brought together and the same time, structure conformation is induced for protein interaction. When intracellular domains of dimers are close to each other, tyrosine kinase are activated for transphosphorylation. During this process, phosphate group are transferred from ATP to tyrosine residues. Multiple sites of tyrosine residues have been identified as kinase activity domains (Tyr-547, 553, 568, 570, 703, 721, 730, 823, 900, 936)[216]. In fact, c-kit activation has been shown involved in regulating cells function in several systems including hematopoietic system, genital system, cardiac system and respiratory system. Our previous data have demonstrated that c-kit^{+} SPCs were involved in vascular remodelling under regulation of SCF after allo-transplantation. However, how does SCF regulate c-kit+ SPCs was still unknown.

Since phosphorylation is activation form of c-kit, we firstly tested if c-kit is phosphorylated after SCF treatment. Phosphate group transfer via protein kinases is one common method for cells to regulate target proteins activity. Several methods were traditional used to detect target protein phosphorylation including kinases activity assay, phosphor-antibodies incubation, and western blot. Recently, cell-based ELISA, intracellular flow cytometry, mass spectrometry and multi-analytic profiling were developed based on signal cell or multiple target points. In our study, classic electrophoretic based western blot assay was employed to detect protein phosphorylation. Several points were needed to be take consideration when detecting phosphorylation proteins. First, since the posttranslational modification was easy to be disrupted, gentle protein harvest was performed to prevent pre-damage of phosphorylated proteins. Second, incubation buffer was replaced to TBST instead of PBST because previous data indicates phosphate group react with substrate in PBST. Our results showed that after SCF treatment, c-kit transformed into phosphorylated form rapidly (Figure 3.9B). This indicated that, binding with SCF stimulated c-kit transformation, to receive the phosphate group from energy providing substrate ATP. As one kind of kinase, multiple intracellular tyrosine sites could receive phosphate group to induce more than one response. In fact, SCF were reported to induce several response in c-kit^{+} cells[216]. However, the role of SCF in regulating vascular SPCs migration is still unknown. Therefore, further downstream signalling factors were tested. As indicated before, small GTPases including Rac1, CDC42 and RhoA are upstream factors that are involved in cell migration instantly after cytokines activation. Small GTPases or known as G-proteins serve as a switch in cytosol. When the bind with GDP, they are inactive whereas when they bind with GTP they are activated. After activated, they transfer phosphate group to downstream targets. Traditional method to detect GTPase activity is co-immunoprecipitation (Co-IP) assay. To test binding between GTP and small GTPases, cell lysate against GTPase would be isolated using microbeads. After electrophoresis, target proteins binding with GTP could be detected using specific antibodies. Recently, another technique called G-LISA is developed to detect small GTPases activity. Similar to ELISA assay, small GTPases effect proteins would be coated in the plate, and only GTP but not GDP bounded G protein could bind on the plate. After luminescence reaction, amount of specific GTP bounded G protein could be detected from absorbance number. Compared with Co-IP assay, G-LISA

assay required less time and can be quantified (Table 4.11). Therefore, our study used G-LISA assay to detect small GTPases activity. For our studies, data showed that after SCF stimulation, mount of active Cdc42, RhoA, and Rac1 within c-kit$^+$ SPCs significantly increased at 0.5min, 1min and 2min, respectively (Figure 3.9C). This indicated that these small GTPases were rapidly activated after stimulation. Then the activated Cdc42 quickly promote F-actin assembly forming filopodia as a signal sensor. Meanwhile, Rac1 regulated lamellipodia formation and matured cell protrusion. Downstream of RhoA is MLC and MLC phosphorylation increase myosin II contractility, providing cells contacting force during migration. Mitogen-activated protein kinases (MAPKs) belongs to protein kinase that functions in several cellular activities. Because our initial results firstly related MAPKs with CDKs for cell proliferation, they were termed as mitogen activated proteins. However, our results showed that they were also related to cell migration. For example, previous studies pointed out that that ERK mutation impaired cell migration[238]. Downstream target of ERK to stimulate cell motility includes MLCK, deadhesion related proteins and calpain. Therefore, we investigated whether MAPK signalling respond after SCF treatment. In western blot result, data showed that MEK/ERK signalling is activated rapidly which facilitates and promotes MLC phosphorylation for cell migration (Figure 3.9B). Our result showed that JNK/c-jun pathway could also be activated by phosphorylation (Figure 3.9B). C-jun is a protein which could bind with c-fos to forms AP-1, one early response transcription factor. Previous data showed that AP-1 could activate cell migration through MMPs release. Our ELISA data showed that after long term SCF regulation, MMP2 but not MMP9 was upregulated which assist ECMs digestion for cell motility (Figure 3.9E). In summary, after SCF treatment on c-kit$^+$ SPCs, SCF/c-kit axis is activated, which promote multiple pathways to regulate cell migration.

Table 4.11 Small GTPases activity assay

	Co-IP	**GLISA**
Lysate amount	Large	Small
Time consuming	High	Low
Quantification	Semi	Yes

4.12 VEGF Induced c-kit$^+$ SPCs Migration

As indicated before, VEGF family is a group of important molecules in vascular biology to induce ECs migration. Our data indicated that VEGF were also involved in c-kit$^+$ SPCs regulation. We assessed VEGF expression after allo-transplantation *in vivo*. Data showed that after transplantation, VEGF distributed in all the neointima (Figure 3.10A). This was possibly due to ECs death caused VEGF release. Although VEGF has been shown to induce angiogenesis, the effect of VEGF on SPCs was unknown. Therefore, transwell assay was used to detect the role of VEGF on c-kit$^+$ SPCs migration. From our result, it was shown that VEGF significantly increased c-kit$^+$ SPCs migration (Figure 3.10B). In single cell level, VEGF could induce c-kit$^+$ SPCs cytoskeleton rearrangement (Figure 3.10C). Protein Kinase B (Akt) is an important kinase downstream of VEGF kinase receptor. Akt could promote various cell function including survival, metabolism, proliferation and migration. By western blot, our study showed that Akt could be rapidly phosphorylated after VEGF commitment on c-kit$^+$ SPCs (Figure 3.10D). Meanwhile, phosphorylated Akt transfer phosphor group to downstream FAK leading to adhesion kinase activation for cell motility (Figure 3.10D). Our data also showed that Akt inhibitor could significantly reduce VEGF induced cell migration (Figure 3.10E). These data indicated that similar to SCF, VEGF acted as a chemoattractant for c-kit$^+$ SPCs. Signalling pathway in SCF and VEGF on c-kit$^+$ SPCs are drawn in Figure 4.11-12.

Figure 4.11-12.

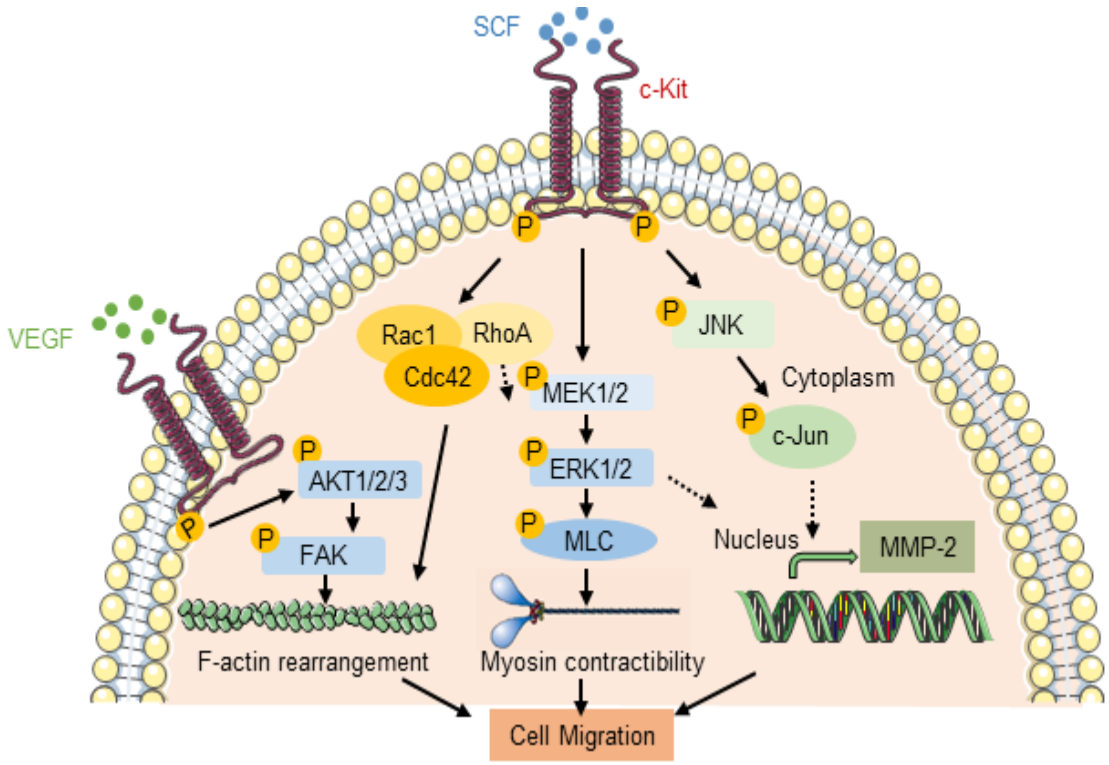

Figure 4.11-12 Schematic diagram illustrating possible mechanisms regulating c-Kit$^+$ SPC migration. SCF stimulates c-Kit phosphorylation and induces activation of downstream small GTPases, MEK/ERK and JNK/c-Jun pathways. Activation of Rac1 and Cdc42 facilitates F-actin rearrangement to form cell protrusion. MLC can be phosphorylated through MEK/ERK signaling and increases myosin contractibility. Activation of MEK/ERK and JNK/c-Jun pathways may further promote MMP-2 expression. VEGF stimulates AKT1/2/3 phosphorylation and activates downstream FAK. These signaling pathways activated by SCF/c-Kit axis or VEGF concomitantly contribute to cell migration.

4.13 Future Work and Perspectives

In summary, we demonstrate here that a recipient non-bone marrow source of c-kit$^+$ SPCs give rise to both SMCs and ECs, contributing to neointima formation in an allograft transplantation model. Cytokines such as SCF and VEGF promote cell migration. These findings may provide novel insights into pathogenesis of neointima formation and further potential therapeutic implications for vascular diseases. However, several issues are left unanswered and will need to be addressed in future studies.

Firstly, although our study indicates that a non-bone marrow source of c-kit$^+$ SPCs play a key role in both neointima formation and EC regeneration after allo-transplantation the precise source of these c-kit$^+$ SPCs is still unclear. Tissues including the vessel wall, spleen, liver, heart and lungs are all reported to harbour SPCs. Therefore, they are potential candidate sources of c-kit$^+$ SPCs. In future studies, if tagged c-kit$^+$ SPCs can be successfully cultured from these specific tissues and then transplanted back into vascular allograft animals, function of these cells could be tested *in vivo*. In our studies, the fate of c-kit$^+$ SPCs were tracked by lineage tracing studies. However, the role of other populations of SPCs such as sca-1$^+$ and CD34$^+$ cells is still unknown. Meanwhile, the relationship between each SPCs population is also unclear. Our study indicates that these SPCs populations overlap to a certain degree. Therefore, in future studies, lineage tracing studies targeting sca-1$^+$ and CD34$^+$ cells are necessary to address their fate. In the future work, if combined lineage tracing technique such as double, or even triple system based for these populations can be developed, the relationship between these cells can be expected to be demonstrated. In addition, our study also demonstrated the role of c-kit$^+$ SPCs in a vascular allo-graft mouse model. However, atherosclerosis*/* arteriosclerosis is not limited to a vascular allo-transplantation mouse model. Other atherosclerosis types including spontaneous, vascular injury and vein graft induced atherosclerosis are also reported. In future, if c-kit$^{kit/CreER}$; ROSA26-RFP mice can be applied in these mouse model the difference in c-kit$^+$ SPCs function can be compared in different mouse models.

Our study also showed that only recipient c-kit$^+$ SPCs are involved in vascular graft induced neointima formation. c-kit$^+$ SPCs from donor animals were possibly killed by

the recipient immune system. However, results from some other studies are not totally the same. Some human studies have concluded that donor SPCs were responsible for neointima formation. A possible reason for this variation is that, immunosuppression drugs were not used in our animal model. In the clinic, immunosuppression drugs are regularly used to prevent immunoreaction, which partly explains the preservation of donor SPCs after surgery. Therefore, in future works, immunosuppression drugs can be applied in our animal model, to clarify whether this difference is because of these drugs. Furthermore, these kinds of studies are also helpful in observing the effect of immunosuppression drugs on both donor and recipient SPCs, which can help improve clinic treatment. Another issue need to be addressed, is our vascular mouse model. Although vascular allograft mouse model perfectly mimic vascular pathology after allo-transplantation, it was not entirely the same with solid organ transplantation. In fact, apart from transplanted vessel itself, graft is also affected by nearby graft parenchymal cells such as liver cells, cardiomyocytes and pulmonary cells. Therefore, further solid organ allo-transplantation mouse models are advice to perform, though high level of difficulties. In this way, heart, liver and kidney transplantation, can be better mimicked in lineage tracing mouse model. This will give us more comprehensive information concerning solid organ allo-transplantation instead of sorely focusing on certain aspects. Further, as state before, immunoreaction is one of the main causes of allo-transplantation induced vasculopathy or arteriosclerosis. However, role of immunoreaction on SPCs are still unknown. We speculate that immunoreaction could do harm to SPCs, but this still need further studies to demonstrate. Meanwhile, if harmed SPCs can be acquired, comparison in disease model can be achieved between these cells and healthy SPCs. With this, new role of immunoreaction in allo-transplantation induced vasculopathy can be addressed. Similarly, effect other risk factors can be addressed by this strategy.

Thirdly, our results proposed that SCF and VEGF promote c-kit^{+} SPCs migration, which potentially contribute to neointima formation. This was verified by result that SCF significantly decreased vascular allograft induced lesion. However, in circulation, distribution of cytokines network is far more complex. Therefore, role of other chemoattractant and the relationship between each other could be examined in future studies. Moreover, although we provided the evidence that these cells can be attracted to the lesion, the underlying cell differentiation mechanism is still unknown. Data from

my colleague showed that TGFβ as a cytokine could stimulate c-kit$^+$ SPCs for SMCs differentiation via glucose metabolism regulation (Figure 4.13). However, further studies on other molecules are still needed, which could give us better understanding in allo-transplantation induced vasculopathy pathology.

Figure 4.13

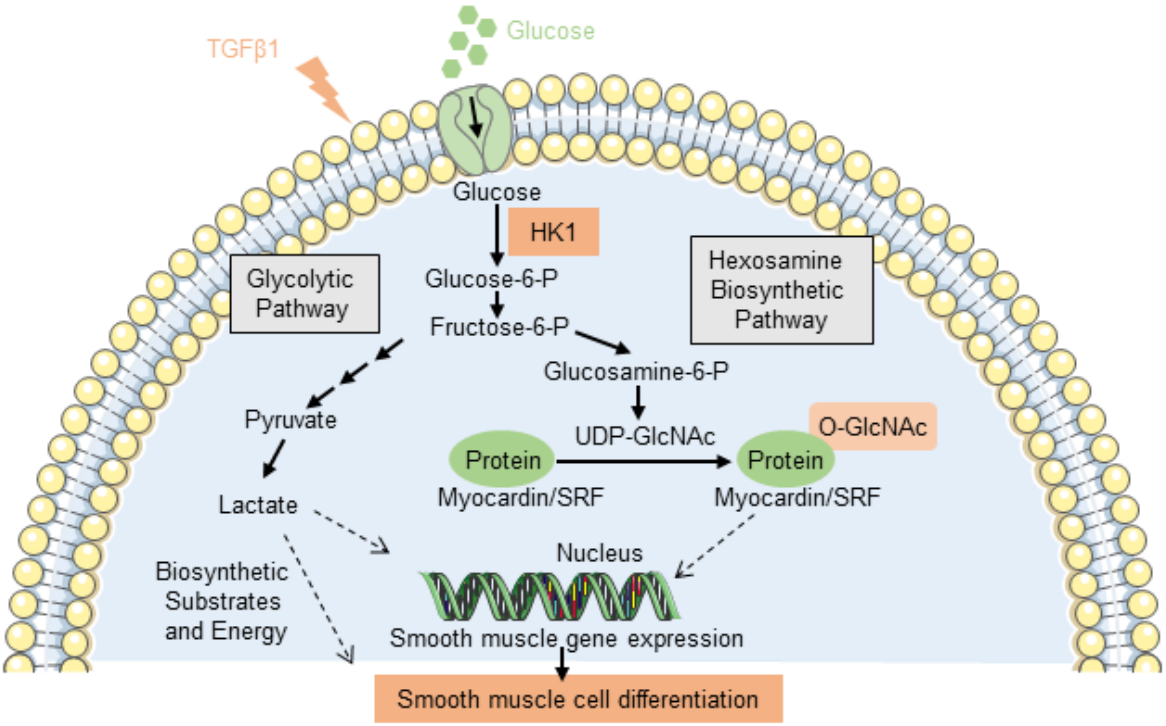

Figure 4.13 Schematic diagram illustrating possible mechanisms regulating c-Kit$^+$ SPC differentiation. TGFβ1 increases glucose uptake and activates glucose metabolism in c-Kit$^+$ SPCs. HK1-dependent glucose metablism leads to activation of the downstream glycolytic pathway and hexosamine biosynthetic pathway. The glycolytic pathway may provide biosynthetic substrates and energy for cell growth and differentiation. The hexosamine biosynthetic pathway provides UDP-N-acetylglucosamine (UDP-GlcNAc), a substrate for protein O-GlcNAcylation, to increase O-GlcNAcylation of SRF and myocardin, which may further regulate smooth muscle gene expression.

Chaper 5: Conclusion

5.1. SPCs are one group of important cells distributing in aorta;

5.2. c-kit$^+$ SPCs involved in endothelial cells homeostasis;

5.3. After vascular allograft surgery, donor c-kit$^+$ SPCs were induced to death;

5.4. Recipient but not donor source of c-kit$^+$ SPCs contributed to vascular allograft induced arteriosclerosis formation;

5.5. Non-bone marrow derivation of c-kit$^+$ SPCs were responsible for ECs and SMCs repopulation after vascular allo-transplantation;

5.6. From vascular allograft, c-kit$^+$ SPCs could be harvested and these cells showed high heterogeneous character;

5.7. As chemoattractant, both SCF and VEGF induced c-kit$^+$ SPCs migration after vascular allograft surgery;

5.8. c-kit blocking antibody ACK2 could partially inhibit SCF induced c-kit$^+$ SPCs migration and decrease vascular allo-transplantation induced lesion area;

5.9. SCF/c-kit axis is crucial in c-kit$^+$ SPCs migration via regulating cell cytoskeleton rearrangement and ECMs regulation.

Chaper 6: Publications and Abstracts

6.1. Publication and Manuscripts

Kokkinopoulos I, Wong MM, Potter CMF, Xie Y, Yu B, Warren DT, Nowak WN, Le Bras A, **Ni Z**, Zhou C, Ruan X, Karamariti E, Hu Y, Zhang L, Xu Q. Adventitial sca-1(+) progenitor cell gene sequencing reveals the mechanisms of cell migration in response to hyperlipidemia. *Stem cell reports*. 2017;9:681-696.

Ni Z., Deng J., Potter CMF., Nowak WN., Zhang Z., Hu Y.; Xu Q. Recipient Stem/Progenitor Cells Dominantly Repopulate Smooth Muscle Cells of Transplant Arteriosclerosis in Mouse Model. Submitted.

6.2. Abstracts

Xie Y., Potter C., Le Bras A., Nowak W., Gu W., **Ni Z**., Hu Y., Zhang L., Xu Q. Leptin Induces Sca-1 + Progenitor Cell Migration Enhancing Neointimal Lesions in Vessel-Injury Mouse Models. University of Fribourg, Switzerland, 7-9 November 2016. Poster Presentation.

Ni Z., Deng J., Potter CMF., Nowak WN., Zhang Z., Hu Y.; Xu Q. Recipient Stem/Progenitor Cells Repopulate Allograft Vessels. In preparation. King's BHF Centre of Research Excellence Postgraduate Symposium, London, 15 May 2018. Oral Presentation.

Chaper 7: References

1. Sakai T, Hosoyamada Y. Are the precapillary sphincters and metarterioles universal components of the microcirculation? An historical review. The journal of physiological sciences : JPS. 2013;63:319-331
2. Birbrair A, Zhang T, Wang ZM, Messi ML, Mintz A, Delbono O. Pericytes at the intersection between tissue regeneration and pathology. Clinical science. 2015;128:81-93
3. Colvin M, Smith JM, Hadley N, Skeans MA, Carrico R, Uccellini K, Lehman R, Robinson A, Israni AK, Snyder JJ, Kasiske BL. Optn/srtr 2016 annual data report: Heart. American journal of transplantation : official journal of the American Society of Transplantation and the American Society of Transplant Surgeons. 2018;18 Suppl 1:291-362
4. Kim WR, Lake JR, Smith JM, Schladt DP, Skeans MA, Harper AM, Wainright JL, Snyder JJ, Israni AK, Kasiske BL. Optn/srtr 2016 annual data report: Liver. American journal of transplantation : official journal of the American Society of Transplantation and the American Society of Transplant Surgeons. 2018;18 Suppl 1:172-253
5. Hart A, Smith JM, Skeans MA, Gustafson SK, Wilk AR, Robinson A, Wainright JL, Haynes CR, Snyder JJ, Kasiske BL, Israni AK. Optn/srtr 2016 annual data report: Kidney. American journal of transplantation : official journal of the American Society of Transplantation and the American Society of Transplant Surgeons. 2018;18 Suppl 1:18-113
6. Hogan PG, Chen L, Nardone J, Rao A. Transcriptional regulation by calcium, calcineurin, and nfat. Genes & development. 2003;17:2205-2232
7. Morelon E, Stern M, Kreis H. Interstitial pneumonitis associated with sirolimus therapy in renal-transplant recipients. The New England journal of medicine. 2000;343:225-226
8. Vitko S, Viklicky O. Cyclosporine renal dysfunction. Transplantation proceedings. 2004;36:243S-247S
9. Lund LH, Khush KK, Cherikh WS, Goldfarb S, Kucheryavaya AY, Levvey BJ, Meiser B, Rossano JW, Chambers DC, Yusen RD, Stehlik J, International Society for H, Lung T. The registry of the international society for heart and lung transplantation: Thirty-fourth adult heart transplantation report-2017; focus theme: Allograft ischemic time. The Journal of heart and lung transplantation : the official publication of the International Society for Heart Transplantation. 2017;36:1037-1046
10. Lu WH, Palatnik K, Fishbein GA, Lai C, Levi DS, Perens G, Alejos J, Kobashigawa J, Fishbein MC. Diverse morphologic manifestations of cardiac allograft vasculopathy: A pathologic study of 64 allograft hearts. The Journal of heart and lung transplantation : the official publication of the International Society for Heart Transplantation. 2011;30:1044-1050
11. Colvin-Adams M, Harcourt N, Duprez D. Endothelial dysfunction and cardiac allograft vasculopathy. Journal of cardiovascular translational research. 2013;6:263-277
12. Rogers NJ, Lechler RI. Allorecognition. American journal of transplantation : official journal of the American Society of Transplantation and the American Society of Transplant Surgeons. 2001;1:97-102
13. van Loosdregt J, van Oosterhout MF, Bruggink AH, van Wichen DF, van Kuik J, de Koning E, Baan CC, de Jonge N, Gmelig-Meyling FH, de Weger RA. The chemokine and chemokine receptor profile of infiltrating cells in the wall of arteries with cardiac allograft vasculopathy is indicative of a memory t-helper 1 response. Circulation. 2006;114:1599-1607
14. Smyth LA, Harker N, Turnbull W, El-Doueik H, Klavinskis L, Kioussis D, Lombardi G, Lechler R. The relative efficiency of acquisition of mhc:Peptide complexes and cross-presentation depends on dendritic cell type. Journal of immunology. 2008;181:3212-3220
15. Jones ND, Van Maurik A, Hara M, Gilot BJ, Morris PJ, Wood KJ. T-cell activation, proliferation, and memory after cardiac transplantation in vivo. Annals of surgery. 1999;229:570-578
16. Tambur AR, Pamboukian SV, Costanzo MR, Herrera ND, Dunlap S, Montpetit M, Heroux A. The presence of hla-directed antibodies after heart transplantation is associated with poor allograft outcome. Transplantation. 2005;80:1019-1025
17. Diujvestijn AM, Derhaag JG, van Breda Vriesman PJ. Complement activation by anti-endothelial cell antibodies in mhc-mismatched and mhc-matched heart allograft rejection: Anti-mhc-, but not anti non-mhc alloantibodies are effective in complement activation. Transplant international : official journal of the European Society for Organ Transplantation. 2000;13:363-371
18. Obhrai J, Goldstein DR. The role of toll-like receptors in solid organ transplantation. Transplantation. 2006;81:497-502

19. Huibers M, De Jonge N, Van Kuik J, Koning ES, Van Wichen D, Dullens H, Schipper M, De Weger R. Intimal fibrosis in human cardiac allograft vasculopathy. Transplant immunology. 2011;25:124-132
20. Kitchens WH, Chase CM, Uehara S, Cornell LD, Colvin RB, Russell PS, Madsen JC. Macrophage depletion suppresses cardiac allograft vasculopathy in mice. American journal of transplantation : official journal of the American Society of Transplantation and the American Society of Transplant Surgeons. 2007;7:2675-2682
21. Saiki T, Ezaki T, Ogawa M, Maeda K, Yagita H, Matsuno K. In vivo roles of donor and host dendritic cells in allogeneic immune response: Cluster formation with host proliferating t cells. Journal of leukocyte biology. 2001;69:705-712
22. Win TS, Rehakova S, Negus MC, Saeb-Parsy K, Goddard M, Conlon TM, Bolton EM, Bradley JA, Pettigrew GJ. Donor cd4 t cells contribute to cardiac allograft vasculopathy by providing help for autoantibody production. Circulation. Heart failure. 2009;2:361-369
23. Tanaka K, Albin MJ, Yuan X, Yamaura K, Habicht A, Murayama T, Grimm M, Waaga AM, Ueno T, Padera RF, Yagita H, Azuma M, Shin T, Blazar BR, Rothstein DM, Sayegh MH, Najafian N. Pdl1 is required for peripheral transplantation tolerance and protection from chronic allograft rejection. Journal of immunology. 2007;179:5204-5210
24. Izawa A, Ueno T, Jurewicz M, Ito T, Tanaka K, Takahashi M, Ikeda U, Sobolev O, Fiorina P, Smith RN, Hynes RO, Abdi R. Importance of donor- and recipient-derived selectins in cardiac allograft rejection. Journal of the American Society of Nephrology : JASN. 2007;18:2929-2936
25. Chong AS, Alegre ML, Miller ML, Fairchild RL. Lessons and limits of mouse models. Cold Spring Harbor perspectives in medicine. 2013;3:a015495
26. Corry RJ, Winn HJ, Russell PS. Primarily vascularized allografts of hearts in mice. The role of h-2d, h-2k, and non-h-2 antigens in rejection. Transplantation. 1973;16:343-350
27. Li Q, Peng Q, Xing G, Li K, Wang N, Farrar CA, Meader L, Sacks SH, Zhou W. Deficiency of c5ar prolongs renal allograft survival. Journal of the American Society of Nephrology : JASN. 2010;21:1344-1353
28. Schenk S, Kish DD, He C, El-Sawy T, Chiffoleau E, Chen C, Wu Z, Sandner S, Gorbachev AV, Fukamachi K, Heeger PS, Sayegh MH, Turka LA, Fairchild RL. Alloreactive t cell responses and acute rejection of single class ii mhc-disparate heart allografts are under strict regulation by cd4+ cd25+ t cells. Journal of immunology. 2005;174:3741-3748
29. Nozaki T, Amano H, Bickerstaff A, Orosz CG, Novick AC, Tanabe K, Fairchild RL. Antibody-mediated rejection of cardiac allografts in ccr5-deficient recipients. Journal of immunology. 2007;179:5238-5245
30. Mombaerts P, Iacomini J, Johnson RS, Herrup K, Tonegawa S, Papaioannou VE. Rag-1-deficient mice have no mature b and t lymphocytes. Cell. 1992;68:869-877
31. Uehara S, Chase CM, Kitchens WH, Rose HS, Colvin RB, Russell PS, Madsen JC. Nk cells can trigger allograft vasculopathy: The role of hybrid resistance in solid organ allografts. Journal of immunology. 2005;175:3424-3430
32. Shi C, Russell ME, Bianchi C, Newell JB, Haber E. Murine model of accelerated transplant arteriosclerosis. Circulation research. 1994;75:199-207
33. Koulack J, McAlister VC, Giacomantonio CA, Bitter-Suermann H, MacDonald AS, Lee TD. Development of a mouse aortic transplant model of chronic rejection. Microsurgery. 1995;16:110-113
34. Dietrich H, Hu Y, Zou Y, Dirnhofer S, Kleindienst R, Wick G, Xu Q. Mouse model of transplant arteriosclerosis: Role of intercellular adhesion molecule-1. Arteriosclerosis, thrombosis, and vascular biology. 2000;20:343-352
35. Zou Y, Dietrich H, Hu Y, Metzler B, Wick G, Xu Q. Mouse model of venous bypass graft arteriosclerosis. The American journal of pathology. 1998;153:1301-1310
36. Nagano H, Mitchell RN, Taylor MK, Hasegawa S, Tilney NL, Libby P. Interferon-gamma deficiency prevents coronary arteriosclerosis but not myocardial rejection in transplanted mouse hearts. The Journal of clinical investigation. 1997;100:550-557
37. Skoskiewicz MJ, Colvin RB, Schneeberger EE, Russell PS. Widespread and selective induction of major histocompatibility complex-determined antigens in vivo by gamma interferon. The Journal of experimental medicine. 1985;162:1645-1664
38. Sharrocks AD, Brown AL, Ling Y, Yates PR. The ets-domain transcription factor family. The international journal of biochemistry & cell biology. 1997;29:1371-1387
39. Garrett-Sinha LA. Review of ets1 structure, function, and roles in immunity. Cellular and molecular life sciences : CMLS. 2013;70:3375-3390

40. Asahara T, Murohara T, Sullivan A, Silver M, van der Zee R, Li T, Witzenbichler B, Schatteman G, Isner JM. Isolation of putative progenitor endothelial cells for angiogenesis. Science. 1997;275:964-967
41. Werner N, Kosiol S, Schiegl T, Ahlers P, Walenta K, Link A, Bohm M, Nickenig G. Circulating endothelial progenitor cells and cardiovascular outcomes. The New England journal of medicine. 2005;353:999-1007
42. Rohde E, Malischnik C, Thaler D, Maierhofer T, Linkesch W, Lanzer G, Guelly C, Strunk D. Blood monocytes mimic endothelial progenitor cells. Stem cells. 2006;24:357-367
43. Rohde E, Bartmann C, Schallmoser K, Reinisch A, Lanzer G, Linkesch W, Guelly C, Strunk D. Immune cells mimic the morphology of endothelial progenitor colonies in vitro. Stem cells. 2007;25:1746-1752
44. Ingram DA, Mead LE, Tanaka H, Meade V, Fenoglio A, Mortell K, Pollok K, Ferkowicz MJ, Gilley D, Yoder MC. Identification of a novel hierarchy of endothelial progenitor cells using human peripheral and umbilical cord blood. Blood. 2004;104:2752-2760
45. Yoder MC, Mead LE, Prater D, Krier TR, Mroueh KN, Li F, Krasich R, Temm CJ, Prchal JT, Ingram DA. Redefining endothelial progenitor cells via clonal analysis and hematopoietic stem/progenitor cell principals. Blood. 2007;109:1801-1809
46. Balaji S, Han N, Moles C, Shaaban AF, Bollyky PL, Crombleholme TM, Keswani SG. Angiopoietin-1 improves endothelial progenitor cell-dependent neovascularization in diabetic wounds. Surgery. 2015;158:846-856
47. Dimmeler S, Fleming I, Fisslthaler B, Hermann C, Busse R, Zeiher AM. Activation of nitric oxide synthase in endothelial cells by akt-dependent phosphorylation. Nature. 1999;399:601-605
48. Gu Z, Kaul M, Yan B, Kridel SJ, Cui J, Strongin A, Smith JW, Liddington RC, Lipton SA. S-nitrosylation of matrix metalloproteinases: Signaling pathway to neuronal cell death. Science. 2002;297:1186-1190
49. Heissig B, Hattori K, Dias S, Friedrich M, Ferris B, Hackett NR, Crystal RG, Besmer P, Lyden D, Moore MA, Werb Z, Rafii S. Recruitment of stem and progenitor cells from the bone marrow niche requires mmp-9 mediated release of kit-ligand. Cell. 2002;109:625-637
50. Schioppa T, Uranchimeg B, Saccani A, Biswas SK, Doni A, Rapisarda A, Bernasconi S, Saccani S, Nebuloni M, Vago L, Mantovani A, Melillo G, Sica A. Regulation of the chemokine receptor cxcr4 by hypoxia. The Journal of experimental medicine. 2003;198:1391-1402
51. Shepherd RM, Capoccia BJ, Devine SM, Dipersio J, Trinkaus KM, Ingram D, Link DC. Angiogenic cells can be rapidly mobilized and efficiently harvested from the blood following treatment with amd3100. Blood. 2006;108:3662-3667
52. Qin G, Ii M, Silver M, Wecker A, Bord E, Ma H, Gavin M, Goukassian DA, Yoon YS, Papayannopoulou T, Asahara T, Kearney M, Thorne T, Curry C, Eaton L, Heyd L, Dinesh D, Kishore R, Zhu Y, Losordo DW. Functional disruption of alpha4 integrin mobilizes bone marrow-derived endothelial progenitors and augments ischemic neovascularization. The Journal of experimental medicine. 2006;203:153-163
53. Ingram DA, Mead LE, Moore DB, Woodard W, Fenoglio A, Yoder MC. Vessel wall-derived endothelial cells rapidly proliferate because they contain a complete hierarchy of endothelial progenitor cells. Blood. 2005;105:2783-2786
54. Fang S, Wei J, Pentinmikko N, Leinonen H, Salven P. Generation of functional blood vessels from a single c-kit+ adult vascular endothelial stem cell. PLoS biology. 2012;10:e1001407
55. Naito H, Kidoya H, Sakimoto S, Wakabayashi T, Takakura N. Identification and characterization of a resident vascular stem/progenitor cell population in preexisting blood vessels. The EMBO journal. 2012;31:842-855
56. Zengin E, Chalajour F, Gehling UM, Ito WD, Treede H, Lauke H, Weil J, Reichenspurner H, Kilic N, Ergun S. Vascular wall resident progenitor cells: A source for postnatal vasculogenesis. Development. 2006;133:1543-1551
57. Bearzi C, Leri A, Lo Monaco F, Rota M, Gonzalez A, Hosoda T, Pepe M, Qanud K, Ojaimi C, Bardelli S, D'Amario D, D'Alessandro DA, Michler RE, Dimmeler S, Zeiher AM, Urbanek K, Hintze TH, Kajstura J, Anversa P. Identification of a coronary vascular progenitor cell in the human heart. Proceedings of the National Academy of Sciences of the United States of America. 2009;106:15885-15890
58. Psaltis PJ, Simari RD. Vascular wall progenitor cells in health and disease. Circulation research. 2015;116:1392-1412
59. Kajstura J, Rota M, Hall SR, Hosoda T, D'Amario D, Sanada F, Zheng H, Ogorek B, Rondon-Clavo C, Ferreira-Martins J, Matsuda A, Arranto C, Goichberg P, Giordano G, Haley KJ, Bardelli

S, Rayatzadeh H, Liu X, Quaini F, Liao R, Leri A, Perrella MA, Loscalzo J, Anversa P. Evidence for human lung stem cells. The New England journal of medicine. 2011;364:1795-1806
60. Suzuki T, Suzuki S, Fujino N, Ota C, Yamada M, Suzuki T, Yamaya M, Kondo T, Kubo H. C-kit immunoexpression delineates a putative endothelial progenitor cell population in developing human lungs. American journal of physiology. Lung cellular and molecular physiology. 2014;306:L855-865
61. Liu Q, Huang X, Zhang H, Tian X, He L, Yang R, Yan Y, Wang QD, Gillich A, Zhou B. C-kit(+) cells adopt vascular endothelial but not epithelial cell fates during lung maintenance and repair. Nature medicine. 2015;21:866-868
62. Orlic D, Kajstura J, Chimenti S, Jakoniuk I, Anderson SM, Li B, Pickel J, McKay R, Nadal-Ginard B, Bodine DM, Leri A, Anversa P. Bone marrow cells regenerate infarcted myocardium. Nature. 2001;410:701-705
63. Murry CE, Soonpaa MH, Reinecke H, Nakajima H, Nakajima HO, Rubart M, Pasumarthi KB, Virag JI, Bartelmez SH, Poppa V, Bradford G, Dowell JD, Williams DA, Field LJ. Haematopoietic stem cells do not transdifferentiate into cardiac myocytes in myocardial infarcts. Nature. 2004;428:664-668
64. Janssens S, Dubois C, Bogaert J, Theunissen K, Deroose C, Desmet W, Kalantzi M, Herbots L, Sinnaeve P, Dens J, Maertens J, Rademakers F, Dymarkowski S, Gheysens O, Van Cleemput J, Bormans G, Nuyts J, Belmans A, Mortelmans L, Boogaerts M, Van de Werf F. Autologous bone marrow-derived stem-cell transfer in patients with st-segment elevation myocardial infarction: Double-blind, randomised controlled trial. Lancet. 2006;367:113-121
65. van Berlo JH, Kanisicak O, Maillet M, Vagnozzi RJ, Karch J, Lin SC, Middleton RC, Marban E, Molkentin JD. C-kit+ cells minimally contribute cardiomyocytes to the heart. Nature. 2014;509:337-341
66. Hu Y, Davison F, Zhang Z, Xu Q. Endothelial replacement and angiogenesis in arteriosclerotic lesions of allografts are contributed by circulating progenitor cells. Circulation. 2003;108:3122-3127
67. Quaini F, Urbanek K, Beltrami AP, Finato N, Beltrami CA, Nadal-Ginard B, Kajstura J, Leri A, Anversa P. Chimerism of the transplanted heart. The New England journal of medicine. 2002;346:5-15
68. Hillebrands JL, Klatter FA, van Dijk WD, Rozing J. Bone marrow does not contribute substantially to endothelial-cell replacement in transplant arteriosclerosis. Nature medicine. 2002;8:194-195
69. Sakihama H, Masunaga T, Yamashita K, Hashimoto T, Inobe M, Todo S, Uede T. Stromal cell-derived factor-1 and cxcr4 interaction is critical for development of transplant arteriosclerosis. Circulation. 2004;110:2924-2930
70. Rossig L, Urbich C, Bruhl T, Dernbach E, Heeschen C, Chavakis E, Sasaki K, Aicher D, Diehl F, Seeger F, Potente M, Aicher A, Zanetta L, Dejana E, Zeiher AM, Dimmeler S. Histone deacetylase activity is essential for the expression of hoxa9 and for endothelial commitment of progenitor cells. The Journal of experimental medicine. 2005;201:1825-1835
71. Yang JY, Wang Q, Wang W, Zeng LF. Histone deacetylases and cardiovascular cell lineage commitment. World journal of stem cells. 2015;7:852-858
72. Qu K, Wang Z, Lin XL, Zhang K, He XL, Zhang H. Micrornas: Key regulators of endothelial progenitor cell functions. Clinica chimica acta; international journal of clinical chemistry. 2015;448:65-73
73. Di Bernardini E, Campagnolo P, Margariti A, Zampetaki A, Karamariti E, Hu Y, Xu Q. Endothelial lineage differentiation from induced pluripotent stem cells is regulated by microrna-21 and transforming growth factor beta2 (tgf-beta2) pathways. The Journal of biological chemistry. 2014;289:3383-3393
74. Meng S, Cao J, Wang L, Zhou Q, Li Y, Shen C, Zhang X, Wang C. Microrna 107 partly inhibits endothelial progenitor cells differentiation via hif-1beta. PloS one. 2012;7:e40323
75. Eisen H, Kobashigawa J, Starling RC, Valantine H, Mancini D. Improving outcomes in heart transplantation: The potential of proliferation signal inhibitors. Transplantation proceedings. 2005;37:4S-17S
76. Owens GK. Regulation of differentiation of vascular smooth muscle cells. Physiological reviews. 1995;75:487-517
77. Majesky MW, Dong XR, Regan JN, Hoglund VJ. Vascular smooth muscle progenitor cells: Building and repairing blood vessels. Circulation research. 2011;108:365-377
78. Treisman R. Transient accumulation of c-fos rna following serum stimulation requires a conserved 5' element and c-fos 3' sequences. Cell. 1985;42:889-902

79. Minty A, Kedes L. Upstream regions of the human cardiac actin gene that modulate its transcription in muscle cells: Presence of an evolutionarily conserved repeated motif. Molecular and cellular biology. 1986;6:2125-2136
80. Miano JM. Serum response factor: Toggling between disparate programs of gene expression. Journal of molecular and cellular cardiology. 2003;35:577-593
81. Norman C, Runswick M, Pollock R, Treisman R. Isolation and properties of cdna clones encoding srf, a transcription factor that binds to the c-fos serum response element. Cell. 1988;55:989-1003
82. Wang D, Chang PS, Wang Z, Sutherland L, Richardson JA, Small E, Krieg PA, Olson EN. Activation of cardiac gene expression by myocardin, a transcriptional cofactor for serum response factor. Cell. 2001;105:851-862
83. Wang DZ, Li S, Hockemeyer D, Sutherland L, Wang Z, Schratt G, Richardson JA, Nordheim A, Olson EN. Potentiation of serum response factor activity by a family of myocardin-related transcription factors. Proceedings of the National Academy of Sciences of the United States of America. 2002;99:14855-14860
84. Qiu P, Ritchie RP, Fu Z, Cao D, Cumming J, Miano JM, Wang DZ, Li HJ, Li L. Myocardin enhances smad3-mediated transforming growth factor-beta1 signaling in a carg box-independent manner: Smad-binding element is an important cis element for sm22alpha transcription in vivo. Circulation research. 2005;97:983-991
85. Miralles F, Posern G, Zaromytidou AI, Treisman R. Actin dynamics control srf activity by regulation of its coactivator mal. Cell. 2003;113:329-342
86. Sata M, Saiura A, Kunisato A, Tojo A, Okada S, Tokuhisa T, Hirai H, Makuuchi M, Hirata Y, Nagai R. Hematopoietic stem cells differentiate into vascular cells that participate in the pathogenesis of atherosclerosis. Nature medicine. 2002;8:403-409
87. Hu Y, Zhang Z, Torsney E, Afzal AR, Davison F, Metzler B, Xu Q. Abundant progenitor cells in the adventitia contribute to atherosclerosis of vein grafts in apoe-deficient mice. The Journal of clinical investigation. 2004;113:1258-1265
88. Passman JN, Dong XR, Wu SP, Maguire CT, Hogan KA, Bautch VL, Majesky MW. A sonic hedgehog signaling domain in the arterial adventitia supports resident sca1+ smooth muscle progenitor cells. Proceedings of the National Academy of Sciences of the United States of America. 2008;105:9349-9354
89. Roostalu U, Aldeiri B, Albertini A, Humphreys N, Simonsen-Jackson M, Wong JKF, Cossu G. Distinct cellular mechanisms underlie smooth muscle turnover in vascular development and repair. Circulation research. 2018;122:267-281
90. Kramann R, Goettsch C, Wongboonsin J, Iwata H, Schneider RK, Kuppe C, Kaesler N, Chang-Panesso M, Machado FG, Gratwohl S, Madhurima K, Hutcheson JD, Jain S, Aikawa E, Humphreys BD. Adventitial msc-like cells are progenitors of vascular smooth muscle cells and drive vascular calcification in chronic kidney disease. Cell stem cell. 2016;19:628-642
91. Sainz J, Al Haj Zen A, Caligiuri G, Demerens C, Urbain D, Lemitre M, Lafont A. Isolation of "side population" progenitor cells from healthy arteries of adult mice. Arteriosclerosis, thrombosis, and vascular biology. 2006;26:281-286
92. Tang Z, Wang A, Yuan F, Yan Z, Liu B, Chu JS, Helms JA, Li S. Differentiation of multipotent vascular stem cells contributes to vascular diseases. Nature communications. 2012;3:875
93. Nguyen AT, Gomez D, Bell RD, Campbell JH, Clowes AW, Gabbiani G, Giachelli CM, Parmacek MS, Raines EW, Rusch NJ, Speer MY, Sturek M, Thyberg J, Towler DA, Weiser-Evans MC, Yan C, Miano JM, Owens GK. Smooth muscle cell plasticity: Fact or fiction? Circulation research. 2013;112:17-22
94. Tang Z, Wang A, Wang D, Li S. Smooth muscle cells: To be or not to be? Response to nguyen et al. Circulation research. 2013;112:23-26
95. Majesky MW, Horita H, Ostriker A, Lu S, Regan JN, Bagchi A, Dong XR, Poczobutt J, Nemenoff RA, Weiser-Evans MC. Differentiated smooth muscle cells generate a subpopulation of resident vascular progenitor cells in the adventitia regulated by klf4. Circulation research. 2017;120:296-311
96. Frid MG, Kale VA, Stenmark KR. Mature vascular endothelium can give rise to smooth muscle cells via endothelial-mesenchymal transdifferentiation: In vitro analysis. Circulation research. 2002;90:1189-1196
97. Atkinson C, Horsley J, Rhind-Tutt S, Charman S, Phillpotts CJ, Wallwork J, Goddard MJ. Neointimal smooth muscle cells in human cardiac allograft coronary artery vasculopathy are of donor origin. The Journal of heart and lung transplantation : the official publication of the International Society for Heart Transplantation. 2004;23:427-435

98. Hu Y, Davison F, Ludewig B, Erdel M, Mayr M, Url M, Dietrich H, Xu Q. Smooth muscle cells in transplant atherosclerotic lesions are originated from recipients, but not bone marrow progenitor cells. Circulation. 2002;106:1834-1839
99. Yu B, Wong MM, Potter CM, Simpson RM, Karamariti E, Zhang Z, Zeng L, Warren D, Hu Y, Wang W, Xu Q. Vascular stem/progenitor cell migration induced by smooth muscle cell-derived chemokine (c-c motif) ligand 2 and chemokine (c-x-c motif) ligand 1 contributes to neointima formation. Stem cells. 2016;34:2368-2380
100. Wong MM, Winkler B, Karamariti E, Wang X, Yu B, Simpson R, Chen T, Margariti A, Xu Q. Sirolimus stimulates vascular stem/progenitor cell migration and differentiation into smooth muscle cells via epidermal growth factor receptor/extracellular signal-regulated kinase/beta-catenin signaling pathway. Arteriosclerosis, thrombosis, and vascular biology. 2013;33:2397-2406
101. Xie Y, Potter CMF, Le Bras A, Nowak WN, Gu W, Bhaloo SI, Zhang Z, Hu Y, Zhang L, Xu Q. Leptin induces sca-1(+) progenitor cell migration enhancing neointimal lesions in vessel-injury mouse models. Arteriosclerosis, thrombosis, and vascular biology. 2017;37:2114-2127
102. Sundberg-Smith LJ, DiMichele LA, Sayers RL, Mack CP, Taylor JM. The lim protein leupaxin is enriched in smooth muscle and functions as an serum response factor cofactor to induce smooth muscle cell gene transcription. Circulation research. 2008;102:1502-1511
103. Margariti A, Xiao Q, Zampetaki A, Zhang Z, Li H, Martin D, Hu Y, Zeng L, Xu Q. Splicing of hdac7 modulates the srf-myocardin complex during stem-cell differentiation towards smooth muscle cells. Journal of cell science. 2009;122:460-470
104. Xiao Q, Zeng L, Zhang Z, Hu Y, Xu Q. Stem cell-derived sca-1+ progenitors differentiate into smooth muscle cells, which is mediated by collagen iv-integrin alpha1/beta1/alphav and pdgf receptor pathways. American journal of physiology. Cell physiology. 2007;292:C342-352
105. Huang H, Xie C, Sun X, Ritchie RP, Zhang J, Chen YE. Mir-10a contributes to retinoid acid-induced smooth muscle cell differentiation. The Journal of biological chemistry. 2010;285:9383-9389
106. Xie C, Huang H, Sun X, Guo Y, Hamblin M, Ritchie RP, Garcia-Barrio MT, Zhang J, Chen YE. Microrna-1 regulates smooth muscle cell differentiation by repressing kruppel-like factor 4. Stem cells and development. 2011;20:205-210
107. Elia L, Quintavalle M, Zhang J, Contu R, Cossu L, Latronico MV, Peterson KL, Indolfi C, Catalucci D, Chen J, Courtneidge SA, Condorelli G. The knockout of mir-143 and -145 alters smooth muscle cell maintenance and vascular homeostasis in mice: Correlates with human disease. Cell death and differentiation. 2009;16:1590-1598
108. Xin M, Small EM, Sutherland LB, Qi X, McAnally J, Plato CF, Richardson JA, Bassel-Duby R, Olson EN. Micrornas mir-143 and mir-145 modulate cytoskeletal dynamics and responsiveness of smooth muscle cells to injury. Genes & development. 2009;23:2166-2178
109. Wang Z, Wang DZ, Hockemeyer D, McAnally J, Nordheim A, Olson EN. Myocardin and ternary complex factors compete for srf to control smooth muscle gene expression. Nature. 2004;428:185-189
110. Mekada K, Abe K, Murakami A, Nakamura S, Nakata H, Moriwaki K, Obata Y, Yoshiki A. Genetic differences among c57bl/6 substrains. Experimental animals. 2009;58:141-149
111. Kumar V, Kim K, Joseph C, Kourrich S, Yoo SH, Huang HC, Vitaterna MH, de Villena FP, Churchill G, Bonci A, Takahashi JS. C57bl/6n mutation in cytoplasmic fmrp interacting protein 2 regulates cocaine response. Science. 2013;342:1508-1512
112. Beermann F, Orlow SJ, Lamoreux ML. The tyr (albino) locus of the laboratory mouse. Mammalian genome : official journal of the International Mammalian Genome Society. 2004;15:749-758
113. Bosma GC, Custer RP, Bosma MJ. A severe combined immunodeficiency mutation in the mouse. Nature. 1983;301:527-530
114. Hoebe K, Jiang Z, Tabeta K, Du X, Georgel P, Crozat K, Beutler B. Genetic analysis of innate immunity. Advances in immunology. 2006;91:175-226
115. Lois C, Hong EJ, Pease S, Brown EJ, Baltimore D. Germline transmission and tissue-specific expression of transgenes delivered by lentiviral vectors. Science. 2002;295:868-872
116. Ding S, Wu X, Li G, Han M, Zhuang Y, Xu T. Efficient transposition of the piggybac (pb) transposon in mammalian cells and mice. Cell. 2005;122:473-483
117. Zambrowicz BP, Imamoto A, Fiering S, Herzenberg LA, Kerr WG, Soriano P. Disruption of overlapping transcripts in the rosa beta geo 26 gene trap strain leads to widespread expression of beta-galactosidase in mouse embryos and hematopoietic cells. Proceedings of the National Academy of Sciences of the United States of America. 1997;94:3789-3794

118. Doyle A, McGarry MP, Lee NA, Lee JJ. The construction of transgenic and gene knockout/knockin mouse models of human disease. Transgenic research. 2012;21:327-349
119. Sangiorgi E, Capecchi MR. Bmi1 is expressed in vivo in intestinal stem cells. Nature genetics. 2008;40:915-920
120. Giraldo P, Montoliu L. Size matters: Use of yacs, bacs and pacs in transgenic animals. Transgenic research. 2001;10:83-103
121. Donehower LA, Harvey M, Slagle BL, McArthur MJ, Montgomery CA, Jr., Butel JS, Bradley A. Mice deficient for p53 are developmentally normal but susceptible to spontaneous tumours. Nature. 1992;356:215-221
122. Lonberg N. Human antibodies from transgenic animals. Nature biotechnology. 2005;23:1117-1125
123. Araki K, Araki M, Miyazaki J, Vassalli P. Site-specific recombination of a transgene in fertilized eggs by transient expression of cre recombinase. Proceedings of the National Academy of Sciences of the United States of America. 1995;92:160-164
124. Gronostajski RM, Sadowski PD. The flp recombinase of the saccharomyces cerevisiae 2 microns plasmid attaches covalently to DNA via a phosphotyrosyl linkage. Molecular and cellular biology. 1985;5:3274-3279
125. Osz J, Brelivet Y, Peluso-Iltis C, Cura V, Eiler S, Ruff M, Bourguet W, Rochel N, Moras D. Structural basis for a molecular allosteric control mechanism of cofactor binding to nuclear receptors. Proceedings of the National Academy of Sciences of the United States of America. 2012;109:E588-594
126. Beliakoff J, Whitesell L. Hsp90: An emerging target for breast cancer therapy. Anti-cancer drugs. 2004;15:651-662
127. McDevitt MA, Glidewell-Kenney C, Jimenez MA, Ahearn PC, Weiss J, Jameson JL, Levine JE. New insights into the classical and non-classical actions of estrogen: Evidence from estrogen receptor knock-out and knock-in mice. Mol Cell Endocrinol. 2008;290:24-30
128. Goodsell DS. The molecular perspective: Tamoxifen and the estrogen receptor. Stem cells. 2002;20:267-268
129. Feil R, Wagner J, Metzger D, Chambon P. Regulation of cre recombinase activity by mutated estrogen receptor ligand-binding domains. Biochemical and biophysical research communications. 1997;237:752-757
130. Zhang Y, Riesterer C, Ayrall AM, Sablitzky F, Littlewood TD, Reth M. Inducible site-directed recombination in mouse embryonic stem cells. Nucleic acids research. 1996;24:543-548
131. Chen X, He Y, Lu F. Autophagy in stem cell biology: A perspective on stem cell self-renewal and differentiation. Stem cells international. 2018;2018:9131397
132. Kretzschmar K, Watt FM. Lineage tracing. Cell. 2012;148:33-45
133. Anastassiadis K, Fu J, Patsch C, Hu S, Weidlich S, Duerschke K, Buchholz F, Edenhofer F, Stewart AF. Dre recombinase, like cre, is a highly efficient site-specific recombinase in e. Coli, mammalian cells and mice. Disease models & mechanisms. 2009;2:508-515
134. He L, Li Y, Li Y, Pu W, Huang X, Tian X, Wang Y, Zhang H, Liu Q, Zhang L, Zhao H, Tang J, Ji H, Cai D, Han Z, Han Z, Nie Y, Hu S, Wang QD, Sun R, Fei J, Wang F, Chen T, Yan Y, Huang H, Pu WT, Zhou B. Enhancing the precision of genetic lineage tracing using dual recombinases. Nature medicine. 2017;23:1488-1498
135. Casanova E, Lemberger T, Fehsenfeld S, Mantamadiotis T, Schutz G. Alpha complementation in the cre recombinase enzyme. Genesis. 2003;37:25-29
136. Beerli RR, Barbas CF, 3rd. Engineering polydactyl zinc-finger transcription factors. Nature biotechnology. 2002;20:135-141
137. Boch J, Scholze H, Schornack S, Landgraf A, Hahn S, Kay S, Lahaye T, Nickstadt A, Bonas U. Breaking the code of DNA binding specificity of tal-type iii effectors. Science. 2009;326:1509-1512
138. Wiedenheft B, Sternberg SH, Doudna JA. Rna-guided genetic silencing systems in bacteria and archaea. Nature. 2012;482:331-338
139. Shalem O, Sanjana NE, Hartenian E, Shi X, Scott DA, Mikkelson T, Heckl D, Ebert BL, Root DE, Doench JG, Zhang F. Genome-scale crispr-cas9 knockout screening in human cells. Science. 2014;343:84-87
140. Wilson T, Hastings JW. Bioluminescence. Annual review of cell and developmental biology. 1998;14:197-230
141. Alam J, Cook JL. Reporter genes: Application to the study of mammalian gene transcription. Analytical biochemistry. 1990;188:245-254

142. Shaner NC, Steinbach PA, Tsien RY. A guide to choosing fluorescent proteins. Nature methods. 2005;2:905-909
143. Notta F, Doulatov S, Laurenti E, Poeppl A, Jurisica I, Dick JE. Isolation of single human hematopoietic stem cells capable of long-term multilineage engraftment. Science. 2011;333:218-221
144. Lowell S, Jones P, Le Roux I, Dunne J, Watt FM. Stimulation of human epidermal differentiation by delta-notch signalling at the boundaries of stem-cell clusters. Current biology : CB. 2000;10:491-500
145. Friedrich G, Soriano P. Promoter traps in embryonic stem cells: A genetic screen to identify and mutate developmental genes in mice. Genes & development. 1991;5:1513-1523
146. Muzumdar MD, Tasic B, Miyamichi K, Li L, Luo L. A global double-fluorescent cre reporter mouse. Genesis. 2007;45:593-605
147. Livet J, Weissman TA, Kang H, Draft RW, Lu J, Bennis RA, Sanes JR, Lichtman JW. Transgenic strategies for combinatorial expression of fluorescent proteins in the nervous system. Nature. 2007;450:56-62
148. Snippert HJ, van der Flier LG, Sato T, van Es JH, van den Born M, Kroon-Veenboer C, Barker N, Klein AM, van Rheenen J, Simons BD, Clevers H. Intestinal crypt homeostasis results from neutral competition between symmetrically dividing lgr5 stem cells. Cell. 2010;143:134-144
149. Mayor R, Etienne-Manneville S. The front and rear of collective cell migration. Nature reviews. Molecular cell biology. 2016;17:97-109
150. Ananthakrishnan R, Ehrlicher A. The forces behind cell movement. International journal of biological sciences. 2007;3:303-317
151. Pampaloni F, Lattanzi G, Jonas A, Surrey T, Frey E, Florin EL. Thermal fluctuations of grafted microtubules provide evidence of a length-dependent persistence length. Proceedings of the National Academy of Sciences of the United States of America. 2006;103:10248-10253
152. Nolen BJ, Littlefield RS, Pollard TD. Crystal structures of actin-related protein 2/3 complex with bound atp or adp. Proceedings of the National Academy of Sciences of the United States of America. 2004;101:15627-15632
153. Haffner C, Jarchau T, Reinhard M, Hoppe J, Lohmann SM, Walter U. Molecular cloning, structural analysis and functional expression of the proline-rich focal adhesion and microfilament-associated protein vasp. The EMBO journal. 1995;14:19-27
154. DesMarais V, Ghosh M, Eddy R, Condeelis J. Cofilin takes the lead. Journal of cell science. 2005;118:19-26
155. Hartwig JH, Bokoch GM, Carpenter CL, Janmey PA, Taylor LA, Toker A, Stossel TP. Thrombin receptor ligation and activated rac uncap actin filament barbed ends through phosphoinositide synthesis in permeabilized human platelets. Cell. 1995;82:643-653
156. Welch MD, Mullins RD. Cellular control of actin nucleation. Annual review of cell and developmental biology. 2002;18:247-288
157. Pollard TD, Borisy GG. Cellular motility driven by assembly and disassembly of actin filaments. Cell. 2003;112:453-465
158. Etienne-Manneville S, Hall A. Rho gtpases in cell biology. Nature. 2002;420:629-635
159. Merlot S, Firtel RA. Leading the way: Directional sensing through phosphatidylinositol 3-kinase and other signaling pathways. Journal of cell science. 2003;116:3471-3478
160. Jay DG. The clutch hypothesis revisited: Ascribing the roles of actin-associated proteins in filopodial protrusion in the nerve growth cone. Journal of neurobiology. 2000;44:114-125
161. Henson JH, Svitkina TM, Burns AR, Hughes HE, MacPartland KJ, Nazarian R, Borisy GG. Two components of actin-based retrograde flow in sea urchin coelomocytes. Molecular biology of the cell. 1999;10:4075-4090
162. Emsley J, Knight CG, Farndale RW, Barnes MJ, Liddington RC. Structural basis of collagen recognition by integrin alpha2beta1. Cell. 2000;101:47-56
163. Choi CK, Vicente-Manzanares M, Zareno J, Whitmore LA, Mogilner A, Horwitz AR. Actin and alpha-actinin orchestrate the assembly and maturation of nascent adhesions in a myosin ii motor-independent manner. Nature cell biology. 2008;10:1039-1050
164. Li Z, Lee H, Zhu C. Molecular mechanisms of mechanotransduction in integrin-mediated cell-matrix adhesion. Experimental cell research. 2016;349:85-94
165. Carisey A, Tsang R, Greiner AM, Nijenhuis N, Heath N, Nazgiewicz A, Kemkemer R, Derby B, Spatz J, Ballestrem C. Vinculin regulates the recruitment and release of core focal adhesion proteins in a force-dependent manner. Current biology : CB. 2013;23:271-281

166. Dumbauld DW, Shin H, Gallant ND, Michael KE, Radhakrishna H, Garcia AJ. Contractility modulates cell adhesion strengthening through focal adhesion kinase and assembly of vinculin-containing focal adhesions. Journal of cellular physiology. 2010;223:746-756
167. Wendt T, Taylor D, Trybus KM, Taylor K. Three-dimensional image reconstruction of dephosphorylated smooth muscle heavy meromyosin reveals asymmetry in the interaction between myosin heads and placement of subfragment 2. Proceedings of the National Academy of Sciences of the United States of America. 2001;98:4361-4366
168. Matsumura F, Hartshorne DJ. Myosin phosphatase target subunit: Many roles in cell function. Biochemical and biophysical research communications. 2008;369:149-156
169. Ponti A, Machacek M, Gupton SL, Waterman-Storer CM, Danuser G. Two distinct actin networks drive the protrusion of migrating cells. Science. 2004;305:1782-1786
170. Riento K, Ridley AJ. Rocks: Multifunctional kinases in cell behaviour. Nature reviews. Molecular cell biology. 2003;4:446-456
171. Small JV, Kaverina I. Microtubules meet substrate adhesions to arrange cell polarity. Current opinion in cell biology. 2003;15:40-47
172. Zhao X, Guan JL. Focal adhesion kinase and its signaling pathways in cell migration and angiogenesis. Advanced drug delivery reviews. 2011;63:610-615
173. Webb DJ, Parsons JT, Horwitz AF. Adhesion assembly, disassembly and turnover in migrating cells -- over and over and over again. Nature cell biology. 2002;4:E97-100
174. Cheresh DA, Leng J, Klemke RL. Regulation of cell contraction and membrane ruffling by distinct signals in migratory cells. The Journal of cell biology. 1999;146:1107-1116
175. Han DC, Shen TL, Guan JL. Role of grb7 targeting to focal contacts and its phosphorylation by focal adhesion kinase in regulation of cell migration. The Journal of biological chemistry. 2000;275:28911-28917
176. West KA, Zhang H, Brown MC, Nikolopoulos SN, Riedy MC, Horwitz AF, Turner CE. The ld4 motif of paxillin regulates cell spreading and motility through an interaction with paxillin kinase linker (pkl). The Journal of cell biology. 2001;154:161-176
177. Webb DJ, Donais K, Whitmore LA, Thomas SM, Turner CE, Parsons JT, Horwitz AF. Fak-src signalling through paxillin, erk and mlck regulates adhesion disassembly. Nature cell biology. 2004;6:154-161
178. Amento EP, Ehsani N, Palmer H, Libby P. Cytokines and growth factors positively and negatively regulate interstitial collagen gene expression in human vascular smooth muscle cells. Arteriosclerosis and thrombosis : a journal of vascular biology / American Heart Association. 1991;11:1223-1230
179. Kadler KE, Baldock C, Bella J, Boot-Handford RP. Collagens at a glance. Journal of cell science. 2007;120:1955-1958
180. Corsi A, Xu T, Chen XD, Boyde A, Liang J, Mankani M, Sommer B, Iozzo RV, Eichstetter I, Robey PG, Bianco P, Young MF. Phenotypic effects of biglycan deficiency are linked to collagen fibril abnormalities, are synergized by decorin deficiency, and mimic ehlers-danlos-like changes in bone and other connective tissues. Journal of bone and mineral research : the official journal of the American Society for Bone and Mineral Research. 2002;17:1180-1189
181. Pozzi A, Wary KK, Giancotti FG, Gardner HA. Integrin alpha1beta1 mediates a unique collagen-dependent proliferation pathway in vivo. The Journal of cell biology. 1998;142:587-594
182. Brown EJ, Frazier WA. Integrin-associated protein (cd47) and its ligands. Trends in cell biology. 2001;11:130-135
183. Orr AW, Lee MY, Lemmon JA, Yurdagul A, Jr., Gomez MF, Bortz PD, Wamhoff BR. Molecular mechanisms of collagen isotype-specific modulation of smooth muscle cell phenotype. Arteriosclerosis, thrombosis, and vascular biology. 2009;29:225-231
184. Colorado PC, Torre A, Kamphaus G, Maeshima Y, Hopfer H, Takahashi K, Volk R, Zamborsky ED, Herman S, Sarkar PK, Ericksen MB, Dhanabal M, Simons M, Post M, Kufe DW, Weichselbaum RR, Sukhatme VP, Kalluri R. Anti-angiogenic cues from vascular basement membrane collagen. Cancer research. 2000;60:2520-2526
185. Chang JH, Javier JA, Chang GY, Oliveira HB, Azar DT. Functional characterization of neostatins, the mmp-derived, enzymatic cleavage products of type xviii collagen. FEBS letters. 2005;579:3601-3606
186. Hinek A, Keeley FW, Callahan J. Recycling of the 67-kda elastin binding protein in arterial myocytes is imperative for secretion of tropoelastin. Experimental cell research. 1995;220:312-324
187. Wolinsky H, Glagov S. A lamellar unit of aortic medial structure and function in mammals. Circulation research. 1967;20:99-111

188. Mochizuki S, Brassart B, Hinek A. Signaling pathways transduced through the elastin receptor facilitate proliferation of arterial smooth muscle cells. The Journal of biological chemistry. 2002;277:44854-44863
189. Yamamoto M, Fujita K, Shinkai T, Yamamoto K, Noumura T. Identification of the phenotypic modulation of rabbit arterial smooth muscle cells in primary culture by flow cytometry. Experimental cell research. 1992;198:43-51
190. Urban Z, Riazi S, Seidl TL, Katahira J, Smoot LB, Chitayat D, Boyd CD, Hinek A. Connection between elastin haploinsufficiency and increased cell proliferation in patients with supravalvular aortic stenosis and williams-beuren syndrome. American journal of human genetics. 2002;71:30-44
191. Li DY, Brooke B, Davis EC, Mecham RP, Sorensen LK, Boak BB, Eichwald E, Keating MT. Elastin is an essential determinant of arterial morphogenesis. Nature. 1998;393:276-280
192. Ekmekci H, Ekmekci OB, Sonmez H, Ozturk Z, Domanic N, Kokoglu E. Evaluation of fibronectin, vitronectin, and leptin levels in coronary artery disease: Impacts on thrombosis and thrombolysis. Clinical and applied thrombosis/hemostasis : official journal of the International Academy of Clinical and Applied Thrombosis/Hemostasis. 2005;11:63-70
193. Yousif LF, Di Russo J, Sorokin L. Laminin isoforms in endothelial and perivascular basement membranes. Cell adhesion & migration. 2013;7:101-110
194. Bonnans C, Chou J, Werb Z. Remodelling the extracellular matrix in development and disease. Nature reviews. Molecular cell biology. 2014;15:786-801
195. Page-McCaw A, Ewald AJ, Werb Z. Matrix metalloproteinases and the regulation of tissue remodelling. Nature reviews. Molecular cell biology. 2007;8:221-233
196. Raffetto JD, Khalil RA. Matrix metalloproteinases and their inhibitors in vascular remodeling and vascular disease. Biochemical pharmacology. 2008;75:346-359
197. Itoh Y, Takamura A, Ito N, Maru Y, Sato H, Suenaga N, Aoki T, Seiki M. Homophilic complex formation of mt1-mmp facilitates prommp-2 activation on the cell surface and promotes tumor cell invasion. The EMBO journal. 2001;20:4782-4793
198. Ammarguellat FZ, Gannon PO, Amiri F, Schiffrin EL. Fibrosis, matrix metalloproteinases, and inflammation in the heart of doca-salt hypertensive rats: Role of et(a) receptors. Hypertension. 2002;39:679-684
199. Ley K, Laudanna C, Cybulsky MI, Nourshargh S. Getting to the site of inflammation: The leukocyte adhesion cascade updated. Nature reviews. Immunology. 2007;7:678-689
200. Lamalice L, Le Boeuf F, Huot J. Endothelial cell migration during angiogenesis. Circulation research. 2007;100:782-794
201. Kansas GS. Selectins and their ligands: Current concepts and controversies. Blood. 1996;88:3259-3287
202. Shamri R, Grabovsky V, Gauguet JM, Feigelson S, Manevich E, Kolanus W, Robinson MK, Staunton DE, von Andrian UH, Alon R. Lymphocyte arrest requires instantaneous induction of an extended lfa-1 conformation mediated by endothelium-bound chemokines. Nature immunology. 2005;6:497-506
203. Phillipson M, Heit B, Colarusso P, Liu L, Ballantyne CM, Kubes P. Intraluminal crawling of neutrophils to emigration sites: A molecularly distinct process from adhesion in the recruitment cascade. The Journal of experimental medicine. 2006;203:2569-2575
204. Muller WA. Leukocyte-endothelial-cell interactions in leukocyte transmigration and the inflammatory response. Trends in immunology. 2003;24:327-334
205. Shaw SK, Bamba PS, Perkins BN, Luscinskas FW. Real-time imaging of vascular endothelial-cadherin during leukocyte transmigration across endothelium. Journal of immunology. 2001;167:2323-2330
206. Engelhardt B, Wolburg H. Mini-review: Transendothelial migration of leukocytes: Through the front door or around the side of the house? European journal of immunology. 2004;34:2955-2963
207. Weis S, Cui J, Barnes L, Cheresh D. Endothelial barrier disruption by vegf-mediated src activity potentiates tumor cell extravasation and metastasis. The Journal of cell biology. 2004;167:223-229
208. Dejana E, Languino LR, Polentarutti N, Balconi G, Ryckewaert JJ, Larrieu MJ, Donati MB, Mantovani A, Marguerie G. Interaction between fibrinogen and cultured endothelial cells. Induction of migration and specific binding. The Journal of clinical investigation. 1985;75:11-18
209. Byzova TV, Goldman CK, Pampori N, Thomas KA, Bett A, Shattil SJ, Plow EF. A mechanism for modulation of cellular responses to vegf: Activation of the integrins. Molecular cell. 2000;6:851-860

210. Pintucci G, Yu PJ, Saponara F, Kadian-Dodov DL, Galloway AC, Mignatti P. Pdgf-bb induces vascular smooth muscle cell expression of high molecular weight fgf-2, which accumulates in the nucleus. J Cell Biochem. 2005;95:1292-1300
211. Pickering JG, Uniyal S, Ford CM, Chau T, Laurin MA, Chow LH, Ellis CG, Fish J, Chan BM. Fibroblast growth factor-2 potentiates vascular smooth muscle cell migration to platelet-derived growth factor: Upregulation of alpha2beta1 integrin and disassembly of actin filaments. Circulation research. 1997;80:627-637
212. Nelson PR, Yamamura S, Kent KC. Extracellular matrix proteins are potent agonists of human smooth muscle cell migration. Journal of vascular surgery. 1996;24:25-32; discussion 32-23
213. Hendrickson RJ, Cappadona C, Yankah EN, Sitzmann JV, Cahill PA, Redmond EM. Sustained pulsatile flow regulates endothelial nitric oxide synthase and cyclooxygenase expression in co-cultured vascular endothelial and smooth muscle cells. Journal of molecular and cellular cardiology. 1999;31:619-629
214. Gambillara V, Montorzi G, Haziza-Pigeon C, Stergiopulos N, Silacci P. Arterial wall response to ex vivo exposure to oscillatory shear stress. Journal of vascular research. 2005;42:535-544
215. Kramer N, Walzl A, Unger C, Rosner M, Krupitza G, Hengstschlager M, Dolznig H. In vitro cell migration and invasion assays. Mutation research. 2013;752:10-24
216. Lennartsson J, Ronnstrand L. Stem cell factor receptor/c-kit: From basic science to clinical implications. Physiol Rev. 2012;92:1619-1649
217. Ogawa M, Matsuzaki Y, Nishikawa S, Hayashi S, Kunisada T, Sudo T, Kina T, Nakauchi H, Nishikawa S. Expression and function of c-kit in hemopoietic progenitor cells. The Journal of experimental medicine. 1991;174:63-71
218. Hu Y, Zou Y, Dietrich H, Wick G, Xu Q. Inhibition of neointima hyperplasia of mouse vein grafts by locally applied suramin. Circulation. 1999;100:861-868
219. Nobes CD, Hall A. Rho, rac, and cdc42 gtpases regulate the assembly of multimolecular focal complexes associated with actin stress fibers, lamellipodia, and filopodia. Cell. 1995;81:53-62
220. Totsukawa G, Yamakita Y, Yamashiro S, Hartshorne DJ, Sasaki Y, Matsumura F. Distinct roles of rock (rho-kinase) and mlck in spatial regulation of mlc phosphorylation for assembly of stress fibers and focal adhesions in 3t3 fibroblasts. J Cell Biol. 2000;150:797-806
221. Reunanen N, Westermarck J, Hakkinen L, Holmstrom TH, Elo I, Eriksson JE, Kahari VM. Enhancement of fibroblast collagenase (matrix metalloproteinase-1) gene expression by ceramide is mediated by extracellular signal-regulated and stress-activated protein kinase pathways. J Biol Chem. 1998;273:5137-5145
222. Yin T, Li L. The stem cell niches in bone. The Journal of clinical investigation. 2006;116:1195-1201
223. Gibson BW, Boles NC, Souroullas GP, Herron AJ, Fraley JK, Schwiebert RS, Sharp JJ, Goodell MA. Comparison of cesium-137 and x-ray irradiators by using bone marrow transplant reconstitution in c57bl/6j mice. Comparative medicine. 2015;65:165-172
224. Duran-Struuck R, Dysko RC. Principles of bone marrow transplantation (bmt): Providing optimal veterinary and husbandry care to irradiated mice in bmt studies. Journal of the American Association for Laboratory Animal Science : JAALAS. 2009;48:11-22
225. Hruban RH, Long PP, Perlman EJ, Hutchins GM, Baumgartner WA, Baughman KL, Griffin CA. Fluorescence in situ hybridization for the y-chromosome can be used to detect cells of recipient origin in allografted hearts following cardiac transplantation. The American journal of pathology. 1993;142:975-980
226. Xu Q. Stem cells and transplant arteriosclerosis. Circulation research. 2008;102:1011-1024
227. Rahmani M, Cruz RP, Granville DJ, McManus BM. Allograft vasculopathy versus atherosclerosis. Circulation research. 2006;99:801-815
228. Alexander MR, Owens GK. Epigenetic control of smooth muscle cell differentiation and phenotypic switching in vascular development and disease. Annual review of physiology. 2012;74:13-40
229. Yoshii SR, Mizushima N. Monitoring and measuring autophagy. International journal of molecular sciences. 2017;18
230. Xu Q, Zhang Z, Davison F, Hu Y. Circulating progenitor cells regenerate endothelium of vein graft atherosclerosis, which is diminished in apoe-deficient mice. Circulation research. 2003;93:e76-86
231. Hill JM, Zalos G, Halcox JP, Schenke WH, Waclawiw MA, Quyyumi AA, Finkel T. Circulating endothelial progenitor cells, vascular function, and cardiovascular risk. The New England journal of medicine. 2003;348:593-600

232. Nakata Y, Shionoya S. Vascular lesions due to obstruction of the vasa vasorum. Nature. 1966;212:1258-1259
233. Iwata H, Manabe I, Fujiu K, Yamamoto T, Takeda N, Eguchi K, Furuya A, Kuro-o M, Sata M, Nagai R. Bone marrow-derived cells contribute to vascular inflammation but do not differentiate into smooth muscle cell lineages. Circulation. 2010;122:2048-2057
234. Bentzon JF, Weile C, Sondergaard CS, Hindkjaer J, Kassem M, Falk E. Smooth muscle cells in atherosclerosis originate from the local vessel wall and not circulating progenitor cells in apoe knockout mice. Arteriosclerosis, thrombosis, and vascular biology. 2006;26:2696-2702
235. Shimizu K, Sugiyama S, Aikawa M, Fukumoto Y, Rabkin E, Libby P, Mitchell RN. Host bone-marrow cells are a source of donor intimal smooth- muscle-like cells in murine aortic transplant arteriopathy. Nature medicine. 2001;7:738-741
236. Evrard SM, Lecce L, Michelis KC, Nomura-Kitabayashi A, Pandey G, Purushothaman KR, d'Escamard V, Li JR, Hadri L, Fujitani K, Moreno PR, Benard L, Rimmele P, Cohain A, Mecham B, Randolph GJ, Nabel EG, Hajjar R, Fuster V, Boehm M, Kovacic JC. Endothelial to mesenchymal transition is common in atherosclerotic lesions and is associated with plaque instability. Nature communications. 2016;7:11853
237. Yasuda H, Galli SJ, Geissler EN. Cloning and functional analysis of the mouse c-kit promoter. Biochemical and biophysical research communications. 1993;191:893-901
238. Huang C, Jacobson K, Schaller MD. Map kinases and cell migration. Journal of cell science. 2004;117:4619-4628